SIMULTANEOUS WATER AND ENERGY OPTIMIZATION IN SHALE EXPLORATION

Doris Oluwafunmilayo Oke (378635)

A thesis submitted in fulfillment of the requirements for the degree

of

Doctor of Philosophy (Chemical Engineering)

Submitted to

School of Chemical and Metallurgical Engineering, Faculty of Engineering and the Built Environment, University of Witwatersrand, Johannesburg, South Africa.

Johannesburg, 2019

DECLARATION

I declare that this thesis is my own unaided work. It is being submitted for the degree of Doctor of Philosophy in Chemical Engineering to the University of the Witwatersrand, Johannesburg. It has not been submitted before for any other degree or examination in any other University.

Doris Oke

13th day of September, 2019

ABSTRACT

Because of several environmental challenges associated with the development of shale resources around the world especially in the area of water management as well as flaring of co-produced gas. It is important to find a better strategy that can alleviate these environmental issues by developing a more integrated approach to address the challenges of the water-energy nexus in shale exploration.

This thesis presents a mathematical framework for simultaneous optimization of water and energy usage in hydraulic fracturing using superstructure-based optimization technique. First, a continuous time formulation for scheduling is developed for the hydraulic fracturing activities. Recycle/reuse of fracturing water (flowback water) is achieved through purification of flowback wastewater using thermally driven membrane distillation (MD). A detailed design model for this technology is incorporated within the water network superstructure in order to account for the design specifications and the energy requirement of the system. The feasibility of utilizing the co-produced gas that is traditionally flared as a potential source of energy for MD is also examined. The applicability of the proposed model is determined using a case study which is a representative of Marcellus shale play.

Next, the mathematical formulation is extended to account for shale gas production, processing, distribution, usage in power generation, and transmission of produced power in which the effect that the type of gas to be produced in a particular shale play/region will have on the infrastructure development is investigated. The study considers natural gas as fuel for commercial, industrial and residential customers, as well as fuel for electric power generation, with the goal of maximizing the overall profit. The resultant model is applied to a case study, which is a representative of Marcellus shale play. The application of the model results in 23.2 % reduction in freshwater consumption, 18.6 % savings in the total cost of freshwater and 42.7 % reduction in the energy requirement of the regenerator. The thermal energy consumption is in the order of 160×10^3 kJ/m^3 of water. Two types of gas are considered: wet gas and dry gas. The results indicate that the cost incurred in the network involving wet gas is 41.76 % higher than the network involving dry gas due to the processing requirement of wet gas.

In addition, the multi-contaminant property of flowback water is investigated through implementation of an on-site pre-treatment technology to remove contaminants like total suspended solid (TSS), Total organic compound (TOC), oil, grease and scaling materials whereby, specification for water reuse can be achieved. This is achieved by considering

detailed ultrafiltration model in order to evaluate the sustainability of the system in terms of energy consumption and associated costs. The study also looks into the feasibility of using the gas that would otherwise be flared to generate electrical energy for the membrane system via an onsite gas generator. The application of the proposed model in a case study results in 21.4 % reduction in the amount of water required for fracturing and 10.3 % reduction in the amount of energy needed by the regenerator. The system consumes 0.109 kWh/m^3 of energy at an operating pressure of 3.69 bar. This indicates a very low-energy consumption compared to a typical energy requirement for wastewater reclamation which usually ranges between 0.8 and 1.0 kWh/m^3 for membrane filtration. The study indicates the possibility of reducing the operating cost of the regeneration network by 61 % if the electrical energy needed is generated onsite using the gas that would otherwise be flared.

The effect of using multiple/ hybrid treatment technologies in maximizing hydraulic fracturing wastewater reuse while accounting for the sustainability of the process in terms of energy and associated cost is also investigated. The study considers ultrafiltration and membrane distillation processes as possible pre-treatment and desalination technologies for flowback water management. Two different scenarios are considered to cover possible flowback water composition in hydraulic fracturing in terms of salinity. Application of the proposed model to a case study leads to 24.13 % reduction in the amount of water required for fracturing. In terms of energy requirements, the approach led to 31.6 % reduction in the required thermal energy in membrane distillation and 8.62 % in the energy requirement for UF. For flowback water with moderate TDS concentration, 93.6 % of the wastewater reuse comes from pre-treated water by ultrafiltration and 6.4 % from membrane distillation. However, as the flowback water salinity becomes higher, the percentage of pre-treated water that could be reused reduced to 81.1 % and the percentage supply through membrane distillation increased to 18.9 %. In all cases, the results indicate that the decision to allow the pre-treated water to pass through desalination technology strictly depends on the volume of water required by a particular wellpad and the salinity of the wastewater.

In general, although the obtained results may not generally applicable to all shale plays, the proposed framework and supporting models aid in understanding the potential impact of using scheduling and optimization techniques in addressing flowback wastewater management.

LISTS OF PUBLICATIONS

JOURNAL PUBLICATIONS

Oke, D., Mukherjee, R., Sengupta, D., Majozi, T., El-Halwagi, M.M., 2019. Optimization of water-energy nexus in shale gas exploration: From production to transmission. Energy, 183, 651-669.

Oke, D., Majozi, T., Mukherjee, R., Sengupta, D., El-Halwagi, M.M., 2018. Simultaneous energy and water optimization in shale exploration. Processes, 6, 86.

CONFERENCE PUBLICATIONS

Oke, D., Mukherjee, R., Sengupta, D., Majozi, T., El-Halwagi, M.M., 2019. Using ultrafiltration for flowback water management in shale gas exploration: multicontaminant consideration. Computer Aided Chemical Engineering, 47, 347-352.

Oke, D., Majozi, T., Mukherjee, R., Sengupta, D., El-Halwagi, M.M., 2018. Water, energy and shale gas optimization: from production to transmission. Proceeding of the 13th SDEWES Conference on Sustainable Development of Energy, Water and Environment Systems, Palermo, Italy. 30 September - 4 October 2018.

Oke, D., Majozi, T., Mukherjee, R., Sengupta, D., El-Halwagi, M.M., 2018. Simultaneous energy and water Optimization in shale exploration. Computer Aided Chemical Engineering, 44, 1957-1962.

DEDICATION

This thesis is dedicated to God Almighty, you are the source and the help of my life and l will forever be grateful to you. To my loving and ever caring husband, Ibrahim Musayayi and my lovely children, IreOluwa Samuel and IranlowoOluwa Emmanuel (you are mummy’s friends), thank you for your support, encouragement and for believing in me. You are the best I ever have, and I will forever love you.

ACKNOWLEDGEMENTS

I wish to express my special gratitude to my supervisor Prof. T. Majozi for his support, insight and technical guidance throughout this work. I would like to sincerely thank the National Research Foundation (NRF) of South Africa for funding this project.

I also want to acknowledge the technical inputs and insights of Prof. M.M. El-Halwagi, Dr. Rajib Mukherjee and Dr. Debalina Sengupta of Texas A&M University.

My special love goes to my parent, Mr. and Mrs. Remi Oke for their full support even when everything seems impossible, you are the best parent in the whole world and you will live to eat the fruit of your labor. To my mother in-law, Mrs. Mary Musayayi for her understanding and for the values you instill in my husband, l love you mummy. My deep appreciation also goes to my late grandmother, Mrs. Olajiire Esther Akintaro, thank you for taking care of me from infant and the unending love you showed me until your last day, I can never forget you maami. To my siblings, Temilade, Bisola and Babatunde, it is a privilege to have you and l cherish you all.

To my colleagues in Sustainable Process Engineering research group, for the teamwork and for making the environment conducive throughout the research period.

Lastly, to all my family members, thank you for being there for me in one way or the other, l love you all.

Table of Contents

LIST OF FIGURES

LIST OF TABLES

CHAPTER ONE

INTRODUCTION

1.1. Background

The "shale revolution" has triggered a dramatic change in oil and natural gas production globally. The revolution starts in the US from where it is spreading to other part of the world. From 2007 to 2015, the US has witnessed an increase in the amount of shale gas produced from 2 to 15 trillion cubic feet per year (Al-Douri et al., 2017), with estimates of continued growth to support monetization projects (Zhang and El-Halwagi, 2017). Due to shale revolution, oil and natural gas production in the US has increased by approximately 73% and 65% (from 2008- 2016) respectively as shown in Figure 1.1. Figure 1.2 compares the natural gas prices between US, Japan and Germany which shows that the gas production boom in the US has resulted in plummeting gas price, which dropped from its 2008 high of $8.84 per million Btu (MMBtu) to $2.94 per MMBtu in July 2012 (Gay et al., 2012). In 2015, shale gas production accounted for over half of total natural gas production in the United State and is predicted to increase to 79 billion cubic feet per day (Bcf/d) by 2040 from 37 billion cubic feet per day (Bcf/d) in 2015 (EIA, 2016).

Natural gas has been found to be the largest source of energy production in the US with 33% of all energy production in 2016 and the largest source of electrical generation since July 2015 (EIA, 2018). The fast growth in electricity production from natural gas is associated with low price of natural gas and smaller carbon footprint compared to coal. Coals have been recognised as a limited resource and the process by which it is translated to electricity has a much negative impact on the environment than natural gas.

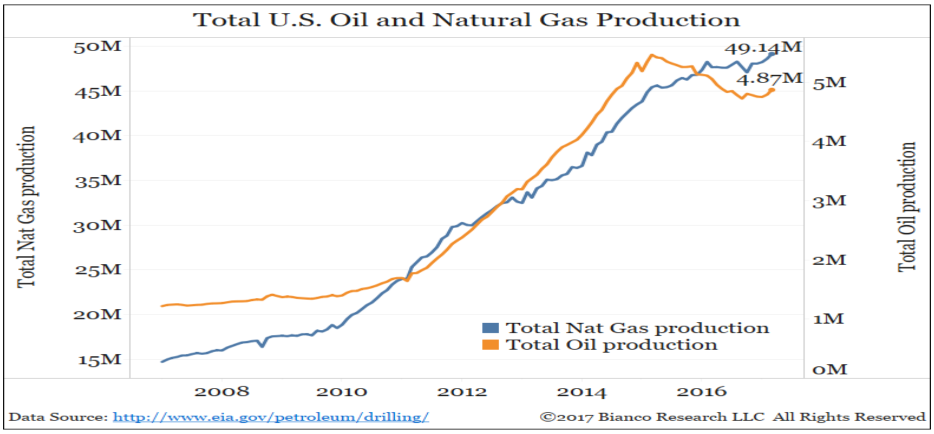

Figure 1.1. US natural gas and oil production (Bianco, 2017)

Figure 1.2. Comparison of world natural gas prices (Aguilera and Radetzki, 2013)

However, the process by which shale gas is produced known as hydraulic fracturing is associated with several environmental challenges among which are: water usage and wastewater discharge as well as flaring of co-produced gas. The summary of this is given in Figure 1.3 below.

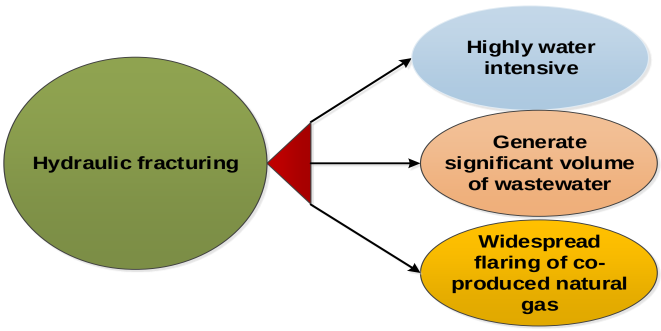

Figure 1.3. Problems associated with hydraulic fracturing

Water management decisions within shale gas production can be grouped into two main categories, i.e. the usage of water in the process of hydraulic fracturing and managing the effluent generated from drilling and production. The production of shale gas typically requires 7,000 to 18,000 m^3 of water to fracture and drill a typical well (Arthur et al., 2008, Yang et al., 2014a, Gregory et al., 2011). A main challenge associated with water usage in hydraulic fracturing is relatively short time within which the large volume of fracturing fluid is needed (Yang et al., 2014a). Another issue of contention that has impeded the ongoing progress in the shale gas production processes is water contamination. Two categories of wastewater are generated after hydraulic fracturing: flowback water and produced water. Flowback water is the wastewater that returns to the surface within the first few weeks after hydraulic fracturing, it is depicted by high flowrate and the volume generated range between 10-40% of the initial injected fluid (Yang et al., 2014a). The contaminants found in flowback water include total suspended solid (TSS), metals, organics and total dissolved solid (TDS), with the TDS value range between 20,000 mg/L to 300,000 mg/L depending on the shale formation and how long the water remains underground (Arthur et al., 2008, Yang et al., 2014a). Produced water on the other hand is the wastewater generated in the production stages. It is made up of the formation water and the injected fracturing fluid generally characterized by high salinity. In selecting appropriate options for the effective management of high volume of the generated flowback water, several factors have to be considered. These include environmental regulation, amount and types of contaminant in the wastewater and economics factors. Thus, water consumption in shale gas production is a serious matter making water resource management an important operational and environmental issue (Hasaneen and El-Halwagi, 2017, Petrakis, 2008). The increase in the cost of freshwater and disposal of generated wastewater, limitations in providing fresh water for fracturing, and the concerns about the negative environmental impact of shale gas wastewater have spurred the interest in identifying cost-effective technologies that can reduce the usage of fresh water and the discharge of wastewater in shale gas production.

The proper management of water resources require wastewater treatment for reuse and/or recycling which can be accomplished by the use of water treatment units, categorised as membrane or non-membrane processes. Flowback water reuse in hydraulic fracturing demands low salinity as high salinity can lead to formation damage, affect performance of some friction reducers and damage the drilling equipment (Elsayed et al., 2015). The choice of the treatment technology depends on the level of purity required, mobility and economics of the process. Special attentions are recently being given to membrane processes in the area of water and wastewater treatments because of various advantages they exhibit over the conventional methods. However, the membrane-based process for water treatment is energy intensive; therefore, minimising energy when exploring membrane technology for water regeneration reuse is also of great importance. In this study, consideration is given to ultrafiltration (UF) and membrane distillation (MD) as the membrane technologies of interest. There are various benefits associated with the use of UF and MD in the areas of water recycle and/or reuse as well as desalination particularly in shale exploration (Elsayed et al., 2013, Elsayed et al., 2015, Shaffer et al., 2013, ERM, 2014, Dahmn and Chapman, 2014). These include:

- UF and MD are both characterised by a smaller footprint because of high surface area to volume ratio of the membrane.
- Both systems have the advantage of modularity and mobility, which allow for easy movement within wellpads.
- Suitability of MD for high-level salinity flowback/produced water, which is the one of the main attributes of wastewater from hydraulic fracturing operation.
- MD is characterised with low-level heating and ability to operate with moderate temperature and pressure while UF is classified as a low pressure driven membrane process with moderate energy requirement. This is considered as an added advantage due to the availability of wasted energy from flaring that can serve as energy source for these technologies.
- Both have the tendency for high water recovery.

In addition to the water management issue faced in hydraulic fracturing is the widespread flaring of the co-produced natural gas. Flaring is the burning of natural gas which cannot be refined or sold. Flaring is carried out frequently in most of the industrial plants especially in managing unusual or irregular occurrence. Flaring in most industries is carried out to decrease hazard in the course of distress in an industrial operation, to get rid of associated gases, or to safely manage process start up and shutdown (Kamrava et al., 2015). In order to minimize flaring in industries, legislative acts should be implemented so that industries will take necessary precautions. Another way of achieving this is by recovery and efficient utilization of the flaring streams (Kazi et al., 2016). In the context of shale exploration, flaring is common in areas where oil and gas are co-produced with no sufficient infrastructure for gathering the gas. Because of this drawback, the producer either choses to build the pipeline or gathering facilities, flare the gas or find a useful way of utilizing the gas on site (Glazer et al., 2014). Although facts about the rate of flaring after well completion is yet to be published, information from the literature suggests that the time at which gas is mostly flared coincide with the time when substantial volume of flowback water is recovered. According to Glaizer et al. (2014), flaring of gas is mostly done in the first 10 producing days after initial completion or recompletion of a well. For example, 15041 wells were completed in Texas in 2012 which led to the flaring of 1.36 billion m^3 (48 billion ft^3) of natural gas. The estimated rate of flare based on these figures can be set at 9600 m^3 per well per day, though variation might occur based on a particular well (Glazer et al., 2014). In general, as indicated in Figure 1.4, flaring is found to be a waste of resources globally resulting in serious environmental problems such as air, thermal and light pollution (Wikramanayake and Bahadur, 2016).

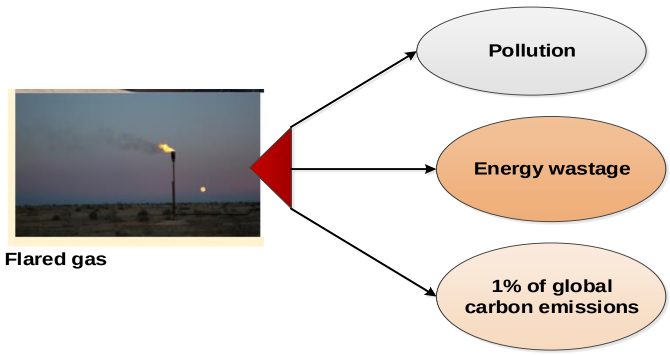

Figure 1.4. Problems associated with flaring

Thus, it is imperative to develop a more integrated approach to address the challenges of the water-energy nexus in shale gas production. The possible solution is to find a better strategy that can alleviate these environmental issues simultaneously. One such strategy is by utilization of the co-produced gas that would otherwise be flared after well completion for onsite wastewater treatment thereby reducing wastewater disposal and rate of gas flaring as well as reduction in freshwater supply during hydraulic fracturing.

Therefore, this study focuses on the synthesis and optimization of an integrated shale gas, water and membrane network that simultaneously optimizes the hydraulic fracturing schedule as well as water and energy consumption using continuous time mathematical formulation for scheduling. Freshwater consumption is minimized by exploring regeneration reuse within the network through purification of flowback water using ultrafiltration (UF) and membrane distillation (MD) regenerator units. A detailed design of these regenerators is incorporated to determine the optimal operating conditions for efficient energy use.

1.2. Motivation

The first motivation behind this work is the scheduling time representation, for a typical well, there is high initial gas or oil production rate. The decline rate of 60 to 90 % is expected after 3 years, consequently the operators need to regularly drill new wells which results in scheduling problem. Studies that have considered wellpad scheduling along with water management in hydraulic fracturing have either adopted the discrete time scheduling formulation or assumed a fixed schedule. The major limitation of discretizing the time horizon is the explosive binary dimension that could lead to higher computational time and suboptimal solution. In order to overcome this limitation, continuous time scheduling formulation is adopted in this study. The pros and cons of discrete and continuous time scheduling formulation is given in Figure 1.5.

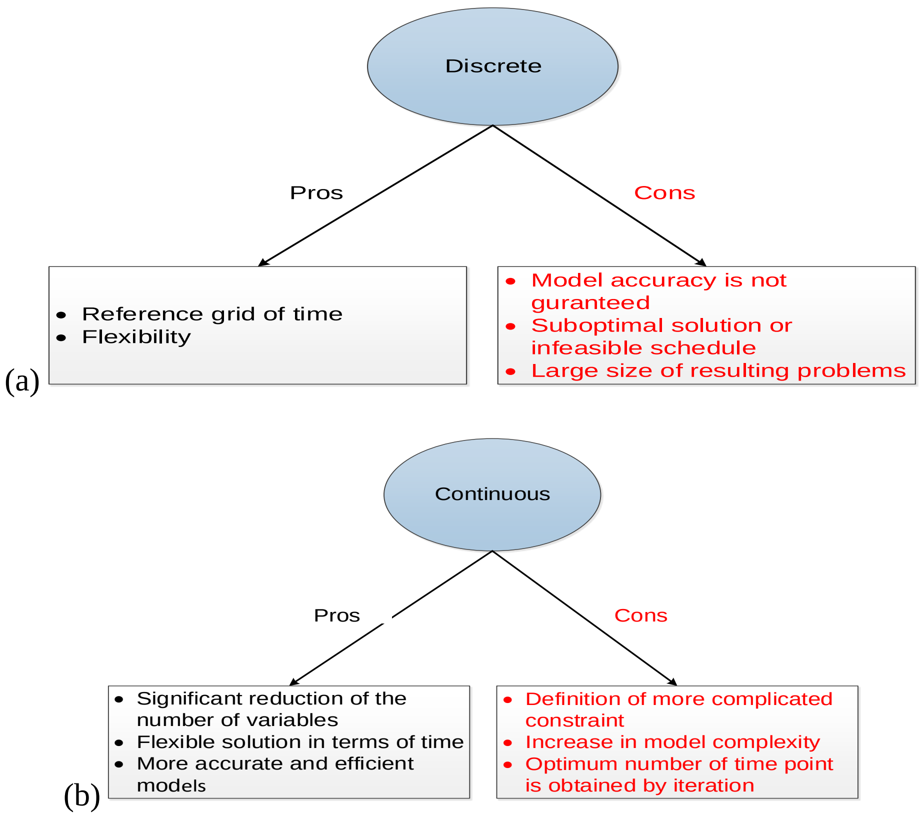

Figure 1.5. a) Pros and cons of discrete time formulation. b) Pros and cons of continuous time formulation.

The second motivation is the regenerator design (black-box vs detailed). Most of the research done in this area has represented the wastewater treatment unit as a “black box” or uses “short cut" regenerator model (Yang et al., 2014b) due to the complexity of the regenerator design. In black-box approach, fixed removal ratio of contaminant or fixed outlet concentration of the regenerated water is used in modelling the performance of a regenerator. Thereby using a linear cost function, which is a function of the amount of water fed into the regenerator to estimate the cost of regeneration. However, this approach does not give the true cost representation of the project and does not allow opportunity to minimize the energy requirement of the regenerator.

Another motivation behind the study is to check the feasibility of using the gas that would otherwise be flared especially in oil producing wells as source of energy for the regenerators as indicated in Figure1.6.

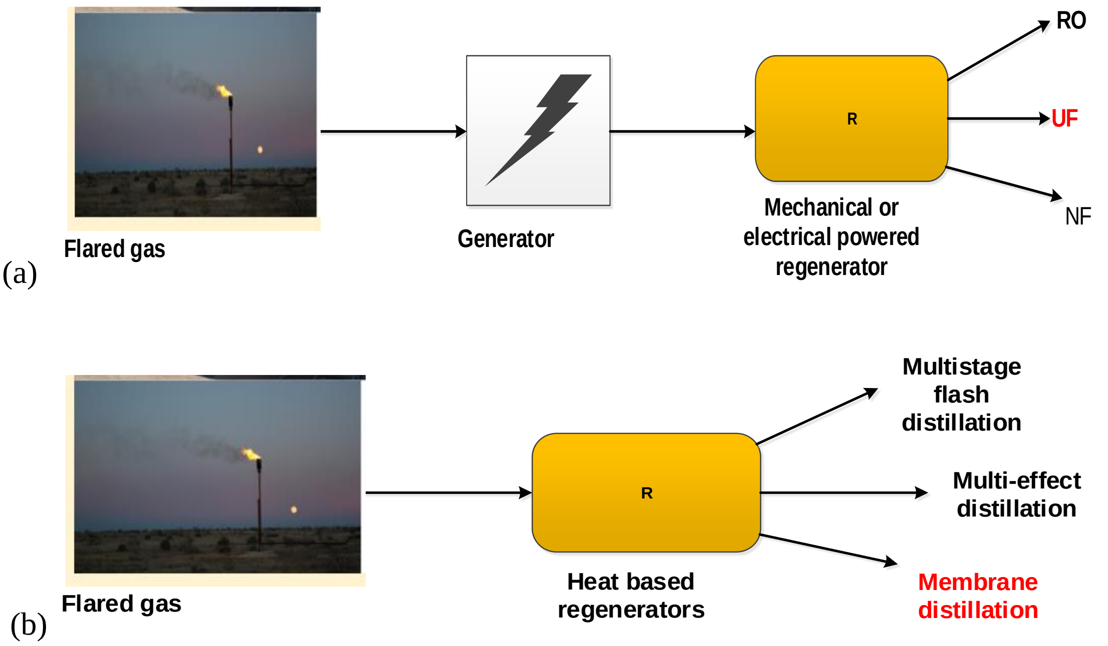

Figure 1.6. (a) Flare gas as source of energy in electrical and mechanical based regenerator (b) Flare gas as source of energy for heat-based regenerator.

Studies available in literature for the utilization of the co-produced gas that is flared after well completion is either focused on the onsite atmospheric water harvesting (Wikramanayake and Bahadur, 2016) using the captured gas or using it as a source of heat (Glazer et al., 2014), for heat-based regenerators. However, it needs to be mentioned that the work by Glazer et al. (2014) is done based on analytical framework and not in the context of mathematical optimization.

The production of shale gas resources also depend extensively on production costs in addition to different environmental impacts associated with the development of shale gas plays as depicted in Figure 1.7. The shale gas production system is a complex multistage network and variety of decisions must be made in each stage of this system. One way of classifying the quality of shale gas depends on the natural gas liquid (NGLs) contents, which lead to the terminology of dry gas and wet gas as shown in Figure 1.8. Dry gas is almost pure methane with trace NGLs, thereby may not require further processing. While the dominant component in wet gas is also methane, the amount of NGLs is significant enough to require further processing. Hence, accurate size and capacities of the processing plants as well as the distribution lines are critical in the optimization problem for overall economic performance. In addition, focus has always been on wet gas without considering the impact of dry gas on the capacities of the infrastructure development. Therefore, discerning the optimal design and operations of the shale gas supply chain has great economic potential.

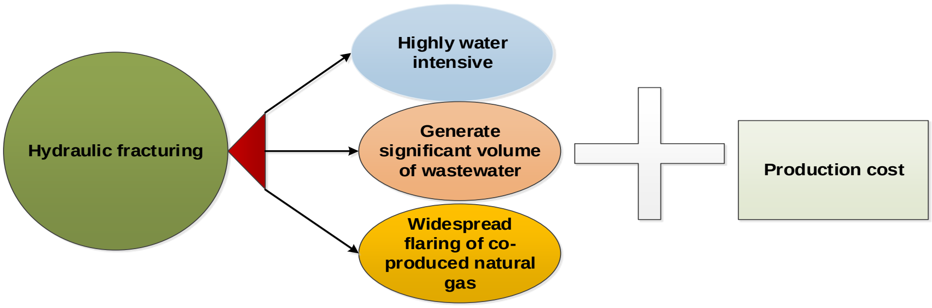

Figure 1.7. Additional challenges with shale gas development

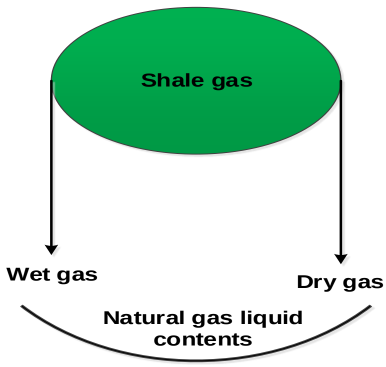

Figure 1.8. Classification of shale gas

This work addresses the drawbacks by developing a systematic approach for water, shale gas and membrane network with a background process of hydraulic fracturing as summarized in

Figure 1.9. To the best of the author's knowledge, there is no existing work in literature that consider water and energy minimization simultaneously in shale gas development using detailed ultrafiltration and membrane distillation technologies with a background process. It aims to determine the hydraulic fracturing performance by simultaneously optimizing the fracturing schedule and reducing the usage of freshwater. Reduction in freshwater consumption is achieved by exploring regeneration reuse within the process. Flowback water regeneration is achieved by purification using ultrafiltration and membrane distillation, which consequently gives a more accurate cost evaluation of the water network, and the energy consumption of the regenerators is optimized. The regenerator is modelled to operate semi-continuously and this requires the use of storage tanks to ensure a smooth connection between the regenerator and fracturing tasks.

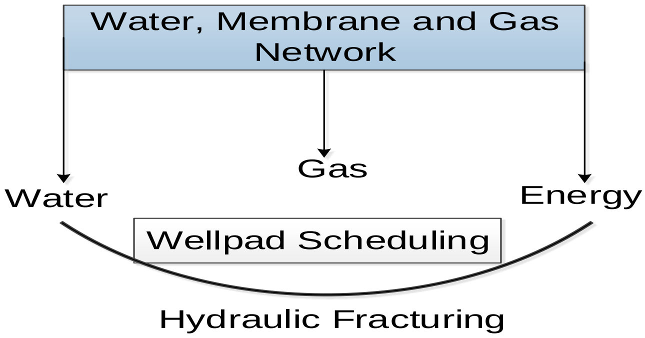

Figure 1.9. Summary of motivation

1.3. Research objectives

The objectives of the research can be summarized as follow:

- The objective is to synthesize an optimal integrated water, shale gas and membrane network and to determine the design of the ultrafiltration and membrane distillation subnetworks that corresponds with the optimal network. The optimal configuration is one that minimizes freshwater use and regeneration energy.
- To develop a mathematical model for hydraulic fracturing scheduling based on continuous time formulation.
- To investigate the feasibility of using co-produced gas that would otherwise be flared as energy source for ultrafiltration and membrane distillation.
- To investigate the effect of optimizing water, energy and shale gas production simultaneously on the overall process.

- To explore the practical application of using ultrafiltration membrane technology as a pre-treatment for membrane distillation.
- To investigate the application of the proposed model in a typical shale gas site using literature case studies.

1.4 Thesis lay out

This thesis consists of seven chapters including this chapter (Chapter 1) that provides the background, motivation for the research, and the overall objective of this study. The layout is schematically represented in Figure 1.10.

Chapter 2 is the literature review, which includes the general overview on water scarcity around the globe and the general knowledge on process integration and optimization, general overview on shale revolution and the process of hydraulic fracturing, water management in hydraulic fracturing, different technology available for flowback water treatment, overview of membrane technology and overview of existing studies on water management in shale exploration.

The developed mathematical formulation to achieve the objectives stated above are presented in chapter 3, 4, 5 and 6.

Chapter 7 concludes the thesis with a summary of the findings and recommendations. References to all articles used in the study are provided at the end of each chapter.

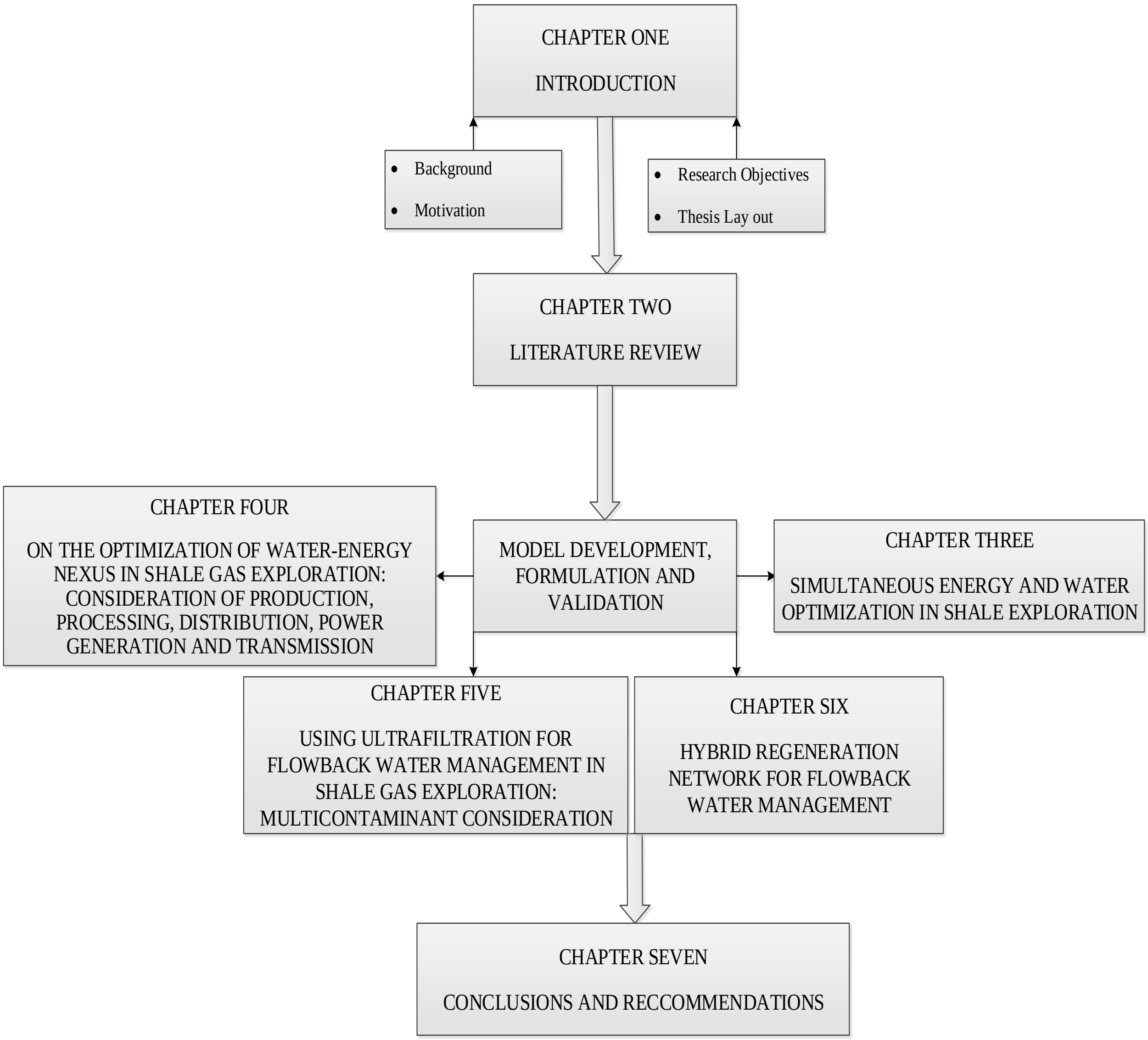

Figure 1.10. Thesis Layout

References

Al-Douri, A., Sengupta, D., El-Halwagi, M.M., 2017. A review of downstream processing of chemical and fuels, Journal of Natural Gas Engineering, Volume 45,pp. 436-455.

Arthur, J.D., Bohm, B., Layne, M., 2008. Hydraulic fracturing considerations for natural gas wells of the Marcellus Shale. The Ground Water Protection Council 2008 Annual Forum, Cincinnati, OH, September 21–24, 1-16.

Dahm, K., Chapman, M., 2014. Produced water treatment primer: Case studies of treatment applications. Science and Technology Research Report, 1-70.

Elsayed, N.A., Barrufet, M.A., Eljack, F.T., El-Halwagi, M.M., 2015. Optimal design of thermal membrane distillation systems for the treatment of shale gas flowback water. International Journal of Membrane Science and Technology 2, 1-9.

Elsayed, N.A., Barrufet, M.A., El-Halwagi, M.M., 2013. Integration of thermal membrane distillation networks with processing facilities. Journal of Industrial and Engineering Chemistry Research 53, 5284-5298.

Environmental report management (ERM), 2014. Recovered water management study in shale wells. ERM project 0243719 final report, 1-61.

Gay, M.O., Fletcher, S., Meyer, N., Gross, S., 2012. Water Management in Shale Gas Plays. Technical Report. HIS Water White Paper, 1-10.

Glazer, Y.R., Kjellsson, J.B., Sanders, K.T., Webber, M.E., 2014. Potential for using energy from flared gas for on-site hydraulic fracturing wastewater treatment in Texas. Environmental Science and Technology Letter 1, 300-304.

Gregory, K.B., Vidic, R.D., Dzombak, D.A., 2011. Water management challenges associated with the production of shale gas by hydraulic fracturing. Elements 7(3), 181-186.

Hasaneen, R., El-Halwagi, M.M., 2017. Integrated process and microeconomic analyses to enable effective environmental policy for shale gas in the United States, Journal of Clean Technologies and Environmental Policy, 19, 1775-1789.

Kamrava, S., Gabriel, K.J., El-Halwagi, M.M., Eljack, F.T., 2015. Managing abnormal operation through process integration and cogeneration systems. Journal of Clean Technology and Environmental Policy 17, 119-128.

Kazi, M.K., Eljack, F., Elsayed, N.A., El-Halwagi, M.M., 2016. Integration of energy and wastewater treatment alternatives with process facilities to manage industrial flares during normal and abnormal operations: A multi-objective extendible optimization framework. Journal of Industrial and Engineering Chemistry Research 55, 2020–2034.

Petrakis, S., 2008. Reduce cooling water consumption: New closed loop cooling method improves process cooling tower operations. Journal of Hydrocarbon Processing, 95-98.

US Energy Information Administration (EIA), Natural gas in the United States. accessed 27 June, 2018. https://www.revolvy.com/page/Natural-gas-in-the-United-States

Shaffer, D. L., Chavez, L. H. A., Ben-Sasson, M., Castrillon S. R., Yip, N. Y., Elimelech, M., 2013. Desalination and reuse of high-salinity shale gas produced water: drivers, technologies, and future directions. Environmental Science andTechnology 47, 9569–9583.

Wikramanayake, E., Bahadur, V., 2016. Flared natural gas-based onsite atmospheric water harvesting (AWH) for oilfield operations. Environment Research Letters 11, 1748-9326.

Yang, L., Salcedo-Diaz, R., Grossmann, I.E., 2014b. Water network optimization with wastewater regeneration models. Journal of Industrial and Engineering Chemistry Research 53, 17680–17695.

Yang, L., Grossmann, I.E., Manno, J., 2014a. Optimization models for shale gas water management. Journal of American Institute of Chemical Engineers, 60, 3490-3501.

Zhang, C., El-Halwagi, M.M., 2017. Estimate the capital cost of shale-gas monetization projects. Chemical Engineering Progress 113,28-32.

CHAPTER TWO

LITERATURE REVIEW

2.1. Water: A finite but sustainable resource

The most common substance on earth is water; it covers virtually three quarters of the earth's surface. Water is distributed to different areas of the planets by the rain cycle powered by the energy of the sun. In order to prevent the rise in economic development and environmental degeneration, water management has to be carried out according to the principle of sustainable development, as water is a very crucial resource for both social and economic growth. Two major factors have contributed to the global scarcity of water as represented in Figure 2.1. These are hydrological variability and high human use. The continual rise in the degree of industrialization and urbanization, rising standard of living, growth in population and activities related to agriculture are greatly influencing the quality and utilization of available water sources. The extensive utilization of this finite resource by the contemporary society signifies urgency for a shift in water treatment presently and in time to come (Holtzhausen, 2002).

According to the report by the organization for economic co-operation and development, OECD (2012a), increased in strains on freshwater availability is projected through 2050. This is because of the fact that water stress regions like North and South Africa as well as South and Central Asia have been projected to experience an increase in population growth of about 2.3 billion people (OECD, 2012a, WWAP, 2016). Another report by 2030 WRG (2009) has predicted global water deficit of 40 % by 2040. FAO (2016) states that 70 % of the global freshwater withdrawal is used in Agricultural activities and this is projected to increase by 20 % by 2050 if necessary measures are not taken. The percentage used by the industry is capped at about 19 % of the global freshwater withdrawal with 15 % for energy and electricity generation and 4 % for manufacturing and other large industries (FAO, 2014f, IEA, 2012b). The remaining 11 % is for domestic and municipal use (WWAP, 2012, FAO, 2016) as depicted in Figure 2.2. In addition, the current report shows that 40 % of the world population is now living in water stressed area and by 2025, this is projected to increase to 50-65 % and half of the world population will be affected by 2050 (FWW, 2018). The predicted water that will be available per person in 2025 is depicted in Figure 2.3. Hence, relevant management tactics need to be enforced to optimize how the water sources are utilized (Mack, 2005, Oke, 2014).

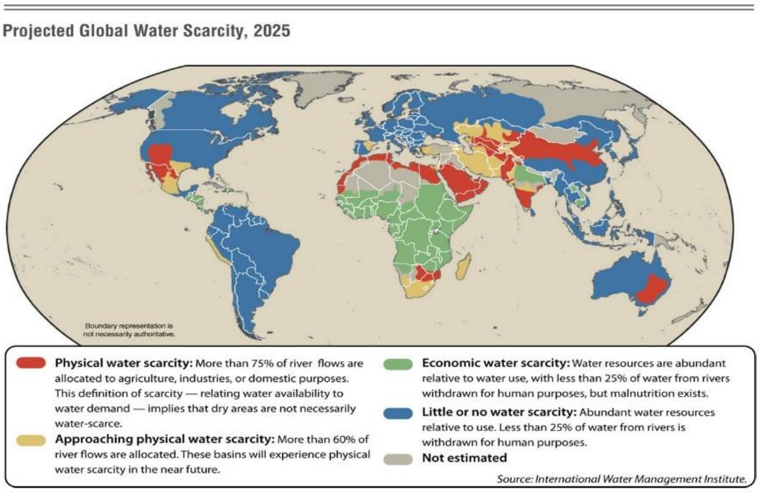

Figure 2.1. Projected water scarcity in 2025 (Council, 2008)

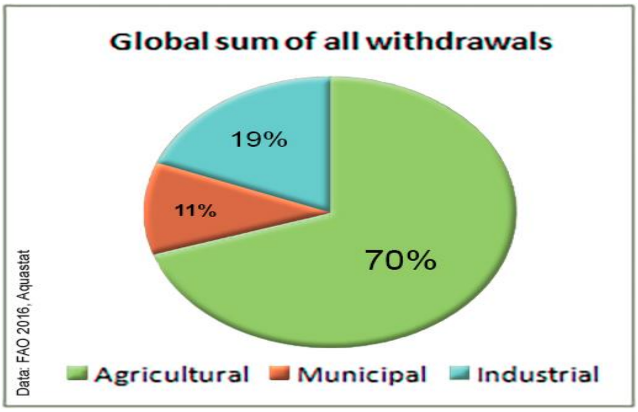

Figure 2.2. Global freshwater withdrawal based on sector (FAO, 2016)

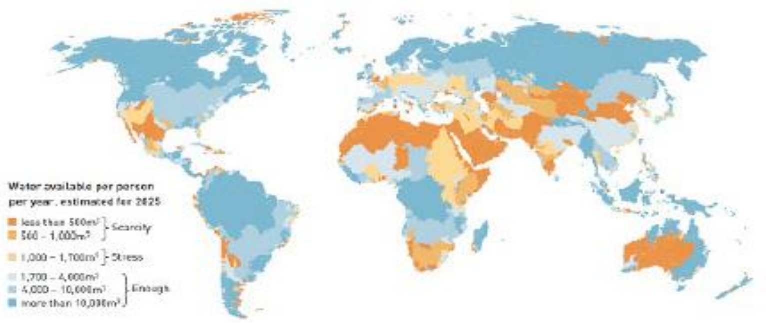

Figure 2.3. Predicted water availability per person in 2025 (FWW, 2018)

Three fundamental strategies have been outlined by the South Africa national legislation under the National Water Acts (1998) to protect water resources. These are:

- Conservation of all important water resources.

- Resource sustainability, i.e. overall resource usage that ensures no lasting degeneration in term of any quantifiable measures (e.g. quality and quantity) (Wright and Xu, 2000).
- Managing water resource of all water user groups in an integrated manner.

Based on the third principle, industries are encouraged to reassess their water management approaches and intensify water reuse and recycling.

2.2. Water in industry

Water is the most commonly used raw material in process industries, as well as an abundant component of chemical, petrochemical, petroleum refining, mining and mineral extraction, food and drink, pulp and paper and many other industries (Mack, 2005). Because of current and projected future water scarcity around the globe, awareness and motivation amongst the larger consumers for optimization of water utilization is growing. The growth is as a result of strong economic motivations like increase in cost of wastewater treatment, higher environmental standards and the increasing shortage and cost of good quality water sources (Alva-Algảez et al., 1998).

There are three rudimentary means to achieve water use minimization (Wang and Smith, 1994, Alva-Argảez et al., 1998, Zhelev and Bhaw, 2000):

- Decrease in fresh water usage by initiating changes in the process.
- Reuse of process water in areas where high quality water is not key and lower quality water will not adversely affect the process into which it is being added.
- Lowering costs of water treatment by employing low-cost treatments and reusing the treated water.

The third option can be divided into regeneration reuse and regeneration recycling. The first involves partial recycling to remove contaminants that may affect the process into which the water is being added. The regeneration recycling requires that the treatment remove any contaminants that may build up, as the treated water will pass through the same process from which it was taken.

Industries around the globe are been pressurized internationally to lower their fresh water consumption and effluent generation. In order to achieve this, many industries have been attracted to a technique called water pinch analysis as a ‘ cleaner production’ technique. The purpose of this technique is to reduce freshwater usage and wastewater generation by evaluating the existing or future industrial complexes and identifying areas where changes such as those previously stated can be applied (Gianadda et al., 2002, Zhelev and Bhaw, 2000).

2.3. Process integration and optimisation

Process integration is a comprehensive strategy to process design, which highlights the process unanimity and examines the synergies amongst various unit operations from the beginning, instead of optimizing them independently. It can also be referred to as unified process design or process synthesis (El-Halwagi, 1997 and 2006). In the chemical engineering setting, process integration can be described as an integrated method to process design and optimization, in which the synergies amongst various unit operations are used to promote effective resources utilization and cost minimization (El-Halwagi, 1997 and 2006). The major benefit of process integration lies in the consideration of a system as a whole (i.e. unified or comprehensive approach) to enhance their design and/or operation. In addition, this approach is generally used in combination with simulation and mathematical optimization tools for identification of better ways in which systems (new or existing) can be integrated, thereby reducing capital and/or operating costs. Process integration approaches are usually used at the start of a project (e.g. a new plant or the enhancement of those already in existence) for screening out likely alternatives, for optimizing the design and/or operation of a process plant. This approach has offered enabling tools for the design of sustainable water network in process industries.

2.4. Water minimization in process industries

The increase in water demand in the process industry may lead to vulnerability of the industry to water scarcity around the globe in combination with the drive to achieve sustainable development. The optimal water network synthesis has been a major issue in process system design and its allied industries (Khor et al., 2011). Process integration has offered enabling tools for the design of sustainable water network like water recycle, reuse, regeneration-recycle and regeneration-reuse, thereby reducing fresh water usage and wastewater generation. Water network optimization has evolved into an important tool of sustainability, as it helps in realising both economic and environmental advantages associated with the use of the above-mentioned supporting tools (Mafukidze and Majozi, 2016). Water using operations in process industries can be classified as either fixed load or fixed flow operations. In fixed load operations, water is used as only mass separating agent to eliminate a fixed amount of pollutants partially from the stream rich in contaminant (Wang and Smith, 1994; Polley and Polley, 2000; Prakash and Shenoy, 2005). In this kind of problem, each water using operation is characterised with fixed load of contaminant by specifying the allowable maximum inlet and outlet concentration. These types of operations are generally categorised as quality controlled and are modelled as mass transfer units (Souifi et al., 2018). Fixed flow operations on the other hand are classified as quantity controlled, as mass transfer is not required. Analysis using this approach is based on the segregation of the water using processes into sink (consumed fixed amount of water) and source (produced fixed amount of water). Generally, two main methods are used to address the problem of water network synthesis, viz. insights-based techniques and mathematical optimization-based techniques. These two techniques are applicable to both continuous and batch processes.

2.4.1. Insights-based technique

Insight-based technique usually involves water pinch analysis algorithms, which were developed for heat and mass integration originally. This technique offers low computational burden in solutions generation, nevertheless, significant problem simplifications is often required. Pinch-targeting methods can be mostly classified into two classes: graphical methods using composite curves and numerical methods. Although graphical methods provide physical insight and intuitive (Wang and Smith, 1994, 1995), they are however tedious and not accurate solution for complex problem (Souifi et al., 2018). On the other hand, numerical methods rely on algebraic accuracy and are therefore amendable for computer programming. The insight-based technique involves two-step approach namely targeting and design for water network synthesis that features flows of freshwater and wastewater that are minimum (Gouws et al., 2010). The targeting approach involves the minimum freshwater and wastewater flowrate setting based on restriction of concentration and flowrate. Based on the restriction data, water pinch analysis is able to simultaneously locate the minimum flowrate target for fresh water and wastewater prior to designing the detailed network (Souifi et al., 2018). In order to achieve the target been set, a network design is then carried out (Foo et al., 2006). The most common targeting graphical technique on water pinch analysis is the limiting composite curve proposed by Wang and Smith (1994). It involved developing a water pinch analysis to identify targets for minimum fresh water that can be used and wastewater that can be discarded. Determination of a limiting water profile for each unit based on the allowable contaminant concentration and mass load of contaminant was done as the first step. The second step entails plotting the limiting composite curve for all water using operations by adding the contaminant load within each concentration interval as shown in Figure 2.4. A water supply line is then drawn from the origin and counter-clockwisely rotated until the line touches the limiting composite curve to achieve a pinch point. This is carried out to target the minimum flow rate of fresh water to the entire water system.

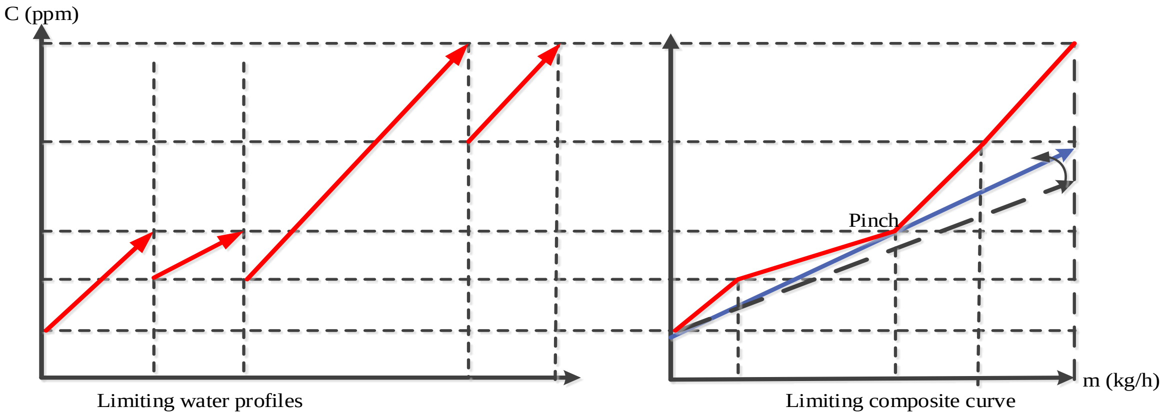

Figure 2.4. Construction of limiting water profiles and limiting composite curve

Various insight-based techniques have been proposed for both fixed load and fixed flow problems for targeting for water reuse and recycle in continuous as well as batch processes. Among the first proposed graphical technique for water network synthesis in continuous processes is the limiting composite curve proposed by Wang and Smith, (1994) developed for fixed load problems. The water-source and water-sink composites of Dhole et al. (1996) and the concept of evolutionary table proposed by Sorin and Bedard, (2001) were the first targeting techniques developed for fixed flowrate problem. Hallale (2002) introduced the method of water surplus diagram, which serves as a promising tool in finding the true minimum water flow rates in the fixed flow rate problems. The material recovery pinch diagram method, which helped in overcoming the iterative steps of the water surplus diagram was proposed by El-Halwagi et al. (2003) and Prakash and Shenoy (2005). Manan et al. (2004) proposed the water cascade analysis (WCA) method and Foo et al. (2006) improved upon the method. Almutlaq et al. (2005) developed another pinch method, which is also tabular in nature known as algebraic targeting approach. Bandyopadhyay et al. (2006) proposed a technique that combines algebraic and graphical methods called the source composite method. Detail of each of these methods can be found in a review paper by Foo et al. (2009).

The first technique for wastewater minimisation in batch processes was proposed by Wang and Smith (1995) in which the pinch technique of Wang and Smith (1994) was modified to consider time as primary constraint and concentration as secondary constraint. The specific problem is divided into concentration intervals and time subinterval and the existing processes are grouped in each concentration interval thereby allow the reuse of effluents from one concentration interval to the subsequent interval. In the interval where no effluent was available for reuse, freshwater was used to meet the requirement. However, the method can only be applied to fixed load problems and to processes operating in a semi continuous mode. This may not be applicable for strictly batch processes as it allowed occurrence of water reuse between processes with overlapping time interval.

Majozi et al. (2006) developed another graphical targeting technique for fixed load problems by modifying the method of Wang and smith (1995) to cater for strictly batch operations. Two approaches were proposed for carrying out the targeting steps. The first approach is similar to that of Wang and Smith (1995) in which time is taken as primary constraint and concentration as secondary constraint. The second approach involves treating concentration as primary constraint and time as secondary constraint. For each time interval, concentration vs water demand diagram is drawn and any surplus water was transferred to higher concentration subinterval for reuse in the same time interval or stored for later use if it meets the requirement of the water using operations in terms of concentration.

The algebraic targeting and network design technique proposed by Foo et al. (2005) was the first approach used for fixed flow problem. Two-stage approach for targeting and design for batch water network was proposed based on the water cascade analysis of Manan et al. (2004) developed for continuous processes. The two-stage approach involves identification of minimum water flow by targeting using a time-dependent water cascade analysis and the rules stipulated by Hallale, (2002) was used in performing network synthesis for each time interval. Information from the sub-networks of each interval was then used to develop the time-water network that serves as the overall network. Although, the study also allows consideration for storage tank, inability to allow water sources of different concentration to mix will result in large number of storage tanks in scenarios where significant number of sources require storage.

Liu et al. (2007a, b) proposed an algebraic targeting technique capable of handling both fixed load and fixed flow problems. The technique is referred to as the time-dependent concentration interval analysis (CIA) which involves segregating water sinks and sources in their respective time intervals before carrying out the targeting step using the concentration interval table (CIT). The first step in using the CIT procedure is to arrange the contaminants concentration in descending order and within the respective interval, water flow is then located. In each concentration interval, the impurity load is determined by multiplying water flow with the concentration difference across the interval. The cascading of the impurity load is then carried out all through the concentration intervals after which the minimum freshwater flow is estimated by dividing the cumulative mass load by the equivalent concentration level. The process is then repeated for all time interval to calculate the total minimum freshwater flow.

Other significant research contributions using insight-based approach include the network design technique using a quantity-time diagram of Chen and Lee (2008) and the algebraic technique proposed by Charturvedi and Bandyopadhyay (2012). However, the major assumption associated with all insight-based technique is that the water using processes operating procedure is known beforehand and these techniques therefore can only be applied if the operating schedule is given. This limitation does not allow for optimization of the production schedule as this can allow for possibility for higher water recovery compare to fixed schedule. In addition, insight-based techniques cannot be applied to problems with multiple contaminants and are therefore restricted to problems with single contaminant.

2.4.2. Mathematical optimization-based technique

Mathematical optimization-based technique in contrast, permits water network synthesis problems to be treated in their full complexity by taking into consideration different topological constraints, multiple contaminants and representative cost functions. However, this method is associated with high computational time necessary to attain optimality particularly in large-scale problems. (Khor et al., 2012). The optimization-based method mostly involves a superstructure network construction, which serves as depiction of design substitutes for the process under investigation. The use of superstructure permits process to be characterized individually by common set of constraint wherein the optimization can take place (Gouws et al., 2010). Another important feature associated with mathematical based model is the objective function, which vary depending on how the problem is addressed and the nature of the mathematical model.

The first research work that addressed the water network synthesis using superstructure-based optimization in continuous processes is the work of Takama et al. (1980) in which a non-linear model was proposed. The non-linear model incorporates water using processes and regeneration units for a multicontaminant system. The work of Takama et al. (1980) was later extended by Rossiter and Nath (1995). Research on water network synthesis in this area has however increased over the time (Gunaratnam et al., 2005, Bringas et al., 2007, Tan et al., 2007b, San Roman et al., 2007, Karuppiah and Grossmann, 2006, Karuppiah and Grossmann, 2008, Tan et al., 2009, Ahmetovic and Grossmann, 2010, Faria and Bagajewicz, 2010a, Poplewski et al., 2010, Mafukidze and Majozi, 2016, Abass and Majozi, 2016, Buabeng-baidoo and Majozi, 2016). Optimization-based techniques with incorporation of mass integration strategies (El-Halwagi et al., 1996, Gabriel & El-Halwagi, 2005) and property-integration framework (Napoles-Rivera et al., 2010, Ng et al., 2010, Ponce-Ortega et al., 2009, Ponce-Ortega et al., 2010) have also been developed for reuse/recycle and regeneration networks.

In batch processes, mathematical based techniques for water minimization involve model formulations, which comprise of various constraints to capture the water and contaminant balances across the water using processes, process operation, capacity and time dimension. This can be categorized into two classes depending on how time dimension is treated. The first class is the group that treats time dimension as a parameter in which water is minimized within a given schedule. This category of problem is assumed to be much simpler to solve compare to when the schedule is to be determined as part of the solution algorithm (Gouws et al., 2010). Among those approaches in this category are the ones proposed by Almató et al. (1997), Almató et al. (1999), Kim and Smith (2004), Majozi (2005a), Li and Chang (2006), Shoaib et al. (2008), Rabie and El-Halwagi (2008), Ng et al. (2008), Chen et al. (2008), Chen et al. (2009), Chen et al. (2010), Lee et al. (2010), and Lee et al. (2014).

The other group of mathematical based optimization technique in batch network treats time dimension as a variable thereby water minimization and schedule that give the minimum water target are determined simultaneously. The main advantage of this approach is that the determination of global minimum water flow and/or cost can be achieved for a variety of operational requirements (Gouws et al., 2010). Among various approaches in this category are those developed by Majozi (2005b), Majozi (2006), Cheng and Chang (2007), Gouws and Majozi (2008), Majozi and Gouws (2009), Adekola and Majozi (2011), Chaturvedi and Bandyopadhyay (2014a), and Adekola and Majozi (2017).

It should be noted that, despite the limitations of insight-based techniques, the approach has offered a simpler depiction of the problem, which helps in building efficient mathematical programming models. Recent works (Oliver et al., 2008, Foo, 2010, Chaturvedi et al., 2016) are proving that combining the two approaches in a synergistic manner, that is, using conceptual insights to aid better models formulation for mathematical programming, is now appearing to be the best efficient alternative. Graphical insights are of importance in practice because they allow the engineer to incorporate many factors that mathematical programming does not consider. Thus, the field has advanced from a paradigm where a graphical insight was used to achieve a design to another where a mathematical is used (Bagajewicz, 2000). Graphical techniques give a clear understanding of a process through visualization, algebraic techniques provide an effective computational framework and mathematical programming allows complex problems to be handled in an effective way. However, selecting an appropriate approach depends on the users based on the specific needs and nature of the problem (Klemeš, 2013).

In accordance with abovementioned trend, this work will focus on the superstructure optimization approach for water network synthesis in shale exploration.

2.5. Shale oil and gas exploration

Shale gas is defined as natural gas that is found trapped within shale formations. The source, reservoir and seal for the natural gas is the shale. Shale gas has been the major source of natural gas supplies in the United from the beginning of this century and this is spreading to other shale gas reserves around the world. One of the unconventional sources of natural gas is Shale gas; others include coalbed methane, tight sandstones, and methane hydrates as illustrated in Figure 2.5. Due to low matrix permeability of shale formation, specific well design approach, which involve a combination of horizontal drilling and fracture stimulation, is required for large-scale development (Al-Douri et al., 2017).

Oil and natural gas locked in the tight impermeable formations have been considered in the past as uneconomical resources to produce. However, this perspective has changed due to technologically advancement in directional drilling and reservoir stimulation as the global energy markets have witnessed dramatic change due to the exploration of these unconventional formations as depicted in Figure 2.6 (Michael and Tiemann, 2015). The enormous development of shale oil and gas production started in important areas such as West Texas and North Dakota, changing the USA crude oil and natural gas markets in an intense and lasting way. Low natural gas price, which is due to production of shale gas, has given rise to a swift reformation of the energy generation industry as coal utilization decrease and power plants turn to natural gas. US has been described by the independent energy statistical agency as “the uncontested global oil and gas leader over the next numerous decades.” Figure 2.7 shows the statistics of oil and gas production in the USA compared to Russia and Saudi Arabia.

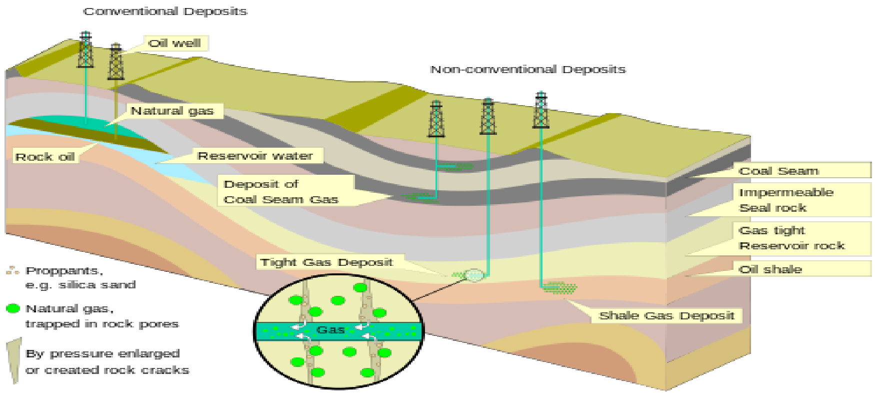

Figure 2.5. An illustration of shale gas compared to other types of gas deposits. (EIA, 2014, Michael and Tiemann, 2015)

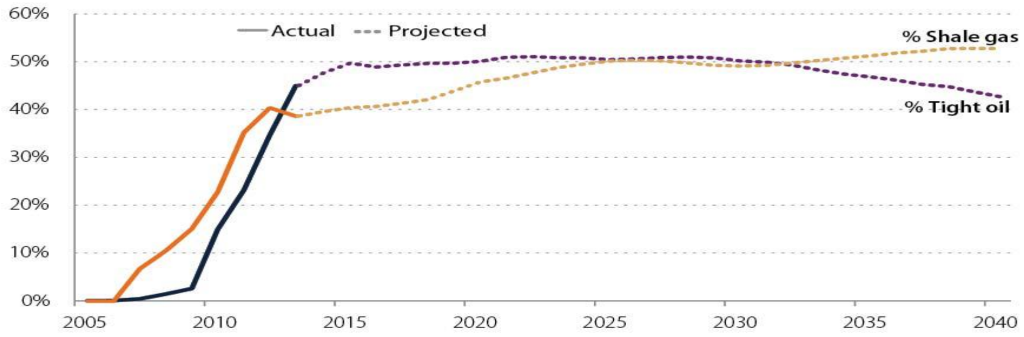

Figure 2.6. Percentage of oil and natural gas from shale oil and gas (EIA, 2014, Michael and Tiemann, 2015)

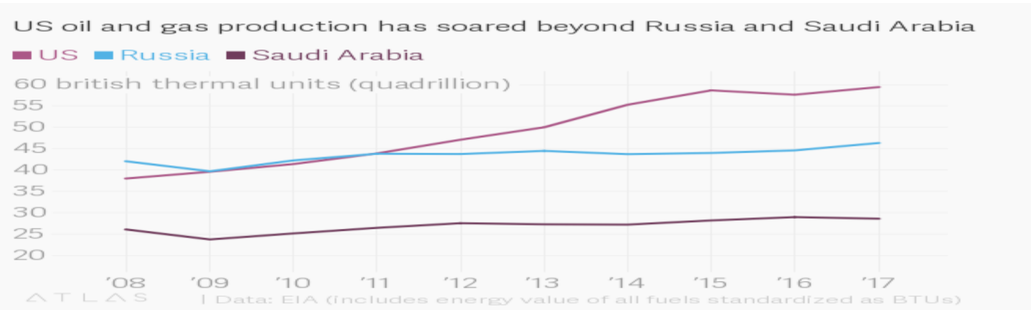

Figure 2.7. USA oil and gas production compared to other countries of the world (www.theatlas.com)

2.5.1 Shale reservoir in the world

The discovery of abundant unconventional shale resources across the globe recently has resulted in increased potential supply of oil and natural gas. Tables 2.1 and 2.2 show the lists of countries with highest technically recoverable shale oil and gas resources. While countries such as USA have succeeded in efficient exploration of the available resources, others such as China and Canada are still in the initialization mode. This data indicates global shale gas production by selected country in 2015, with estimated statistics for 2040. In 2015, shale gas production in the US is estimated to be approximately 37 billion cubic feet per day, making it the biggest shale gas producer across the globe. This is expected to increase to 80 billion cubic feet per day in 2040. The development of shale gas in other parts of the world has remained tentative. Countries such as Canada, Argentina, Poland, and China have commenced exploration while countries like France and Bulgaria have chosen to ban the development or wait (Rahm and Riha 2014). Presently, US, Canada, China, and Argentina are the only countries producing shale gas in commercial scale. Commercial production is anticipated to commence in Mexico and Algeria by 2030 and 2020, respectively. By 2040, 70 percent of shale gas production worldwide is expected to come from these countries.

Table 2.1. Estimated technically recoverable shale gas resources (EIA, 2015)

Country	Technically Recoverable Shale gas (Tcf)
China	1115
Argentina	802
Algeria	707
USA	665
Canada	573
Mexico	545
Australia	437
South Africa	390
Russia	285
Brazil	245

Table 2.2. Estimated technically recoverable shale oil resources (EIA, 2015)

Country	Technically Recoverable Shale Oil (Billions of Barrels)
Russia	75
USA	58
China	32
Argentina	27
Libya	26
Australia	18
Venezuela	13
Mexico	13
Pakistan	9
Canada	9

The shale gas reservoirs location evaluated by the United States Energy Information Agency (EIA, 2015) are shown in Figures 2.8 and 2.9. The EIA's assessment indicates technically recoverable gas resources from shales in the amount of 7,576 trillion cubic feet (TCF) in more than 40 countries assessed. This figure has increased from the time when the survey was first conducted in 2011, which estimated 6,622 TCF of the resource. The global leader in terms of shale gas reserves is China, with over 1,115 TCF. The fourth country behind China, Argentina, and Algeria is U.S. based on the assessment (EIA, 2015).

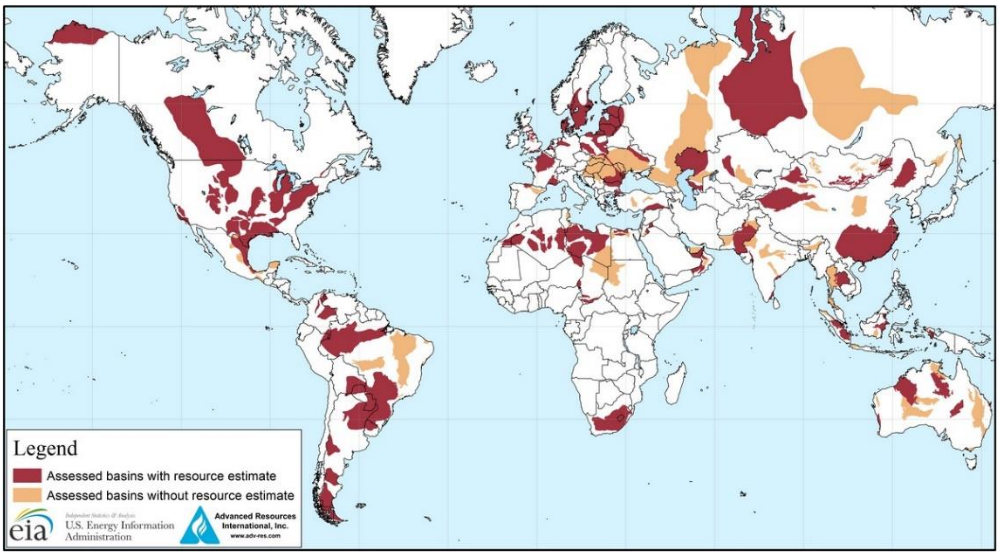

Figure 2.8. Shale reserves around the world (EIA, 2015)

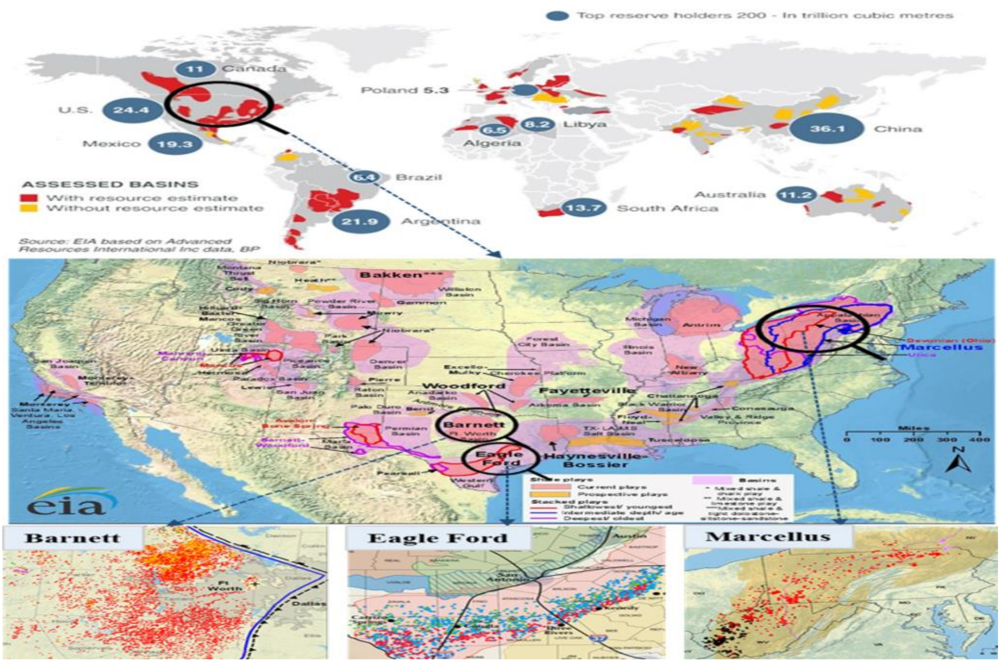

Figure 2.9. Overview of shale resources around the world (EIA, 2015, Gao and You, 2017)

2.5.2. Shale reserves in the USA

Overview of the shale gas play distribution for the lower 48 states in the US is given in Figure 2.10. The biggest gas producing play currently is the Marcellus Shale underlying portions of the states of Pennsylvania (PA), Ohio (OH), West Virginia (WV), and New York (NY) (Rahm and Riha 2014). Additional main gas plays in the US presently comprise the Haynesville, located in the states of Texas (TX) and Louisiana (LA), the Barnett in TX, and the Fayetteville in Arkansas (AR) as depicted in Table 2.3. There are five states responsible for about 65 % of the total United State dry gas production as shown in Table 2.4 and Figure 2.11 respectively (EIA, 2017) and Figure 2.12 provides an overview of dry gas production from different shale play from 2004 to 2018.

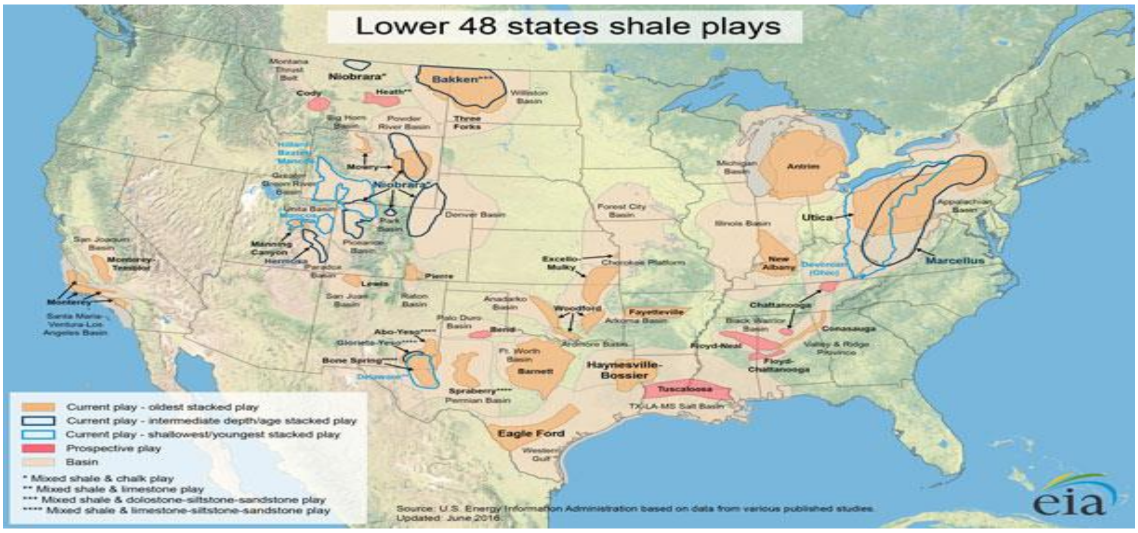

Figure 2.10. Shale play in the US (EIA, 2017)

Table 2.3. Key contributors to the US shale gas production from 2014- 2040 (Al-Douri et al., 2017)

Shale play	Percentage contribution (%)
Marcellus	32
Haynesville/Bossier	17
Eagle Ford	11
Barnett	8
Utica	6
Faytteville	6
Woodford	4

Table 2.4. Dry gas production states in the US (EIA, 2017)

State	Dry gas production (%)
Texas	24
Pennsylvania	20
Oklahoma	9
Louisiana	6
Wyoming	5

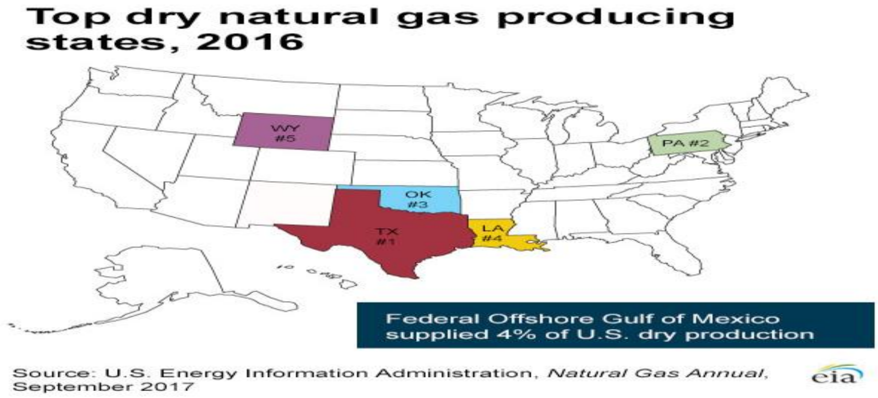

Figure 2.11. Dry natural gas producing states in the US (EIA, 2017)

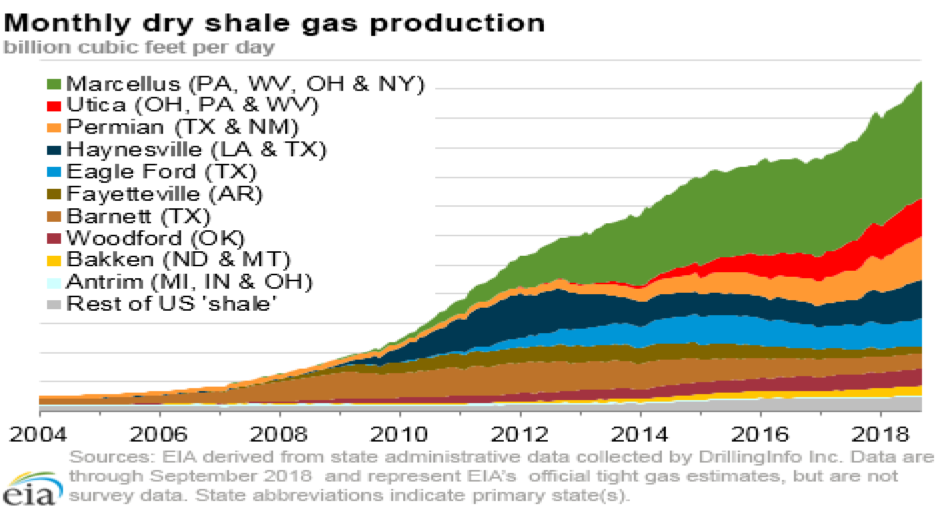

Figure 2.12. Dry gas production in the US (EIA, 2017)

2.6. Shale gas system

The shale gas production system consists of a complex structure among which are acquisition of water required for fracturing, production of shale gas, managing wastewater generated from fracturing, processing of the produced shale gas, natural gas transportation and the end use as shown in Figure 2.13. Various decision is required regarding each of this network structure in order to allow for optimal design and operations of the total network, hence maximizing the economic potential.

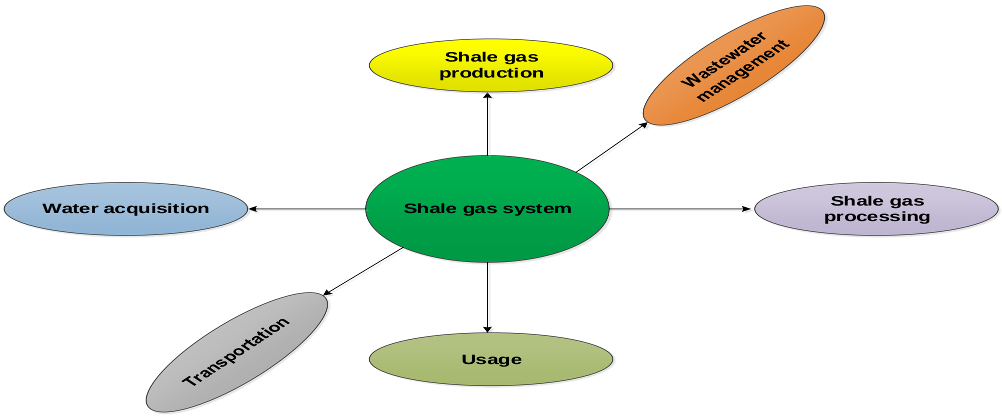

Figure 2.13. Overview of shale gas system

2.6.1. Wellpad development and production

Wellpads development and production involve series of stages that includes: site preparation, drilling, completion, and production as depicted in Figure 2.14.

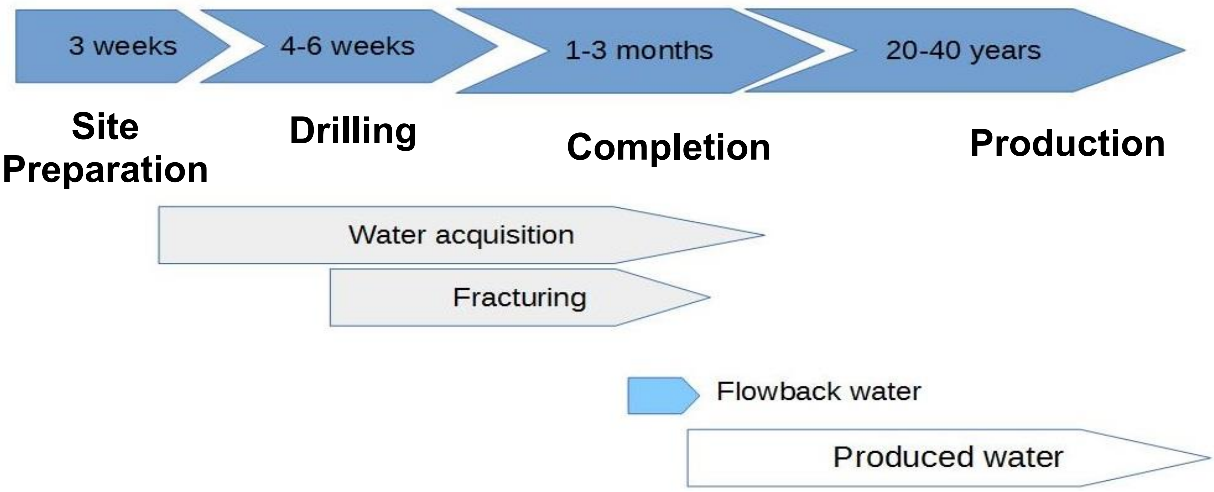

Figure 2.14. Wellpad development timeline (adapted from Yang et al., 2014a).

2.6.1.1. Site preparation

The first step involved the exploration of the potential shale wells through geologic assessment and obtaining the drilling permits. There are series of steps required for the shale site construction after the drilling permits have been obtained. These include: clearance of proposed site to accommodate equipment, road construction for access to the area, impoundments construction to handle the drilling and fracturing fluids produced in the course of the processes, installation of transportation infrastructure e.g. gathering pipelines, injection lines, water supply lines etc. and construction of storage facilities (Hefley et al., 2011, Gao and You 2017, Gao et al., 2017).

2.6.1.2. Drilling

There are two major drilling techniques used for the development and exploration of oil and natural gas formations namely vertical and horizontal drilling. Vertical drilling involves drilling a well straight down into the earth till the drill bit reaches the formation being developed while in horizontal drilling depending on seismic and other geological data, the well under development is drilled to a particular length and then turned horizontally to a set lateral length. The advancement in horizontal, or directional, drilling has played a major role in today's success with shale plays (Rodriguez and Soeder, 2015). The major advantage of horizontal drilling compared with vertical drilling is that it allows operators to drill multiple wells at a single shale site/pad thereby leading to more gas/oil production with fewer bores, improves shale gas production efficiency; reduce environmental footprint and less capital investment (Hughes 2013). A comparison of vertical and directional wells is shown in Figure 2.15. It is important to have a larger contact area between wellbore and target formation in shales as their low permeability necessitates large volumes of rock to be intersected in order to produce economic volumes of hydrocarbons (Rodriguez and Soeder, 2015). This process can go on for few months depending on the length, depth and the number of horizontal wells that require drilling (Speight, 2013).

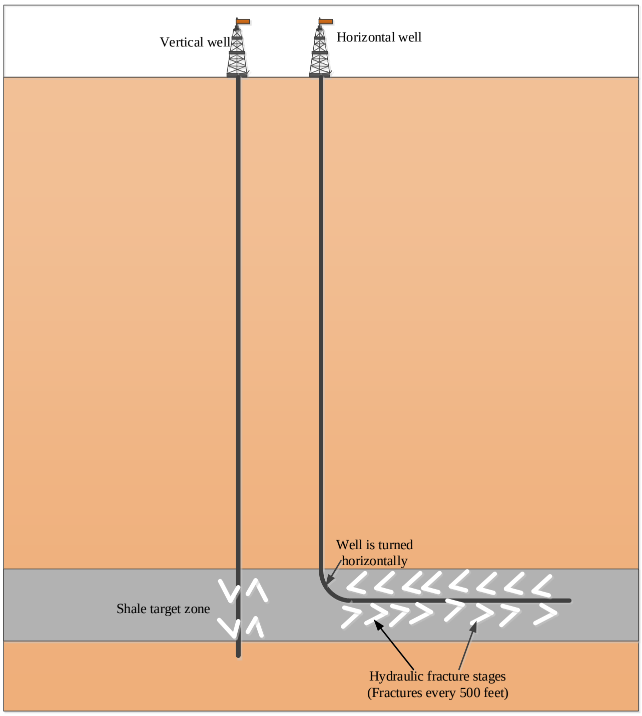

Figure 2.15. Comparison between vertical and horizontal drilling **(**Rodriguez and Soeder, 2015, Soeder and Kappel, 2009)

2.6.1.3. Completion

The well completion stage occurs after drilling phase has been completed and this phase refers to as the process by which a well is made ready for shale gas production (Gao and you, 2017). There are three different main stages required in this phase namely: perforation, hydraulic fracturing and production (Holditch, 2012, Brzycki, 2016). In the perforation stage, an electric current is sent to a perforating gun through a wire, which results in a charge that shoots hole through the casing into the shale. Hydraulic fracturing stage involves the injection of mixture of sand, water and chemical additives at a very high pressure to break the shale formation while production stage involves the construction of wellhead and pipeline gathering for natural gas production. During the period of drilling and/or hydraulic fracturing, a continuous supply of drilling/ fracturing fluid is essential.

2.6.1.4. Hydraulic fracturing

The method used in extracting gas from deep underground is referred to as Fracking, or hydraulic fracturing. The technique involves digging wells up to 4 km deep. The small size and lack of permeability of unconventional formations make them relatively resistance to hydrocarbon flow thereby require natural or artificial fracture for the trapped oil and gas to be released. The method uses a mixture of water, sand and chemicals, which is injected into each well under high-pressure (up to 70 Mpa). As depicted in Figures 2.16a and b, the fluid is injected down the wellbore through an isolated steel pipe to fracture the gas-holding subsurface rock formation in order to release the gas, which is then transported to the surface. The horizontal portion of the well is fractured, or stimulated, in a number of stages as shown in Figure 2.17. A fixed amount of water is required for each stage. The first stage to be stimulated is the one situated close to the end of the well, and then the stage is temporarily plugged to prevent flow back in order to allow for the fracturing of the next stage. This action is repeated along the full length of the horizontal portion of the well until the last stage is completed. Typically, each crew can frac at the rate of up to four stages per day (Yang et al., 2014a).

When all the stages have been fractured, the plugs are drilled out and the pressure is released out thereby leading to reverse flow of fluid in which water and excess sand flow up to the surface through the isolated steel pipe (ERM, 2014).

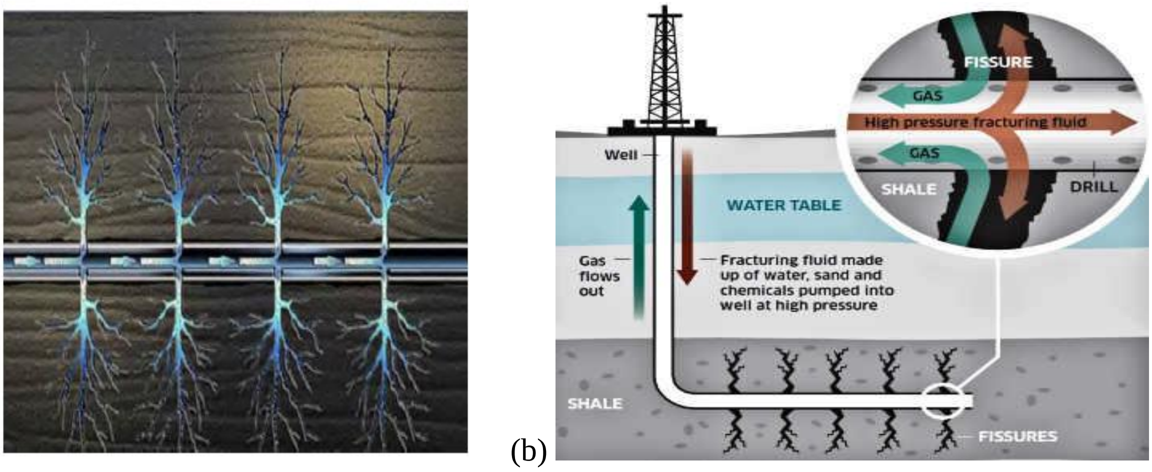

(a) (b)

Figure 2.16. Process of hydraulic fracturing (GWPC, 2018)

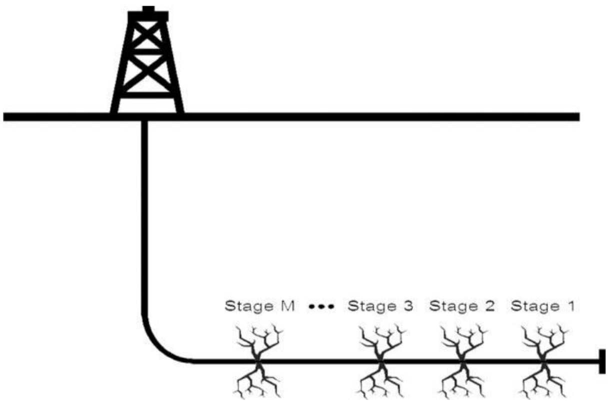

Figure 2.17. Horizontal well hydraulic fracturing stages (Yang et al., 2014a).

2.6.1.5. Composition of frac fluid

Analysis of the geological characteristics of the shale formation to be fractured is the determining factor for the final composition of the fluid to be used in hydraulic fracturing. There are three types of frac fluid design available for hydraulic fracturing and the composition of the frac fluid depends on the design appropriate for the shale play. These designs include slickwater, linear gel and cross-link gel. A typical hydraulic fracturing fluid consists of water, proppant (usually sand) and chemical additives as shown in Figure 2.18 with water taking about 90 % of the volume while sand and chemical additives take about 9.5 % and 0.5 % respectively. Proppant is used in hydraulic fracturing to keep the fractures open thereby allow free flow of oil and gas from the formation up the wellbore in conjunction with the portion of the injected fluid to be recovered (ERM, 2014).

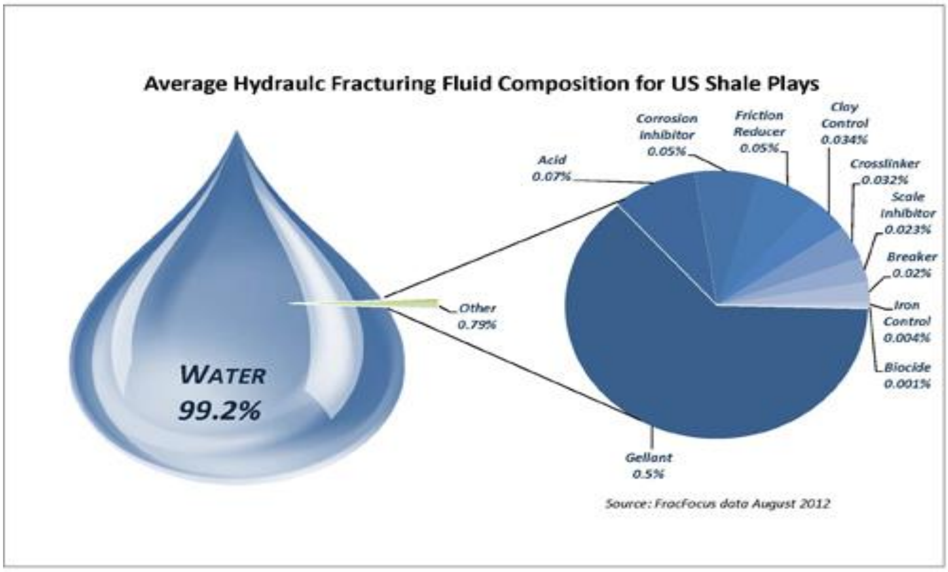

Figure 2.18. Frac fluid composition (Veil, 2014, GWPC, 2018).

The types of chemical additives used, the main compound and the purpose of usage in hydraulic fracturing is presented in Table 2.5.

Table 2.5. Chemical additives used in hydraulic fracturing (Veil, 2014, GWPC and All, 2009)

Additive	Main compounds	Purpose
Diluted acid (15 %)	Hydrochloric acid or Muriatic acid	Dissolution of minerals and initiates cracks in the rock
Biocides	Glutaraldehyde	Elimination of bacteria from water that produces corrosive byproducts
Breaker	Ammonium persulfate	Promote delayed of gel polymer chains breakdown
Corrosion Inhibitor	N, n-dimethyl formamide	Prevention of pipe corrosion
Cross linker	Borate salts	Fluid viscosity maintenance
Friction reducer	Polyacrylamide or Mineral oil	Minimizes friction between fluid and pipe
Gel	Guar gun or hydoxyethyl cellulose	Thicken the water to promote sand suspension

2.7. Environmental impact of shale exploration

The potential environmental and health impacts associated with tight oil and shale gas exploration has been an issue of global concern especially as shale gas reserve around the globe is increasing. These include potential direct impacts to the quality of groundwater and surface water, water supplies, air pollution and possible seismicity/earthquake (Michael and Tiemann, 2015).

2.7.1. Water issue

The production of shale gas requires substantial volume of water depending on the geological formation, depth to target formation and length of lateral of the shale play (Rahm and Riha 2014). Typically, 7,000 to 18,000 m^3 of water is required to fracture and drill a typical well (Arthur et al., 2008, Yang et al., 2014a, Gregory et al., 2011). About 90 % of the required water is used in hydraulic fracturing while the remaining 10 % is necessary for drilling. As significant as these values might be, study in literature (Gregory et al., 2011) shows that the water used in fracking makes up a smaller percentage (<1%) of the total water used in industries. In addition, Figure 2.19 gives a breakdown of water consumption for extraction and processing of various fuels and it shows that natural gas (shale gas) has the lowest water consumption compared to other fuels. The Figure also signifies that water use in shale gas production compared to other energy sources is lower per unit of energy generated and if natural gas displace coal in generating electricity at a combined cycle gas plant, the volume of water consumed per unit of energy generated could reduce by 80 % (Mielke et al., 2010, Yang et al., 2014a). However, the challenge associated with water usage in hydraulic fracturing is the large volume, which is needed within a short time, and particular area of shale-associated withdrawals can create water quantity issues (Yang et al., 2014a, Arthur et al., 2010). The rise in freshwater demand in hydraulic fracturing is placing pressure on water sources as the competitive demand of fresh water by other sectors like industrial, municipal, and agricultural has led to increase in fresh water cost and the reduction in water availability (Boschee, 2014). Problems associated with water utilization include the effects that huge withdrawals might have on groundwater resources, streams and aquatic life, and other competing uses particularly in water stress regions (Arthur et al., 2010, Grubert and Kitasei, 2010). Such effects can be regional or localized and can vary seasonally or with longer-term variations in precipitation. Shale gas development might also be restricted in water stressed regions due to competition in demands from other consumers, along with decreasing aquifers water levels because of urban and agricultural development. Another issue of contention in shale gas production processes is the management of the huge amounts of wastewater generated during natural gas production. Two categories of wastewater generated are flowback water from hydraulic fracturing operations and produced water from shale formations. Managing this large volume of water has emerged as a concern for producers in terms of quality and costs as restriction placed on surface discharge of wastewater has increased and the capacity for disposal using underground injection well is limited in most of the Shale regions (Acharya, 2011). Thus, water consumption in shale gas production is a serious matter making water resource management an important operational and environmental issue (Hasaneen and El-Halwagi, 2017).

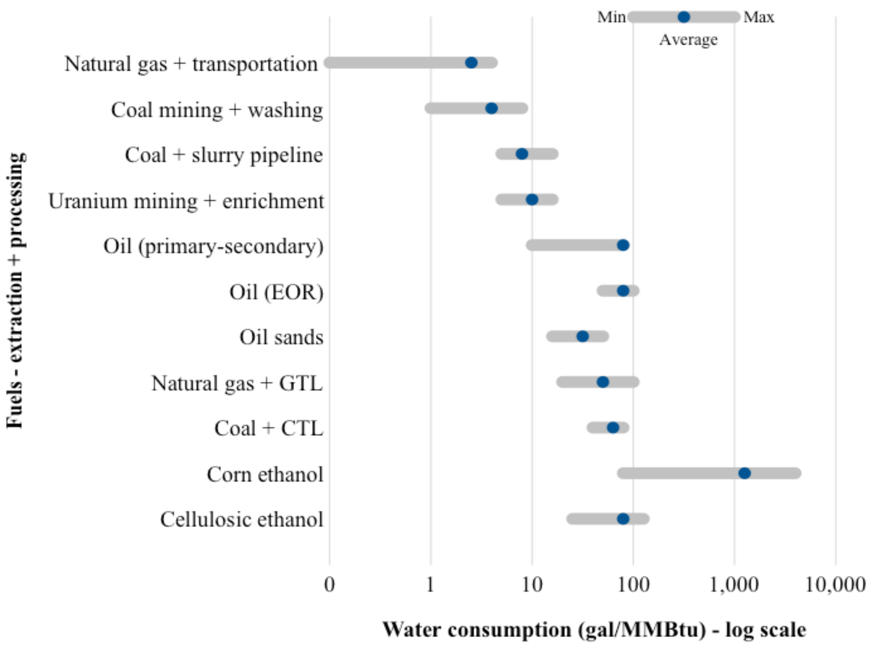

Figure 2.19. Water consumption for extraction and processing of fuels (adapted from Mielke et al., 2010).

2.7.2. Air Emissions / Greenhouse Gas (GHG) Emissions

At different stages in oil and natural gas production is air pollution. The sources of this emission include the construction of pipeline, drilling and completion of well, water management activities, processing of natural gas, storage, and transmission equipment. Major pollutants of concern include methane, volatile organic compounds (VOCs), nitrogen oxides, sulfur dioxide, particulate matter, and other hazardous air pollutants (Lattanzio, 2016). A major source of methane and VOC emissions is the oil and gas industry, these emissions form ozone (smog) upon reaction with nitrogen oxides. (EPA, 2012). Figure 2.20 shows the rate of methane leakage from the natural gas system in the US. Based on the 100-year global warming potential, methane has been found to be 25 times more potent than carbon dioxide as a greenhouse gas (GHG). (Howarth et al., 2011). Any leakage of shale gas during the production or transmission may result in non-negligible environmental impacts (Gao and You, 2017). Although the life cycle greenhouse gas emission in shale gas is much lower than coal, it is still comparable to that of conventional gas (Burnham et al., 2011). It has been estimated recently by the National Oceanic and Atmospheric Administration (NOAA) that four percent of methane produced by the gas wells in Weld County, Colorado is escaping into the atmosphere. Other contaminants released through various drilling procedures are benzene, toluene, xylene and ethyl benzene (BTEX), carbon monoxide, formaldehyde and metals contained in diesel fuel combustion.

Exposure to these pollutants can result in short-term illness, cancer, organ damage, nervous system disorders and birth defects or even death.

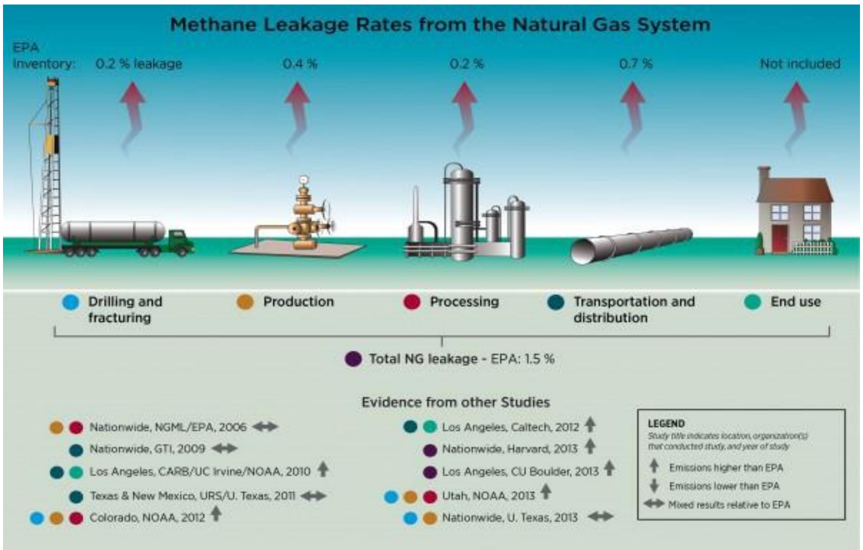

Figure 2.20. Methane leakage from natural gas system (FAG, 2018)

Crystalline silica, in the form of sand, can results in silicosis (an incurable but preventable lung disease) when inhaled by workers as sand is a key component of fracking process. Air samples from eleven fracking sites in the US were analysed by the National Institute for Occupational Safety (NIOSH) and it was found that all the sites surpassed relevant occupational health criteria for exposure to respirable crystalline silica. It was found that the silica concentrations in 31% of the samples surpassed the NIOSH exposure limit by a factor of 10, which means that wearing appropriate respiratory equipment by the workers would not guarantee adequate protection.

2.7.3. Gas Flaring

Flaring is the burning of natural gas, which cannot be refined or sold. Flaring is carried out frequently in most of the industrial plants especially in managing unusual or irregular occurrence. Flaring in most industries is carried out to decrease hazard in the course of distress in an industrial operation, to get rid of associated gases, or to safely manage process start up and shutdown (Kamrava et al., 2015). Flaring is common in areas where oil and gas are co-produced with no sufficient infrastructure for gathering the gas. Because of this drawback, the producer either choses to build the pipeline or gathering facilities, flare the gas or find a useful way of utilizing the gas on site (Glazer et al., 2014).

The U.S. has increased the amount of flared gas more than any other nation in the past five years, though Russia still burns off far more than any other country (Hoffman, 2012). Figure 2.21 shows a glimpse of Natural gas flares from a flare-head at the Orvis State well in the United State. According to Hoffman (2012), 30 percent of the natural gas in the Bakken Shale oil fields of North Dakota, is flared off because of lack of gathering equipment. This amount of wasted gas is estimated at up to $100 million a year. In addition, 15041 wells were completed in Texas in 2012 which led to the flaring of 1.36 billion m^3 (48 billion ft^3) of natural gas (Glaizer et al., 2014). In general, flaring is found to be a waste of resources globally resulting in serious environmental problems such as air, thermal and light pollution.

Figure 2.21. Natural gas flares from a flare-head at the Orvis State well (Hoffman, 2012)

2.7.4. Trucking

In order to transport the required equipment's, water and chemical to and from the shale sites, large number of truck trips is required. About 4,000 to 6500 truck is required to complete a wellpad (90 % associated with fracturing) (Yang et al., 2014a). This may result in road damage, increase noise pollution, air pollution and road accident in communities with shale resources. Roads in many of these regions cannot support the weight and number of large trucks causing an average overall impact on pavement life reductions of approximately 30 % (Energy in Texas (ET), 2013).

2.7.5. Earthquakes/ Seismicity

Additional issue connected with deep-well oil and gas drilling is earthquakes. Although hydraulic fracturing only triggers microseisemic event too small to be detected except with sensitive instruments but the earthquakes associated with injection of wastewater into permitted Class II injection wells are of serious concern. The type of earthquakes triggered by the underground injection of fracking wastewater is refer to as induced seismic. Though most of the tremors are trivial in magnitude (the strongest measured is 5.2), those that are big enough to be felt by people have also been connected with some injection wells that accept flowback and produced water from hydraulically fractured wells. According to the United States Government Accountability Office, GAO (2014), about 144,000 such class II disposal wells in the US accept wastewater of over 2 billion US gallons (7.6 Gl) every day. From 1967 to 2000, about 21 large earthquakes per year were recorded in states like Arkansas, Colorado, New Mexico, Ohio, Oklahoma, Texas, and Virginia. However, these states have recorded more 200 earthquakes from 2010 to 2012 with 188 in 2011 (Shih et al., 2016, Ellsworth, 2013). Figure 2.22 below illustrates the recent increase in earthquake activity in the central United States.

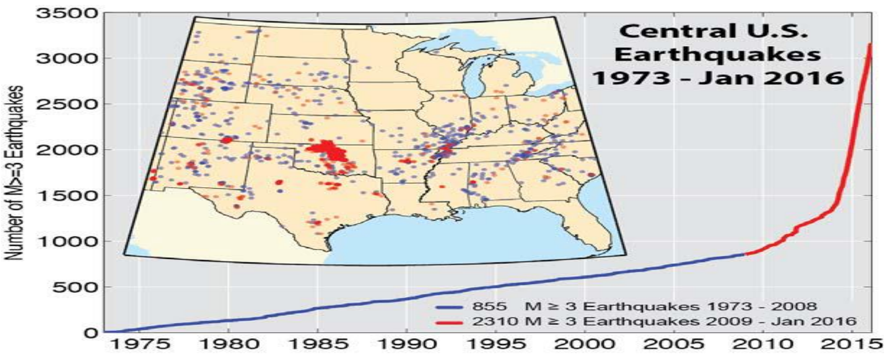

Figure 2.22. Earthquakes in central United State (adapted from Shih et al., 2016, USGS, 2018)

2.8. Water management

2.8.1. Process flow

Mapping the water process flow is essential to understanding the cost implications and decision driver associated with water management in shale gas plays. The modelling and analysis of water-related costs are built upon this framework. The shale gas development water cycle consists of various steps such as freshwater acquisition, transportation, injection, storage, treatment, and disposal as shown in Figure 2.23. Water management decision within shale gas production can be categorized into two primary categories: water usage in the hydraulic fracturing process and the management of wastewater generated from drilling and production. Of the total water used in shale gas production, roughly 90 % is for hydraulic fracturing, while 10 % is required for drilling process (Yang et al., 2014a).

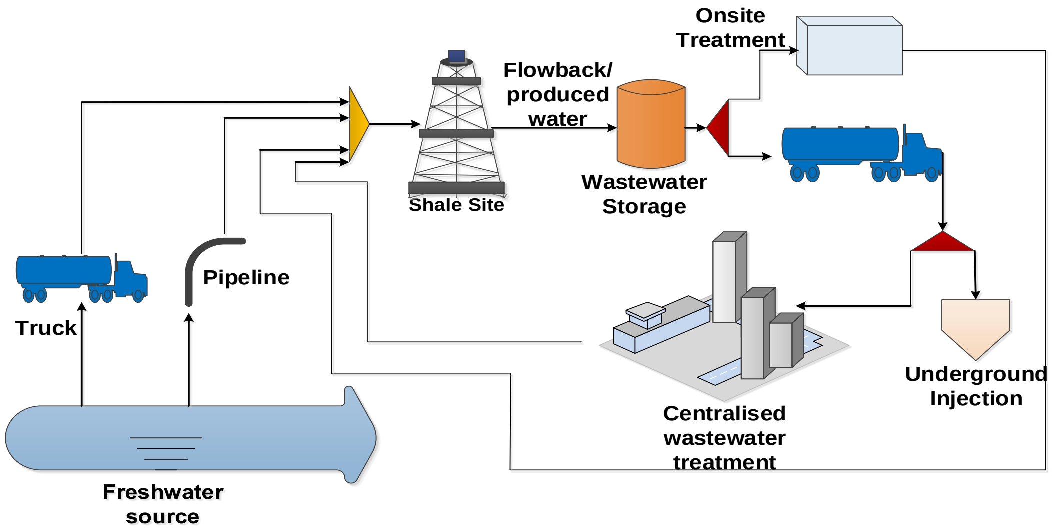

Figure 2.23: Overview of water management in shale gas production

2.8.1.1. Water acquisition

There are two sources from which water can be withdrawn for shale gas production, which are conventional, and unconventional sources. Conventional sources include surface water, ground water, treated wastewater and cooling water while unconventional sources include acid mine drainage (AMD) and using natural gas liquid as frac fluid. The most common of these sources is surface water such as rivers or lake. For example, the dominant water source used for shale gas production processes in Pennsylvania comes from river and streams (Shih et al., 2016, EPA 2015b) while in Marcellus Shale 40 % of surface water used come from small rivers, creeks and streams (Kuwayaman et al., 2015a). However, issues typically associated with water withdrawal from any of these sources especially the surface and ground water include complexity in obtaining permit for withdrawal, access near the shale site and seasonal variation in water availability (Yang et al., 2014a).

2.8.1.2. Transportation

Water management decisions in hydraulic fracturings are mainly influenced by transportation costs. Freshwater can be transported to the shale site using two modes of transportation, which include trucking and/or piping as shown in Figure 2.24. To bring a typical wellpad into completion, approximately 4000-6500 one-way truck trips are required. Although, transporting freshwater through truck allows for flexibility of operation from well to well, it leads to environmental issues such as road damage, noise pollution, air pollution, and require high cost. Hence, due to the high cost of trucking and other environmental impacts, operators are encouraged to draw water from sources that are close by through piping. Transporting water through pipeline is associated with lower cost, however, due to lack of infrastructure, temporary pipe networks are always used as permanent pipeline are heavily regulated.

(a)  (b) 

Figure 2.24. Water transportation in Shale development. (a) Trucking (b) Piping (Yang et al., 2014a)

2.8.1.3. Storage

Freshwater acquired by truck and/or pipeline is typically stored in the freshwater open impoundment while, wastewater is generally stored in pits or storage tanks prior to treatment. Although wastewater storage using pit allows storage of hundreds of thousands of barrels of water with lower cost, however it has some environmental risks such as surface spills, leaking or overflowing pit which can lead to groundwater contamination, odours and air contamination (Ramirez, 2009, Adams et al. 2011, Shih et al., 2016). Storage of wastewater using storage tanks (frac tanks) on the other hand are characterised with smaller capacities and higher cost but are more flexible in terms of operation and with less environmental risks (Gay and Slaughter, 2014). Therefore, due to risks associated with wastewater storage, heavy regulation is placed on it and the best management practise has been recognised as using frac tanks (enclosed tank) (Lewis, 2012).

2.8.2 Wastewater production and management

Wastewater management is the primary driver of water-related costs. Fracturing a shale gas well requires two to six million gallons of water depending on the formation geology and operational procedure. At the subsequent or later stage when hydraulic fracturing is completed, some percentage of the injected water returns to the surface either as flowback water or produced water containing different contaminants. Flowback water is the water-based solution that returns to the surface within the first few weeks after the completion of hydraulic fracturing operation, it is depicted by high flowrate typically around 700 L/min (Schwab and Cammarota, 2018). Produced water on the other hand is the wastewater generated in the production stages. It is made up of the formation water and the injected fracturing fluid generally characterized by high salinity and low flowrate typically 4 L/min. A wastewater production forecast for the Marcellus play suggests that Pennsylvania wells will generate over 15 million m^3 by 2025 (Gay et al., 2012). The wastewater generated varies in quantity and quality with different authors reporting different values in literature. Carrero-Parreño et al. (2017) reports that the value of flowback water that returns during the first two weeks varies between 10 and 80 % of the injected fluid, Gay et al. (2012) reports that 20-80% of this water is recovered during the flow back period, with the remainder being temporarily lost to the formation. Other authors report values of 8–15 % (Lutz et al., 2013), 10–40 % (Gregory et al., 2011, Yang et al., 2014a) and 5-70 % (Schwab and Cammarota, 2018).

2.8.2.1. Wastewater Characteristics

Flowback water is not a uniform raw material from a process development perspective. The physical and chemical properties of flowback water differ significantly subject to the geographic location of the shale play, the geological formation, and the chemicals used in the course of drilling and fracturing processes. Furthermore, the properties and volume of the wastewater water differ throughout the lifetime of the well (ERM, 2014, Glazer et al., 2015, Carrero-Parreño et al., 2017). The types of contaminants and the level of salinity in the wastewater depend on the types of chemical additives used during fracturing and how long the water has stayed underground. The composition and volume of generated wastewater vary depending on the geological formation of the shale play but with general predominant trend of decreasing flowrate and increasing TDS concentration (Yang eta al., 2014a, Yang et al., 2015, Carrero-Parreño et al., 2017) as shown in Figure 2.25. Among various contaminants found in hydraulic fracturing wastewater are high level of total dissolved solid (TDS), scaling ions, total organic compound (TOC), total suspended solids (TSS) and other materials. Tables 2.6 and 2.7 present usual flowback water compositions from several shale gas wells as adapted from Carrero-Parreño et al. (2017) and Schwab and Cammarota (2018) respectively. Constituents of concern include dissolved and suspended organics, like oil and grease; suspended solids, like formation solids, corrosion and scale products, and bacteria; additives such as proppants, friction reducers, biocides, and corrosion inhibitors; naturally occurring radioactive material, precisely barium and radium isotopes; and TDS (Shih et al., 2016, Schwab and Cammarota, 2018).

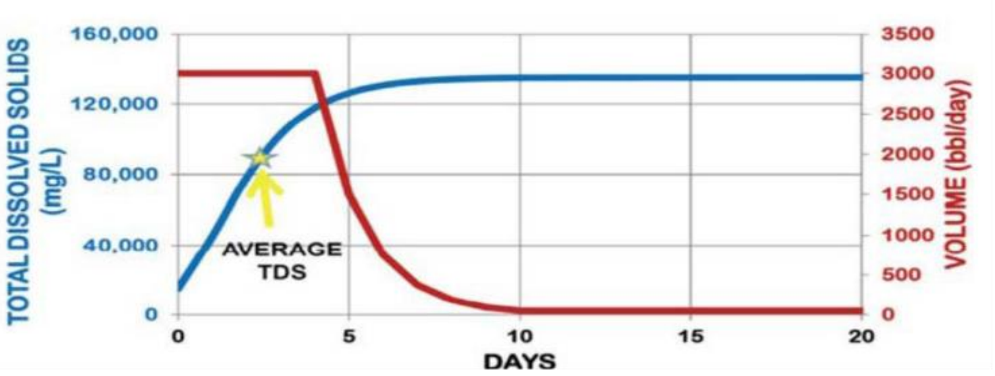

Figure 2.25. Flowback water vs. TDS profile (Yang et al., 2014a).

Table 2.6. Random flowback water composition from Barnett and Appalachian plays (Carrero –Parreño et al., 2017)

Parameter	Well 1	Well 2	Well 3	Well 4
TDS (mg/L)	200,006	54,230	110,847	9,751
TSS (mg/L)	3,220	881	1,530	168
TOC (mg/L)	200	89	138	38
Fe (mg/L)	92	60	105	40
Ca (mg/L)	14,680	4,800	3600	241
Mg (mg/L)	4,730	1,707	899	49
Ba (mg/L)	98	112	127	1
Oil and grease (mg/L)	0	0	18	0

Table 2.7. Some physicochemical properties of effluents from shale gas production (Schwab and Cammarota, 2018)

Parameter	Min	Max	Average	Parameter	Min	Max	Average
TDS (mg/L)	8,180	189,000	67,462.5	Alkalinity (mg/L)	118	255	187.2
TSS (mg/L)	nd	570	248.3	Hardness (mg/L)	196	63.6	19,316.8
TOC (mg/L)	3	1,048	456.2	pH	5.7	7.6	6.7
Fe (mg/L)	4.2	160	61.9	COD (mg/L)	20	4,440	1,910
Ca (mg/L)	319	22,200	7,885.9	SO_4^{2-} (mg/L)	nd	414	36.5
Mg (mg/L)	31	2,260	923.6	NO_3^- (mg/L)	nd	18.1	10.3
Ba (mg/L)	0	3,169	1,139.6	PO_4^{3-} (mg/L)	nd	90	9.5
Oil and grease (mg/L)	nd	594	82.6	Al (mg/L)	Nd	13.3	2.4
Br (mg/L)	52.5	970	537.4	Cl (mg/L)	4,600	107,000	55,884.7
Methane (mg/L)	1.8	10,500	3,420	Ethane (mg/L)	nd	2,730	816

nd: not detected

2.8.2.2. Wastewater Management

Due to the importance of water in the process of hydraulic fracturing, industries are faced with challenges of defining wastewater management strategies that are sustainable environmentally and economically. The water quality parameters differ greatly across geographies and throughout the operational life of the well, increasing the complexity of water management decisions. There are various wastewater management options available but are influenced by many factors such as the infrastructure in existence, properties of shale, economics of gas production, and the social and political condition of a particular play (Lutz et al., 2013, Rahm and Riha, 2014). For the growth of this vast energy source coupled with concerns globally over the quality and quantity of fresh water, novel strategies for water management that will allow natural gas extraction to be sustainable environmentally and feasible economically will be critical (Gregory et al., 2011). In addition, to safeguard the groundwater and surface water resources, production of shale gas resources will necessitate innovative flowback management. Management options for flowback water being adopted presently vary from shale to shale depending on the economic factor and the geological formation of the shale play due to variation in the volume and composition of flowback water. These options can be categorized into two, which are disposal and treatment options. The conventional method across the industry is the disposal of produced and flowback water into injection wells. Nevertheless, this method has become restricted by operational capacities, location, and environmental concerns, amongst other issues. Disposal option include underground injection, surface discharge and pond evaporation. Each option significantly depends on environmental regulation, discharge outlet availability, transportation safety to the discharge outlet and abundance supply of fresh water resources as disposal is just an option for wastewater discharge but does not promote water reuse (Elsayed et al., 2015). Three different factors have been identified to tackle the challenges of water management in hydraulic fracturing (ERM, 2014). These includes:

- Minimization of freshwater required for hydraulic fracturing by the use of non-freshwater sources such as brackish water or other media like waterless frac fluid.
- Maximization of reuse.
- Improvement of treatment technologies.

Therefore, producing companies are considering water recycling/reuse technologies that permit effective wastewater treatment and reuse in the next fracturing operation.

Treatment options on the other hands provides an opportunity for wastewater reuse or discharge. These options include onsite partial treatment, which allows reuse/recycling for fracturing other wells and transportation to a centralized wastewater facility for reuse or for surface water discharge (Arthur et al., 2005, Shih et al., 2016, Krupnick, 2013). Several factors need to be considered in order to select an appropriate treatment technology for flowback water management. Among these factors are: the volume of flowback water, the composition in terms of salinity and other critical contaminants, the desired level of treatment, mobility and economics. The contaminant levels that are usually of concern are TDS, TSS, calcium and sulphate (Yang et al 2014a). Treatment technologies are common feature of water management practices and are selected based on the end use of treated water. These are categorized as membrane and non-membrane processes and in most cases; multiple treatment technologies are required to meet the expected water requirement criteria. Table 2.8 shows a train of various established water treatment processes available for treating wastewater from oil and gas industries. Among these are coagulation, sedimentation, membrane processes such as ultrafiltration/microfiltration, softening, electrocoagulation etc. (Bole-Rentel, 2015, Guerra et al., 2011, ERM, 2014, Carrero-Parreño et al., 2017). The kinds of water treatment required differ for different drilling and hydraulic fracturing processes as varieties of organic and inorganic compounds are used in fracturing fluids to optimize formation fracturing and transportation. In order to promote maximization of shale gas recovery, there must be compatibility between the salinity, water composition and the hydraulic fracturing fluid chemistry and formation, as high salinity can lead to formation damage, affect performance of some friction reducers and damage the drilling equipment (Elsayed et al., 2015). The specification for wastewater reuse in the Marcellus shale is given in Table 2.9 as an example. Therefore, it is important that accurate amount and quality of water be used in the processes, to ensure that any interference with the fracturing fluid performance by any unwanted contaminant is avoided.

Naturally Occurring Radioactive Materials (NORMs) such as uranium, thorium and radium have not been accounted for in Table 2.9 because it is believed that their concentration in shale gas wastewater are generally not close to the dangerous value (Carrero –Parreño et al., 2017).

Different alternatives for flowback water management is given in Figure 2.26, from the figure the first alternative is the onsite reuse of the wastewater in which the flowback water is blended with freshwater to fracture other wells without treatment. However, operational problems from high level of contaminants can occur as the compatibility of salinity and composition of water used with the hydraulic fracturing water chemistry and formation is of paramount importance to maximize shale gas recovery (Reyntjens and Johnson, 2013, Carrero-Parreño et al., 2017, Elsayed et al., 2015, Hayes 2012). Another alternative is for the water to undergo pre-treatment mainly to remove scaling materials, TSS, and organics after which the pre-treated water can be used directly or blend with freshwater to meet the frac fluid criteria depending on the salinity.

Table 2.8. Available pre-treatment and treatment options for oil and gas wastewater (ERM, 2014, Guerra et al., 2011, Carrero –Parreño et al., 2017)

Mechanism	Target parameters
Filtration	Large solids e.g. sand and mineral scales
Coagulation/flocculation	Heavy metals, TSS
Oxidation	Organics and metal removal
Electrocoagulation	TSS, heavy metals
Oil/water separator	Oil
Floatation	TSS, oil
Hydrocyclone	Oil
Reverse osmosis	TDS
Ultrafiltration	TSS, heavy metals, microbes, colloidal natural organic matters
Chemical biocides	Microbes
UV light	Microbes
Ozone	microbe
Softening	Scale forming cations e.g.Ca, Mg, Ba etc.
Membrane distillation	TDS
Crystallization	TDS
Nanofiltration	TDS
Forward osmosis	TDS

Table 2 .9. Specification for flowback water reuse in Marcellus Shale play (Carrero –Parreño et al., 2017)

Parameter	Maximum value recommended	
	1	2
TSS (mg/L)	50	
TDS (mg/L)	50,000-65,000	50,000
TOC (mg/L)	<25	
Total hardness (mg/L)	2,500	26,000
Total alkalinity (mg/L)		300
pH	6-8	
Bacteria (/mL)	<100	
Chloride (mg/L)	20,000-30,000	45,000
Sulfates (mg/L)		50
Ca (mg/L)		8000
Fe (mg/L)	20	10
Na (mg/L)		36,000
K (mg/L)		1,000
Ca (mg/L)		8,000
Mg (mg/L)		1,200
Ba (mg/L)		10
Sr (mg/L)		10
Mn (mg/L)		10

The main consideration in the treatment of flowback/ produced water is to reduce the TDS concentration, so that it meets the standard for discharge or reuse. The removal of TDS has been considered as one of the most challenging because of the energy intensive processes required (Yang et al., 2014a, ERM, 2014, Bole-Rentel, 2015, Carrero-Parreño et al., 2017, GAO, 2012) as TDS concentration can range from 40,000 mg/L to as high as 300,000 mg/L depending on the shale play. Therefore, desalination as the last alternative is required for flowback with high salinity to allow for reuse, recycle or surface discharge. Two categories of desalination processes namely thermal and membrane technologies can be used for treatment of flowback water with high salinity depending on the water composition. Example of these processes include reverse osmosis (RO), forward osmosis (FO), membrane distillation (MD) and mechanical vapour recompression. While forward osmosis can be used to treat flowback water with medium TDS level typically less than 70,000 mg/L, reverse osmosis can only operate with TDS level below 40,000 mg/L. On the other hand, membrane distillation can operate with TDS level as high as 300,000 mg/L and mechanical vapour recompression is also suitable for high salinity water up to 200, 000 mg/L. In line of the aforementioned, the focus of this study is on membrane processes as membrane technologies are getting special recognition as substitutes to conventional water treatment and as a means of improving wastewater for reuse.

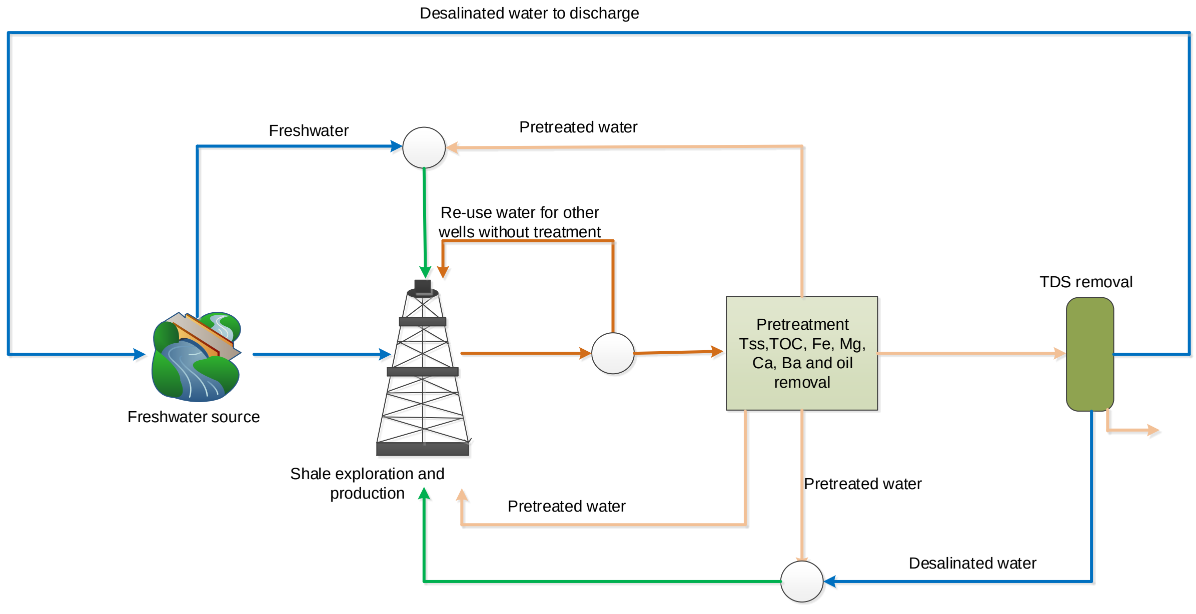

Figure 2.26. Alternative for flowback water management (Carrero-Parreño et al., 2017)

2.9. Membrane network

Membrane technology covers all engineering approaches for the transport of substances between two fractions with the help of permeable membranes. In general, mechanical separation processes for separating gaseous or liquid streams use membrane technology. The special recognitions been received by membrane processes in the area of water and wastewater treatments are as a result of various advantages they exhibit over the conventional methods (Thoola, 2014, ERM, 2014, Judd and Jefferson, 2003). These include:

- No or little necessity for chemical additives
- High rejection factor
- High quality permeates
- Inexistence of a phase change thereby consume less/ moderate energy.

The mode of operation for membrane processes is depicted in Figure 2.27**.** In the figure, the stream into the membrane system is separated into two, the first portion called the permeate is the fraction that permeates through the membrane and the portion which contain the impermeable materials is called the retentate. Membrane separation processes vary depending on the mechanisms of separation, size of the separated particles and driving force. The major criteria on which the classification depend is the driving force, which can be through a pressure difference, temperature difference, concentration difference, or electrical potential (Thoola, 2014). The widely used membrane processes are the pressure driven membranes that include microfiltration, ultrafiltration, nanofilteration, and reverse osmosis. Detail informations on membrane processes, their mode of operation and the driving force are given in Table 2.10. The membrane networks selected for the purpose of this research are ultrafiltration and Membrane distillation treatment technologies. Ultrafiltration is selected as one of the preferred option for flowback water pre-treatment and membrane distillation as option for desalination technology considered suitable for oil and gas wastewater treatment (Reyntjens and Johnson, 2013, ERM, 2014, Bole-Rentel, 2015).

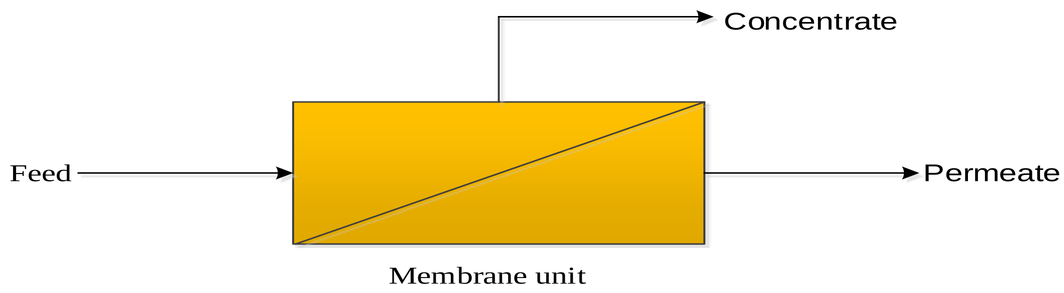

Figure 2.27. Membrane separation principle

Table 2.10. Classification of membrane processes (Buonomenna et al., 2012)

Separation process	Driving force	Mode of separation
Microfiltration (MF)	Pressure difference	Size exclusion
Ultrafiltration (UF)	Pressure difference	Size exclusion
Nanofiltration (NF)	Pressure difference	Size exclusion
Reverse osmosis	Pressure difference	Diffusion
Pervaporation (PV)	Concentration difference	Solution-diffusion
Dialysis (D)	Concentration difference	Diffusion
Membrane distillation (MD)	Temperature difference	Diffusion
Electrodialysis (ED)	Electrical potential	Ion exchange

2.9.1. Ultrafiltration (UF)

Ultrafiltration (UF) is a type of membrane filtration that depends on forces such as pressure or concentration gradients for separation through a semipermeable membrane. The membrane allows the passage of water and solutes of low molecular weights in the permeate whereas the retention of suspended solids and high molecular weight solutes occur in the retentate. Ultrafiltration membranes are characterised based on the molecular (MWCO) of the membrane used. Ultrafiltration allows filtration of bigger particles and are therefore only utilised for pre-treatment or removal of particulates. This membrane filter water through a porous membrane using pressure or suction. Ultrafiltration pore sizes range from 0.01–0.1 µm and need low transmembrane pressure (1–30 psi) to function (Guerra et al., 2011). During operation, one or more feed components are deposited on the surface of the membrane, or within the membrane pores, which results in fouling of the membrane and leads to flux reduction through the membrane (Guadix et al., 2004). The reversal of this undesirable occurrence may be achieved by chemical cleaning and, consequently, UF processes operates in a cyclic manner in which individual cycle consists of a period of filtration followed by a cleaning period.

UF systems can either operate with cross-flow or dead-end flow as presented in Figures 2.28 and 2.29 respectively. The flow of the feed solution is perpendicular to the membrane surface in dead-end filtration. In contrast, in cross flow systems the flow passes parallel to the membrane surface. Dead-end configurations are batch processes suitable for solution with low suspended solids. This process leads to accumulation of solids at the surface of the membrane hence; frequent back flushes and cleaning is required to maintain high flux. In continuous processes, cross-flow configurations are ideal as continuous flushing of solids from the surface of the membrane results in a thinner cake layer and reduce resistance to permeation. Membrane can be made from either polymeric or ceramic materials. Ceramic membranes can achieve high flux rates, strong mechanically, chemically and thermally stable and are much more resilient compared to polymeric membranes (Guerra et al., 2011). A tubular configuration is usually used with an inside-out flow path, where the feed water flows inside the membrane channels and permeates through the support structure to the outside of the module. Typically, these membranes consist of at least two layers—a porous support layer and a separating layer. Ceramic membranes are capable of particulates, organic matter, oil and grease, and metal oxides removal, their lifetime is longer and cleaning can be achieved with more aggressive chemicals; however, they are usually expensive than polymeric materials. In terms of energy requirements, ceramic membranes require lower energy than polymeric membranes (Dahmn and Chapman, 2014).

Ultrafiltration is one of the most effective techniques for treatment of oily wastewater, particularly for flowback/produced water, in contrast to the traditional separation methods due to its high efficiency for oil removal (Ahmadun et al., 2009). Ultrafiltration (UF) is a pre-treatment technology for the removal of particles and colloidal material from flowback water before further membrane treatment. UF can be used to remove contaminants such as trace particulates, oil and grease, biological and organic constituent as well as large molecular weight organic compounds. Ultrafiltration module is usually used in combination with other treatment methods like hydrocyclones for sand and oil separation, followed by microfiltration or ultrafiltration for smaller particles and colloidal material, before a desalting process for on-site treatment of flowback/produced water. There are numerous advantages associated with the use of UF in the areas of water recycle and/or reuse particularly in shale exploration (ERM 2014, Dahmn and Chapman, 2014, Anselme and Jacobs, 1996, Ahmadun et al., 2009). These include:

- UF is characterised by a smaller footprint per volume of water treated.
- Modular and mobile system which allow for easy movement within wellpads.
- Consistent constituent removal.
- It is able to operate with moderate energy, which can allow for channelling the gas that would otherwise be flared as fuel to generate the energy requirement.
- High water recovery (> 95 %).
- No necessity for chemical additives.

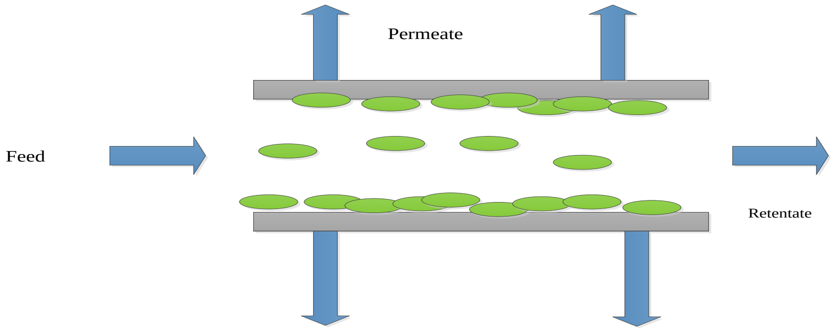

Figure 2.28. Schematic of cross flow operation

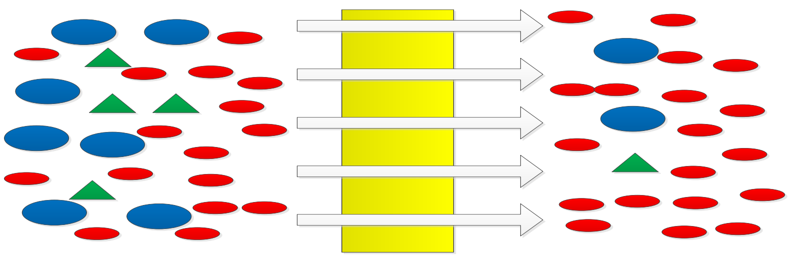

Figure 2.29. Schematic of dead-end operation

2.9.2. Membrane distillation (MD)

Membrane distillation has emerged as a promising technology in wastewater treatment and has gained high level of interest in industries especially where high purity separation is of great importance. It is capable of treating wastewater from oil and gas effectively (Elsayed et al., 2015). However, the suitability of membrane distillation in wastewater treatment depends on the type of contaminant in the wastewater for in order to produce pure water; the contaminant should be non-volatile solutes. In MD, the feed is pre-treated to a temperature below boiling point, which ranges between 323-363 K in the case of water treatment application. The water vapour then travels through a hydrophobic, microporous membrane. The vapour is condensed on the permeate side using the stored permeate and collected as pure liquid as shown in Figure 2.30. The use of hydrophobic membrane is to ensure that the membrane pores are free of condensation. The driving force in membrane distillation is the chemical potential difference across the membrane which depends on the difference between the vapour pressure of the feed and the permeate sides. There are various benefits associated with the use of MD in the areas of water recycle and/or reuse as well as desalination particularly in shale exploration (Elsayed et al., 2013, Elsayed et al., 2015). These include:

- Low-level heating and ability to operate with moderate temperature and pressure; this is a very crucial factor in shale exploration due to availability of wasted energy from flaring which can be used as energy source for MD.
- Ability to treat highly concentrated feed with modest pre-treatment and less fouling, which is the case with water generated from hydraulic fracturing.
- Compact size and modular nature: MD is characterized with a small footprint due to high surface area to volume ratio of the membrane. It can also be easily adjusted to the require capacity by removal or addition of MD modules which allow easy movement from one wellpad to the other.
- High rejection factor with high purity permeate. Ideally, complete rejection of solute is expected in MD.

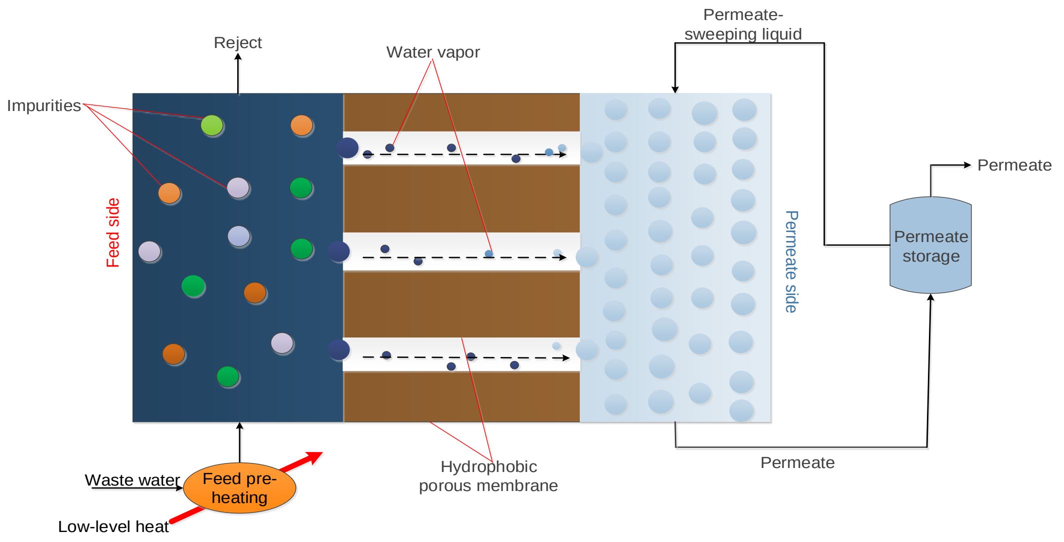

Figure 2.30. Schematic of membrane distillation

Consideration must be given to both heat and mass transfer from the feed side to the permeate side of the membrane. Three basic mechanisms control mass transfer in membrane distillation; these are Knudsen diffusion, molecular diffusion and Poiseuille. Mass and heat transfer take place across three sections (Elsayed et al., 2013, Yun et al., 2006), mass transfer takes place in the boundary layer of the membrane on the feed side, across the membrane and on the permeate side boundary layer. Heat transfer on the other hand takes place from the bulk of the feed to the interface of the membrane through a boundary layer via convection, across the membrane via conduction and latent heat associated with the vaporized flux, and through the boundary layer from the interface of the membrane to the bulk of the permeate via convection. In order to describe mass transfer through the membrane, models such as Knudsen diffusion, molecular diffusion or incorporation of both have been established to yield quality results (Yun et al., 2006).

Some of the drawbacks associated with membrane distillation are the low permeate flux, temperature polarization due to high susceptibility of the permeate flux to the condition of the feed temperature (due to non-isothermal nature of MD) and high rate of heat lost by conduction through the membrane (Alkhudhiri et al., 2012, Elsayed et al., 2013).

Various configurations of MD have been reported in literature (Elsayed et al., 2013; Yun et al., 2006) with variation based on mode of vapour collection on the permeate side and the method of the driving force enhancement across the membrane. Among these configurations are direct contact membrane distillation (DCMD), vacuum membrane distillation (VMD), air gap membrane distillation (AGMD) and sweeping gas membrane distillation (SGMD) (Alkhudhiri et al., 2012, Elsayed et al., 2013, Yun et al., 2006)). The focus of this study is on direct contact membrane distillation (DCMD) which is found to be the most commonly used configuration. The pre-heated feed solution is in direct contact with the side surface of hot membrane in this configuration thereby allow evaporation to take place at feed-membrane surface. Some of the merits associated with DCMD are ease of construction, operation, maintenance and stability in operation compared to other configurations (Elsayed et al., 2015).

2.10. Shale gas composition and processing

Shale gas is a complex mixture and the compositions of gas produced from different wells will vary. The typical composition of shale gas is shown in Table 2.11. The main component of shale gas is methane with other different compounds, which may be present in varying proportion (Younger, 2004). Shale gas usually comprises of heavier hydrocarbons, viz. ethane, propane, butanes, etc. and other impurities, like carbon dioxide, nitrogen, and hydrogen sulfide besides the main component, methane, (NETL, 2013, Younger, 2004). The heavier hydrocarbons are jointly referred to as natural gas liquids (NGLs) after processing and purification into final products. Shale gas can be grouped into two types depending on the natural gas liquid (NGLs) contents namely dry gas and wet gas. Natural gas liquids are hydrocarbons with generally higher market values than methane gas. These hydrocarbons include ethane, propane, butane and heavier components. Dry gas is virtually pure methane with trace NGLs, thereby may not require further processing. While the main component in wet gas is also methane, the quantity of NGLs is substantial enough to necessitate additional processing (Gao et al., 2017, EIA, 2006).

Table 2.11 Typical composition of shale gas (Yang, 2016, Younger, 2004)

Component	Chemical formula	Percentage composition (%)
Methane	CH_4	70-90
Ethane	C_2H_6	0-9
Propane	C_3H_8	0-9
Butane	C_4H_{10}	0-9
Pentane	C_5H_{12}	0-9
Carbon Dioxide	CO_2	0-8
Oxygen	O_2	0-0.2
Nitrogen	N_2	0-5
Hydrogen Sulfide	H_2S	0-5
Rare gases	A, He, Ne, Xe	trace

Natural gas processing involves the separation of different hydrocarbons and fluids from the pure natural gas, to produce dry natural gas what generally known as ‘pipeline quality’. Major transportation pipelines typically enforce restrictions on the make-up of the natural gas that is allowed into the pipeline (Natgas, 2013). However, as shale gas from different plays differ in composition and also there is variability in the compositional makeup of wells within the same play, the processing requirements depend on the well that is producing the gas (Al-Douri et al., 2017). Figure 2.31 below shows a schematic representation of a typical shale gas processing plant. The processing steps involve the condensate and water removal, acid gas removal (carbon dioxide and hydrogen sulphide), dehydration, mercury removal (if applicable), nitrogen elimination and NGLs recovery.

The first step after the raw gas has been brought to the surface is to remove water and condensate by lowering the gas pressure to the operating pressure of the gathering line thereby allow the gas to cool and some of the water of saturation condenses out. However, as the gas is been transported to the processing plant, further cooling of the gas to ground temperature is likely which encourages hydrate formation and plugging of pipeline. Therefore, in order to avoid this condition, either the gas is heated up to keep it above its hydrate point or gas dehydration is perform at the well site (Younger, 2004). At the processing plant, the gas passes through a separator to remove the liquids after which it is sent to the sweetening unit for acid gas removal using sweetening agents like monoethanol amine, Sulphinol etc. The product of the sweetening unit is then dehydrated to remove the remaining water vapour after which it undergoes mercury removal (if necessary) and nitrogen rejection. The gas stream is then sent to the fractionation units where natural gas liquids are separated from pipeline-quality. The pipeline-quality gas with typical composition after NGLs recovery as shown in Table 2.12 is sent from processing unit to the end users through distribution lines and the NGLs serve as raw materials in chemical industries to produce various products that can be used in manufacturing industries as raw materials (Al-Douri et al., 2017, Siirola, 2014, Marano et al., 2015).

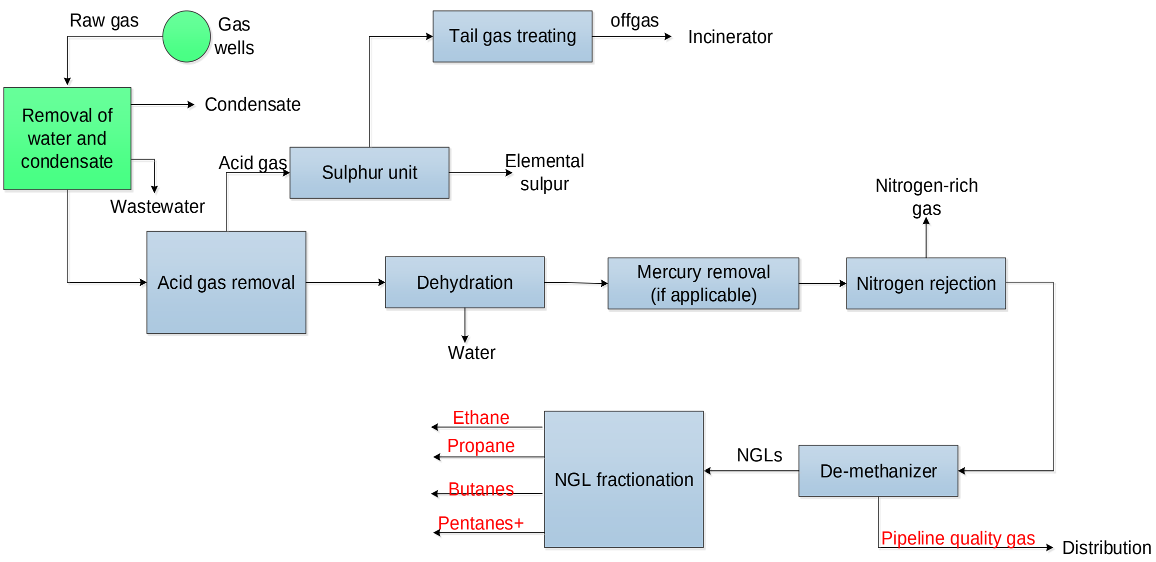

Figure 2.31. Typical shale gas processing plant (Al-Douri et al., 2017)

Table 2.12. Natural gas pipeline quality (adapted from Al-Douri et al., 2017)

Component	Composition (mol %)
Methane	95.4
Ethane	3.89
Propane	0.04
Carbon Dioxide	2.00
Nitrogen	0.08
Hydrogen Sulfide	4×10^{-6}

2.11. Shale gas/ Natural gas transportation

The transportation of natural gas to the processing plants and to the market hub where pricing and selling of natural gas take place is majorly done through pipeline systems. The pipeline systems consist of pipeline, compressors, valves and monitoring devices (Gao and You, 2017a). The natural gas transmission pipelines connect the gas wells to the processing plants, various receipt points and finally to the main end users' area. They are usually pipeline with wide diameter and long distance depending on the types and exists in three different forms (EIA, 2018) which are:

- Interstate natural gas pipelines, which operate and distribute natural gas across state borders.
- Hinshaw pipeline: receives natural gas from interstate lines and distribute to customers within a state border for consumption.
- Intrastate pipelines: operate and transport natural gas within a state border.

After the transportation of natural gas to the communities where it will be consumed, it flows into mains, which are pipelines with smaller diameters. The natural gas is then transported to the final end users for consumption through smaller service lines (EIA, 2018).

2.12. Natural gas storage

There exists fluctuation in the daily and seasonal demand of natural gas, therefore, storage facilities are necessary during the period of low demand for the following reasons (EIA, 2018,)

- To ensure sufficient supply during period of high demand
- To serve as natural gas inventory management tool
- To serve as seasonal natural gas supply backup and deals with fluctuation in price

Natural gas storage facilities can be an underground facilities or smaller volume tanks, which can exist above or below ground. These facilities are usually in three categories as presented in Figure 2.32 (EIA, 2018) namely:

- Depleted natural gas or oil field: This is the most common type of underground storage and consist of those formations that are no longer in use because they have been tapped of all recoverable natural gas or oil (Natgas, 2013). They are the type of storage facilities close to consuming areas and are commonly used to store natural gas and oil in the United States.
- Salt caverns: Salts caverns are underground salt deposits, which may exist in two forms namely: salt beds and salt domes. Salt caverns are usually leached from bedded salts formation in the Midwest, Northeast and Southeast states while in the Gulf coast states, these storage facilities are mainly in salt dome formations. Their rate of withdrawal and injection is typically higher than the natural gas working capacity.
- Aquifers: These are porous underground permeable rock formations and their development is more costly compare to depleted gas reservoir, therefore, common in areas where depleted gas reservoir does not exist. This is mostly used in the Midwest where water-bearing sedimentary rock formations are tuned to reservoir for natural gas.

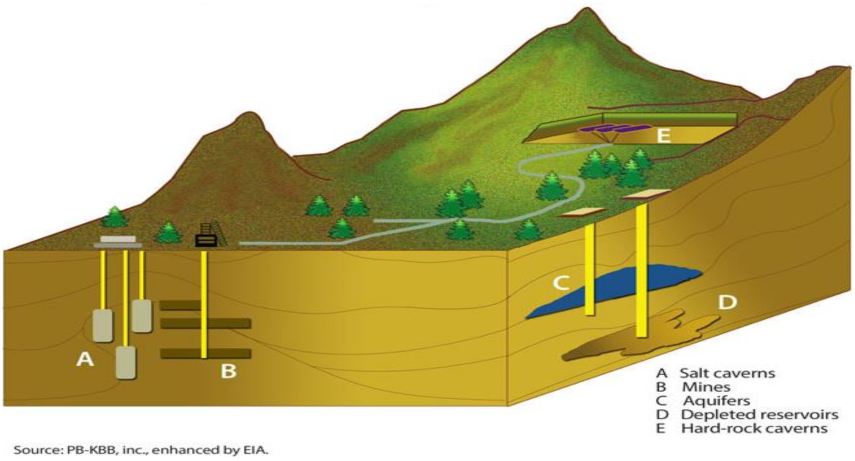

Figure 2.32: Natural gas storage facilities (EIA, 2018)

2.13. Natural gas end use

Natural gas consumption is predicted to rise from 120 trillion cubic feet (Tcf) in 2012 to 203 Tcf in 2040. It accounts for the largest source of energy in world primary energy consumption, which is estimated to increase by 41% in two decades (EIA, 2016, Arredondo-Ramírez et al., 2016). The major fuel in the electric power and industrial sectors is natural gas and is found to be an attractive choice for new generating plants in electric power sector because of its fuel efficiency (EIA, 2016). Figure 2.33 shows the detail of US natural gas consumption by sector in 2016 based on the data from Energy Information Administration (EIA) (CCES, 2018).

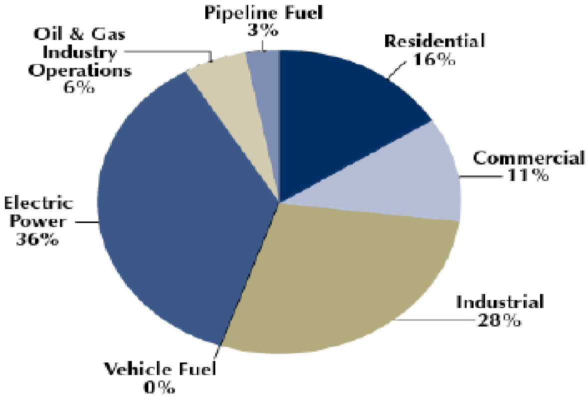

Figure 2.33. Natural gas consumption by sector in the USA (CCES, 2018)

On a yearly basis, natural gas consumption worldwide for industrial and electric power sector is going to increase by an average of 1.7%, and 2.2% respectively from 2012 to 2040 (EIA, 2016). The industrial and electric power sectors together account for 73% of the total increase in world natural gas consumption, and is estimated to increase to 74% of total natural gas consumption through 2040. From Figure 2.33, 36 % of US natural gas consumption is consumed in electric power sector to generate electricity. In the industrial sector, natural gas serves as raw material for various chemical products and as source of heat with about 28 % of total US natural gas consumption while commercial and residential sectors take up 11 % and 16 % respectively majorly for heating purposes.

2.14. Natural gas vs Coal

Natural gas has been found to be a source of clean energy production compared to other fossil fuels such as coal or petroleum products. In order to implement plans for the reduction of carbon dioxide (CO2) emissions, natural gas usage is been promoted to replace carbon-intensive fossil fuels. Some of the advantages that natural gas has over other fossil fuels are: for every unit of electricity generated using natural gas, the emission of carbon dioxide is minimal. The carbon dioxide emission from natural gas is found to be 30% lower than emission from oil and 45% lower than coal. In addition, when natural gas is compared to other fossil fuels in terms of the quantity of nitrogen oxides, sulphur dioxide, particulates and mercury discharge, the quantity release by natural gas is minimal (Natgas, 2013, Oke et al., 2019a). Hence, replacing other fossil fuels with natural gas can lead to a potential reduction in the emission of these harmful pollutants.

2.15. Shale gas Production profile

The shale gas production profile is referred to as the decline curve, it is characterised by a rate of production with a sharp initial decline rate and much slower decline rate after a few years (Blumsack, 2017). The production profile help in the determination of how profitable shale gas wells are in comparison with conventional gas wells and whether specific shale energy development projects are likely to pay off. Figure 2.34 illustrates a typical shale gas production decline curve for two different cases of estimated ultimate recoverable reserves (EUR) as adapted from Blumsack (2017) in which there is hyperbolically decline in the gas production initially and later reflect exponential decline.

Generally, for a single well, shale gas production profile reflects a high rate of production initially, and then a significant decline rate of 60% to 90% after the first three years (Gao and You, 2017, EIA, 2012). This characteristic is because of depletion in pressure and inherently low permeability of the shale reservoir. Consequently, shale gas operators have to drill new wells regularly or refracture existing ones to maintain a stable production profile (Hughes, 2014) thereby leads to scheduling problem.

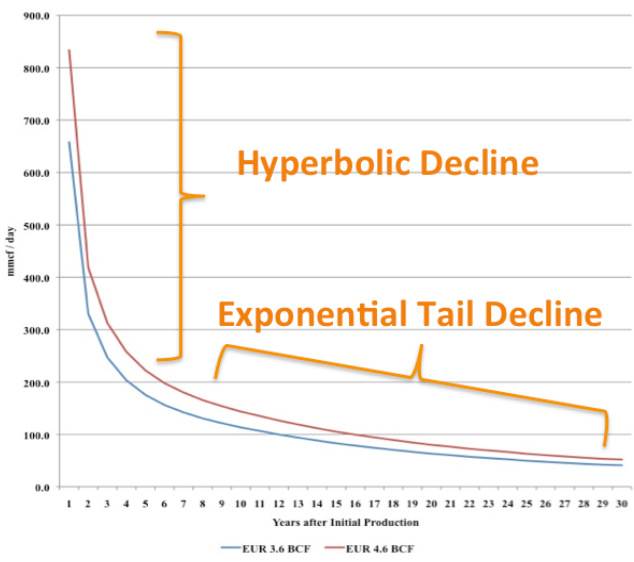

Figure 2.34. Wellpad production profile (Blumsack, 2017).

2.16. Scheduling

Scheduling is an important decision-making process which covers various aspect of process industries. It has a great impact on process operations as one of the core areas by dealing with where, when and how available resources are allocated to execute a collection of tasks over time given certain requirements (Pinto and Grossmann, 1998). Traditionally, the main goal of scheduling in process industries is to either optimize plant performance characteristics or plant economic term (Behdani et al., 2007). Although scheduling may apply to traditionally continuous processes, it is mostly used for batch processes. A wide range of products are produced using batch mode in chemical industries (e.g. pharmaceutical, polymer, food and many specialty chemical) especially those produced in small quantities and for which there can be change in production processes or demand pattern (Mockus and Reklaitis, 1999,).

Scheduling in batch processes can be categorized into three categories depending on the length of time horizon namely: short term, medium term and long term. Short term scheduling deals with time horizon of shorter length ranging between several hours or days. Medium term scheduling focuses on the determination of detailed production schedule involving time horizon of medium time while long term scheduling considers a long time horizon and involve high-level decision making (Dhamdhere, 2006). There are various aspects to be considered in batch process scheduling amongst which are time representation, production recipe representation, representation of event within the time horizon and others. In addition, three major components are always part of scheduling problems (Pinto and Grossmann, 1998). These are assignment of tasks to equipment, activities sequencing, and utilization timing of equipment and resources by the processing tasks.

2.16.1. Time representation

The important aspect to be considered in any scheduling problem is the time representation as the computational intensity and size of the resultant mathematical model is highly influenced by how time is treated (Behdani et al., 2007). There are two approaches used for time dimension in batch processes, which are based on whether the schedule event can occur at any time in the time horizon of interest or at some predefine time points (Mendez et al., 2006). These approaches are the discrete time and continuous time formulations. Discrete time formulations involve even discretization of time horizon of interest. The time horizon of interest is divided into number of time intervals of uniform durations as depicted in Figure 2.35a **(**Kondili et al., 1993**)** and the event such as the beginning and the ending of a task are associated with the boundaries of these time intervals. This time representation approach leads to a model structure, which is simpler and easier to solve and it provides a reference grid of time for all operation competing for shared resources. Some of the disadvantages associated with discrete time formulations are:

- This approach is by definition only approximation of the actual problem due to concept of discretization and continuous nature of time.
- Achieving an accurate approximation of the original problem involve using a sufficiently small time interval thereby leading to large model with high computational intensity.
- Reduction of the domain of timing decisions may result in sub-optimal or infeasible solution.

However, despite these limitations, discrete time formulations have been applied efficiently in variety of industrial applications where a reasonable number of intervals is enough for accurate problem representation (Mendez et al., 2006).

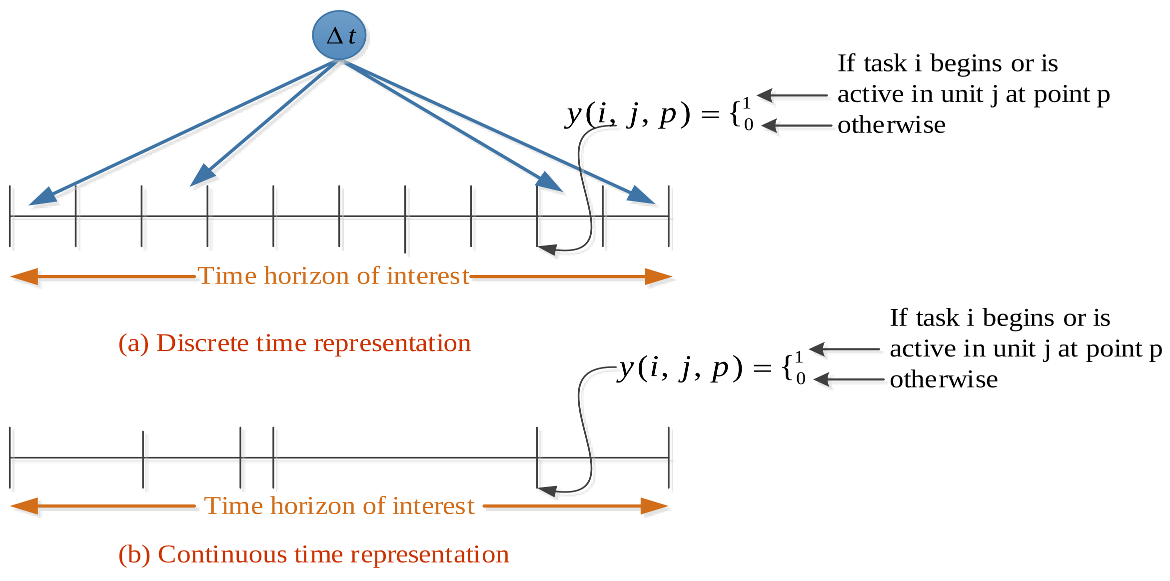

Figure 2.35. Discrete and continuous time representation (Majozi, 2010)

To overcome the limitations of discrete time formulations, continuous time representations were introduced as depicted in Figure 2.35b. These approaches allow events to take place at any point in the continuous domain of time (Behdani et al., 2007) by using a set of continuous variables to define the exact time at which an event occurs. This results in flexibility in terms of time as tasks are allowed to start or end at any time within the time horizon. It also results in mathematical models of smaller size and less computational intensity due to possible elimination of a major fraction of the inactive event time interval assignment (Floudas and Lin, 2004). However, the major shortcoming of continuous time formulations is the determination of optimum number of time points as the number of time points is not known priori and needs to be determined by iteration until there is no improvement in the objective function.

2.16.2. Recipe representation

Another aspect that is of great importance in batch plant scheduling is the recipe representation. Processing sequences involved in batch plant production cycle can be complex as many interconnected operations are involved. However, simplified representation of batch processes can aid in the development of effective scheduling models. Among the most used of these representations are the State Task Network (STN), the State Sequence Network (SSN) and the Resource Task Network (RTN).

In STN, processes are represented as a collection of different material states that are transformed by task carried out in a processing unit i.e. a processing task consumes and produces states. (Harjunkoski et al., 2014). Kondili et al. (1993) proposed the State Task Network recipe representation, to deal with the ambiguity associated with processing network representation using traditional flowsheet. State Task Network uses three main entities for clear representation of batch recipe namely the state nodes usually denoted by circles, the task nodes denoted by rectangles and the arcs. The state nodes represent all processed material within the batch plant that include the feeds, intermediates and final products, task nodes stand for the various process operation involved in the transformation of one or more input state to one or more output states whilst arcs indicate the flow of states by linking states and tasks. An illustration of STN representation for a simple batch process consisting of three processing units processing one material each to produce another material is given in Figure 2.36a.

The State Sequence network (SSN) shares a form of similarity with the STN and it was proposed by Majozi and Zhu, (2001). The distinction between the two representations is the absence of task declaration in SSN but uses only state nodes for recipe representation as shown in Figure 2.36b. The existence of a task in this representation is implied by the presence of an arc, which denote a transformation of one state to another (Majozi, 2010). Adoption of SSN representation for batch process scheduling usually results in fewer binary variables, which in turn leads to reduction in the size of the resulting model.

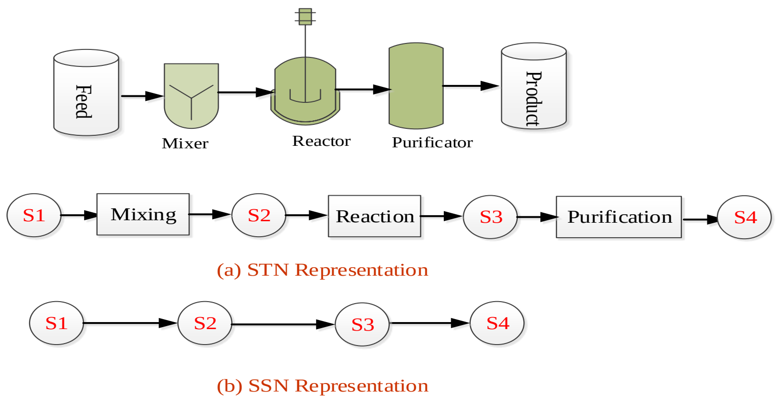

Figure 2.36. STN and SSN representation of a batch process (Majozi, 2010)

The State Task Network was extended to the Resource Task Network by Pantelides, (1993) in which all resources required in batch process plant are described in a unified manner. The Resource Task Network (RTN) representation uses a uniform treatment framework for all available resources by assuming that processing and storage tasks consume and release resources at their beginning and ending times (Mendenz et al., 2006). The representation consists of a resource node and task node as depicted in Figure 2.37. The circle does not only represent states but also other resources required in the batch process like processing units and vessels.

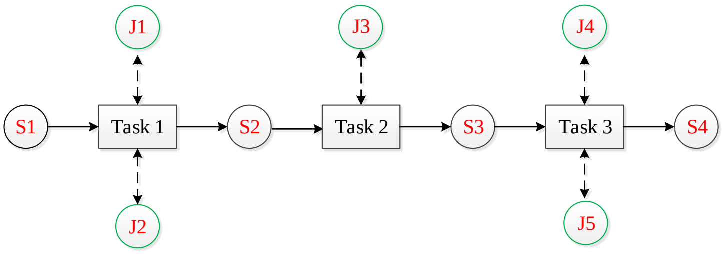

Figure 2.37. RTN representation of a batch process

2.16.3. Representation of events within the time horizon

Scheduling models rely on various concepts or techniques that arrange the event of schedule over time. These concepts or techniques greatly depend on the time representation employed in a particular model. Discrete time formulation employs global time interval as only option for both general networks and sequential processes. In continuous time formulation on the other hand, general network processes employ event-based models, which are categorized into global time points and unit-specific time events while sequential processes rely on approaches based on slots and precedence. Although the concept of slot and precedence are used in sequential processes initially, however it has also been extended to general network processes.

2.16.3.1. Global time intervals

In these type of models, predefined common and fixed time grids are used to represent different events taking place in different units such as starting or finishing time of tasks. A schematic representation of a global time interval concept is depicted in Figure 2.38 for a process involving two units allocated to process of five batches. Global time interval only allows the beginning and the ending of a task to occur at a point of the grid i.e. interval boundaries thereby results in reduction of the scheduling model to an allocation problem (Mendez, et al., 2006)

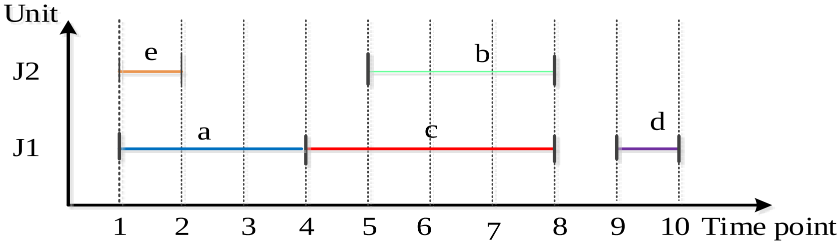

Figure 2.38. Global time intervals (discrete)

2.16.3.2. Global time point

The representation of global time point corresponds to a generalization of global time interval. Although, both concepts involve definition of a common time grid, however global time point requires a variable time interval which is not known priori as depicted in Figure 2.39 thereby making the duration of each interval to become a decision variable in the optimization (Mendez, et al., 2006, Floudas and Lin, 2004).

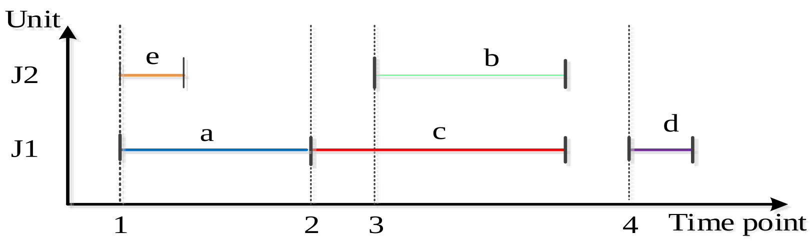

Figure 2.39. Global time points (continuous)

2.16.3.3. Unit-specific time events

These techniques use a definition of different variable time grid for each shared resource and allow the start of different tasks taking place in different units at the same time point to occur at different moments as depicted in Figure 2.40**.** The advantage of this technique compared to global event is that it usually requires fewer number of event points due to the heterogeneous location of event points for different units and defining an event as the starting of task only (Floudas, and Lin 2004).

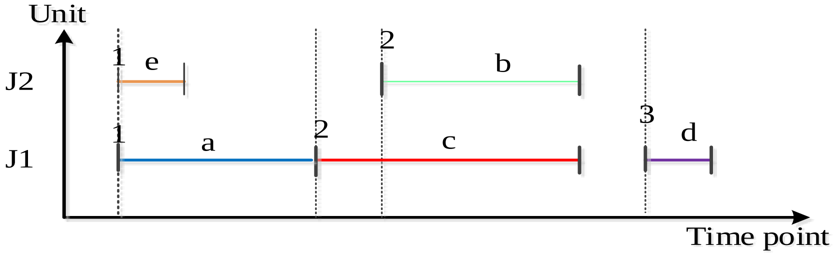

Figure 2.40. Unit specific time events (continuous)

2.16.3.4. Slot based techniques

These techniques are based on the definition of predefined time slots of unknown duration for each processing unit in order to allocate them to various tasks to be executed. Slot based models can be categorized into synchronous and asynchronous models as depicted in Figure 2.41.

Synchronous representations use common slots across all units while in asynchronous models, different slots are postulated for different units. This allows for more flexibility regarding timing decision and require fewer time slots due to its similarity with unit-specific time event.

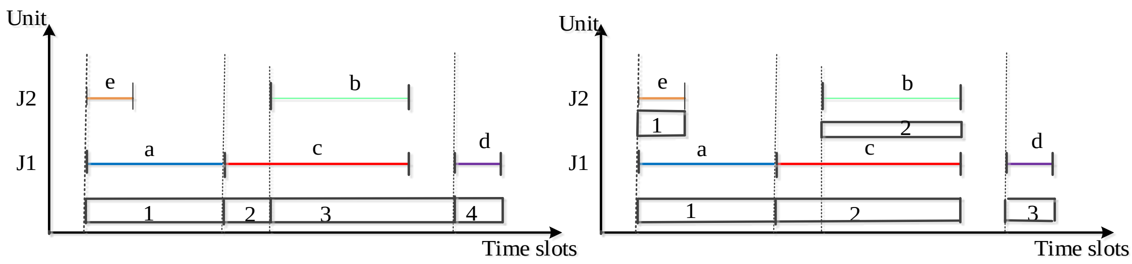

Figure 2.41. Slot based representations (continuous)

2.16.3.5. Precedence-based techniques

Precedence-based techniques are used in batch plants to determine the optimal task sequencing in each processing units and can be subdivided into immediate and general precedence models. In the immediate precedence models, only the immediate predecessor of a batch in a unit is considered while in general precedence models, consideration is given to all predecessors of a batch in a particular unit. An example to illustrate these two techniques is given in Figure 2.42. From the figure, task e is the immediate predecessor of task b performed in unit J1 while task a is the immediate predecessor of task c and task c is the immediate predecessor of task d in unit J2. However, in general precedence-based models, tasks a and c are both considered as predecessors of task d. The major advantage associated with the general precedence-based models is that a single sequencing variable can be defined for allocating each pair of batch tasks to the same-shared resource thereby result in simpler formulations when compared to the immediate precedenc- based models (Mendez et al., 2006). The major disadvantage associated with precedence-based models in general is that as the number of batches to be scheduled increase, the number of sequencing variables also increase and therefore generate large-scale models for real case application.

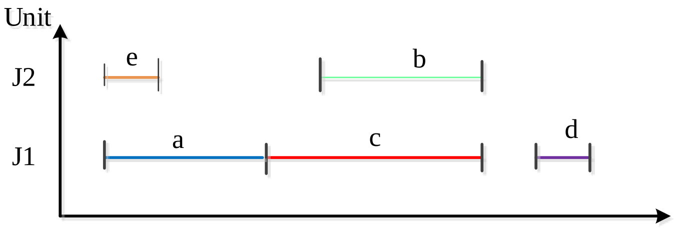

Figure 2.42. Precedence-based representation

2.17. Existing mathematical models on water management in shale gas exploration

Several studies in literature have focused on optimization strategies for water management in hydraulic fracturing.

Gay et al. (2012) focused on water treatment, transport and disposal as key concern in shale gas development. They developed a model to explore the cost implications of decisions about water treatment, transportation and disposal. The analysis considered a hypothetical well in the Marcellus play.

Kitwadkar (2014) addressed the logistic such as strategies for defining the location of a mobile treatment plant as the development plan continues over the development field. An approach, which depend on a multi criteria decision analysis (MCDA), was developed to optimise where the mobile treatment facilities will be located. The criterias for MCDA comprise well density, ease of access and piping minimisation if piping is used and volume of water produced. Three scenarios namely baseline, retroactive and proactive were considered to examine the effect of current and future circumstances on the proposed locations. The results from these scenarios were used to compare the piping distances from each well to the treatment facilities to minimize the cost of piping. The obtained results showed that the well density and water production are the significant criterial for placing the treatment facilities. The distance between wells generating wastewater to the treatment facilities and the distance between the treatment facilities to the wells, where the water will be reused played a significant role, as both cannot be fully satisfied at the same time.

Grossmann (2014) addressed the optimisation model for investment, operation and water management in shale gas supply chain. The objective is to develop an advanced mixed-integer programming method that optimise the design and operation of the supply chain infrastructure as well as optimising the use and cost of water management for hydraulic fracturing operation; while accounting for its environmental impact. However, most of the above publications area focused on the environmental impact of hydraulic fracturing or on the techno economic analysis and optimisation of specific water management options.

Yang et al. (2014a) proposed a mathematical model to optimise water use life cycle in shale development through a discrete-time scheduling formulation taking into account the uncertainty in water availability. The model considered a short-term operation with the objective of minimizing the expected transportation, treatment, storage and disposal cost taking into account the revenue from gas production. However, the focus of the model is mainly on the operational scheduling problem with no consideration regarding the associated strategic design decisions involve in shale gas development. Therefore, the model was later extended by Yang et al. (2015) to account for longer-term operations and capture the investment decisions for water management options such as pipelines, water treatment and impoundments in order to maximize the gross profit. The investment decision captured is only a part of investment decisions associated with shale gas development as it only focused on water management without capturing the aspect related to shale gas production.

Gao and You (2015a) proposed an optimisation model similar to the model proposed by Yang et al. (2015) for water management system design and operation in shale gas production process. The objective aimed at profit maximisation per unit of fresh water consumed. The model is formulated as a mixed-integer linear fractional programming (MILFP) problem, taking into account the economic performance and water use efficiency related to shale gas production. However, a fixed schedule was assumed for the wellpad fracturing, the schedule of the wellpads cannot be overlooked because of the impact it may have on the revenue.

Gao and You (2015b) developed a mathematical model for the life cycle economic and environmental optimization of shale gas supply chain network design and operations. The proposed model aimed at the maximization of both economic and environmental performance of shale gas network through developing a functional unit-based life cycle optimization. The economic indicator is based on the levelized cost of electricity generated from shale gas while environmental indicator is taken as the greenhouse gas emissions per unit amount of energy generated.

Bartholomew and Mauter (2016) developed a multiobjective MILP model that relied on the discrete time scheduling formulation of Yang et al. (2015) which aimed in determining water management approach that promotes reduction of financial, human health and environment (HHE) cost related to water management shale gas production. The model described a systematic analysis of the trade-offs in financial costs and the impacts of HHE related to several water management approaches used in hydraulic fracturing. The model demonstrated that the criteria pollutants and greenhouse gases are important with respect to financial costs of water management, therefore needs to be incorporated in water management decision.

Lira-Barragán et al. (2016) developed an optimization framework to deal with the uncertainties associated with management of water in shale gas production. The major variations related to hydraulic fracturing water usage and the time-based return of flowback water were considered and scenarios were generated to manipulate the uncertainties. The proposed formulation aimed at finding a strategic plan that put into consideration the risks associated with the uncertainties in shale gas developments. Probability curves of costs and water requirement were generated for visualization of risk associated with the uncertainties and for adequate equipment sizing. However, the proposed formulation considered a fixed schedule to implement the approach.

Guerra et al. (2016) proposed a mixed integer quadratically constrained programming (MIQCP) mathematical framework that integrate water management and design of shale gas supply chain. Different modelling, simulation and optimization tools usually used in the energy sector to evaluate how viable new energy sources are both technically and economically were considered. The objective is the maximization of the net present value. The proposed model showed that a better decision in the production of gas and wastewater is possible if different alternatives for the design of well-pad are included in the supply chain design.

Shih et al. (2016) proposed a multiobjective framework for hydraulic fracturing water management, which incorporate four major decision bodies in shale gas development. These are the oil and gas well developers and operators, centralized wastewater treatment facility planners and operators, environmental regulators and social planners. The proposed model can be used for simultaneous decision regarding water, infrastructure and environmental issue in shale gas development. However, the proposed formulation is still at the development stage and yet to be applied to a case study.

López‑Díaz et al. (2018) proposed a multi-objective optimization framework for the optimal design of efficient water network in shale gas production taking into consideration the economic and environmental criteria. The economic aspects aimed in minimizing the total annualised cost associated with the water network while the environmental aspect accounted for the minimisation of effect associated with total dissolved solid concentration in discharged wastewater streams and freshwater consumption using the eco-indicator 99 methodology. The approach aimed in determining the freshwater requirements, volumes of flowback water collected and later treated, reused and disposed, along with the optimal storage and treatment units capacities. However, as the developed framework required fracking schedule to implement the approach, fixed schedule is used for the implementation.

Other publications have focused mainly on water treatment technologies available for flowback/produced water in hydraulic fracturing.
Carrero –Parreño et al. (2017) developed an optimization model for the simultaneous synthesis of water pre-treatment systems (WPS) in which a multistage superstructure is proposed for the optimal WPS design, comprising numerous water pre-treatment options. Hence, the optimal sequence of pre-treatment with minimum cost, in accordance with the inlet water composition and wastewater-desired destination is identified using the superstructure. However, the water pre-treatment systems were modelled via short-cut models based on contaminant removal ratios.

Onishi et al. (2017a) proposed a rigorous optimization framework that considered the synthesis of single and multiple-effect evaporation (SEE/MEE) systems simultaneously, taking into consideration the mechanical vapor recompression (MVR) and energy recovery. The objective aimed at enhancing the energy efficiency of the system by reducing brine discharges thus zero liquid discharge is achieved. The proposed formulation is majorly designed for purification of produced water with high salinity.

Onishi et al. (2017b) also developed a non-linear programming (NLP) optimization approach for the simultaneous synthesis of single and multiple-effect evaporation (SEE/MEE) systems design, with vapor recompression cycle and thermal integration for the treatment of flowback water with high-salinity in which the system is investigated for zero liquid discharge. Evaluation to determine the optimal configuration of the process under various feed salinity was carried out using sensitivity analysis. The proposed formulation indicates that the reduction in the brine discharges leads to a cost effective process, thereby promotes decrease in the environmental impact associated with energy consumption and disposal of waste.

Elsayed et al. (2015) proposed an optimization method based on multi-period formulation for the treatment of shale gas flowback water, which take into account the fluctuation in the contaminant concentration and flowrate using membrane distillation. The model highlights the relationship between water recovery and cost and shows that the conflicting objective regarding cost and water recovery can be effectively dealt with using the proposed approach. However, these treatment technologies were modelled as standalone and not within the overall shale gas and water network.

Some other studies have also explored the possibility of using the gas that would otherwise be flared in shale production as a source of energy required in water management. Wikramanayake and Bahadur (2016) introduced an idea of utilizing the energy of natural gas (that would have been flared) for onsite atmospheric water harvesting (AWH) for oilfield operations. Several technical pathways to harvest atmospheric moisture using the energy of natural gas were analysed and a modelling framework was developed to quantify the dependence of water harvest rates on flared gas volumes and ambient weather.

Glaizer et al. (2014) proposed an analytical framework to understand the viability of simultaneous mitigation of water and gas flaring challenges face in oil and gas industries by using energy from flared natural gas for on-site treatment of wastewater, thus decreasing flared gas, quantity of wastewater, and the amount of freshwater required for subsequent shale production. However, it needs to be mentioned that the work by Glazer et al. (2014) is done based on analytical framework and not in the context of mathematical optimization.

2.18. Research gaps

The literature review has highlighted the importance of water and wastewater management in shale gas development exploring the tools available to achieve this goal and research on the efficient water management strategies are still ongoing. Water and energy usage in the process industries are interdependent. The process of hydraulic fracturing requires a large volume of water and energy is also required to treat wastewater generated from hydraulic fracturing effectively. Most of the existing studies on shale gas water management only focused on flowback/ produced water treatment and technologies available for flowback water pre-treatment or treatment. Others considered the design and synthesis of only the wastewater treatment subnetworks without considering the background process i.e. the scheduling of wellpads from where the flowback water is generated.

The studies that focused on the background process however have either adopted the discrete time scheduling formulation for the wellpad fracturing or assumed a fixed schedule. A limitation of discretizing the time horizon is the explosive binary dimension that could lead to higher computational time and suboptimal solution. Assuming a fixed schedule is a huge drawback as this has a great effect on the overall profit.

In addition, most of the research that accounted for wastewater treatment within the background process of hydraulic fracturing have represented the wastewater treatment unit as a "black box" or using short-cut models due to the complexity of the regenerator design accounting for single contaminant mainly total dissolve solid (TDS). The use of "black box" approach and short-cut models adopted to simplify the regenerator performance do not explicitly account for the full design specifications, true cost representation of the process and associated energy.

Furthermore, studies available on utilization of gas that would otherwise be flared have focused on analytical framework for thermal energy-based regenerators. Missing from literature is a synthesis and optimization approach for an integrated water, natural gas infrastructure and membrane network that optimizes water and energy simultaneously in hydraulic fracturing operation using continuous time mathematical formulation for scheduling. This is achieved by embedding a subnetwork of detailed MD and UF regenerator models into water and shale gas network model. The regenerator models incorporate detailed cost correlations that are functions of the design variables and the feasibility of using gas that would otherwise be flared as source of electrical and thermal energy for the regenerators is investigated.

References

Abass, M., Majozi, T., 2016. Optimization of integrated water and multiregenerator membrane systems. Industrial and Engineering Chemistry Research 55, 1995-2007.

Acharya, H. R., Henderson, C., Matis, H., Kommepalli, H., Moore, B., Wang, H., 2011. Cost-effective recovery of low-TDS frac flowback water for re-use, US Department of Energy, National Energy Technology Laboratory, Morgantown, WV.

Adams, M. B., Pamela J. E., Ford, W.M., Johnson, J.B., Schuler, T.M., Gundy, M.T., Wood, F., 2011. Effects of development of a natural gas well and associated pipeline on the natural and scientific resources of the Fernow Experimental Forest. General Technical Report NRS-76. Newtown Square, PA: Northern Research Station, Forest Service, US Department of Agriculture.

Adekola, O., Majozi, T., 2011. Wastewater minimization in multipurpose batch plants with a regeneration unit: Multiple contaminants. Computers and Chemical Engineering 35, 2824-2836.

Adekola, O., Majozi, T., 2017. Wastewater minimization in batch plants with sequence dependent changeover. Computers and Chemical Engineering 97, 85-103.

Aguilera, R.F., Radetzki, M., 2013. Shale gas and oil: fundamentally changing global energy markets. Oil and Gas Journal. https://www.ogj.com/articles/print/volume-111/issue-12/exploration-development/shale-gas-and-oil-fundamentally-changing-global-energy-markets.htm. Accessed 26 December 2018.

Ahmetovic, E., Grossmann, I. E., 2010. Strategies for the Global Optimization of Integrated Process Water Networks. ESCAPE 20.

Ahmadun, F., Pendashteh, A., Abdullah, L.C., Biak, D.R. A., Madaeni, S.S., Abidin, Z.Z., 2009. Review of technologies for oil and gas produced water treatment. Journal of Hazardous Material 170, 530-551.

Al-Douri, A., Sengupta, D., El-Halwagi, M.M., 2017. A review of downstream processing of chemical and fuels. Journal of Natural Gas Engineering, Volume 45,pp. 436-455.

Alkhudhiri, A., Darwish, N., Hila, N., 2012. Membrane distillation: A comprehensive review, Desalination 287, 2-18.

Almató, M., Espuna, A. & Puigjaner, L., 1999. Optimization of water use in batch process industries. Computers and Chemical Engineering 23, 1427-1437.

Alva-Argaez, A., Kokossis, A.C., Smith, R., 1998. Waste water minimization of industrial systems using an integrated approach. Computers and Chemical Engineering 22, 5741-5744.

Almutlaq, A.M, Kazantzi, V., El-Halwagi, M.M., 2005. An algebraic approach to targetting waste discharge and impure fresh usage via material recycle/reuse network. Clean Technology and Environmental Policy 7(4), 294-305

Anselme, C., Jacobs, E.P., 1996. Ultrafiltration, in: Water treatment membrane processes. (ed.) Mallevialle, J., Odendaal, P.E., Wiesner, M. R. American Water Works Association Research Foundation. Lyonnaise des Eaux. Water Research Commission of South Africa. McGraw-Hill.

Arthur, J.D., Bohm, B., Layne, M., 2008. Hydraulic fracturing considerations for natural gas wells of the Marcellus Shale. The Ground Water Protection Council 2008 Annual Forum, Cincinnati, OH, September 21–24, 1-16.

Bagajewicz, M.J., 2000. A review of recent design procedures for water networks in refineries and process plants. Computer and Chemical Engineering 24, 2093-2113.

Bartholomew, T.V., Mauter, M.S., 2016. Multiobjective optimization model for minimizing cost and environmental impact in shale gas water and wastewater management. Journal of ACS Sustainable Chemistry and Engineering 4, 3728-3735.

Bandyopadhyay, S., Ghanekar, M. D., Pillai, H. K., 2006. Process water management. Industrial and Engineering Chemistry Research 45(15), 5287-5297.

Behdani, B., Pishvaie, M.R., Rashtchian, D., 2007. Optimal scheduling of mixed batch and continuous processes incoporating utility aspects. Chemical Engineering and Processing 46, 271-281.

Bianco research, 2017. The shifting geography of U.S. oil and gas production. Accessed 6 September, 2019.

Bole-Rentel, T., 2015. Shale Gas 101: Introduction to water impacts. WWWF Technical report, 1-64.

Boschee, P., 2014. Produced and flowback water recycling and reuse - economics, limitations, and technology. Society of Petroleum Engineers 3(1).

Blumsack, S., 2017. Production decline for shale gas wells, energy markets, policy, and regulation (EME 801), The Pennsylvania State University, USA.

Buonomenna, M.G., Golemme, G., Perrotta, E., 2012. Membrane operations for industrial applications, In: Advances in Chemical Engineering, (eds) Z. Nawaz, InTech.

Buabeng-Baidoo, E., Majozi, T., 2016. Industrial and Engineering Chemistry Research 54, 9394−9406.

Burnham, A., Han, J., Clark, C.E., Wang, M., Dunn, J.B., Palou-Rivera, I., 2011. Life-cycle greenhouse gas emissions of shale gas, natural gas, coal, and petroleum. Environmental Science and Technology 46, 619–627.

Carrero-Parreño, A., Onishi,V.C., Salcedo-Díaz, R., Ruiz-Femenia, R., Fraga, E. S., Caballero, J.A., Reyes-Labarta, J. A., 2017. Optimal pretreatment system of flowback water from shale gas production. Journal of Industrial and Engineering Chemistry Research 56, 4386−4398.

Centre for Climate and Energy Solutions (CCES), 2018. Natural Gas. https://www.c2es.org/content/natural-gas/. Accessed 26 November 2018.

Chen, C.L., Lee, J.Y., 2008. A graphical technique for the design of water-using networks in batch processes. Chemical Engineering Science, 63, 3740-3754.

Chaturvedi, N. D., Bandyopadhyay, S., 2012. A rigorous targeting to minimize resource requirement in batch processes. Industrial and Engineering Chemistry Research 51, 8015-8024.

Chaturvedi, N. D., Bandyopadhyay, S., 2014a. Simultaneous targeting for the minimum water requirement and the maximum production in a batch process. Journal of Cleaner Production 77, 105-115.

Chaturvedi, N. D., Manan, Z. A., Alwi, S. R. W., Bandyopadhyay, S., 2016. Effect of multiple water resources in a flexible-schedule batch water network. Journal of Cleaner Production,1-8.

Cheng, K. F., Chang, C. T., 2007. Integrated water network design for batch processes. Industrial and Engineering Chemistry Research 46, pp. 1241-1253.

Dahm, K., Chapman, M., 2014. Produced water treatment primer: Case studies of treatment applications. Science and Technology Research Report, 1-70.

Dhamdhere, D. H., 2006. Operating systems: A concept-based Approach. 2nd ed. New Delhi: Tata McGraw-Hill.

Dhole, V. R., Ramchandi, N., Tainsh, R. A., Wasilewski, M., 1996. Make your process water pay itself. Chemical Engineering,103(1), 100-103.

Energy Information Administration (EIA), 2016. Shale gas production drives world natural gas production growth. Accessed on 6 September, 2019.

Energy Information Administration (EIA), 2018. Delivery and Storage of Natural Gas. Accessed on 11 November, 2018.

https://www.eia.gov/energyexplained/index.php?page=natural_gas_delivery

Energy Information Administration (EIA), 2017, Where our natural gas comes from https://www.eia.gov/energyexplained/index.php?page=natural_gas_where.Accessed 11November, 2018.

Energy Information Administration (EIA), 2018. Natural gas storage. 2018 http://naturalgas.org/naturalgas/storage/. Accessed 11 November, 2018.

Energy Information Administration (EIA), 2012. Annual Energy Outlook 2012 with Projections to 2035. http://www.eia.gov/forecasts/aeo/pdf/0383(2012).pdf. Accessed 7 November, 2018.

Energy in Texas: Educational series, 2013. Technical report. Texas Department of Transportation. https://consumerenergyalliance.org/2013/08/energy-in-texas/. Accessed 7 December 2018.

El-Halwagi, M. M., Hamad, A. A., Garrison, G. W., 1996. Synthesis of waste interception and allocation networks. Journal of American Institute of Chemical Engineer 42(11), 3087–3101.

El-Halwagi, M. M., 1997. Pollution Prevention through Process Integration, Academic Press.

El-Halwagi, M. M., 2006. Process Integration, Elsevier.

El-Halwagi, M. M., Gabriel, F., Harrel, D., 2003. Rigorous Graphical Targeting for Resource Conservation via Material Reuse/Recycle Networks. Industrial Engineering and Chemical Research , 42(2003), 4319-4328.

Elsayed, N.A., Barrufet, M.A., Eljack, F.T., El-Halwagi, M.M., 2015. Optimal design of thermal membrane distillation systems for the treatment of shale gas flowback water. International Journal of Membrane Science and Technology 2, 1-9.

Elsayed, N.A., Barrufet, M.A., El-Halwagi, M.M., 2013. Integration of thermal membrane distillation networks with processing facilities. Journal of Industrial and Engineering Chemistry Research 53, 5284-5298.

Ellsworth, W. L., 2013. Injection-Induced Earthquakes. Science 341(6142).

Environmental report management (ERM), 2014. Recovered water management study in shale wells. ERM project 0243719 final report, 1-61.

Environmental Protection Agency (EPA), 2015b. Case study analysis of the impacts of water acquisition for hydraulic fracturing on local water availability. Washington, DC. https://www.epa.gov/hfstudy/case-study-analysis-impacts-water-acquisition-hydraulic-fracturing-local-water-availability

Environmental Protection Agency (EPA), 2012. Overview of final amendments to air regulations for the oil and natural gas industry: Fact Sheet. http://www.epa.gov/airquality/oilandgas/pdfs/20120417fs.pdf.

Energy Information Administration (EIA), 2015. Energy explained : Where our natural gas comes from. https://www.eia.gov/energyexplained/index.php?page=natural_gas_where. Accessed 12 December 2018.

Faria, D. C., Bagajewicz, M. J., 2010a. On the appropriate modelling of process plant water systems. American Institute of Chemical Engineers 53(3), 668-689.

Floudas, C. A., Lin, X., 2004. Continuous-time versus discrete-time approaches for scheduling of chemical processes: a review. Computers and Chemical Engineering 28, 2109-2129.

Foo, D. C. Y., Manan, Z. A., Tan, Y. L., 2006. Use cascade analysis to optimize water networks. Chemical Engineering Progress 102(7), 45–52.

Foo, C. Y., Manan, Z. A., Tan, Y. L., 2005. Synthesis of maximum water recovery network for batch process systems. Journal of Cleaner Production 13, 1381-1394.

Foo, D. C. Y., 2009. State-of-the-art review of pinch analysis techniques for water network synthesis. Industrial and Engineering Chemistry Research , 48(11), 5125-5159.

Foo, D. C. Y., 2010. Automated targeting for batch process integration. Industrial and Engineering Chemistry Research 49, 9899-9916.

Food and Agriculture Organization of the United Nations (FAO), 2011. The state of the world's land and water resources for food and agriculture: Managing systems at risk.

Food and Agriculture Organization of the United Nations (FAO), 2014f. Country Report: Russian Federation. Global Forest ResourcesAssessment 2015. Rome, Italy. 87

Food and Agriculture Organization of the United Nations (FAO), 2016. The State of World Fisheries and Aquaculture 2016.Contributing to food security and nutrition for all. Rome, Italy. 1-200

Fracking around the globe (FAG), 2018. Fracking and the Environment, https://frackingaroundtheglobe.wordpress.com/3-fracking-and-the-environment/, accessed 6 November 2018.

Freshwater watch (FWW), 2018. https://freshwaterwatch.thewaterhub.org/content/water-limited-resource. Accessed, 7th November 2018.

Gabriel, F. B., El-Halwagi, M. M., 2005. Simultaneous synthesis of waste interception and material reuse networks: Problem reformulation for global optimization. Environmental Progress 24(2), 171–180.

Gay, M.O., Fletcher, S., Meyer, N., Gross, S., 2012. Water Management in Shale Gas Plays. Technical Report. HIS Water White Paper, 1-10.

Gay, M., Slaughter, A., 2014. Water management, a new paradigm for the oil and gas sector. https://ihsmarkit.com/research-analysis/q11-water-management-a-new-paradigm-for-the-oil-and-gas-sector.html. Accessed 12 December 2018.

Gao, J., You, F., 2015a, Optimal design and operations of supply chain networks for water management in shale gas production: MILFP model and algorithm for the water-enegy nexus. Journal of American Institute of Chemical Engineers 61, 1184-1208.

Gao, J., You, F., 2015b. Shale gas supply chain design and operations toward better economic and life cycle environmental performance: MINLP model and global optimization algorithm, ACS Sustainable Chemistry and Engineering 3, 1282-1291.

Gao, J., You, F., 2015c. Deciphering and handling uncertainty in shale gas supply chain design and optimization: Novel modelling framework and computational efficient solution algorithm. Journal of American Institute of Chemical Engineers 61, 3739-3760.

Gao, J., He, C., You, F., 2017. Shale gas process and supply chain optimization, in: Advances in Energy Systems Engineering (eds) G.M. Kopanos. Springer International Publishing, Switzerland.

Gao, J., You, F., 2017aa. Design and optimization of shale gas energy systems: Overview, research challenges, and future directions. Computers and Chemical Engineering 106, 699–718.

Gao, J., You, F., 2017. Game theory approach to optimal design of shale gas supply chains with consideration of economics and life cycle greenhouse gas emissions. Journal of AmericanInstitute of Chemical Engineers 63, 2671-2693.

General Accountability Office (GAO), 2012. Information on the quantity, quality, and management of water produced during oil and gas production. GAO-12-156. Washington, DC.

Gianadda, P., Brouckaert, C.J., Sayer, R., Buckley, C.A., 2002. The application of pinch analysis to water. Regent and effluent management in a chlor-alkali facility. Water Science and Technology, 46(9), 21-28.

Glazer, Y.R., Kjellsson, J.B., Sanders, K.T., Webber, M.E., 2014. Potential for using energy from flared gas for on-site hydraulic fracturing wastewater treatment in Texas. Environmental Science and Technology Letter 1, 300-304.

Glazer, Y. R., Davidson, F. T., Webber, M. E., 2015. Flaring our way out of a water crisis. Earth magazine. accessed 25 April 2017.

Gouws, J.F., Majozi, T., Foo, D.C.Y., Chen, C., Lee, J., 2010. Water minimization techniques for batch processes. Industrial Engineering Chemistry Research 49, 8877–8893.

Gouws, J.F., Majozi, T., 2008. Impact of multiple storage in wastewater minimisation for multicontaminant batch plants: Towards zero effluent. Industrial Engineering Chemistry Research 47, 369-379.

Gouws, J.F., Majozi, T., 2009. Usage of inherent storage for minimisation of wastewater in multipurpose batch plants. Chemical Engineering Science 64, 3545-3554.

Gregory, K.B., Vidic, R.D., Dzombak, D.A., 2011. Water management challenges associated with the production of shale gas by hydraulic fracturing. Elements 7(3), 181-186.

Grubert, E., Kitasei, S., 2010. How energy choices affect fresh water supplies: A comparison of US Coal and Natural Gas. Worldwatch Institute Briefng Paper 2, Washington, DC, 2010.

Ground Water Protection Council (GWPC), All Consulting (AC), 2009. Modern shale gas development in the United States: A Primer, Prepared for the U.S. Department of Energy, Office of Fossil Energy, and National Energy Technology Laboratory. 1-96.

Ground water protection council (GWPC), 2018. Chemical use in hydraulic fracturing. https://fracfocus.org/water-protection/drilling-usage. Accessed 7 December 2018.

Grossmann, I.E., 2014. Optimization Models for Optimal Investment, Drilling and Water Management in Shale Gas Supply Chains. A CPSE Seminar.

Guadix, A., Sorensen, E., Papageorgiou, L.G., Guadix, E.M., 2004. Optimal design and operation of continuous ultrafiltration plants. Journal of Membrane Science 235, 131-138.

Guerra, O.J., Calderon, A.J., Papageorgiou, L.G., Siirola, J.J., Reklaitis, G.V., 2016. An optimization framework for the integration of water management and shale gas supply chain design. Journal of Computer and Chemical Engineering 92, 230-255.

Guerra, K., Dahm, K., Dundorf, S., 2011. Oil and gas produced water management and Beneficial use in the western United States.Science and Technology Program Report 57, 1-129.

Gunaratnam, M., Alva-Argáez, A., Kokossis, A., Kim, J. K., Smith, H., 2005. Automated Design of Total Water Systems. Industrial Engineering and Chemical Research 44(3), 588-599.

Groundwater Protection Council (GWPC), 2018. Chemical use in hydraulic fracturing. https://fracfocus.org/water-protection/drilling-usage. Accessed 27 October, 2018.

Hallale, N., 2002. A New Graphical Targeting Method for Wastewater Minimization. Advanced Environmental Research, 6(30), 377-390.

Harjunkoski, I., Maravelias, C.T., Bongers, P., Castro, P.M., Engell, S., Grossmann, I.E., Hooker, J., Méndez, C., Sand, G., Wassick, J., 2014. Scope for industrial applications of production scheduling models and solution methods. Computers and Chemical Engineering, V 62, 161-193.

Hasaneen, R., El-Halwagi, M.M., 2017. Integrated process and microeconomic analyses to enable effective environmental policy for shale gas in the United States, Journal of Clean Technologies and Environmental Policy, 19, 1775-1789.

Hayes, T., Severin, B. F., 2012. Barnett and Appalachian shale water management and reuse technologies. Project report by Gas Technology Institute for Research Partnership to Secure Energy for America (RPSEA); RPSEA: Houston, TX, 1−125.

Hefley, W.E., Seydor, S.M., Bencho, M.K., Chappel, I., Dizard, M., Hallman, J., Herkt,J., Jiang, P.J., Kerec, M., Lampe, F., 2011. The Economic Impact of the Value Chain of a Marcellus Shale Well. Pitt Business Working Papers.University of Pittsburgh.

Hoffman, J., 2012. Potential health and environmental effects of hydrofracking in the Williston Basin, Montana. Geology and Human Health .Topical Resources. Accessed 7 December, 2018. https://serc.carleton.edu/NAGTWorkshops/health/case_studies/hydrofracking_w.html

Holtzhausen, L., 2002. The war for water, fighting the battle for the last drop. Water Sewage and Effluent 22 (2), 26-29.

Howarth, R.W., Santoro, R., Ingraffea, A., 2011. Methane and the greenhouse-gas footprint of natural gas from shale formations. Climatic Change 106, 679–690.

Holditch, S.A., 2012. Getting the gas out of the ground. Chemical Engineering Progress 108, 41–48.

Hughes, J.D., 2014. Drilling deeper: A reality check on U.S. government forecasts for a Lasting tight oil & shale gas boom. Post Carbon Institute, California, Santa Rosa 95404.1-307.

Hughes, J. D., 2013. A reality check on the shale revolution. Nature 494(7437), 307–308.

International Energy Agency (IEA), 2012b. World energy outlook 2012. IEA/OECD, Paris, France.

Karuppiah, R., Grossmann, I. E., 2006. Global optimisation for the synthesis of integrated water systems in chemical processes. Computers and Chemical Engineering 30, 650-673.

Kamrava, S., Gabriel, K.J., El-Halwagi, M.M., Eljack, F.T., 2015. Managing abnormal operation through process integration and cogeneration systems. Journal of Clean Technology and Environmental Policy 17, 119-128.

Kazi, M.K., Eljack, F., Elsayed, N.A., El-Halwagi, M.M., 2016. Integration of energy and wastewater treatment alternatives with process facilities to manage industrial flares during normal and abnormal operations: A multi-objective extendible optimization framework. Journal of Industrial and Engineering Chemistry Research 55, 2020–2034.

Khor, C.S., Foo, D.C., El-Halwagi, M.M., Tan, R.R., Shah, N. A., 2011. Superstructure optimization approach for membrane separation-based water regeneration network synthesis with detailed nonlinear mechanistic reverse osmosis model. Industrial and Engineering Chemistry Research 50, 13444–13456.

Khor, C., Chachuat , B., Shah, N., 2012. A superstructure optimisation approach for water network synthesis with membrane separation-based regenerators. Computers and Chemical Engineering, 42, 48-63.

Kim, J.K., Smith, R., 2004. Automated design of discontinuous water systems. Trans IChemE, Part B, Process Safety and Environmental Protection 82(B3), 238-248.

Kitwadkar, A.H., 2014. GIS based location optimization for mobile produced water treatment facilities in shale gas operations. Master Thesis. Colorado State University, Colorado.

Klemeš, J.J., 2013. Handbook of process integration (PI): Minimization of energy and water use. (eds) Klemes, J.J. Woodhead publishing, Cambridge.

Kondili, E., Pantelides, C.C., Sargent, R. W. H., 1993. A general algorithm for short term scheduling of batch operations-I. MILP formulation. Computers and Chemical Engineering, V 17, 211-227.

Kuwayama, Y., Olmstead, S., Krupnick, A., 2015a. Water quality and quantity impacts of hydraulic fracturing. Current Sustainable/Renewable Energy Reports 2(1), 17-24.

Krupnick, A., 2013. Managing the risks of shale gas – resources for the future. Centre for Energy Economics and Policy.

Lattanzio, R. K., 2016. An overview of air quality issues in natural gas systems. CRS Report R42833,1-21.

Lee, S. J., Alwi, S. R. W., Lim, S. L., Manan, Z. A., 2014. Minimum water network design for fixed schedule and cyclic operation batch processes with minimum storage capacity and inter-connections. Journal of Cleaner Production 77, 65-78.

Lewis, A. 2012. Wastewater generation and disposal from natural gas wells in Pennsylvania, Master’s Thesis, Duke University, Durham.

Li, B. H., Chang, C. T., 2006. A mathematical programming model for discontinuous water-reuse system design. Industrial and Engineering Chemistry Research 45, 5027-5036.

Lira-Barragán, L., Ponce-Ortega, J.M., Guillén-Gosálbez, G.,El-Halwagi, M.M., 2016. Optimal water management under uncertainty for shale gas production. Journal of Industrial and Engineering Chemistry Research 55, 1322–1335.

Liu, Y., Yuan, X., Luo, Y., 2007a. Synthesis of water utilization system using concentration interval analysis method (I) Non-mass transfer based operation. Chinese Journal of Chemical Engineering 15, 361-368.

Liu, Y., Yuan, X., Luo, Y., 2007b. Synthesis of water utilization system using concentration interval analysis method (II) discontinuous process. Chinese Journal of Chemical Engineering 15(3), 369-375.

Lutz, B.D., Lewis, A.N., Doyle, M.W., 2013, Generation, transport, and disposal of wastewater associated with Marcellus shale gas development. Journal of Water Resources Research 49, 647-656.

Mack, C.L., 2005. Screening of technologies for the recovery of rhodium (III) metal ions from a precious metal refinery wastewater. Master Thesis. Rhodes University, South Africa.

Mafukidze, N.Y., Majozi, T., 2016. Synthesis and optimisation of an integrated water and membrane network framework with multiple electrodialysis regenerators. Computers and Chemical Engineering 85, 151–161.

Majozi, T., 2010. Batch Chemical Process Integration: Analysis, Synthesis and Optimisation. London: Springer.

Majozi, T., Brouckaert, C. J., Buckley, C. A., 2006. A graphical technique for wastewater

minimization in batch processes, Journal of Environmental Management 78: 317-329.

Majozi, T., 2005a. An effective technique for wastewater minimization in batch processes. Journal of Cleaner Production 13,1374-1380.

Majozi, T., 2005b. Wastewater minimization using central reusable water storage in batch plants. Computers and Chemical Engineering 29, 1631-1646.

Manan, Z. A., Tan, Y. L., Foo, D. C. Y., 2004. Targeting the minimum water flowrate using water cascade analysis. American Institute of Chemical Engineers Journal, 50(2004), 3169-3183.

Marano, J., Spivey, J.J., Morreale, B., 2015. Chemical synthesis. Chemical Engineering Progress 111(8), 58-62.

Mendez, C. A., Cerda, J., Grossmann, I.E., Harjunkoski, I., Fahl., M., 2006. State-of-the-art review of optimization methods for short-term scheduling of batch processes. Computers and Chemical Engineering, 30, 913-946.

Mielke, E., Anadon, L.D., Narayanamurti, V., 2010. Water consumption of energy resource extraction, processing, and conversion: A review of the literature for estimates of resource extraction, processing to fuels, and conversion to electricity. Discussion Paper #2010-15. Energy Technology Innovation Policy Discussion Paper Series, 1-52.

Mockus, L., Reklaitis, G.V., Continuous time representation approach to batch and continuous process scheduling.1. MINLP formulation. Journal of Industrial Engineering Chemistry Research 38, 197-203.

Napoles-Rivera, F., Ponce-Ortega, J. M., El-Halwagi, M. M., Jimenez-Gutierrez, A., 2010. Global optimization of mass and property integration networks with in-plant property interceptors. Chemical Engineering Science, 65(15), 4363–4377.

Natural gas (Natgas), 2013.Natural gas and the environment. http://naturalgas.org/environment/naturalgas/. Accessed 7 December, 2018.

National water act, 1998. Guide to the national water act.Department of Water Affairs and Forestry. South Africa.

NETL, 2013. Modern shale gas development in the United States: An update. National Energy Technology Laboratory. https://www.netl.doe.gov/File%20Library/Research/Oil-Gas/shale-gas-primer-update-2013.pdf. Accessed 6, November 2018.

Ng, D., Foo, C.Y., Rabie, A., El-Halwagi, M.M., 2008. Simultaneous synthesis of property-based water reuse/recycle and interception networks for batch processes. American Institute of Chemical Engineer 54 (10), 2624–2632.

Oke, D., Mukherjee, R., Sengupta, D., Majozi, T., El-Halwagi, M.M., 2019. Optimization of water-energy nexus in shale gas exploration: From production to transmission. Energy, 183, 651-669.

Oke, D., 2014. Purification of platinum group metals process stream using saccharomyces cerevisiae waste yeast biomass. Master Thesis. University of Witwatersrand, South Africa.

Oliver, P., Rodriguez, R., Udaquiola, S., 2008. Water use optimization in batch process industries. Part 1: design of the water network. Journal of Cleaner Production16, 1275-1286.

Onishi, V.C., Carrero-Parreño, A., Reyes-Labarta, J.A., Fraga, E. S., Caballero, J.A., 2017a. Desalination of shale gas produced water: A rigorous design approach for zero-liquid discharge evaporation systems. Journal of Cleaner Production 140, 1399-1414.

Onishi, V.C., Carrero-Parreño, A., Reyes-Labarta, J.A., Ruiz-Femenia, R., Salcedo-Díaz, R.E., Fraga, S., Caballero, J.A., 2017b. Shale gas flowback water desalination: Single vs multiple-effect evaporation with vapor recompression cycle and thermal integration. Desalination 404, 230-248.

Organisation for Economic Co-operation and Development (OECD), 2012a. OECDWater Outlook to 2050: The OECD calls for early and strategic action. OECD Publishing, Paris.

Pantelides, C.C., 1993. Unified framework for optimal process planning and scheduling, in Proceedings of the second international conference on foundations of computer-aided process operations. (Eds.)Rip-pin, D.W.T., Hale, J.C., Davis, J. Crested Butte, Colorado, 253-274.

Pinto, J.M., Grossmann, I.E., 1998. Assignment and sequencing models for the scheduling of process systems. Annals of Operation Research 81, 433-466.

Polley, G.T., Polley, H.L., 2000. Design better water networks. Chemical Engineering Progress 96, 47–52.

Ponce-Ortega, J.M., Hortua, A.C., El-Halwagi, M.M., Jiménez -Gutierrez, A., 2009. A property-based optimization of direct recycle networks and wastewater treatment processes. American Institute of Chemical Engineer 55 (9), 2329–2344.

Ponce-Ortega, J.M., Jime´nez-Gutierrez, A., El-Halwagi, M.M., 2010. Global optimization

for the synthesis of property-based recycle and reuse networks including environmental constraints. Computers and Chemical Engineering 34, 318–330.

Poplewski, G., Walczyk, K., Jezowski, J., 2010. Optimization-based method for calculating water networks with user specified characteritics. Chemical Engineering Research and Design 88(2009), 109-120.

Prakash, R., Shenoy, U. V., 2005. Targeting and desgn of water networks for fixed flowrates and fixed contminants load operations. Chemical Engineering Science , 60(1), 255-268.

Ramirez, P., 2009. Reserve pit management: Risks to migratory birds. Environmental Contaminants Program, U.S. Fish & Wildlife Service, Region 6.

Ratner, M., Tiemann, M., 2015. An Overview of Unconventional Oil and Natural Gas: Resources and Federal Actions. Congress Research services Report, 1-34.

Rahm B. G., Riha, S. J., 2014. Evolving shale gas management: water resource risks, impacts, and lessons learned. Journal of Environmental Science Processes and Impacts,16(1400), 1-13.

Reyntjens, K., Johnson, A., 2013. Ensuring sustainable shale operations through water management. Dow Water & Process Solutions, 1-94.

Rodriguez, R.S., Soeder D.J., 2015. Evolving water management practices in shale oil & gas development, Journal of Unconventional Oil and Gas Resources 10, 18–24.

Rossiter, A. P., Nath, R., 1995. Wastewater minimization uisng nonlinear programming. In: Waste Minimization Through Process Design ,(Ed)Rossiter A. P. McGraw - Hill.

Souifi, M., Souissi, A., Salouhi, M., 2018. Rigorous targeting approach for water reuse and wastewater minimization in industrial processes. Journal of Materials and Environmental Sciences 9(2), 591-604.

Schwab, M.C., Cammarota, M.C. 2018. Composition and treatment of effluent from shale gas production. Clean Technologies and Environmental Policy, 1-13.

Shaffer, D. L., Chavez, L. H. A., Ben-Sasson, M., Castrillon S. R., Yip, N. Y., Elimelech, M., 2013. Desalination and reuse of high-salinity shale gas produced water: drivers, technologies, and future directions. Environmental Science andTechnology 47, 9569–9583.

Shih, J., Swiedler, E., Krupnick, A., 2016. A Model for Shale Gas Wastewater Management, Discussion Paper, 1-68.

Shoaib, A.m., Aly, S.M., Awad, M.E. Foo, D.C.Y., El-Halwagi, M.M., 2008. A hierarchical approach for the synthesis of batch water network. Computer and Chemical Enginnering 32, 530-539.

Siirola, J., 2014. The impact of shale gas in the chemical industry. Journal of American Institute of Chemical Engineers 60 (3), 810-819.

Soeder, J.D., Kappel, W.M., 2009. Water resources and natural gas production from the Marcellus shale: U.S. Geological Survey Fact Sheet , 2009–3032.

Speight, J.G., 2013. Production technology, In: Shale Gas Production Processes. (Ed.) Speight, J.G. Gulf Professional Publishing, Boston, 69–100.

Stackelberg, H.V., 2010. Market Structure and Equilibrium. Springer Science &Business Media.

Takama, N., Kuriyama, T., Shiroko, K., Umeda, T., 1980. Optimal planning of water allocation in industry. Computers and Chemical Engineering , 4(80), 251-258.

Thoola, M.I., 2014. Performance characteristics of bio-ultrafiltration on local surface water. Master dissertation, Durban University of Technology.

Tan, Y. L., Manan, Z. A.,Foo, D. C. Y., 2007. Retrofit of water network with regeneration using water pinch analysis. Trans IChemE, Part B, Safety and Environmental Protection, 85(B4),305-317.

Tan, R. R., Ng, D. K. S., Foo, D. C. Y., Aviso, K. B., 2009. A superstructure model for the synthesis of single-contaminant water networks with partitioning regenerators. Process Safety and Environmental Protection 87, 197-205.

US Energy Information Administration (EIA), Natural gas in the United States. accessed 27 June, 2018. https://www.revolvy.com/page/Natural-gas-in-the-United-States.

US Geological Survey(USGS), 2018. Earthquake Hazards Program. https://earthquake.usgs.gov/research/induced/overview.php. Accessed 26 December 2018.

Veil, J., 2014. Shale gas water management experiences from North America. Society of Petroleum Engineers distinguished lecturer program. 1-61.

Wang, Y. P., Smith, R., 1994. Wastewater minimisation. Chemical Engineering Science 49, 981-1006.

Wang, Y. P., Smith, R., 1995. Time Pinch Analysis. Trans IChemE 73, 905-914.

Wikramanayake, E., Bahadur, V., 2016. Flared natural gas-based onsite atmospheric water harvesting (AWH) for oilfield operations. Environment Research Letters 11, 1748-9326.

World Water Assessment Programme (WWAP), 2012. The United Nations World Water Development Report 4: Managing Water under Uncertainty and Risk. Paris, UNESCO.

World Water Assessment Programme (WWAP). 2016. The United Nations World Water Development Report 2016: Water and Jobs. Paris, UNESCO."

2030 Water Resources Group (WRG), 2009. Charting our water future. http://www.mckinsey.com/client_service/sustainability/latest_thinking/charting_our_water_future.Accessed 14 March 2018.

Wright, K.A., Xu, Y., 2000. A water balance approach to the sustainable management of groundwater in South Africa. Water SA 26(2), 167-170.

Yang, L., Salcedo-Diaz, R., Grossmann, I.E., 2014b. Water network optimization with wastewater regeneration models. Journal of Industrial and Engineering Chemistry Research 53, 17680–17695.

Yang, L., Grossmann, I.E., Manno, J., 2014a. Optimization models for shale gas water management. Journal of American Institute of Chemical Engineers, 60, 3490-3501.

Yang, Y., 2016. A study of shale gas production and its supply chain. MSC Thesis, University of Pittsburgh, USA.

Yang, L., Grossmann, I.E., Mauter, M.S., Dilmore, R.M., 2015. Investment optimization model for freshwater acquisition and wastewater handling in shale gas production, Journal of American Institute of Chemical Engineers 61, 1770-1782.

Younger, A.H., 2004. Natural gas processing principles and technology - Part 1. University of Calgary, Alberta, Canada.

Yun, Y., Ma, R., Zhang, W., Fane, A.G., Li, J., 2006. Direct contact membrane distillation mechanism for high concentration NaCl solutions. Desalination 188, 251–262.

Zhang, C., El-Halwagi, M.M., 2017. Estimate the capital cost of shale-gas monetization projects. Chemical Engineering Progress 113,28-32.

Zhelev, T.K., Bhaw, N., 2000. Combined water-oxygen pinch analysis for better wastewater treatment management. Waste management 20, 665-670.

CHAPTER THREE

SIMULTANEOUS ENERGY AND WATER OPTIMIZATION IN SHALE EXPLORATION

Introduction

This chapter focuses on the synthesis and optimization of an integrated water and membrane network that simultaneously optimizes water and energy consumption in hydraulic fracturing using continuous time mathematical formulation for scheduling. Recycle/reuse of fracturing water is achieved through purification of flowback wastewater using thermally driven membrane distillation (MD). Since MD is an energy intensive process, a detailed design model for this technology is incorporated within the water network superstructure in order to allow for simultaneous optimization of water, operation and/or capital cost as well as energy used. The study also examines the feasibility of utilizing the co-produced gas that is traditionally flared as a potential source of energy for the membrane distillation.

3.1. Problem statement

The problem statement in this chapter can be stated as follows.

Given:

- Number of freshwater sources (interruptible and uninterruptible)
- Set of wellpads *S* to be fractured with known volume of water required for fracturing and maximum allowable contaminant concentration in the fracturing fluid.
- Total number of frac stages for each wellpad
- Earliest fracturing date for each wellpad
- Set of wastewater injection wells *D*
- Volume of water required per stage
- Minimum and maximum number of stages that can be fractured per day
- Time horizon of interest
- Network of regenerator
- Gas storage facility
- Historical stream data for the interruptible source

Determine the optimal configuration of the total network that gives:

- Optimal fracturing schedule of the wellpads
- Minimum freshwater intake and wastewater generation

- Optimal operation and design conditions of the regenerator such as number of membrane modules and the energy consumption
- Feasibility of using captured flared gas as energy source for the regenerator.

The assumptions made in the model formulation are as follow:

- The wells in each wellpad are aggregated (Yang et al., 2014a).
- Each wellpad is connected to exactly one of the impoundments through piping (Yang et al., 2014a).
- The number of fracturing stages that could be fractured per day is kept constant at 4 instead of allowing it to be variable between 2-4 stages (Yang et al., 2014a).
- The flowback water from the fractured wellpad is assumed to be 25% (Yang et al., 2015) of the initial water used.
- The capacity of the wastewater tank and fracturing tank on each wellpad varies depending on its water requirement.
- The water treatment unit is located onsite and can be moved from one wellpad to the other.
- The historical flowrate data for the interruptible water source from each calendar year is treated as a scenario each with equal probability (Yang et al 2014a).

3.2. Superstructure representation

Based on the problem statement, the superstructure in Figure 3.1 is developed. In the superstructure, two types of freshwater sources are considered (interruptible and uninterruptible sources) (Yang et al., 2014a). Uninterruptible source is a big water body with guaranteed water availability throughout the year but the mode of transportation is through trucking. The interruptible source is a nearby source that requires piping but with uncertain water availability all year round. These two sources are considered because water management decisions are primarily influenced by transportation costs (Yang et al., 2014a). In order to complete a typical wellpad, roughly 4000-6500 one-way truck trips are needed. Hence, due to the high cost of trucking and other environmental impact related to drawing water from uninterruptible source, operators are encouraged to draw water from sources that are close by through piping (Yang et al., 2014a). The water from any of these sources can be stored in any of the impoundment *t* prior to its usage. *S* represents a set of wellpad to be fractured in which the fracking fluid is blended using freshwater from the impoundment and the recycled water from the fracturing tank. The maximum concentration of TDS into the wellpads is kept at an upper limit of 50,000 ppm (Yang et al., 2015, Bartholomew and Mauter, 2016). The flowback water generated from the fractured wellpad in the first two weeks after fracturing is assumed to be 25% of the initial water used. This flowback water can be sent to regenerator *R* for treatment or any of the injection well *D* for disposal. The flowback water sent to regenerator *R* is treated before it is sent to the fracturing tank for reuse in the next wellpad. The product of a particular wellpad after stimulation can be either oil and gas or gas only depending on the geological formation of the shale play. For a wellpad that produces oil and gas, the co-produced gas can be captured and stored in the gas storage facility from where it is supplied to the regenerator *R* as fuel, which in turn produces the heat energy needed, by the regenerator while the oil is sent to the market. In the case of gas producing well, part of the gas can be diverted into the gas storage facility for wastewater treatment while the rest can be sent to the market.

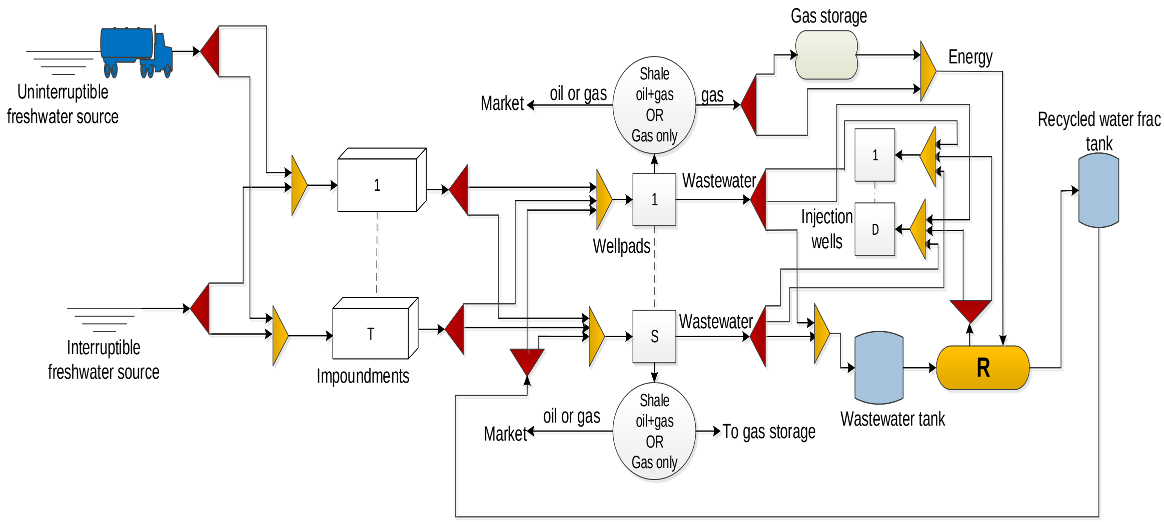

Figure 3.1. Superstructure representation of the water network.

The mode of operation of the regenerator is as stated below:

- Transfer of water from the wastewater tank to the regenerator *R* is done provided there is a wellpad to be fractured. Whenever the regenerator starts operation, it operates continuously until the wastewater tank becomes empty.
- The regenerator only operates if there is a wellpad to be fractured, otherwise it remains inactive.
- The performance of the regenerator is specified based on a variable removal ratio

3.3. Model formulation

The mathematical model presented in this chapter is based on the superstructure given in Figure 3.1. The problem is formulated as a mixed- integer nonlinear programming (MINLP) model, which is divided into two sections developed inside the same structure to simultaneously optimize water and energy. The first section focuses on mass balance and scheduling while the second is based on the detailed membrane distillation model. The scheduling framework adopted here is based on the state task network (STN) and unequal discretization of time horizon, which involves time point *n* occurring at unknown time. A time point is a precise moment within a given horizon when an event occurs (e.g., start of task, end of task, transfer of materials etc.). It is generally used to track inventory levels and model the occurrence of tasks in batch and semi-batch processes. Among the important decision variables are the 0-1 variables which indicate if a wellpad is fractured or if water is transferred to storage and regeneration. The following three sets of binary variables are used:

$w_{s,n}$ Is assigned a value of 1 if wellpad *s* is stimulated at time point *n.*

$wv_{s,n}$ Is assigned a value of 1 if transfer of water takes place from wellpad *s* to storage at time point *n.*

wr_n Is assigned a value of 1 if transfer of water from storage to regenerator takes place at time point *n.*

In order to explain the model, the constraints characterizing the optimization formulation are described.

3.3.1. Mass balance constraint

It is important to state the mass balances around each wellpad, the impoundment, the wastewater storage tank, the fracturing tank, the injection well and the regenerator.

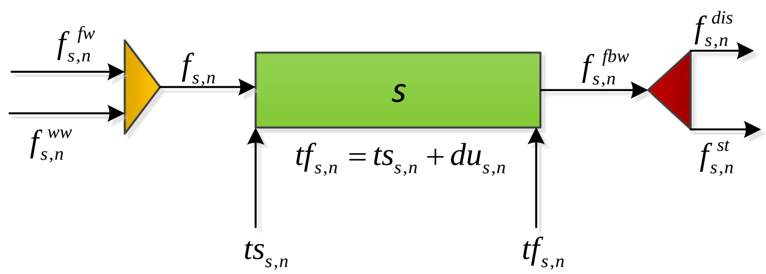

Figure 3.2. Mass balance representation around a wellpad.

The mass balance around a wellpad is conducted in accordance with Figure 3.2. The total volume of water required to fracture wellpad s at time point n, $f_{s,n}$, is given by Equation (3.1) where WR_s is the amount of water required to fracture wellpad *s*, and $w_{s,n}$ is the binary variable that indicate if wellpad *s* is fractured at time point *n.* This water requirement is supplied with freshwater from the impoundment $f_{s,n}^{fw}$ and/or reused water from the fracturing tank $f_{s,n}^{ww}$, which is obtained by Equation (3.2). Equation (3.3) specifies that only freshwater is to be used at the first time point.

$$f_{s,n} = WR_s w_{s,n} \quad \forall s \in S, n \in N \tag{3.1}$$

$$f_{s,n} = f_{s,n}^{fw} + f_{s,n}^{ww} \quad \forall s \in S, n \in N, n \geq 2 \tag{3.2}$$

$$f_{s,n} = f_{s,n}^{fw} \quad \forall s \in S, n \in N, n = 1 \tag{3.3}$$

The flowback water generated in the first two weeks after fracturing $f_{s,n}^{fbw}$ is assumed to be 25% of initial water used and is given by Equation (3.4). Equation (3.5) gives the TDS concentration, $c_{s,n}^{fbw}$ in the wastewater where CS_s is the flowback water concentration of wellpad *s*. The value used is between the average value in the first two weeks after fracturing and the highest value that can be found in typical flowback water as reported in literature. Equation (3.6) states that the flowback water after wellpad fracturing could be discarded as effluent or sent to the wastewater storage where $f_{s,n}^{st}$ **is** the volume of wasewater sent to the storage and $f_{s,n}^{dis}$ is the volume of wastewater sent to disposal from wellpad *s* at time point *n*.

$$f_{s,n}^{fbw} = 0.25 f_{s,n} \quad \forall s \in S, n \in N \tag{3.4}$$

$$c_{s,n}^{fbw} = CS_s w_{s,n} \quad \forall s \in S, n \in N \tag{3.5}$$

$$f_{s,n}^{fbw} = f_{s,n}^{st} + f_{s,n}^{dis} \quad \forall s \in S, n \in N \tag{3.6}$$

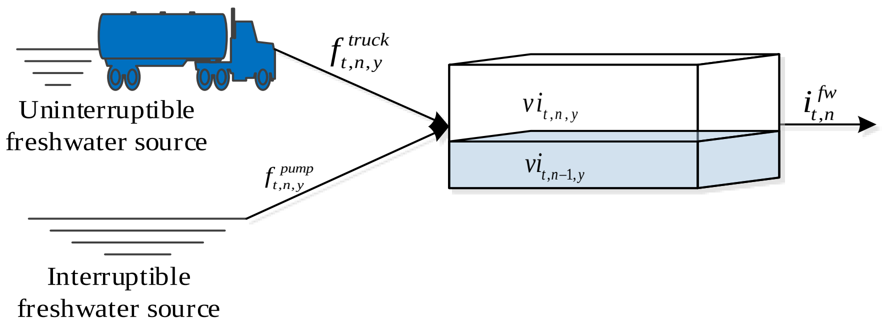

Figure 3.3. Mass balance representation around the impoundment.

The mass balance around the impoundment is conducted in accordance with Figure 3 as given in Equations (3.7) and (3.8). Equation (3.7) describes the total water $i_{t,n}^{fw}$ use from each impoundment *t* at time point *n* given the piping connection $TP_{s,t}$ between impoundment *t* and wellpad s. The volume $vi_{t,n,y}$ of impoundment t at time point n for a given scenario year y is describes by Equation (3.8). The equation States that the volume of freshwater stored in the impoundment consists of the volume stored at the previous time point and the difference between water entering the impoundment through trucking and piping and the total water leaving the impoundment to wellpads. $f_{t,n,y}^{pump}$ is a continuous variable which specifies the amount of water supplied through piping from interruptible source to the corresponding impoundment at time point n and $f_{t,n,y}^{truck}$ is the amount of water supplied through trucking.

$$i_{t,n}^{fw} = \sum_{s \in TP_{s,t}} f_{s,n}^{fw} \quad \forall t \in T, n \in N \tag{3.7}$$

$$vi_{t,n,y} = vi_{t,n-1,y} + f_{t,n,y}^{pump} - i_{t,n}^{fw} + f_{t,n,y}^{truck} \quad \forall t \in T, n \in N, y \in Y \tag{3.8}$$

Equation (3.9) states that the total volume of water disposed fd_n at time point n is the sum of flowback water sent to disposal $f_{s,n}^{dis}$ from wellpad s and the concentrate from the regenerator f_n^{con} . This total amount of water can be disposed into any of the injection well d as given in Equation (3.10) while Equation (3.11) states that the throughput into each of the injection well should not exceed the maximum it can take. ff_n^{dis} is a continous variable indicating the throughput of an injection well d at time point n and $DI^{\max}$, is the parameter indicating the maximum capacity of the injection well.

$$fd_n = \sum_s f_{s,n}^{dis} + f_n^{con} \quad \forall n \in N \tag{3.9}$$

$$fd_n = \sum_d ff_{d,n}^{dis} \quad \forall n \in N \tag{3.10}$$

$$fd_n \le DI^{\max} \quad \forall n \in N \tag{3.11}$$

Equation (3.12) gives the expected production $p_{s,n}$ from wellpad s at time point n, where p_s is a parameter indicating the gas production of wellpad s.

$$p_{s,n} = P_s w_{s,n} \qquad \forall s \in S, n \in N \tag{3.12}$$

3.3.2. Mass balance around the wastewater storage tank and the fracturing tank

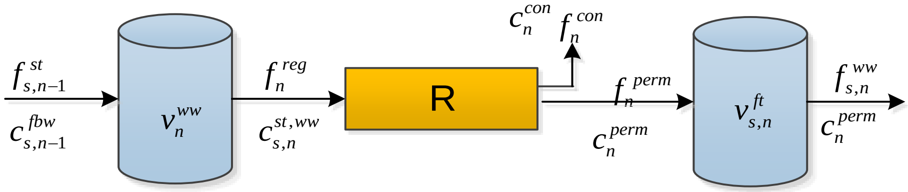

Figure 3.4. Mass balance representation around the storage tank, regenerator and the fracturing tank.

Part of the assumption made in the study is that all the flowback water sent to storage from wellpad *s* fractured at previous time point $f_{s,n-1}^{st}$, is the quantity that is treated by the regenerator f_n^{reg} at time point *n* as stated in Equation (3.13). This gives an indication that the volume of wastewater tank on each wellpad becomes zero at the end of each time point. The concentration of water sent to the treatment unit is given by Equation (3.14) where $c_n^{st,ww}$, is the contaminant concentration into the treatment unit at time point *n.*

$$\sum_s f_{s,n-1}^{st} = f_n^{reg} \quad \forall n \in N, n \geq 2 \tag{3.13}$$

$$\sum_s f_{s,n-1}^{st} c_{s,n-1}^{fbw} = f_n^{reg} c_n^{st,ww} \quad \forall n \in N, n \geq 2 \tag{3.14}$$

The capacity of the treatment wastewater tank v_n^{ww}, at time point *n* is bounded by the volume of flowback water f_n^{reg} to be treated at time point *n* as given in Equation (3.15). Equations (3.16) to (3.18) ensure that the maximum capacity of the tank is not exceeded where $V^{\max}$ and $V^{\min}$ are parameters that indicate the maximum and minimum capacity of the wastewater storage tank respectively. Equation (3.19) ensures that no water is stored in the storage tank at the end of the time horizon.

$$v_n^{ww} = f_n^{reg} \quad \forall n \in N \tag{3.15}$$

$$v_n^{ww} \leq V^{\max} \quad \forall n \in N \tag{3.16}$$

$$f_{s,n-1}^{st} \geq V^{\min} wv_{s,n-1} \quad \forall s \in S, n \in N, n \geq 2 \tag{3.17}$$

$$f_{s,n-1}^{st} \leq V^{\max} wv_{s,n-1} \quad \forall s \in S, n \in N, n \geq 2 \tag{3.18}$$

$$v_n^{ww} = 0 \quad \forall n = /N/ \tag{3.19}$$

The capacity of the fracturing tank $v_{s,n}^{ft}$, on wellpad *s* depends on the volume of wastewater required $f_{s,n}^{ww}$ at the wellpad as defined in Equation (3.20).

$$v_{s,n}^{ft} \geq f_{s,n}^{ww} \quad \forall s \in S, n \in N \tag{3.20}$$

3.3.3. Mass balance around the regenerator

Equation (3.21) states that the total volume of water into the regenerator at time point *n* f_n^{reg} is the sum of the amount collected as permeate f_n^{perm} and amount sent to disposal as concentrate f_n^{con}. The contaminant balance around the regenerator is given in Equation (3.22) where c_n^{perm} represents the outlet concentration of contaminant from the regenerator and c_n^{con} is the contaminant concentration removed from the water by the regenerator at time point *n*. Equation (3.23) states that the inlet contaminant concentration into the regenerator should not exceed the maximum it can take where $C^{\max}$ is the maximum inlet concentration into the regenerator . The performance of the regenerator is a function of the removal ratio (*RR*) of contaminant as stated in Equation (3.24). The quantity of water to be collected as permeate and concentrate depends on the recovery ratio (*LR*) as stated in Equations (3.25) and (3.26) respectively.

$$f_n^{reg} = f_n^{perm} + f_n^{con} \quad \forall n \in N \tag{3.21}$$

$$f_n^{reg} c_n^{st,ww} = f_n^{perm} c_n^{perm} + f_n^{con} c_n^{conc} \quad \forall n \in N \tag{3.22}$$

$$c_n^{st,ww} \le C^{\max} \qquad \forall n \in N \tag{3.23}$$

$$c_n^{perm} = c_n^{st,ww}\left(1 - RR\right) \quad \forall n \in N \tag{3.24}$$

$$LRf_n^{reg} = f_n^{perm} \qquad \forall n \in N \tag{3.25}$$

$$f_n^{con} = \left(1 - LR\right) f_n^{reg} \qquad \forall n \in N \tag{3.26}$$

The amount of wastewater reused at any time point is supplied through the permeate stream from the regenerator as given in Equation (3.27). Equation (3.28) ensures that the maximum allowable concentration into the wellpad is not exceeded where $CS^{\max}$ is the maximum inlet contaminant concentration into wellpad *s*.

$$f_n^{perm} = \sum_s f_{s,n}^{ww} \qquad n \in N \tag{3.27}$$

$$f_n^{perm} c_n^{perm} \le CS^{\max} \sum_s f_{s,n} \quad \forall n \in N \tag{3.28}$$

3.3.4. Scheduling model

The scheduling part of the model captures the time dimension related to the process. These are categorised into three parts namely:

- wellpad scheduling
- wastewater storage tank scheduling and
- the regenerator scheduling

3.3.4.1. Wellpad scheduling

Equation (3.29) is the allocation constraint which specifies that each wellpad *s* has to be fractured exactly once at a given time point *n* in the time horizon.

$$\sum_n w_{s,n} = 1 \quad \forall s \in S$$

Equation (3.30) states that no task can start at the end of the time horizon.

$$w_{s,n} = 0 \quad \forall s \in S, n \in N, n = /N/ \tag{3.30}$$

The duration of each wellpad $du_{s,n}$, is calculated by Equation (3.31) where TR_s is the time required to fracture wellpad *s* .Equations (3.32) and (3.33) gives the finish time of each wellpad $tf_{s,n}$ expressed with big-M constraints, which are only active if wellpad *s* is stimulated at time point *n* where $ts_{s,n}$ is the start time of fracturing wellpad s at time point n .

$$du_{s,n} = TR_s w_{s,n} \quad \forall s \in S, n \in N \tag{3.31}$$

$$tf_{s,n} \le ts_{s,n} + du_{s,n} + H\left(1 - w_{s,n}\right) \quad \forall s \in S, n \in N \tag{3.32}$$

$$tf_{s,n} \ge ts_{s,n} + du_{s,n} - H\left(1 - w_{s,n}\right) \quad \forall s \in S, n \in N \tag{3.33}$$

Equation (3.34) states that the time at which the fracturing of wellpad *s* begins $ts_{s,n}$, is equal to the time at which time point *n* occurs tt_n i.e. the start time of each wellpad must coincide with a time point.

$$ts_{s,n} = tt_n \quad \forall s \in S, n \in N \tag{3.34}$$

Equation (3.35) is the sequence dependent change over time between wellpad *s* and s'. It states that the start time of wellpad s' at time point *n* must be equal or greater than the finish time of wellpad *s* at previous time point plus the crew transition time $CT_s^{s'}$ between wellpad s and s'. Equation (3.36) states that the time at which time point *n* occurs must correspond with the availability time AT_s of wellpad *s*.

$$ts_{s',n} \geq tf_{s,n-1} + CT_s^{s'} w_{s',n} \quad \forall s \in S, s' \in S, s' \neq s, n \in N, n \geq 2 \tag{3.35}$$

$$tt_n \geq \sum_s \left(AT_s w_{s,n} - H\left(1 - w_{s,n}\right)\right) \quad n \in N \tag{3.36}$$

3.3.4.2. Storage tank scheduling

Water usage in hydraulic fracturing and water sent to the storage tank for treatment are linked by Equation (3.37). It states that water can only be transferred from wellpad *s* to the wastewater tank for treatment if wellpad fracturing takes place at that time point. Equations (3.38) and (3.39) ensure that the transfer time of water from a wellpad into storage $tv_{s,n}$ correspond with the time when the fracturing task ends $tf_{s,n}$.

$$wv_{s,n} \leq w_{s,n} \quad \forall s \in S, n \in N \tag{3.37}$$

$$tv_{s,n} \geq tf_{s,n} - H\left(2 - wv_{s,n} - w_{s,n}\right) \quad \forall s \in S, n \in N \tag{3.38}$$

$$tv_{s,n} \leq tf_{s,n} + H\left(2 - wv_{s,n} - w_{s,n}\right) \quad \forall s \in S, n \in N \tag{3.39}$$

3.3.4.3 Regenerator scheduling

Equation (3.40) relates the regeneration and fracturing task starting at time point *n*. It states that water regeneration can only take place at time point n if there is a wellpad to be fractured at that time point. Equations (3.41) and (3.42) ensure that the time at which regeneration starts tr_n coincide with the time at which fracturing task starts at time point *n*. This is because all tasks starting at point *n* must start at the same time but their finish times do not have to coincide. Equation (3.43) gives the duration of regeneration where ttr_n is the finish time of regeneration at time point *n*, f_n^{reg} is the total volume of water into the regenerator at time point n and ff^{MD} is the feed flowrate into the regenerator.

$$wr_n \geq w_{s,n} \quad \forall s \in S, n \in N \tag{3.40}$$

$$tr_n \geq ts_{s,n} - H\left(2 - wr_n - w_{s,n}\right) \quad \forall s \in S, n \in N \tag{3.41}$$

$$tr_n \leq ts_{s,n} + H\left(2 - wr_n - w_{s,n}\right) \quad \forall s \in S, n \in N \tag{3.42}$$

$$ttr_n = tr_n + \left(\frac{f_n^{reg}}{ff^{MD}}\right) wr_n \quad \forall n \in N \tag{3.43}$$

3.3.5. Tightening constraint

Tightening formulations play an important role in finding good solutions for the original problem. Non-addition of tightening constraint can lead to weak relaxation. Equation (44) impose the requirement that the sum of the fracturing durations of all the wellpads $du_{s,n}$ should be lesser or equal to the time horizon H while Equation (45) restricts the sum of the fracturing time of all wellpads starting after tt_n to be smaller than the remaining time where tt_n is the time at which time point *n* occurs.

$$\sum_{s}\sum_{n} du_{s,n} \leq H \tag{3.44}$$

$$\sum_{s}\sum_{n' \geq n} du_{s,n'} \leq H - tt_n \quad \forall n \in N \tag{3.45}$$

3.3.6. Membrane distillation (MD) model

The detailed design model for the membrane distillation unit, which is based on the work of Elsayed et al. (2013), is presented in this section. Various configurations of MD have been reported in literature (Elsayed et al., 2013, Yun et al., 2006) with variation based on mode of vapour collection on the permeate side and the method of the driving force enhancement across the membrane. The focus of this study is on direct contact membrane distillation (DCMD) which is found to be the most commonly used configuration. Some of the merits associated with DCMD are ease of construction, operation, maintenance and stability in operation (Elsayed et al., 2013). Figure 5 illustrates a schematic representation of a typical direct contact membrane distillation unit. The flowback water is pre-heated to effect evaporation and the degree of pre-heating becomes an optimization variable. The vapour passes through the membrane and condensation occurs on the permeate side using stored permeate which is at relatively low temperature than the feed. Consideration must be given to both heat and mass transfer from the feed side to the permeate side of the membrane. Mass and heat transfer take place across three sections (Elsayed et al., 2013, Yun et al., 2006): mass transfer takes place in the boundary layer of the membrane on the feed side, across the membrane and on the permeate side boundary layer. Heat transfer on the other hand takes place from the bulk of the feed to the interface of the membrane through a boundary layer via convection, across the membrane via conduction and latent heat associated with the vaporized flux, and through the boundary layer from the interface of the membrane to the bulk of the permeate via convection. In order to describe mass transfer through the membrane, model such as Knudsen diffusion, molecular diffusion or incorporation of both have been established to yield quality results (Yun et al., 2006).

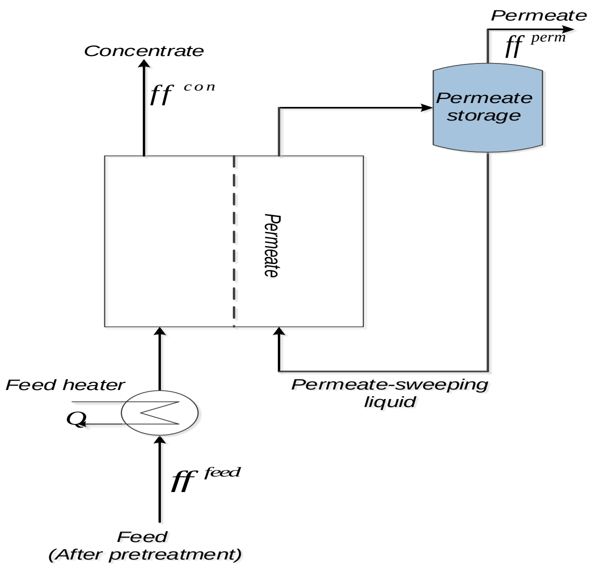

Figure 3.5. Schematic representation of a typical direct contact membrane distillation.

The membrane distillation considered uses GVHP, which is a polyvinylidene fluoride flat sheet membrane used in DCMD. The detail of this is given in Yun et al. (2006).

The following assumptions are made for the constraints in the plant using a set of mathematical equations describing its operation:

- Flowback water contains organics, oils, dissolved solids (TDS) mainly in the form of salts and other contaminants (Gregory et al., 2011). It is assumed that flowback water is pretreated to remove oils, organics and other necessary contaminants. Membrane distillation is used to remove TDS, as this is the main contaminant of interest for water reuse/ recycle in hydraulic fracturing.
- The separation efficiency of the MD modules depends on temperature. This is because the permeate flux is also temperature dependent.

The driving force for the water flux across the membrane, Jw, is the difference in pressure of the water vapour and is defined in Equation (3.46) as:

$$Jw = Bw\left(p_{wf}^{vap}\gamma_{wf}x_{wf} - p_{wp}^{vap}\right) \tag{3.46}$$

where Bw is the membrane permeability p_{wf}^{vap},is the water vapour pressure of the feed, p_{wp}^{vap} is the water vapour pressure of the permeate, γ_{wf} is the activity coefficient of water in the feed and x_{wf} is the mole fraction of water in the feed.

The Antoine equation (Elsayed et al., 2013) is used to estimate the water vapor pressure of the feed and the permeate which depends on temperature as given in Equations (3.47) and (3.48): where T_{mf} and T_{mp} are the temperature of the feed and permeate on the membrane respectively.

$$p_{wf}^{vap} = \exp\left(23.1964 - \frac{3816.44}{T_{mf} - 46.13}\right) \tag{3.47}$$

$$p_{wp}^{vap} = \exp\left(23.1964 - \frac{3816.44}{T_{mp} - 46.13}\right) \tag{3.48}$$

The activity coefficient is dependent on concentration and on the assumption of NaCl as the primary solute, Equation (3.49) (Lawson and Lloyd, 1997) can be used to estimate the activity coefficient where x_{NaCl} is the molar concentration of NaCl in the feed.

$$\gamma_{wf} = 1 - 0.5x_{NaCl} - 10x_{NaCl}^2 \tag{3.49}$$

Sodium Chloride is chosen as the basis of calculation because it is reported to be the dominant species with regards to concentration in flowback /produced water (Camacho et al., 2013; Estrada and Bhamidimarri, 2016; Engle and Rowan, 2014). It makes up over 50% of the total dissolved solids.

The permeability of the membrane Bw depends on the membrane temperature, T_m which differs based on the kind of diffusion. The permeability of membranes in which molecular diffusion occurs is calculated through Equation (3.50) as proposed by Elsayed et al. (2013) where B_{wb} is the temperature-independent base value of membrane permeability.

$$Bw = B_{wb}T_m^{1.334} \tag{3.50}$$

The membrane temperature is the mean value of the bulk temperature of the feed, T_{bf} and permeate T_{bp}, (El-Halwagi, 2012). Therefore, the average temperature in the MD module can be determined by the expression given in Equation (3.51).

$$T_m = \frac{T_{bf} + T_{bp}}{2} \tag{3.51}$$

Mass and salt balance around the MD unit is conducted in accordance with Figure 3 as given in Equations (3.52) - (3.54):

$$ff^{\,feed} = ff^{\,MD} \rho_{water} \tag{3.52}$$

$$ff^{\,feed} = ff^{\,perm} + ff^{\,con} \tag{3.53}$$

$$ff^{\,feed} cf^{\,feed} = ff^{\,perm} cp^{perm} + ff^{\,con} cr^{con} \tag{3.54}$$

where $ff^{\,feed}$ is the total flowrate into MD, $ff^{\,perm}$ and $ff^{\,con}$ are the permeate and concentrate flowrate and, ρ_{water} is the density of water. The amount of water collected as permeate highly depends on the energy, Q, supplied to the unit. Therefore, the heat required by the feed is given in Equation (3.55):

$$Q = ff^{\,feed} C_P \left(T_{bf} - T_{sf} \right) \tag{3.55}$$

where C_p, T_{bf} T_{sf} are the specific heat capacity of the feed stream, temperature of the feed in the bulk and the temperature of feed water into MD respectively. Only a portion of the heat supplied to the unit will be used to vaporize the permeate. This portion is stated as the efficiency factor η. Thus, Equation (3.56) gives the heat balance for the MD unit (Elsayed et al., 2013) where, ΔH_{vw} is the latent heat of vaporization for water.

$$\eta Q = ff^{\,perm} \Delta H_{vw} \tag{3.56}$$

The thermal efficiency of MD, η can be measured using experimental data or semi empirical formula (Elsayed et al., 2013) as indicated in Equation (3.57). Where k_m is the membrane thermal conductivity and δ is the membrane thickness.

$$\eta = 1 - \frac{1.5\frac{k_m}{\delta}\left(T_{mf} - T_{mp}\right)}{Jw\Delta H_{vw} + \frac{k_m}{\delta}\left(T_{mf} - T_{mp}\right)} \tag{3.57}$$

The thermal conductivity of a particular membrane can be determined using Equation (3.58) which is correlated based on the data of Khayet and Matsuura, (2011).

$$k_m = 1.7\times10^{-7} T_m - 4.0\times10^{-5} \tag{3.58}$$

Equation (3.59) as proposed by Elsayed et al. (2013) can be used to determine water vaporization in the feed side of the membrane.

$$\Delta H_{vw} = 3190 - 2.5009 T_{mf} \tag{3.59}$$

The transfer of heat through the boundary layers on the two sides of the membrane results in temperature gradient between the bulk solutions and surface of the membrane known as temperature polarization, θ. This occurrence may lead to significant reduction in the driving force; therefore, it is necessary to consider the temperature gradient across the membrane. Based on this, temperature polarization coefficient (Schofield et al., 1987) may be used to calculate the membrane temperature profile as given in Equation (3.60).

$$\theta = \frac{T_{mf} - T_{mp}}{T_{bf} - T_{bp}} \tag{3.60}$$

In order to estimate the temperature polarization coefficient of a particular membrane, experimental data or correlations may be used (Khayet and Matsuura, 2011, Al-Obaidani et al., 2008). A linear behaviour as a function of the temperature as provided by Khayet and Matsuura, (2011) is given in Equation (3.61).

$$\theta = 1.362 - 0.0026 T_{bf} \tag{3.61}$$

In accordance with the experimental observation, two other simple assumptions are suggested (Elsayed et al., 2013; El-Halwagi, 2012):

The first assumption is that for MD with laminar flows of the feed and the sweeping liquid, the absolute value of the temperature difference between the bulk and the membrane on each side of the membrane is nearly the same, as given in Equation (3.62),

$$T_{bf} - T_{mf} \approx T_{mp} - T_{bp} \tag{3.62}$$

The second assumption is that the membrane temperature is the mean value of the bulk temperature of the feed and permeate as specified in Equation (3.51) above.

The liquid recovery "*LR*"is the fraction of the feed into the regenerator that is recovered as permeate. The fraction of water recovery by the MD unit is given by Equation (3.63).

$$LR = \frac{ff^{perm}}{ff^{feed}} \tag{3.63}$$

The removal ratio "*RR*" is the mass load of contaminant in the concentrate stream of the regenerator as a fraction of the feed. It is assumed to be a variable in this work and is defined as given in Equation (3.64).

$$RR = \frac{ff^{con} cr^{con}}{ff^{feed} cf^{feed}} \tag{3.64}$$

In order to determine the area of the membrane required, A_m, the permeate flow rate is divided by the water flux as given in Equation (3.65).

$$A_m = \frac{ff^{perm}}{Jw} \tag{3.65}$$

The regeneration network takes into account the capital and the operational cost involves in the operation of the unit. These are incorporated in the overall objective function in order that the energy consumed as well as cost associated with regeneration are optimized together with water utilization.

The annualized fixed cost of the MD network, AFC, as proposed by Elsayed et al. (2013) is given by Equation (3.66).

$$AFC = 58.5 A_m + 1115\, ff^{feed} \tag{3.66}$$

The annual operating cost excluding heating, AOC, as proposed by Elsayed et al. (2013) is given by Equation (3.67), where u, is the ratio of recycled reject to raw feed.

$$AOC = \left(1411 + 43\left(1 - LR\right) + 1613\left(1 + u\right)\right) ff^{feed} \tag{3.67}$$

The annual heating cost AHC, is given by Equation (3.68): where AOT is the annual operating time, Q is the heat requred by the feed into MD and OC^{ht} is a parameter indicating the cost of heating.

$$AHC = AOT\left(QOC^{ht}\right) \tag{3.68}$$

3.3.7. Additional constraints

The thermal energy consumption per unit of water treated E^{con} ,is given by Equation (3.69). Equation (3.70) gives the total energy required for treatment at any time point, E_n^{total} . The volume of natural gas needed per time point, V_n^{nat} , is given in Equation (3.71) where ∂_{ED} , is the energy density.

$$E^{cons} = \frac{Q}{ff^{feed}} \tag{3.69}$$

$$E_n^{total} = f_n^{reg} E^{cons} \quad \forall n \in N \tag{3.70}$$

$$V_n^{nat} = \frac{E_n^{total}}{38300\partial_{ED}} \quad \forall n \in N \tag{3.71}$$

3.3.8 Objective function

The objective is to maximize profit, which comprises of the following terms: (1) revenue from gas production, (2) freshwater transportation cost, (3) wastewater treatment cost, (4) disposal cost, (5) wastewater storage cost, and (6) pumping cost to treatment facility as given in Equation (3.72).

$$\max profit = SP^{gas}\sum_{s}\sum_{n} p_{s,n} - \left[\begin{array}{l} \left(OC^{truck,fw}\sum_{t}\sum_{n}\sum_{y}\frac{f_{t,n,y}^{truck}}{NY} + OC^{pump,fw}\sum_{t}\sum_{n}\sum_{y}\frac{f_{t,n,y}^{pump}}{NY}\right) \\ +\left(\left(58.5A_m + 1115ff^{feed}\right) + \left(1411 + 43\left(1-LR\right) + 1613\left(1+u\right)\right)ff^{feed} + AOT\left(QOC^{ht}\right)\right) \\ +\left(OC^{dis}\sum_{s}\sum_{n} f_{s,n}^{dis}\right) \\ +\left(OC^{st,ww}\left(\sum_{s}\sum_{n} v_{s,n}^{ft} + \sum_{n} v_{n}^{ww}\right)\right) \\ +OC^{pump,ww}DS_s\left(\sum_{s}\sum_{n} f_{s,n}^{st} + \sum_{n} f_{n}^{perm}\right) \end{array}\right] \tag{3.72}$$

3.4. Case study

In order to demonstrate the applicability of the proposed model, an example taken from Yang et al. (2014a) is considered. This case study represents the typical Marcellus Shale play. The example considered 14 wellpads, 540 days time horizon, one uninterruptible freshwater source and two interruptible sources connected to impoundments as illustrated in Table 3.1. 30 years historical data were provided for the two interruptible sources. The selected membrane distillation is a polyvinylidene fluoride used in direct-contact membrane distillation. The details of this membrane module are given in Yun et al. (2006) and Elsayed et al. (2013). The permeability of the membrane is a function of the membrane temperature, which varies depending on the type of diffusion. This is calculated based on molecular diffusion through equation (3.50). In order to ensure a complete analysis of the model, three different scenarios are considered. Scenario 1 is the base case, which is the water integration without regeneration i.e. freshwater is considered as only available water source for hydraulic fracturing. Scenario 2 is the case where black box model is used; i.e. water minimisation only and a linear cost function is used in estimating the cost associated with regeneration. Scenario 3 considers water integration involving detailed regenerator where water and energy are optimized simultaneously.

Table 3.1. Wellpad Data (Yang et al., 2014a).

Wellpads	S1	S2	S3	S4	S5	S6	S7	S8	S9	S10	S11	S12	S13	S14
Match with takepoints $TP_{s,t}$	*t2*	*t1*	*t1*	*t1*	*t1*	*t2*	*t2*	*t2*	*t2*	*t2*	*t2*	*t1*	*t1*	*t2*
Earliest fracturing day	1	1	1	1	1	39	1	273	273	273	396	379	379	1
No. of stages	57	61	54	55	64	26	97	88	86	76	63	100	100	87

The parameters and the cost coefficients are given in Table 3.2 while the information regarding the average flowback water and TDS profile for a given wellpad in the first 14-20 days after wellpad fracturing, and the expected gas production for each wellpad are obtained from Yang et al. (2014a).

Table 3.2. Parameters and cost coefficients.

Parameter	Value
Crew transition time (day)	5
Volume of fracturing fluid used per stage (m^3)	950
Freshwater used (%)	85
Storage cost ($\$/m^3$)	0.59
Freshwater trucking cost ($\$/m^3$)	29.35
Freshwater pumping cost ($\$/m^3$)	15.93
Disposal cost ($\$/m^3$)	134.18
Wastewater pumping cost ($\$/km/m^3$)	0.28
Wastewater storage cost ($\$/m^3$)	0.59
Temperature-independent base value of membrane permeability B_{WB} ($kg/m^2.s.pa.K^{1.334}$)	$3.9*10^{-10}$
Membrane thickness (mm)	0.65
Membrane life time (year)	4
Annual operation time (h)	8000
Heating cost ($\$/10^9J$)	5
Supply temperature (K)	293
Specific heat capacity (kJ/kgK)	4
Average TDS concentration of the feed into MD (mg/L)	200,000

3.4.1. Results and discussion

The resulting model was implemented in GAMS and solved using the general-purpose global optimization solver (BARON), which uses a branch-and-reduce algorithm to obtain a solution. Although BARON is not always guaranteed to converge to the global optimum, it has a proven track record in solving non-convex MINLP problems. Performance of BARON and statistics in solving a wide variety of test problems have been reported in literature (MINLPLib, 2018, Nohra and Sahinidis, 2018, Tawarmalani and Sahinidis, 2005). The solution comparison and the computational statistics between the three scenarios are given in Tables 3.3 and 3.4, respectively. The total volume of water required for the 14 wellpads is found to be 818,800 m^3. The results encourage the use of freshwater from the interruptible sources which is achieved through piping, thereby reducing the high cost and environmental issues that are associated with trucking. It should be noted that Scenario 1 which involve the use of freshwater only does not take into account the extra cost associated with the water network like the cost of treatment and storage. Thus, no comparison with regard to profit is done between the three scenarios as shown in Table 3.3. The total revenue for both Scenarios 2 and 3 is found to be $261.24 million and the total profit for Scenario 3 is found to be 0.6% higher than the profit obtained in Scenario 2. This is mainly due to the fact that the cost of wastewater disposal, and treatment cost are higher in Scenario 2 compared to Scenario 3.

Table 3.3. Solution comparison.

	Scenario 1	Scenario 2	Scenario 3
Freshwater Pumped (1,000 m^3)	818.80	640.30	635.30
Freshwater trucked (1,000 m^3)	0	0	0
Regenerated water (1,000 m^3)	0	178.53	183.53
Freshwater save (%)	0	21.80	22.42
Freshwater trucking cost ($ 1,000)	0	0	0
Freshwater pumping cost ($ 1,000)	13,043	10,019	10,012
Disposal cost ($ 1,000)	0	2,119	1,450
Wastewater pumpin cost ($ 1,000)	0	10.01	11.65
Wastewater storage cost ($ 1,000)	0	1,740	1,747
Treatment cost ($ 1,000)	0	11,307	10,575
Revenue ($ 1,000)	-	261,240	261,240
Profit ($ 1,000)	-	235,860	237,340

It is worth mentioning here that the cost of treatment in scenario 3 is higher in this chapter compared to the subsequent chapters because of the operational expenses associated with softening process. In order to allow for thermal –based desalination processes, composition restriction is always imposed on the concentration of scaling forming materials such as calcium, barium and magnesium. This is mostly achieved by softening process using lime or soda ash. The costs of these chemical additives are 0.074 US$/kg for lime and 0.165 US$/kg for soda ash ((Carrero –Parreño et al., 2017). However, this decision is always based on the presence and concentration of the scale forming cations.

Table 3.4. Computational statistics.

	Scenario 1	Scenario 2	Scenario 3
No. of constraint	5,698	9,324	9,418
No. of continuous variables	3,796	6,023	6,103
No. of binary variables	210	435	435
Non-linear terms	-	1,458	1,514
CPU time (s)	0.11	51.82	458.59
No. of slots	14	14	14
No. of time points	15	15	15

The fracturing schedule for each scenario is presented in Figures 3.6-3.8. As can be seen from these figures, the schedules involve different timing and sequences. As the schedule in Figure 3.6 only consider freshwater usage, the wellpads fracturing followed each other depending on the availability time of each wellpad and also on the water availability in the impoundment. The gap between S7 and S8 in Figure 3.6 is due to the fact that S7 is available from day 1 while S8 only becomes available after day 273.

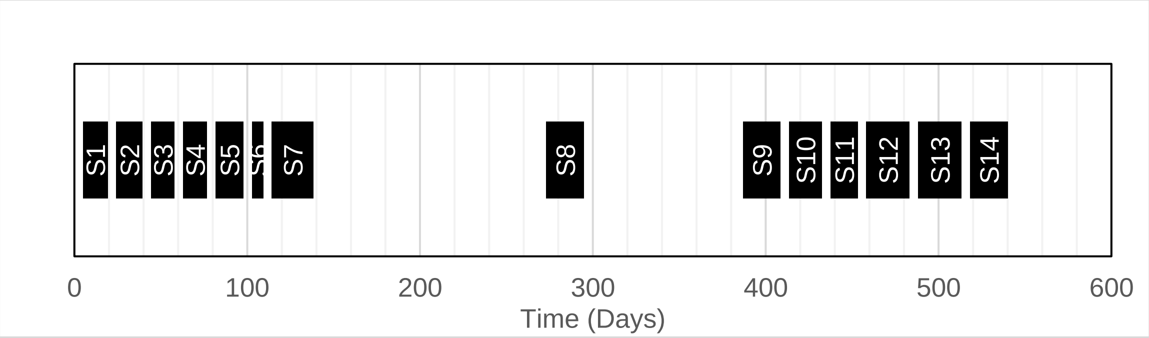

Figure 3.6. Fracturing schedule (Base case).

In Figures 3.7 and 3.8, it is observed that wellpad S6 is fractured last in both schedules. This is because wellpad S6 has the least number of stages which implies that it will require the lowest volume of water for fracturing thereby reducing the volume of wastewater to be disposed in the last time point. The gap between S8 and S9 in Figure 3.6, S5 and S4 in Figure 3.7 and S3 and S5 in Figure 3.8 may be attributed to what is referred to as frac holiday, which depends mainly on water availability for fracturing. According to literature (Yang et al., 2014a), fracturing idle time (holiday) is a flexible period when fracturing crew takes time off usually due to low water availability. Figures 3.7 and 3.8 show that the tightness in fracturing schedule of each group of wellpads which is much more profound in Figure 3.8 improves the effectiveness of flowback water reuse.

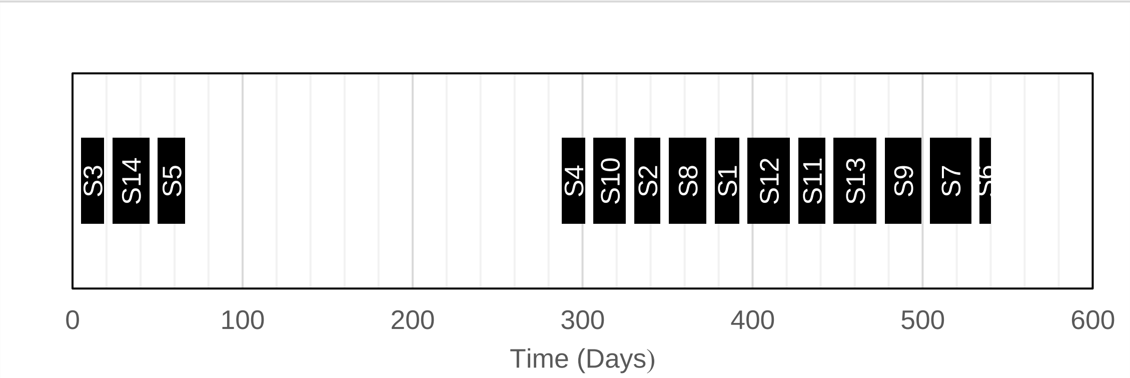

Figure 3.7**.** Fracturing schedule (Scenario 2).

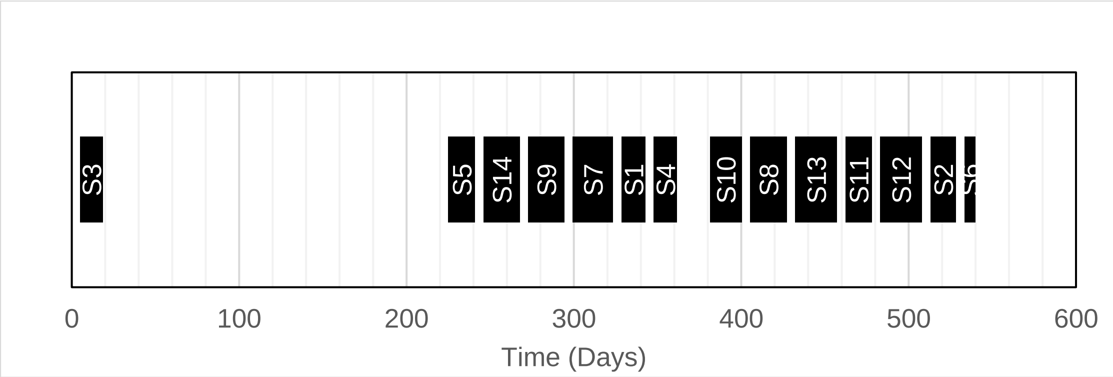

Figure 3.8. Fracturing schedule (Scenario 3).

Figure 3.9 gives a detailed description of how the water-recycling scheme for the optimum scenario (scenario 3) is implemented. The figure summarises the percentage of freshwater and wastewater requirement for each wellpad based on the fracturing schedule given in figure 3.8.

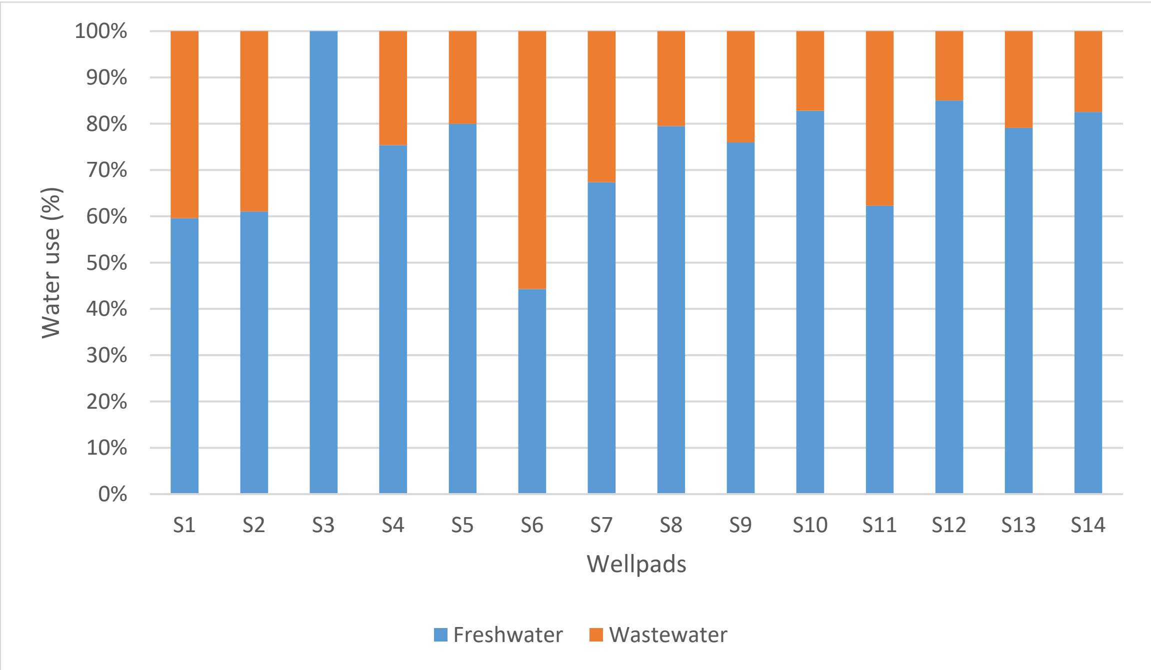

Figure 3.9. Percentage of water used in fracturing operation (Scenario 3)

As a result of effective flowback water reuse, a saving of 183,534.65 m^3 of freshwater is achieved out of the total volume of 818,800 m^3 required for the 14 wellpads. The saving is found to be 21.23 % higher than the study in literature (Yang et al., 2014a), using discrete time formulation. In Scenario 2, 96.7 % of the flowback water is sent to regenerator *(R)* and the remaining 3.3 % is sent to the injection well to be disposed while in Scenario 3, 99.4 % of the flowback water is sent to regenerator (*R)* while the remaining 0.6 % is disposed.

In order to calculate the cost and energy associated with the wastewater regeneration, a cost analysis based on the black box model, standalone model and detailed model was performed. The costs of regeneration are found to be $11.2 million, $9.8 million and $10.5 million respectively. The results show that the deviation of the cost function (black box model) from the actual cost of regeneration (standalone model) is 12.7 %. The result obtained in Scenario 3 show that the optimized cost of regeneration is 6.6 % higher than the cost of MD standalone model. This is because optimizing the temperature of the feed into MD results in a reduction of the water flux thereby increasing the membrane area required which in turn results to an increase in the fixed cost of the membrane. When water minimisation alone is considered, the membrane operated at the maximum feed temperature of 363 K which leads to the maximization of the water flux across the membrane, hence the membrane area and the fixed cost is minimized. However, this does not necessarily indicate that the membrane performance is optimal, which is in agreement with the work of Elsayed et al. (2013). The design specifications for the optimal design of the MD regenerator is given in Table 3.5. The optimal feed temperature is found to be 354 K. The permeate flux; thermal efficiency, thermal energy required and the removal ratio are also given in Table 3.5. The model prediction of 0.013 kg/m^{2}s for the permeate flux at the optimal feed temperature of 354 K agrees with the work of Elsayed et al. (2013) and the experimental data reported by Yun et al. (2006) to be 0.0125 kg/m^{2}s at 351 K.

Table 3.5. Design specification for MD.

Design variables	Optimum values
MD feed temperature (K)	354
Thermal efficiency	0.98
Thermal energy (kJ/day)	610×10^6
Permeate flux (kg/m^{2}s)	0.013
Removal ratio (RR) (%)	1

The simultaneous optimization of both energy and water within the water network results in 12.7 % reduction in the amount of energy required by the regenerator based on the throughput per day. The amount of energy required is reduced from 699×10^6 kJ (equivalent to 18,250 m^3 of natural gas) to 610×10^6 kJ (equivalent to 15,926 m^3 of natural gas). The value of energy consumed by the regenerator is 244×10^3 kJ/m^3 of distillate, which is found to be lesser than the range of thermal energy reported in literature for membrane distillation. The range of thermal energy required by membrane distillation is between 120 and 1700 kWh/m^3 equivalent to between 432×10^3 kJ/m^3 and 6.12×10^6 kJ/m^3 (Camacho et al., 2013; Suarez and Urtubia, 2016). The average volume of flared gas per unit time based on literature (Glazer et al., 2014) as specified under section 1.1 is used in this study and this is compared to the energy requirement of the regenerator. Using gas that would otherwise be flared as the source of heat for the regenerator rendered the heating cost in the objective function to become zero.

3.5. Conclusion

A continuous time scheduling formulation has been developed for simultaneous water and energy optimization in shale play. Two possible sources of freshwater withdrawal for hydraulic fracturing were considered and the Purification of the generated flowback water is achieved using membrane distillation. The importance of optimizing fracturing schedule with water and energy management has been demonstrated by incorporating detailed MD model within the water network. The applicability of the proposed formulation has been demonstrated with a case study and significant reduction in the required freshwater and regeneration energy have been achieved.

In the next chapter, the proposed formulation is extended to account for the shale gas production network and infrastructural development.

Nomenclature

Sets

D	$\{d \mid d$ = injection well$\}$
N	$\{n \mid n$ = time point$\}$
S	$\{s \mid s$ = wellpad$\}$
T	$\{t \mid t$ = an interruptible source and its corresponding impoundment$\}$
$TP_{s,t}$	Match between wellpad *s* and source *t*
Y	$\{y \mid y$ = historical river flowrate data year$\}$

Parameters

AT_s	Availability time of wellpad *s*, day
AOT	Annual operating time, hr
B_{wb}	Temperature independent base value for the permeability, kg/m^2.s.pa.K$^{1.334}$

C_p	Specific heat capacity of the feed stream, KJ/kgK
$C^{\max}$	Maximum inlet concentration into treatment unit, mg/L
Cf^{feed}	Concentration of the feed water into MD, mg/L
$CS^{\max}$	Maximum inlet concentration into wellpad *s*, mg/L
CS_s	Flowback water concentration in wellpad *s*, mg/L
$CT_S^{S'}$	Crew transition time between wellpads, day
$DI^{\max}$	Maximum capacity of an injection well *d*, m^3
DS_s	Distance from wellpad *s* to treatment facility, km
H	Time horizon of interest, day
LR	Liquid recovery for the regenerator
NY	Number of historical year, yr
$OC_s^{pump,fw}$	Freshwater pumping cost, \$/m^3
$OC_s^{truck,fw}$	Freshwater trucking cost, \$/m^3
$OC_s^{pump,ww}$	Wastewater pumping cost, \$/m^3/km
OC^{dis}	Cost of wastewater disposal, \$/m^3
$OC_s^{st,ww}$	Cost of wastewater storage, \$/m^3
OC^{ht}	Cost of heating, \$/10^{9}J
P_s	Gas production of wellpad *s*, m^3
SP^{gas}	Unit price of natural gas, \$/m^3
ST_s	Availability date of wellpad *s*, day
TR_s	Time required fracturing wellpad *s*, day
T_{sf}	Temperature of feed water into the treatment unit, K
u	Ratio of recycled reject to raw feed
$V^{\max}$	Maximum capacity of storage, m^3
$V^{\min}$	Minimum capacity of storage, m^3
WR_s	Amount of water required to fracture wellpad *s*, m^3
X_{NaCl}	Molar concentration of NaCl in the feed
δ	Membrane thickness, mm
∂_{ED}	Energy density, kJ/ m^3

ρ_{water} Density of water, kg/ m^3

Binary variables

$w_{s,n}$ Defines the beginning of stimulating each wellpad *s* at time point *n*

$wv_{s,n}$ Transfer of water from wellpad s to storage at time point *n*

wr_n Transfer of water from storage to regenerator at time point *n*

Continuous variables

A_m Required membrane area, m^2

AFC Annualized fixed capital cost for the regenerator, $/yr

AHC Annualized heating cost for the regenerator, $/yr

AOC Annualized operating cost for the regenerator, $/yr

Bw Membrane permeability, kg/(m^2.pa)

$c_{s,n}^{fbw}$ Flowback water concentration of wellpad *s* at time point *n*, mg/L

$c_n^{st,ww}$ Contaminant concentration into the treatment unit at time point *n*, mg/L

c_n^{perm} Outlet concentration of contaminant from regenerator at time point *n*, mg/L

c_n^{con} Contaminant concentration removed from water by regenerator at time point *n*, mg/L

cp^{perm} Permeate concentration from MD, mg/L

cr^{con} Retentate concentration from MD, mg/L

$du_{s,n}$ Duration of wellpad *s* at time point *n*, day

E^{cons} Thermal energy consumption per unit of water treated, kJ/m^3

E_n^{total} Thermal energy required at time point *n*, kJ

$f_{s,n}$ Total water required to fracture wellpad *s* at time point *n*, m^3

$f_{t,n,y}^{pump}$ Water pumped from interruptible source at time point *n* in scenario year *y*, m^3

$f_{t,n,y}^{truck}$ Water trucked from uninterruptible source at time point *n* in scenario year *y*

$f_{s,n}^{fw}$ Freshwater required to fracture wellpad *s* at time point *n*, m^3

$f_{s,n}^{ww}$ Wastewater required to fracture wellpad *s* at time point *n*, m^3

$f_{s,n}^{fbw}$ Flowback water from wellpad *s* at time point *n*, m^3

$f_{s,n}^{st}$ Flowback water sent to storage tank from wellpad *s* at time point *n*, m^3

$f_{s,n}^{dis}$ Flowback water sent to disposal from wellpad *s* at time point *n*, m^3

f_n^{reg} Total flowback water to be treated at time point *n*, m^3

f_n^{perm} Amount of water collected as permeate from the regenerator at time point *n*, m^3

f_n^{con} Amount of retentate from the regenerator at time point *n*, m^3

fd_n Total water sent to disposal at time point *n*, m^3

$ff_{d,n}^{dis}$ Throughput of an injection well *d* at time point *n*, m^3

ff^{MD} Total flowrate into MD, m^3/day

ff^{feed} Total flowrate into MD, kg/day

ff^{perm} Permeate flowrate from MD, kg/day

ff^{con} Retentate flowrate from MD, kg/day,

$i_{t,n}^{fw}$ Total freshwater required from impoundment *t* for fracturing at time point *n*, m^3

Jw Water flux across the membrane, kg/(m^2.s)

k_m Membrane thermal conductivity, kW/(m.K)

$p_{s,n}$ Expected gas production of wellpad *s* at time point *n*, m^3

p_{wf}^{vap} Water vapour pressure of the feed in MD, pa

p_{wp}^{vap} Water vapour pressure of the permeate in MD, pa

Q Heat required by the feed into MD, kJ/day

RR Regenerator removal ratio

$ts_{s,n}$ Start time of wellpad *s* at time point *n*, day

$tf_{s,n}$ Finish time of wellpad *s* at time point *n*, day

tt_n Time that correspond to time point *n*, day

tr_n Start time of regeneration at time point *n*, day

ttr_n Duration of regeneration at time point *n*, day

$tv_{s,n}$ Time at which water is transferred from wellpad *s* to storage tank at time point *n*, day

T_{mf} Temperature of the feed on the membrane, K

T_{mp}	Temperature of the permeate on the membrane, K
T_m	Membrane average temperature, K
T_{bf}	Temperature of the feed in the bulk, K
T_{bp}	Temperature of permeate in the bulk, K
$vi_{t,n,y}$	Volume of impoundment t at time point n in scenario year y, m^3
v_n^{ww}	Capacity of wastewater tank at time point n, m^3
$v_{s,n}^{ft}$	Capacity of fracturing tank on wellpad s at time point n, m^3
v_n^{nat}	Volume of natural gas needed to produce the required energy at time point n, m^3
x_{wf}	Mole fraction of water in the feed
γ_{wf}	Activity coefficient of water in the feed to the membrane distillation
η	Overall thermal efficiency of the regenerator
ΔH_{vw}	Latent heat of vaporization for water, kJ/kg
θ	Temperature polarization coefficient

Superscript

con	Concentrate
cons	Consumption
dis	Disposal
feed	Feed
ft	Fracturing tank
fw	Freshwater
fbw	Flowback water
gas	Gas
ht	Heating
max	Maximum
min	Minimum
nat	Natural gas
pump	Pumping
perm	Permeate
reg	Regenerator
st	Storage

total	Total
truck	Trucking
vap	Vapour
ww	Wastewater
Subscript	
bp	permeate bulk
bf	Feed bulk
m	Membrane
mp	Membrane permeate
mf	Membrane feed
wf	Feed water
wp	Permeate water

References

Al-Obaidani, S., Curcio, E., Macedonio, F., Di Profio, G., Al-Hinai, H., Drioli, E., 2008. Potential of membrane distillation in seawater desalination: thermal efficiency, sensitivity study and cost estimation. Jounal of Membrane Science 323, 85–98.

Bartholomew, T.V., Mauter, M.S., 2016. Multiobjective optimization model for minimizing cost and environmental impact in shale gas water and wastewater management. Journal of ACS Sustainable Chemistry and Engineering 4, 3728-3735.

Camacho, L.M., Dume´e, L., Zhang, J., Li, J.D., Duke, M., Gomez, J., Gray, S., 2013. Advances in membrane distillation for water desalination and purification applications. Water 5, 94–196.

Estrada, J.M., Bhamidimarri, R. A., 2016. Review of the issues and treatment options for wastewater from shale gas extraction by hydraulic fracturing. Fuel 182, 292-303.

Elsayed, N.A., Barrufet, M.A., El-Halwagi, M.M., 2013. Integration of thermal membrane distillation networks with processing facilities. Journal of Industrial and Engineering Chemistry Research 53, 5284-5298.

El-Halwagi, M.M., 2012. Sustainable design through process integration: Fundamentals and applications to industrial pollution prevention, resource conservation, and profitability enhancement. Butterworth-Heinemann: Oxford, UK.

Engle, M.A., Rowan, E.L., 2014. Geochemical evolution of produced waters from hydraulic fracturing of the Marcellus Shale, northern Appalachian Basin: A multivariate compositional data analysis approach. International Journal of Coal Geology126, 45-56.

Glazer, Y.R., Kjellsson, J.B., Sanders, K.T., Webber, M.E., 2014. Potential for using energy from flared gas for on-site hydraulic fracturing wastewater treatment in Texas. Environmental Science and Technology Letter 1, 300-304.

Gregory, K.B., Vidic, R.D., Dzombak, D.A., 2011. Water management challenges associated with the production of shale gas by hydraulic fracturing. Elements 7(3), 181-186.

Khayet, M., Matsuura, T., 2011. Membrane dstillation: Principles and applications. Elsevier, Amsterdam.

Lawson, K.W., Lloyd, D.R., 1997. Membrane distillation: Review. Journal of Membrane Science 124, 9-25.

MINLPLib, http://www.minlplib.org/, accessed on June 19, 2018.

Nohra, C.J., Sahinidis, N.V., 2018. Global optimization of nonconvex problems with convex-transformable intermediates. Journal of Global Optimization, 1-22.

Schofield, R. W., Fane, A. G., Fell, C. J. D., 1987. Heat and mass transfer in membrane distillation. Journal Membrane Science 33, 299-313.

Suarez, F., Urtubia, R., 2016. Tackling the water-energy nexus: an assessment of membrane distillation driven by salt-gradient solar ponds. Clean Technologies and Environmental Policy 18(6), 1697-1712.

Tawarmalani, M., Sahinidis, N.V., 2005. A polyhedral branch-and-cut approach to global optimization. Mathematical Programming. 103, 225-249.

Yang, L., Grossmann, I.E., Manno, J., 2014a. Optimization models for shale gas water management. Journal of American Institute of Chemical Engineers, 60, 3490-3501.

Yang, L., Grossmann, I.E., Mauter, M.S., Dilmore, R.M., 2015. Investment optimization model for freshwater acquisition and wastewater handling in shale gas production, Journal of American Institute of Chemical Engineers 61, 1770-1782.

Yun, Y., Ma, R., Zhang, W., Fane, A.G., Li, J., 2006. Direct contact membrane distillation mechanism for high concentration NaCl solutions. Desalination 188, 251–262.

CHAPTER FOUR

ON THE OPTIMIZATION OF WATER-ENERGY NEXUS IN SHALE GAS EXPLORATION: CONSIDERATION OF PRODUCTION, PROCESSING, DISTRIBUTION, POWER GENERATION AND TRANSMISSION

Introduction

The production of shale gas resources depends extensively on production costs in addition to different environmental impacts associated with the development of shale gas plays. In particular, the depletion and degradation of water sources, as well as the potential for underground water contamination (Guerra et al., 2016). The shale gas production system is a complex multistage network and includes various components such as water acquisition, shale gas production, wastewater management, shale gas processing, usage and transportation. A variety of decisions must be made in each stage of this system. Hence, to achieve a great economic potential, discerning the optimal design and operations of the shale gas supply chain is of paramount importance. The proposed framework in this chapter takes into account longer-term decisions for water related issues such as investments in water treatment units, impoundments and natural gas infrastructure, which include gathering pipelines, processing facilities, storage facilities and distribution. The mathematical framework proposed in chapter three is extended to account for shale gas production, processing, distribution, usage in power generation, and transmission of produced power.

4.1. Problem statement

The problem addressed in this chapter can be stated as follows. Given are: (i) set of wellpads *S* to be fractured with known volume of water required for fracturing and maximum allowable contaminant concentration in the fracturing fluid. (ii) Total number of frac stages for each wellpad and the earliest fracturing date for each wellpad. (iii) Minimum and maximum number of stages that can be fractured per day and the volume of water required per stage. (iv) A number of freshwater sources are given from which freshwater can be withdrawn for fracking. Two types of freshwater sources are considered which are interruptible and uninterruptible sources. The freshwater withdrawal from the interruptible source is done through piping and water availability is estimated based on the historical data to account for the possible seasonal change. The water availability from the uninterruptible source is guaranteed throughout the year and water transportation is through trucking. (v) Network of regenerator *R* for wastewater treatment. (vi) Set of wastewater injection wells *D* for wastewater disposal. (vii) Set of processing plant *P* for processing shale gas from where natural gas and natural gas liquids are produced. (viii) Set of underground reservoirs *U*, which serve as natural gas inventory management tool or seasonal natural gas supply backup. (ix) Set of power plant *W* with known maximum capacities for electricity generation. (x) Set of distribution company *B* which distribute natural gas to different end users. (xi) Set of power grid *K* for electricity transmission. (xii) The time horizon of interest.

Using the given data, it is required to determine: (i) Selection of freshwater sources. (ii) The fracturing schedule of the wellpads that optimizes water and energy usage. (iii) Optimum design of MD regenerator such as number of membrane modules and energy consumption. (iv) Optimum size of processing plant, underground reservoir and power plant. (v) Capacity of pipelines between wellpads, processing plant, underground reservoir and power plant. (vii) The capacity of electricity transmission line and the power loss through transmission. (viii) Optimal configuration of the total network. The goal is to maximize the total expected profit.
The assumptions made in the model formulation are as follow:

- The wells in each wellpad are aggregated (Yang et al., 2015).
- The shale gas production profile of each wellpad is known.
- The number of fracturing stages that could be fractured per day is kept constant at 4.
- The flowback water from the fractured wellpad in the first two weeks after fracturing operation is assumed to be 25% of the initial water used while the maximum concentration of TDS into the wellpads is kept at an upper limit of 50,000 ppm (Yang et al., 2015, Bartholomew and Mauter, 2016).
- All freshwater pipelines are buried to avoid freezing during winter period in a shale play region where freezing is an issue and each pipeline has enough capacity to transfer fresh water required.
- Price of natural gas, electricity and NGLs to different customers are independent of time.
- Pipelines are placed in between wellpads as the wellpads in each area are assumed to be close in proximity.
- Interruptible freshwater sources are seasonal and availability depends on the average historical flowrate data.
- Composition of shale gas at each wellpad is known.

4.2. Model formulation

Based on the problem statement, the superstructure as shown in Figure 4.1 is developed. This representation is an extension of the proposed superstructure in chapter 3. In the superstructure, freshwater can be acquired from any of the two sources as mentioned before which is then stored in the impoundment *t* prior to its usage. *S* represents a set of wellpad to be fractured in which the fracking fluid is blended using freshwater from the impoundment and the recycled water from the fracturing tank to meet the maximum contaminant concentration into the wellpads. The flowback water generated from the fractured wellpad in the first two weeks after fracturing can be sent to regenerator *R* for treatment or any of the injection well *D* for disposal. The product (shale gas) of a particular wellpad after stimulation can be either wet gas or dry gas depending on the geological formation of the shale play. Both wet gas and dry gas are accounted for in this study. For dry gas with composition of almost pure methane, processing might not be of necessity (Gao et al., 2017). For wet gas, the extracted gas after well completion is transported through pipelines to processing plants where major separation as depicted in Figure 2.31 takes place. The recovered natural gas liquids, which include propane, ethane, butane etc. are sent to NGLs storage where they are sold separately as their market value is much higher than natural gas. The natural gas, which is of "pipeline quality", is transported through pipelines to different consumers. It can be directly transported to power plants for electricity generation, to distribution companies that distribute natural gas to different end users or alternatively to underground reservoirs, which can be depleted natural gas or oil fields, aquifers or salt caverns where it is stored indefinitely mainly to accommodate fluctuations in price and demand. The power generated at the power plant is transmitted to different end users via electrical grid. The size of freshwater impoundments, processing plants, transmission lines as well as the capacity and capital investment for the gas pipeline networks, design specification for the regeneration unit as well as energy consumption, become important matters to be addressed in this work.

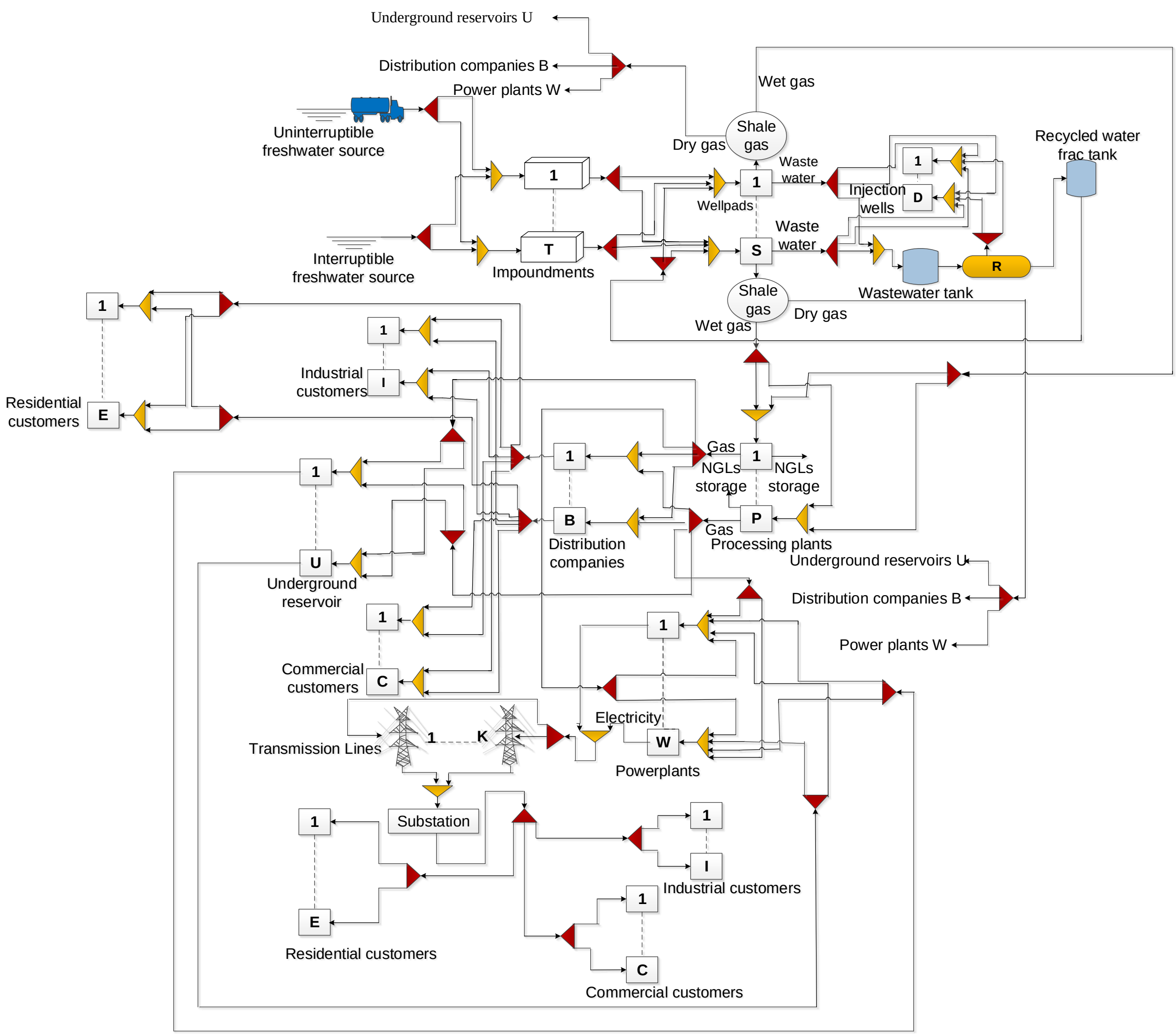

Figure 4.1. Superstructure representation of the total network.

The mathematical formulation developed in this chapter integrates scheduling model, model for water and shale gas network design and synthesis and the membrane distillation design model. The scheduling framework adopted here is based on the state task network (STN) and unequal discretization of time horizon, which involves time point *n* occurring at unknown time.

The objective of the problem is defined in Equation (4.1) as:

$$
\begin{aligned}
\max\ profit = & \Bigg[\left(SP^{ngl}\sum_{p}\sum_{n} ngl_{p,n}\right)+\left(SP^{elec,ind}\sum_{i}\sum_{n}P_{i,n}^{ind}+SP^{elec,com}\sum_{c}\sum_{n}P_{c,n}^{com}+SP^{elec.res}\sum_{e}\sum_{n}P_{e,n}^{res}\right)+\left(SP^{gas,ind}\sum_{b}\sum_{i}\sum_{n} ind_{b,i,n}+SP^{gas,com}\sum_{b}\sum_{c}\sum_{n} com_{b,c,n}+SP^{gas,res}\sum_{b}\sum_{e}\sum_{n} res_{b,e,n}\right)\Bigg] \\
- & \Bigg[\left(OC^{wd,fw}\left(\sum_{t}\sum_{n} f_{t,n}^{truck}+\sum_{t}\sum_{n} f_{t,n}^{pump}\right)\right) \\
& +\left(OC^{truck,fw}\sum_{t}\sum_{n} D_t f_{t,n}^{truck}+OC^{pump,fw}\sum_{t}\sum_{n} f_{t,n}^{pump}+\sum_{a}\sum_{t} CC^{pipe} D_{a,t}\right) \\
& +\left(\left(58.5A_m+1115\, ff^{feed}\right)+\left(1411+43(1-LR)+1613(1+u)\right) ff^{feed}+AOT\left(QOC^{ht}\right)\right) \\
& +\left(OC^{dis}\sum_{n} fd_n+OC^{ww,truck}\sum_{s}\sum_{n} Dd_s\, fd_n\right) \\
& +\left(OC^{st,ww}\left(\sum_{s}\sum_{n} v_{s,n}^{ft}+\sum_{n} v_n^{st,ww}\right)\right) \\
& +\left(OC^{pump,ww} D_s\left(\sum_{s}\sum_{n} f_{s,n}^{trtb}+\sum_{n} f_n^{perm}\right)+CC^{pipe} D_s\right) \\
& +\left(CC^{base,imp}+\sum_{t} IC^{inc,imp} c_t\right) \\
& +\left(\sum_{s}\sum_{n}\left(uc_{s,n}^{drill} NS_s+uc_{s,n}^{prod} pr_{s,n}\right)\right) \\
& +\left(CC^{ref,pro}\sum_{p}\left(\frac{\left(c_p^{cap}\right)^{sfp}}{rcp^{pro}}\right)\frac{chem^{pro}}{rchem^{pro}}+OC^{pro}\sum_{s}\sum_{p}\sum_{n} sp_{s,p,n}\right) \\
& +\left(CC^{ref,pipe}\sum_{s}\sum_{p} D_{s,p}\left(\frac{\left(c_{s,p}^{pipe}\right)^{sft}}{rcp^{pipe}}\right)\frac{chem^{pipe}}{rchem^{pipe}}+OC^{pipe} D_{s,p}\sum_{s}\sum_{p}\sum_{n} sp_{s,p,n}\right) \\
& +\left(OC^{power,gen}\sum_{w}\sum_{n}\left(\sum_{p} pw_{p,w,n}+\sum_{u} uw_{u,w,n}\right)\right) \\
& +\left(\sum_{u}\sum_{n}\left(OC^{inj,nat\,gas}\sum_{p} pu_{p,u,n}+OC^{wd,nat\,gas}\sum_{w} uw_{u,w,n}\right)\right) \\
& +\left(CC^{ref,pipe}\sum_{p}\sum_{u} D_{p,u}\left(\frac{\left(c_{p,u}^{pipe}\right)^{sft}}{rcp^{pipe}}\right)\frac{chem^{pipe}}{rchem^{pipe}}+OC^{pipe} D_{p,u}\sum_{p}\sum_{u}\sum_{n} pu_{p,u,n}\right) \\
& +\left(CC^{ref,pipe}\sum_{p}\sum_{w} D_{p,w}\left(\frac{\left(c_{p,w}^{pipe}\right)^{sft}}{rcp^{pipe}}\right)\frac{chem^{pipe}}{rchem^{pipe}}+OC^{pipe} D_{p,w}\sum_{p}\sum_{w}\sum_{n} pw_{p,w,n}\right) \\
& +\left(CC^{ref,pipe}\sum_{p}\sum_{b} D_{p,b}\left(\frac{\left(c_{p,b}^{pipe}\right)^{sft}}{rcp^{pipe}}\right)\frac{chem^{pipe}}{rchem^{pipe}}+OC^{pipe} D_{p,b}\sum_{p}\sum_{b}\sum_{n} pd_{p,b,n}\right) \\
& +\left(CC^{ref,pipe}\sum_{u}\sum_{w} D_{u,w}\left(\frac{\left(c_{u,w}^{pipe}\right)^{sft}}{rcp^{pipe}}\right)\frac{chem^{pipe}}{rchem^{pipe}}+OC^{pipe} D_{u,w}\sum_{u}\sum_{w}\sum_{n} uw_{u,w,n}\right) \\
& +\left(OC^{ele,trans}\sum_{w}\sum_{n} te_{w,n}\right) \\
& +\left(OC^{st,ngl}\sum_{p}\sum_{n} v_{p,n}^{ngl}\right)\Bigg]
\end{aligned}
\tag{4.1}
$$

Which takes into account the following terms:

(i) Total revenue from electricity, natural gas and natural gas liquid sales (ii) fresh water withdrawal cost (iii) freshwater transportation cost (iv) wastewater treatment cost (v) wastewater disposal cost (vi) wastewater storage cost (vii) wastewater pumping cost (viii) cost of impoundment (ix) cost of wellpad drilling and shale gas production (x) cost of wet gas processing plant (xi) shale gas transportation cost (xii) cost of power generation (xiii) cost of natural gas storage (xiv) natural gas transportation cost (xv) cost of electricity transmission (xiv) cost of power generation (xiii) cost of natural gas liquid storage

The objective function is subject to the following constraints, which consist of allocation constraints, material balances, sequencing constraints, capacity constraints, bounding constraints and the membrane distillation design constraints.

4.2.1. Allocation constraint

Equation (4.2) is the allocation constraint which specifies that each wellpad *s* has to be fractured exactly once at a given time point *n* in the time horizon. A time point is a precise moment within a given horizon (H) when an event occurs.

$$\sum_n w_{s,n} = 1 \quad \forall s \in S \tag{4.2}$$

Equation (4.3) states that the time at which time point *n* occurs tt_n must correspond with the availability time AT_s of wellpad *s*. Where $w_{s,n}$ is the binary variable that indicate if wellpad *s* is fractured at time point *n*.

$$tt_n \geq \sum_s \left(AT_s w_{s,n} - H\left(1 - w_{s,n}\right)\right) \quad \forall n \in N \tag{4.3}$$

4.2.2. Mass balance constraints

Water requirement by each wellpad is supplied with freshwater from the impoundment $f_{s,n}^{fw}$ and/or recycled water from the frac tank $f_{s,n}^{ww}$, which is obtained by Equation (4.4).

$$f_{s,n} = f_{s,n}^{fw} + f_{s,n}^{ww} \quad \forall s \in S, n \in N, n \geq 2 \tag{4.4}$$

Equation (4.5) describes the total water use $i_{t,n}^{fw}$ from each impoundment *t* at time point *n* given the piping connection $TP_{s,t}$ between impoundment *t* and wellpad *s*. The total volume of water $fp_{a,n}^{fw}$ withdrawn from interruptible source *a* at time point *n* is describe in Equation (4.6) given the piping connection $TP_{a,t}$ between river *a* and impoundment *t*. Equation (4.7) states that the volume of water withdrawn from river *a* at any time point should be within its capacity, where binary variable y_a indicates the existence of river *a* and $F_a^{pump,\max}$ is a parameter indicating the maximum volume of water that can be withdrawn from river *a*. The volume of impoundment *t* at any time point *n* is given by Equation (4.8), where $f_{t,n}^{pump}$ is a continuous variable indicating the volume of water supplied through piping to the corresponding impoundment at time point n and $f_{t,n}^{truck}$ is the volume of water supplied through trucking.

$$i_{t,n}^{fw} = \sum_{s \in TP_{s,t}} f_{s,n}^{fw} \quad \forall t \in T, n \in N \tag{4.5}$$

$$f_{t,n}^{pump} = \sum_{a \in TP_{a,t}} fp_{a,n}^{fw} \quad \forall t \in T, n \in N \tag{4.6}$$

$$fp_{a,n}^{fw} \le F_a^{pump,\max} y_a \quad \forall a \in A, n \in N \tag{4.7}$$

$$vi_{t,n} = vi_{t,n-1} + f_{t,n,}^{pump} - i_{t,n}^{fw} + f_{t,n,y}^{truck} \quad \forall t \in T, n \in N \tag{4.8}$$

Equation (4.9) states that the flowback water generated after wellpad fracturing $f_{s,n}^{fbw}$ can be sent to regenerator R for treatment or injection well for disposal. Where $f_{s,n}^{trtb}$ is the volume of wastewater sent to treatment and $f_{s,n}^{dis}$ is the volume sent to disposal from wellpad s at time point n.

$$f_{s,n}^{bw} = f_{s,n}^{trtb} + f_{s,n}^{dis} \quad \forall s \in S, n \in N \tag{4.9}$$

Equation (4.10) is the total shale gas production from wellpad s at time point n, where p_s is a parameter indicating the gas production of wellpad s.

$$p_{s,n} = p_s w_{s,n} \quad \forall s \in S, n \in N \tag{4.10}$$

The total amount of shale gas produced at wellpad s at time point n is transported to different processing plant as indicated in Equation (4.11), where $sp_{s,p,n}$ indicates the amount of shale gas sent from wellpad s to processing plant p ant time point n.

$$pr_{s,n} = \sum_{p} sp_{s,p,n} \quad \forall s \in S, n \in N \tag{4.11}$$

The total methane produced $tm_{p,n}$ at processing plant depends on the average methane composition MC_s of the shale gas and the processing efficiency PE of the processing plant as given in Equation (4.12).

$$tm_{p,n} = \sum_{s} sp_{s,p,n} MC_s PE \quad \forall p \in P, n \in N \tag{4.12}$$

The total amount of natural gas produced at processing plant at time point n should equal to the amount sent to different power plants $pw_{p,w,n}$, distribution companies $pd_{p,b,n}$ and underground reservoir $pu_{p,u,n}$ as given in Equation (4.13).

$$tm_{p,n} = \sum_{w} pw_{p,w,n} + \sum_{b} pd_{p,b,n} + \sum_{u} pu_{p,u.n} \quad \forall p \in P, n \in N \tag{4.13}$$

The amount of natural gas liquid $ngl_{p,n}$ produced at each processing plant is given in Equation (4.14), where NC_s is the average natural gas liquid composition in shale gas at wellpad s at time point n.

$$ngl_{p,n} = \sum_{s} sp_{s,p,n} NC_s PE \quad \forall p \in P, n \in N \tag{4.14}$$

Equation (4.15) gives the balance for the natural gas liquid in processing plant p at time point n where $ngl_{p,n}$ indicates the amount of natural gas liquid produced at time point n and $nls_{p,n}$ is the amount of natural gas liquid sold at time point n.

$$v_{p,n}^{ngl} = v_{p,n-1}^{ngl} + ngl_{p,n} - nls_{p,n} \quad \forall p \in P, n \in N \tag{4.15}$$

Equation (4.16) gives the natural gas balance at underground reservoir u at time point n where $pu_{p,u,n}$ is the amount of natural gas sent to underground reservoir u from processing plant p at time point n and $uw_{u,w,n}$ is the amount of natural gas sent to power plant w from underground reservoir at time point n.

$$v_{u,n}^{und,res} = v_{u,n-1}^{und,res} + \sum_{p} pu_{p,u,n} - \sum_{w} uw_{u,w,n} \quad \forall u \in U, n \in N \tag{4.16}$$

The total amount of electricity generated at power plant at time point n is given by Equation (4.17) where EG denotes the amount of electricity generated per unit shale gas input.

$$te_{w,n} = EG\left(\sum_{p} pw_{p,w,n} + \sum_{u} uw_{u,w,n} \right) \quad \forall w \in W, n \in N \tag{4.17}$$

The power generated in the power station is generated at a lower voltage, which requires to be stepped up to a higher voltage before it is transmitted over a long distance to cater for different consumers. The use of higher voltage (hence lower current in the line) reduces voltage drop in the line resistance and reactance and also results in reduction of transmission losses. Equation

(4.18) gives the total current on the transmission line I_n^{trans} at any given time point n using power formula circuit for 3-phases where V^{trans}, PF are parameters indicating the transmission voltage and power factor respectively.

$$I_n^{trans} = \frac{\sum_w te_{w,n}}{V^{trans} PF \sqrt{3}} \quad \forall n \in N \tag{4.18}$$

The power loss during high voltage transmission p_n^{loss} is given in Equation (4.19) while the amount of power received at the substation p_n^{rec} is given in Equation (4.20) where R^{trans} is a parameter indicating the transmission resistance.

$$P_n^{loss} = \left(I^{trans}\right)^2 R^{trans} \quad \forall n \in N \tag{4.19}$$

$$P_n^{rec} = \sum_w te_{w,n} - P_n^{loss} \quad \forall n \in N \tag{4.20}$$

The power received at the substation is distributed to different end users as given in Equation (4.21). $p_{i,n}^{ind}$, $p_{c,n}^{com}$, $p_{e,n}^{res}$ are continuous variables, which represent power distributed to industrial customers, commercial customers and residential customers respectively. These have to be stepped down to lower voltages based on the required voltage for each end user as indicated in Equation (4.22) –(4.24) where V^{ind}, V^{com}, V^{res} are parameters indicating the transmission voltage for industrial, commercial and residential customers respectively.

$$P_n^{rec} = \sum_i P_{i,n}^{ind} + \sum_c P_{c,n}^{com} + \sum_e P_{e,n}^{res} \quad n \in N \tag{4.21}$$

$$I_n^{trans,ind} = \frac{\sum_i P_{i,n}^{ind}}{V^{ind} PF \sqrt{3}} \quad \forall n \in N \tag{4.22}$$

$$I_n^{trans,com} = \frac{\sum_c P_{c,n}^{com}}{V^{com} PF \sqrt{3}} \quad \forall n \in N \tag{4.23}$$

$$I_n^{trans,res} = \frac{\sum_e P_{e,n}^{res}}{V^{res} PF \sqrt{3}} \quad \forall n \in N \tag{4.24}$$

The amount of natural gas sent to distribution company *b* from processing plant *p* is distributed to different end users as given in Equation (4.25) where $ind_{b,i,n}, com_{b,c,n}, res_{b,e,n}$ represent the amount of natural gas distributed to the industrial, commercial and residential customers respectively.

$$\sum_p pd_{p,b,n} = \sum_i ind_{b,i,n} + \sum_c com_{b,c,n} + \sum_e res_{b,e,n} \quad \forall b \in B, n \in N \tag{4.25}$$

4.2.3. Capacity and Bounding Constraints

Equation (4.26) is the capacity constraint for the processing plant which states that the total amount of shale gas from wellpad *s* at time point *n* processed by each processing plant should not exceed its processing capacity, where c_p^{cap} is a continuous variable that indicate the capacity of processing plant *p*.

$$\sum_s sp_{s,p,n} \le c_p^{cap} \quad p \in P, \forall n \in N \tag{4.26}$$

The total amount of power generated at power plant *w* at time point *n* transmitted by each transmission line *k* should not exceed its transmission capacity tc_k as given in Equation (4.27).

$$\sum_w te_{w,n} \le tc_k \quad \forall k \in K, n \in N \tag{4.27}$$

The total amount of natural gas stored $v_{u,n}^{und,res}$ at underground reservoir *u* at time point *n* cannot exceed its storage capacity $V^{und,res,\max}$ as given in Equation (4.28). Equation (4.29) indicates that the amount of natural gas injected $pu_{p,u,n}$ in each reservoir cannot exceed its injection capacity $IC^{\max,und}$ while Equation (4.30) states that the amount of gas withdrawn $uw_{u,w,n}$ from each underground reservoir *u* at time point *n* cannot exceed its withdrawal ability $WC^{\max,und}$. y_u is a binary variable that indicate the existence of underground reservoir *u*.

$$v_{u,n}^{und,res} \le V^{und,res,\max} y_u \quad u \in U, \forall n \in N \tag{4.28}$$

$$\sum_p pu_{p,u,n} \le IC^{\max,und} y_u \quad u \in U, \forall n \in N \tag{4.29}$$

$$\sum_w uw_{u,w,n} \le WC^{\max,und} y_u \quad u \in U, \forall n \in N \tag{4.30}$$

The amount of natural gas liquids stored $v_{p,n}^{ngl}$ at each processing plants *p* at time point *n* cannot exceed its storage capacity $V^{ngl,\max}$ as given in Equation (4.31) where y_p is a binary variable indicating the existence of a processing plant.

$$v_{p,n}^{ngl} \le V^{ngl,\max} y_p \quad \forall p \in P, n \in N \tag{4.31}$$

The amount of natural gas liquids sold from all the processing plants at time point *n* cannot exceed the demand $NL^{\max}$ as indicated in Equation (4.32)

$$\sum_p nls_{p,n} \le NL^{\max} \quad \forall n \in N \tag{4.32}$$

The amount of gas transported by pipeline is bounded by the capacity of the pipeline which include the pipeline transporting shale gas from wellpad *s* to processing plant *p*, natural gas from processing plant *p* to power plant *w*, distribution company *b*, underground reservoir *u* and from underground reservoir *u* to power plant *w* as given in Equation (4.33) –(4.37)

$$sp_{s,p,n} \le c_{s,p}^{pipe} \quad s \in S, p \in P, \forall n \in N \tag{4.33}$$

$$pw_{p,w,n} \le c_{p,w}^{pipe} \quad p \in P, w \in W, \forall n \in N \tag{4.34}$$

$$pu_{p,u,n} \le c_{p,u}^{pipe} \quad p \in P, u \in U, \forall n \in N \tag{4.35}$$

$$pd_{p,b,n} \le c_{p,b}^{pipe} \quad p \in P, b \in B, \forall n \in N \tag{4.36}$$

$$uw_{u,w,n} \le c_{u,w}^{pipe} \quad u \in U, w \in W, \forall n \in N \tag{4.37}$$

The total amount of natural gas sent from processing plant *p* and underground reservoir *u* to each power plant *w* must not exceed the power plant demand $W^{\max}$ as given by Equation (4.38) while Equation (4.39) states that the total amount of natural gas sent from processing plant *p* to distribution company *b* should not exceed the demand B^{max}. y_w and y_b are binary variables indicating the existence of power plant and distribution company respectively.

$$\sum_p pw_{p,w,n} + \sum_u uw_{u,w,n} \le W^{\max} y_w \quad w \in W, \forall n \in N \tag{4.38}$$

$$\sum_p pd_{p,b,n} \le B^{\max} y_b \quad b \in B, \forall n \in N \tag{4.39}$$

Amount of natural gas sent from distribution Company *b* to different customers should not exceed their demand as given by Equation (4.40) – (4.42)

$$\sum_{b} ind_{b,i,n} \le IND^{\max} \quad i \in I, \forall n \in N \tag{4.40}$$

$$\sum_{b} com_{b,c,n} \le COM^{\max} \quad c \in C, \forall n \in N \tag{4.41}$$

$$\sum_{e} res_{b,e,n} \le RES^{\max} \quad b \in B, \forall n \in N \tag{4.42}$$

The amount of power transmitted to different customers should not exceed their demand as given by Equation (4.43) – (4.45). Based on the information from literature (USEPA, 2018), 28% of power generated per time is used by industrial customers, 35% by commercial customers and 37% by residential customers.

$$\sum_{i} P_{i,n}^{ind} \le 0.28 P_{n}^{rec} \quad \forall n \in N \tag{4.43}$$

$$\sum_{c} P_{c,n}^{com} \le 0.35 P_{n}^{rec} \quad \forall n \in N \tag{4.44}$$

$$\sum_{e} P_{e,n}^{res} \le 0.37 P_{n}^{rec} \quad \forall n \in N \tag{4.45}$$

The capacity of impoundment *t* is bounded by the corresponding capacity range as given in Equation (4.46)

$$T^{\min} \le c_t \le T^{\max} \quad \forall t \in T \tag{4.46}$$

The volume of the impoundment at any time point *n* should not exceed its storage capacity as stated in Equation (4.47)

$$vi_{t,n} \le c_t \quad \forall t \in T, n \in N \tag{4.47}$$

If a processing plant exists, its processing capacity should be bounded by the corresponding capacity range as given in Equation (4.48)

$$cp^{\min} y_p \le c_p^{cap} \le cp^{\max} y_p \quad \forall p \in P \tag{4.48}$$

Equation (4.49) - (4.53) give the capacity of all pipeline transporting gas. $c^{Spipe,\min}$ and $c^{Spipe,\max}$ represent the minimum and maximum capacity of pipeline transporting shale gas, while

$c^{Npipe,\min}$ and $c^{Npipe,\max}$ represent the minimum and maximum capacity of pipeline transporting natural gas respectively.

$$c^{Spipe,\min} y_{s,p}^{sp} \le c_{s,p}^{pipe} \le c^{Spipe,\max} y_{s,p}^{sp} \quad s \in S, p \in P \tag{4.49}$$

$$c^{Npipe,\min} y_{p,w}^{pw} \le c_{p,w}^{pipe} \le c^{Npipe,\max} y_{p,w}^{pw} \quad p \in P, w \in W \tag{4.50}$$

$$c^{Npipe,\min} y_{p,u}^{pu} \le c_{p,u}^{pipe} \le c^{Npipe,\max} y_{p,u}^{pu} \quad p \in P, u \in U \tag{4.51}$$

$$c^{Npipe,\min} y_{p,b}^{pd} \le c_{p,b}^{pipe} \le c^{Npipe,\max} y_{p,b}^{pd} \quad p \in P, b \in B \tag{4.52}$$

$$c^{Npipe,\min} y_{u,w}^{uw} \le c_{u,w}^{pipe} \le c^{Npipe,\max} y_{u,w}^{uw} \quad u \in U, w \in W \tag{4.53}$$

If a transmission line exists, its transmission capacity should be bounded by the corresponding capacity range as given in Equation (4.54)

$$k^{\min} y_k \le tc_k \le k^{\max} y_k \quad \forall k \in K \tag{4.54}$$

4.2.4. Scheduling Constraints

The scheduling part of the model captures the time dimension related to the process. These are categorised into three parts namely:

- wellpad scheduling
- wastewater storage tank scheduling and
- the regenerator scheduling

It is worth mentioning that the scheduling framework with water network constraints have been presented in detail in chapter three. However, important scheduling constraints are provided again to facilitate understanding.

4.2.4.1. Wellpad scheduling

The duration of each wellpad $du_{s,n}$, is calculated by Equation (4.55) where TR_s is the time required to fracture wellpad *s*. Equations (4.56) and (4.57) gives the finish time of each wellpad $tf_{s,n}$ expressed with big-M constraints, which are only active if wellpad *s* is stimulated at time point *n* where $ts_{s,n}$ is the start time of fracturing wellpad s at time point n .

$$du_{s,n} = TR_s w_{s,n} \quad \forall s \in S, n \in N \tag{4.55}$$

$$tf_{s,n} \le ts_{s,n} + du_{s,n} + H\left(1 - w_{s,n}\right) \quad \forall s \in S, n \in N \tag{4.56}$$

$$tf_{s,n} \geq ts_{s,n} + du_{s,n} - H\left(1 - w_{s,n}\right) \quad \forall s \in S, n \in N \tag{4.57}$$

Equation (4.58) is the sequence dependent change over time between wellpad *s* and $s^{'}$. It states that the start time of wellpad $s^{'}$ at time point *n* must be equal or greater than the finish time of wellpad *s* at previous time point plus the crew transition time $CT_s^{s'}$ between wellpad s and s'.

$$ts_{s^{'},n} \geq tf_{s,n-1} + CT_s^{s^{'}} w_{s^{'},n} \quad \forall s \in S, s^{'} \in S, s^{'} \neq s, n \in N, n \geq 2 \tag{4.58}$$

4.2.4.2. Storage tank scheduling

Water usage in hydraulic fracturing and water sent to the storage tank for treatment are linked by Equation (4.59). It states that water can only be transferred from wellpad *s* to the wastewater tank for treatment if wellpad fracturing takes place at that time point. Equations (4.60) and (4.61) ensure that the transfer time of water from a wellpad into storage $tv_{s,n}$ correspond with the time when the fracturing task ends $tf_{s,n}$.

$$wv_{s,n} \leq w_{s,n} \quad \forall s \in S, n \in N \tag{4.59}$$

$$tv_{s,n} \geq tf_{s,n} - H\left(2 - wv_{s,n} - w_{s,n}\right) \quad \forall s \in S, n \in N \tag{4.60}$$

$$tv_{s,n} \leq tf_{s,n} + H\left(2 - wv_{s,n} - w_{s,n}\right) \quad \forall s \in S, n \in N \tag{4.61}$$

4.2.4.3. Regenerator scheduling

Equation (4.62) relates the regeneration and fracturing task starting at time point *n*. It states that water regeneration can only take place at time point n if there is a wellpad to be fractured at that time point. Equations (4.63) and (4.64) ensure that the time at which regeneration starts tr_n coincide with the time at which fracturing task starts at time point *n*. This is because all tasks starting at point *n* must start at the same time but their finish times do not have to coincide. Equation (4.65) gives the duration of regeneration where ttr_n is the finish time of regeneration at time point *n*, f_n^{reg} is the total volume of water into the regenerator at time point n and ff^{MD} is the feed flowrate into the regenerator.

$$wr_n \geq w_{s,n} \quad \forall s \in S, n \in N \tag{4.62}$$

$$tr_n \geq ts_{s,n} - H\left(2 - wr_n - w_{s,n}\right) \quad \forall s \in S, n \in N \tag{4.63}$$

$$tr_n \le ts_{s,n} + H\left(2 - wr_n - w_{s,n}\right) \quad \forall s \in S, n \in N \tag{4.64}$$

$$ttr_n = tr_n + \left(\frac{f_n^{reg}}{ff^{MD}}\right) wr_n \quad \forall n \in N \tag{4.65}$$

4.2.4.4. Membrane distillation (MD) model

The membrane distillation model used is based on the work of Elsayed et al. (2013). This model has been presented in detail in chapter three and will not be discussed in detail in this chapter. However, some of the key equations in the model are provided for better understanding.

The driving force for the water flux across the membrane, Jw, is the difference in pressure of the water vapour and is defined in Equation (4.66) as:

$$Jw = Bw\left(p_{wf}^{vap}\gamma_{wf}x_{wf} - p_{wp}^{vap}\right) \tag{4.66}$$

where Bw is the membrane permeability, p_{wf}^{vap},is the water vapour pressure of the feed, p_{wp}^{vap} is the water vapour pressure of the permeate, γ_{wf} is the activity coefficient of water in the feed and x_{wf} is the mole fraction of water in the feed.

The activity coefficient is dependent on concentration and on the assumption of NaCl as the primary solute, Equation (4.67) (Yun et al., 2006) can be used to estimate the activity coefficient where x_{NaCl} is the molar concentration of NaCl in the feed.

$$\gamma_{wf} = 1 - 0.5x_{NaCl} - 10x_{NaCl}^2 \tag{4.67}$$

The permeability of the membrane Bw depends on the membrane temperature, T_m which differs based on the kind of diffusion. The permeability of membranes in which molecular diffusion occurs is calculated through Equation (4.68) as proposed by Elsayed et al. (2013) where B_{wb} is the temperature-independent base value of membrane permeability.

$$Bw = B_{wb}T_m^{1.334} \tag{4.68}$$

The amount of permeated water is highly dependent on the energy Q provided to the unit. Therefore, the heat required by the feed is given by Equation (4.69).

$$Q = ff^{feed}C_P\left(T_{bf} - T_{sf}\right) \tag{4.69}$$

The membrane area A_m is calculated by dividing the permeate flow rate by the water flux as given in Equation (4.70).

$$A_m = \frac{ff^{perm}}{Jw} \tag{4.70}$$

The annualized fixed cost of the MD network, AFC, as proposed by Elsayed et al. (2013) is given by Equation (4.71).

$$AFC = 58.5A_m + 1115\,ff^{feed} \tag{4.71}$$

The annual operating cost excluding heating, AOC, as proposed by Elsayed et al. (2013) is given by Equation (4.72), where u, is the ratio of recycled reject to raw feed.

$$AOC = \left(1411 + 43\left(1 - LR\right) + 1613\left(1 + u\right)\right) ff^{feed} \tag{4.72}$$

The annual heating cost AHC, is given by Equation (4.73): where AOT is the annual operating time, Q is the heat requred by the feed into MD and OC^{ht} is a parameter indicating the cost of heating.

$$AHC = AOT\left(QOC^{ht}\right) \tag{4.73}$$

4.3. Case study

To illustrate the application of the proposed model, a case study taken from Yang et al. (2015) and Bartholomew and Mauter, (2016) is considered as illustrated in Table 4.1. This case study deals with longer-term decisions for water management in shale exploration. Fourteen wellpads that are geographically distributed in two clusters in a given region with different availability time are considered. There are five nearby interruptible freshwater sources, one uninterruptible freshwater source and two impoundments serving the wellpads in the two areas. The layout for the case study is shown in Figure 4.2. The time horizon considered is 3 years. The major changes from the case study presented in Yang et al. (2015) is as follows:

- The removal of ponds and the addition of one uninterruptible source
- The removal of an impoundment from area 2 and placement of impoundment in area 1
- Choice of modular desalination technology that is placed onsite and can be moved from one wellpad to the other.

Table 4.1. Wellpad Data

Wellpads	S1	S2	S3	S4	S5	S6	S7	S8	S9	S10	S11	S12	S13	S14
Earliest frac day	1	42	133	133	497	497	140	77	133	133	133	497	497	497
# of stages	120	120	210	140	140	210	434	492	280	175	280	175	70	350
# of wells	10	4	6	4	4	6	14	12	8	5	8	5	2	10

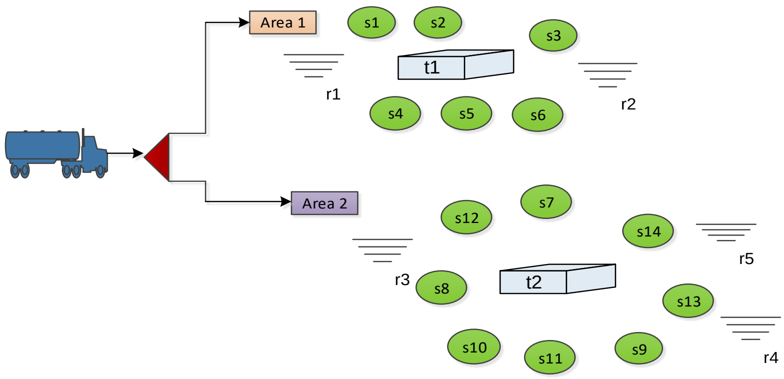

Figure 4.2. Layout for the case study

In addition to the case study in Yang et al. (2015), we consider 3 sets of shale gas processing plants, 4 underground reservoirs for natural gas storage, 5 distribution companies that distribute natural gas to the end users, 3 gas turbine combined cycle power plants with 50% generation efficiency based on lower heating value (LHV) and 3 sets of high voltage transmission line. The parameters and the cost coefficients are given in Table 4.2 while the information regarding the average flowback water and TDS profile for a given wellpad in the first 14-20 days after wellpad fracturing, and the expected gas production for each wellpad are obtained from Yang et al. (2015) respectively. The data pertaining to shale gas optimization were taken from Gao and You (2015a) and the design parameters of the membrane process were adapted from Elsayed et al. (2013).

Two scenarios are considered to ensure the detailed analysis of the model. Scenario 1 is the case where the shale gas considered is wet gas that require further processing before distribution while scenario 2 considered dry gas that require no further processing. Both scenarios consider water and gas integration involving detailed regenerator where water, gas and energy are optimized simultaneously. The implementation of the resulting model was done in GAMS and solved using the general-purpose global optimization solver (BARON).

Table 4.2. Parameters and cost coefficients

Parameter	Value
Crew transition time (day)	5
Volume of frac fluid used per stage (m^3)	950
Freshwater used (%)	85
Wastewater storage cost ($/$m^3$)	0.59
Freshwater trucking cost ($/$m^3$)	29.35
Freshwater pumping cost ($/$m^3$)	15.93
Disposal cost ($/m3)	134.18
Wastewater pumping cost($/km/m3)	0.28
Temperature-independent base value ($kg/m^2.s.pa.K^{1.334}$)	$3.9*10^{-10}$
Impoundment base capital cost ($)	360,000
Impoundment incremental cost ($/$m^3$)	7.40
Cost of pipeline ($/km)	202,000
Cost of freshwater withdrawal ($/$m^3$)	0.99
Reference capital investment for processing plant ($)	21,310,000
Membrane thickness (mm)	0.65
Membrane life time (year)	4
Annual operation time (h)	8000
Heating cost ($/$10^9$J)	5
Supply temperature (K)	293
Specific heat capacity (KJ/kgK)	4
NGL composition in shale gas	0.1-0.2
Natural gas price ($/$m^3$)	0.12
Chemical engineering plant cost index for pipeline	881.9
Chemical engineering plant cost index for processing plant	574
Methane composition in shale gas	0.8-0.9
Chemical engineering plant cost index of the reference year for pipeline	887.6

4.3.1. Cost analysis

The optimum results indicate that, the maximum expected profit is $9.16 billion for scenario 1. The total cost is $41.98 billion, the revenue from electricity, natural gas and natural gas liquid is found to be $51.15 billion. Of the revenue, 65 % is generated from the sale of electricity, 22.84 % from natural gas sale and the remaining 12.14 % comes from the sale of natural gas liquids. The detailed cost breakdown of the optimal solution for the first scenario is given in Figure 4.3. From Figure 4.3, shale gas production cost which include the cost of wellpad drilling and production has the highest percentage, which is 51.7 % of the total cost. Shale gas processing cost, which include the capital investment and operating cost of the processing plant accounts for 42 % while power generation and transmission only account for 4 % and 1.8 % respectively. Water related cost accounts for 0.3 % while transportation and storage cost related to gas is 0.4 % of the total cost, which are found to be negligible.

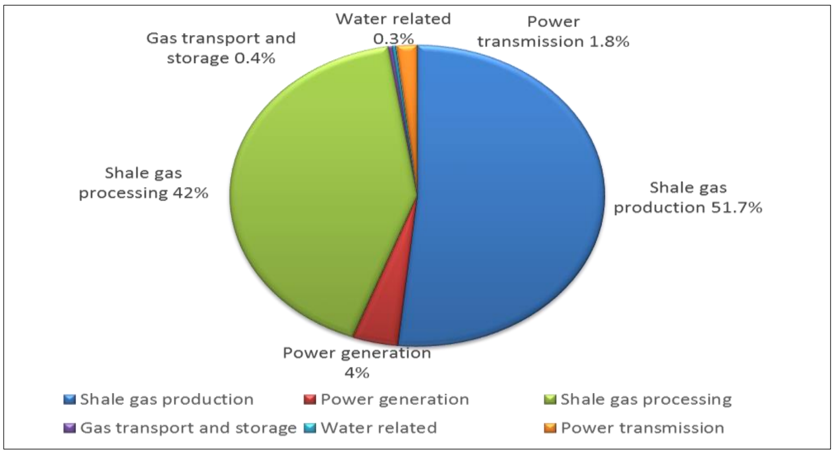

Figure 4.3. Cost breakdown of the optimal case (wet gas)

The optimum results for scenario 2 indicate a total profit of $25.44 billion. The total cost is $24.45 billion, and the revenue generated from the sale of electricity and natural gas amount to $49.89 billion. Of this revenue, 66.65 % is generated from the sale of electricity and 33.35 % from natural gas. The detailed cost breakdown of the optimal solution for the second scenario is given in Figure 4.4. In Figure 4.4, shale gas production cost amounts to 88.8 % of the total cost incurred while power generation and transmission account for 6.8 % and 3.1 % respectively. Water related cost accounts for 0.52 % while transportation and storage cost related to gas is 0.86 % of the total cost.

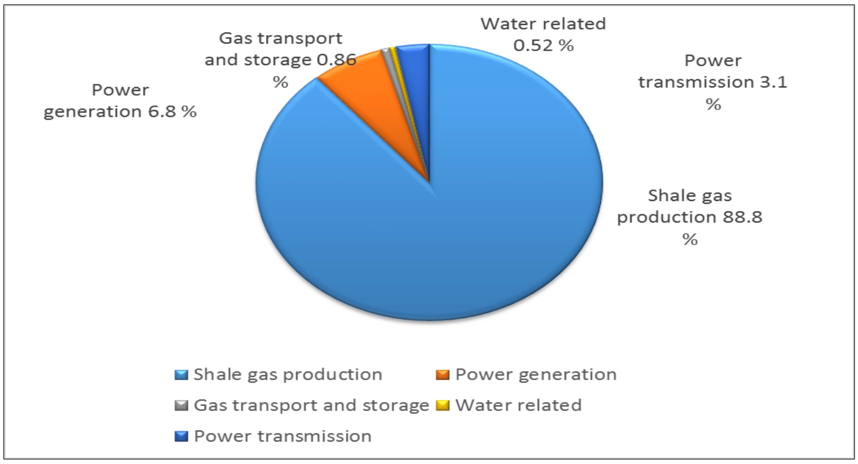

Figure 4.4**.** Cost breakdown of the optimal case (dry gas)

The huge difference in the profit realised in scenario 2 compared to scenario 1 is due to the fact that scenario 2 does not require setting up processing plants as dry gas contain mainly methane which require no further processing. The 2.5 % increase in revenue realised in scenario 1 arises from the sale of natural gas liquid, which according to literature has higher market values than methane gas (Gao et al., 2017).

4.3.2. Optimal network configuration

The optimal configuration of freshwater and shale gas network for wet and dry gas scenario are presented in Figures 4.5 and 4.6 respectively. The results indicate that for the two scenarios, the model proposed freshwater acquisition from interruptible sources through piping as a preferred option thereby reducing the cost and environmental issues that is associated with trucking. All the five interruptible freshwater sources are selected and the capacity of impoundment in the two areas are 850×10^3 m^3 each for the two scenarios. Two processing plants each with different capacities are set up in scenario 1 and the capacity of each of the processing plants are 5.01×10^9 m^3 and 5.39×10^9 m^3 respectively. One underground reservoir is set up in both scenarios to serve as natural gas inventory management tool or seasonal natural gas supply backup and the difference in the preferred option for the reservoir depends on the distance to the processing plants or the wellpads. Both scenarios require four distribution companies that distributes natural gas to various end users. While scenario 1 requires 2 power plants to be set up, scenario 2 requires setting up 3 power plants as the volume of natural gas in scenario 2 is higher than scenario 1 (as the shale gas produced in scenario 1 is made up of methane and NGLs). The transmission capacity for each of the three-transmission line set up is found to be 10×10^6 MW and the average power loss in the two scenarios during electricity transmission per time point is 1.02 %.

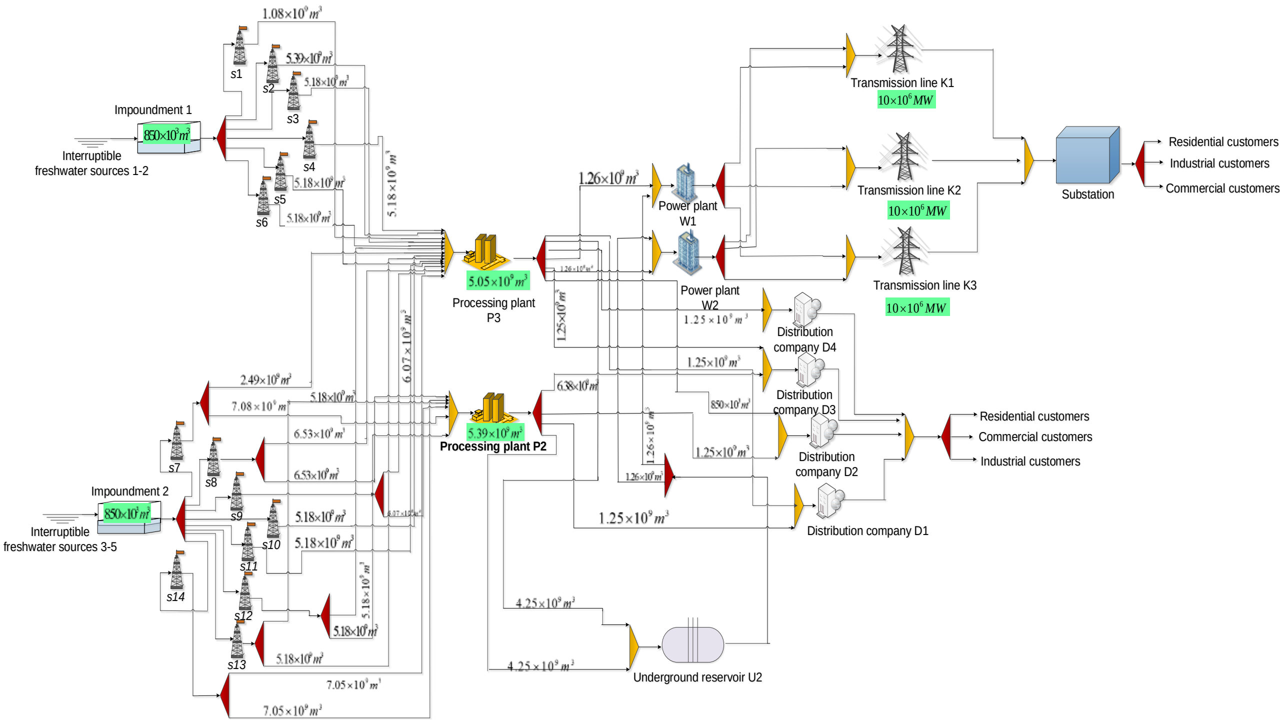

Figure 4.5. Optimal configuration of freshwater and gas network (wet gas).

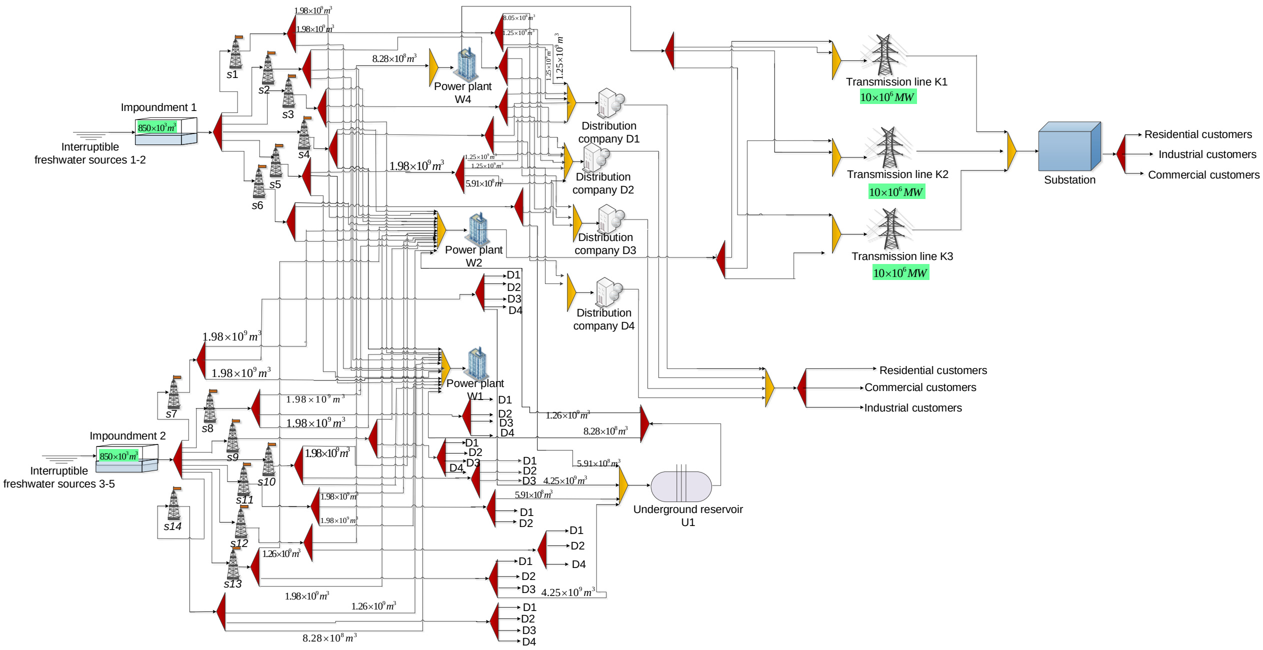

Figure 4.6. Optimal configuration of freshwater and gas network (dry gas).

4.3.3. Fracturing schedule

Table 4.3 gives the computational results and the solution comparisons for the two scenarios considered. The fracturing schedule for each scenario is presented in Figures 4.7and 4.8 respectively. From Figures 4.7 and 4.8, wellpads from the same geographical area follow each other in the schedule in most cases, which will improve the overall logistics. It is worth noted that there is tightness in the fracturing schedule of wellpads in both scenarios, this tightness in schedule may lead to three important factors:

(a) It will bring about steady production of gas which in turn helps in satisfying the market demands as shale gas production for each wellpad is considered to have exponentially decreasing production profile (Yang et al., 2015; Gao and you, 2015a).

(b) It will help in designing more appropriate infrastructure capacities; thereby increase the overall economic performance.

(c) The tightness in fracturing schedules will improves the recycling efficiency of flowback water. Due to efficient reuse of flowback water, a saving of 944,288 m^3 of freshwater is achieved out of the total volume of 4,064,986 m^3 required for the 14 wellpads.

Table 4.3. Solution comparison

	Scenario 1	Scenario 2
Total water used (1,000 m^3)	4,064.98	4,064.98
Freshwater trucked (1,000 m^3)	0	0
Freshwater pumped (1,000 m^3)	3,120.69	3,120.69
Regenerated water (1,000 m^3))	944.29	944.29
Freshwater saved (%)	23.2	23.2
Cost of gas transport and storage ($ 1,000)	167,920	210,270
Cost of shale gas processing ($ 1,000)	17,631,600	NA
Cost of power transmission ($ 1,000)	755,640	757,950
Cost of shale gas production ($ 1,000)	21,703,660	21,711,600
Revenue ($ 1,000)	51,145,000	49,893,000
Profit ($ 1000)	9,159,605	25,441,149
No. of constraints	11,537	12,910
No. of continuous variables	9,868	11,391
No. of binary variables	551	649
Non-linear terms	1,597	1,695
CPU time (s)	81626	84191

Another important thing to note in the fracturing schedule for the two scenario is that scenario 1 choses to fracture wellpads S8, S7 and S9 after S1 and as these 3 wellpads have high number of stages, they require large volume of water especially S8 and S7, this may be the reason why there is huge gap between S1 and S8 as the schedule has to be delayed to allow for enough water to be available. However, in scenario 2, the fracturing schedule are much tighter at the beginning and the delay is not as profound as scenario 1 as wellpads with less numbers of stages are fractured first which makes the finishing time of all the wellpads to be quicker than scenario 1. The common thing to be noted in the two scenarios is that the wellpads that require the largest volume of water i.e. S8, S7, S9, S11and S14 are fractured after each other especially in scenario 2; this will lead to a significant reduction in the amount of freshwater to be withdrawn.

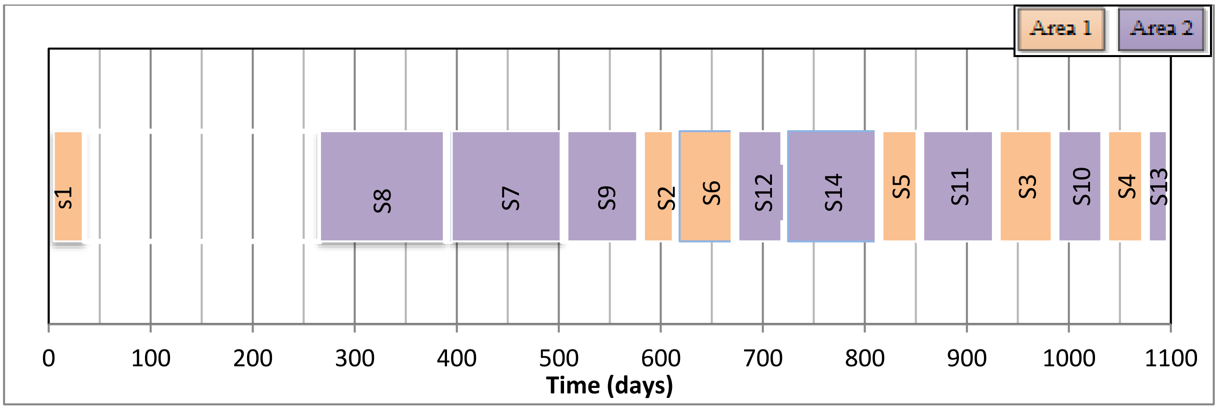

Figure 4.7. Fracturing schedule (Scenario 1)

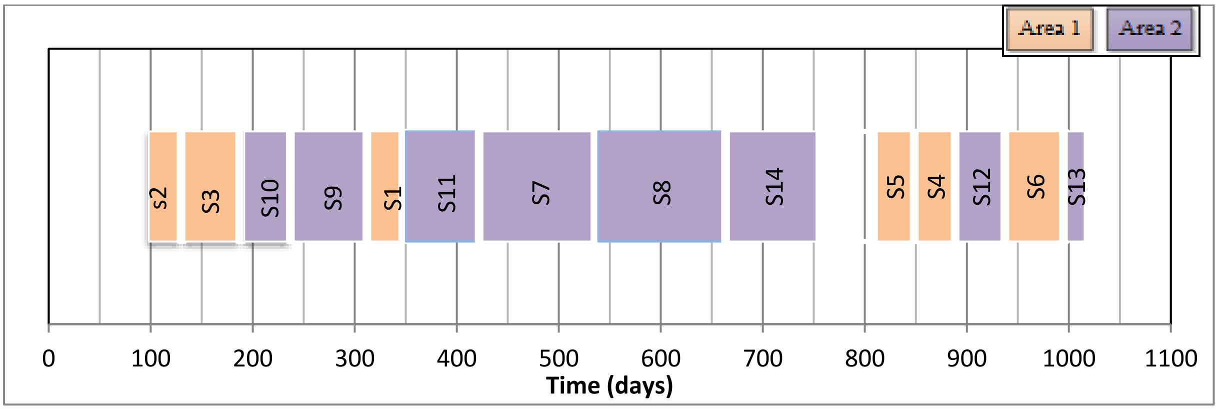

Figure 4.8. Fracturing schedule (Scenario 2)

4.3.4. Regeneration energy

In order to calculate the energy associated with the wastewater regeneration, analysis based on the detailed model and MD standalone model was performed. The optimum throughput from the scenarios (both scenarios have the same throughput) was used in the MD standalone model in order to determine the actual energy needed for regeneration. When MD standalone model is considered, the membrane operated at the maximum feed temperature of 363 K which leads to the maximization of the water flux across the membrane, hence the membrane area and the fixed cost is minimized. However, this does not necessarily correspond to the optimal performance of the membrane. The simultaneous optimization of both energy, water and shale gas within the network for both scenarios results in 42.7 % reduction in the amount of energy required by the regenerator based on the throughput per day. The amount of energy required is reduced from 700×10^{6} kJ to 401×10^{6} kJ. The thermal energy consumption is in the order of 160×10^{3} kJ/m^{3} of water. The design specifications of the MD regenerator required for this process are given in Table 4.4. The optimal feed temperature is found to be 333 K and the permeate flux is 0.005 kg/m^{2}s. The thermal energy required and the removal ratio are given in Table 4.4.

Table 4.4 Design specification for MD.

Design variables	Optimum values
MD feed temperature (K)	333
Thermal efficiency	0.97
Thermal energy (kJ/day)	4×10^{8}
Removal ratio	0.99
Permeate flux (kg/m^{2}s)	0.005

4.4. Conclusion

This work proposes a continuous time scheduling formulation for water-energy nexus optimization in shale gas exploration with emphasis on shale gas production, processing, distribution, power generation and transmission. This entails incorporating detailed MD model within the network to capture the energy requirement associated with water management in shale gas production. Consideration is also given to both wet and dry gas in order to capture the impact the type of gas produced in a particular shale play will have on the infrastructure development and economic performance. It has been established that the type of shale gas to be produced from wellpads in a particular region can have significant effect on the infrastructure development required and the overall economic performance.

NOMENCLATURE

Sets

B $\{b \mid b$ = distribution company$\}$

C $\{c \mid c$ = commercial customer$\}$

D $\{d \mid d$ = injection well$\}$

E {e | e = residential customer}

I {i | i = industrial customers}

K {k | k = transmission line}

N {n | n = time point}

P {p | p = processing plant}

S {s | s = wellpad}

T {t | t = an interruptible source and its corresponding impoundment}

$Tp_{a,t}$ Match between river source a and impoundment t

$TP_{s,t}$ Match between wellpad s and impoundment t

U {u | u = underground reservoir}

W {w | w = power plant}

Parameters

AOT Annual operating time, hr

AT_s Availability time of wellpad s, day

$B^{\max}$ Natural gas demand by distribution company at time point, m^3

B_{wb} Temperature independent base value for the permeability, $kg/m^2.s.pa.K^{1.334}$

C_p Specific heat capacity of the feed stream, KJ/kgK

$c^{Spipe,\min}$ Minimum capacity of pipeline transporting shale gas, m^3

$c^{Spipe,\max}$ Maximum capacity of pipeline transporting shale gas, m^3

$c^{Npipe,\min}$ Minimum capacity of pipeline transporting natural gas, m^3

$c^{Npipe,\max}$ Maximum capacity of pipeline transporting natural gas, m^3

$CC^{base,imp}$ Base capital cost of impoundment, \$

CC^{pipe} Capital cost of pipeline, \$

$CC^{ref,pro}$ Reference capital cost for processing plant, \$

$CC^{ref,pipe}$ Reference capital cost for pipeline transporting gas, $

$cp^{\min}$ Minimum capacity of processing plant, m^3

$cp^{\max}$ Maximum capacity of processing plant, m^3

$chem^{pipe}$ Chemical engineering plant cost index for pipeline

$COM^{\max,}$ Natural gas demand by commercial customers

$D_{a,t}$ Distance between interruptible source *a* and impoundment *t*, km

$D_{s,p}$ Distance between wellpad *s* and processing plant *p*, km

$D_{p,b}$ Distance between processing plant p and distribution company b, km

$D_{p,u}$ Distance between processing plant *p* and underground reservoir *u*, km

$D_{p,w}$ Distance between processing plant *p* and power plant *w*, km

$D_{u,w}$ Distance between underground reservoir *u* and power plant *w*, km

DS_s Distance from wellpad *s* to treatment facility, km

Dd_s Distance from wellpad *s* to disposal, km

$du_{s,n}$ Duration of wellpad *s* fractured at time point *n*, day

EG Electricity generated per unit natural gas input, kWh/m^3

$F_a^{pump,\max}$ Maximum amount of water that can be pumped from river *a*, m^3

H Time horizon of interest, yr

$IC^{inc,imp}$ Incremental cost of impoundment, $\$/m^3$

$IC^{\max,und}$ Injection capacity of underground reservoir, m^3

$IND^{\max,}$ Natural gas demand by industrial customers

$K^{\min}$ Minimum capacity of transmission line, MW

$K^{\max}$ Maximum capacity of transmission line, MW

LR	Liquid recovery for the regenerator
MC_s	Methane composition of wellpad *s*
NC_s	NGL composition of wellpad *s*
$NL^{\max}$	Maximum demand for natural gas liquid at any time point, m^3
$OC_s^{pump,fw}$	Freshwater pumping cost, \$/m^3
$OC_s^{truck,fw}$	Freshwater trucking cost, \$/m^3
$OC^{wd,fw}$	Cost of freshwater withdrawal, \$/m^3
$OC_s^{pump,ww}$	Wastewater pumping cost, \$/km/m^3
OC^{dis}	Cost of wastewater disposal, \$/m^3
$OC_s^{st,ww}$	Cost of wastewater storage, \$/m^3
$OC^{ww,truck}$	Cost of wastewater trucking, \$/km/m^3
OC^{ht}	Cost of heating, \$/10^{9}J
OC^{pipe}	Unit variable cost for pipeline transporting gas, \$/m^3
$OC^{power,gen}$	Cost of power generation from natural gas, \$/m^3
$OC^{st,ngl}$	Cost of NGL storage, \$/m^3
$OC^{inj,nat\,gas}$	Cost of natural gas injection, \$/m^3
$OC^{wd,nat\,gas}$	Cost of natural gas withdrawal, \$/m^3
$OC^{ele,trans}$	Cost of power transmission, \$/kWh
OC^{pro}	Cost of processing plant, \$/m^3
ps_s	Expected shale gas production of wellpad *s*, m^3
PE	Processing efficiency of processing plant
PF	Power factor
R^{trans}	Transmission line resistance, ohm

$RES^{\max,}$ Natural gas demand by residential customers

rcp^{pipe} Reference capacity of pipeline transporting gas, m^3

rcp Reference capacity of processing plant, m^3

$rchem^{pipe}$ Chemical Engineering plant cost index of reference year for pipeline

$rchem^{pro}$ Chemical Engineering plant cost index of the reference year for processing plant

sfp Size factor of processing plant

sft Size factor of pipeline transporting gas

$SP^{gas,ind}$ Unit price of natural gas to industrial customers, \$/m^3

$SP^{gas,com}$ Unit price of natural gas to industrial customers, \$/m^3

$SP^{gas,res}$ Unit price of natural gas to residential customers, \$/m^3

SP^{ngl} Sale price of NGL, \$/m^3 gas

$SP^{ele,com}$ Sale price of electricity to the commercial customers, \$/kWh

$SP^{ele,ind}$ Sale price of electricity to the industrial customers, \$/kWh

$SP^{ele,res}$ Sale price of electricity to the residential customers, \$/kWh

ST_s Availability date of wellpad s , day

$CT_S^{S'}$ Crew transition time between wellpads, day

T_{sf} Temperature of feed water into the treatment unit, K

$T^{\min}$ Minimum capacity of impoundment *t*, m^3

$T^{\max}$ Maximum capacity of impoundment *t*, m^3

u Ratio of recycled reject to raw feed

$uc_{s,n}^{prod}$ Unit cost of shale gas production at wellpad *s* at time point *n*, \$/m^3

$uc_{s,n}^{drill}$ Unit cost of drilling and completion of wellpad *s* at time point *n*, \$

V^{trans} Transmission voltage, kV

V^{ind} Voltage required by industrial customers, kV

V^{com} Voltage required by commercial customers, kV

V^{res} Voltage required by residential customers, kV

$V^{und,res,\max}$ Working gas capacity of underground reservoir, m^3

$V^{und,res,\max}$ Withdrawal capacity of underground reservoir, m^3

$V^{ngl,\max}$ Storage capacity of natural gas liquid, m^3

$W^{\max}$ Power plant demand at any time point, m^3

X_{NaCl} Molar concentration of NaCl in the feed

Binary variables

$w_{s,n}$ Defines the beginning of stimulating each wellpad s at time point n

wr_n Transfer of water from storage to regenerator at time point n

$wv_{s,n}$ Transfer of water from wellpad s to storage at time point n

y_a Binary variable indicating the existence of interruptible source a

y_b Binary variable indicating the existence of distribution company b

y_p Binary variable indicating the existence of processing plant

y_k Binary variable indicating the existence of transmission line k

y_u Binary variable indicating the existence of underground reservoir u

y_w Binary variable indicating the existence of power plant w

$y_{s,p}^{sp}$ Binary variable indicating existence of pipeline between s and p

$y_{p,u}^{pu}$ Binary variable indicating the existence of pipeline between p and u

$y_{p,b}^{pd}$ Binary variable indicating the existence of pipeline between p and d

$y_{p,w}^{pw}$ Binary variable indicating the existence of pipeline between p and w

$y_{u,w}^{uw}$ Binary variable indicating existence of pipeline between *u* and *w*

Continuous variables

A_m Required membrane area, m^2

AFC Annualized fixed capital cost for the regenerator, \$/yr

AHC Annualized heating cost for the regenerator, \$/yr

AOC Annualized operating cost for the regenerator, \$/yr

Bw Membrane permeability, kg/(m^2.pa)

c_t Capacity of impoundment *t*, m^3

c_p^{cap} Capacity of processing plant *p*, m^3

$c_{p,w}^{pipe}$ Capacity of pipeline transporting gas from *p* to *w*, m^3

$c_{p,u}^{pipe}$ Capacity of pipeline transporting gas from *p* to *u*, m^3

$c_{u,w}^{pipe}$ Capacity of pipeline transporting gas from u to w, m^3

$c_{s,p}^{pipe}$ Capacity of pipeline transporting shale gas from *s* to *p*, m^3

$c_{p,b}^{pipe}$ Capacity of pipeline transporting gas from *p* to *b*, m^3

$chem^{pro}$ Chemical Engineering plant cost index for processing plant

$com_{b,c,n}$ Amount of natural gas sent to commercial customer *c* from distribution company *b* at time point *n*, Amp

$f_{s,n}$ Total water required to frac wellpad s at time point n, m^3

$f_{t,n}^{truck}$ Water trucked from uninterruptible source to impoundment t at time point *n*, m^3

$f_{t,n}^{pump}$ Total water pumped from to impoundment t at time point *n*, m^3

$f_{s,n}^{fw}$ Freshwater required to frac wellpad s at time point *n*, m^3

$fp_{a,n}^{fw}$ Freshwater pumped from interruptible source a at time point n, m^3

$f_{s,n}^{ww}$ Wastewater required to frac wellpad s at time point n, m^3

$f_{s,n}^{bw}$ Flowback water from wellpad s at time point n, m^3

$f_{s,n}^{trtb}$ Flowback water sent to treatment facility at time point n, m^3

$f_{s,n}^{dis}$ Flowback water sent to disposal from wellpad s at time point n, m^3

ff^{feed} Total flowrate into MD, kg/day

f_n^{perm} Amount of water collected as permeate from the regenerator at time point n, m^3

f_n^{reg} Total flowback water to be treated at time point n, m^3

ff^{perm} Permeate flowrate from MD, kg/day

ff^{MD} Total flowrate into MD, m^3/day

fd_n Total water sent to disposal at time point n, m^3

$i_{t,n}^{fw}$ Total freshwater required to frac from impoundment t at time point n, m^3

I_n^{trans} Total current on transmission line at time point n, Amp

$I_n^{trans,com}$ Current transmitted to the commercial customers at time point n, Amp

$I_n^{trans,ind}$ Current transmitted to the industrial customers at time point n, Amp

$I_n^{trans,res}$ Current transmitted to the residential customers at time point n, Amp

$ind_{b,i,n}$ Amount of natural gas sent to industrial customer i from distribution company b at time point n, m^3

Jw Water flux across the membrane, kg/(m^2.s)

$ngl_{p,n}$ Amount of NGL produced at processing plant p at time point n, m^3

$nls_{p,n}$	Amount of NGL sold from processing plant *p* at time point *n*, m^3
$pr_{s,n}$	Expected gas production of wellpad s at time point *n*, m^3
p_{wf}^{vap}	Water vapour pressure of the feed in MD, pa
p_{wp}^{vap}	Water vapour pressure of the permeate in MD, pa
P_n^{rec}	Power received at substation at time point *n*, kWh
P_n^{loss}	Power loss during transmission at time point *n*, kWh
$P_{e,n}^{res}$	Power sent to residential customers *e* at time point n, kWh
$P_{i,n}^{ind}$	Power sent to industrial customers *i* at time point n, kWh
$P_{c,n}^{com}$	Power sent to commercial customers *c* at time point n, kWh
$pd_{p,b,n}$	Amount of natural gas sent from processing plant *p* to distribution company *b* at time point *n*, m^3
$pu_{p,u,n}$	Amount of natural gas sent from processing plant *p* to underground reservoir *u* at time point *n*, m^3
$pw_{p,w,n}$	Amount of natural gas sent from processing plant *p* to power plant *w* at time point *n*, m^3
Q	Heat required by the feed into MD, kJ/day
$res_{b,e,n}$	Amount of natural gas sent to residential customer *c* from distribution company *b* at time point *n*, Amp
$sp_{s,p,n}$	Amount of shale gas sent to processing plant *p* from wellpad *s* at time point *n*, m^3
tt_n	Time that correspond to time point n, day
$tf_{s,n}$	Finish time of wellpad *s* at time point *n*, day
$ts_{s,n}$	Start time of wellpad *s* at time point *n*, day

tr_n Start time of regeneration at time point *n*, day

ttr_n Duration of regeneration at time point *n*, day

$tv_{s,n}$ Time at which water is transferred from wellpad *s* to storage tank at time point *n*, day

$tm_{p,n}$ Total methane produced at processing plant *p* at time point *n*, m^3

$te_{w,n}$ Amount of power generated at power plant *w* at time point *n*, kWh

tc_k Capacity of transmission line *k*, MW

T_{bf} Temperature of the feed in the bulk, K

T_m Membrane average temperature, K

$uw_{u,w,n}$ Amount of gas withdrawn from underground reservoir *u* to power plant *w* at time point n, m^3

$v_{p,n}^{ngl}$ Amount of NGL stored at processing plant p at time point n, m^3

$v_{u,n}^{und,res}$ Amount of natural gas stored at underground reservoir *u* at time point n, m^3

$v_n^{st,ww}$ Volume of wastewater tank at *n*, m^3

$v_{s,n}^{ft}$ Capacity of frac tank on wellpad s at time point *n*, m^3

$vi_{t,n}$ Volume of impoundment *t* at time point *n*, m^3

v^{com} Voltage required by commercial customers, kV

v^{res} Voltage required by residential customers, kV

x_{wf} Mole fraction of water in the feed

γ_{wf} Activity coefficient of water in the feed to the membrane distillation

Superscript

base	Base
cap	Capacity
cons	Consumption
com	Commercial
dis	Disposal
drill	Drilling
ele	Electricity
feed	Feed
ft	Frac tank
fw	Freshwater
fbw	Flowback water
gas	Gas
gen	Generated
ht	Heating
ind	Industrial
imp	Impoundment
inc	Incremental
inj	Injection
loss	Loss
max	Maximum
min	Minimum
nat gas	Natural gas
ngl	Natural gas liquid

pro	Processing
*pro*d	Production
pump	Pumping
perm	Permeate
power	Power
pipe	Pipeline
res	Residential
res	Reservoir
ref	Reference
rec	Received
st	Storage
total	Total
truck	Trucking
trans	Transmission
trtb	Treatment
und	Underground
vap	Vapour
wd	Withdrawal
ww	Wastewater

Subscript

bp	Permeate bulk
bf	Feed bulk
m	Membrane

mp Membrane permeate

mf Membrane feed

wf Feed water

wp Permeate water

References

Bartholomew, T.V., Mauter, M.S., 2016. Multiobjective optimization model for minimizing cost and environmental impact in shale gas water and wastewater management. Journal of ACS Sustainable Chemistry and Engineering 4, 3728-3735.

Elsayed, N.A., Barrufet, M.A., El-Halwagi, M.M., 2013. Integration of thermal membrane distillation networks with processing facilities. Journal of Industrial and Engineering Chemistry Research 53, 5284-5298.

United State Environmental Protection Agency (USEPA), 2018. Energy and the environment: Electricity customers. https://www.epa.gov/energy/electricity-customers; accessed 4 July 2018.

Gao, J., He, C., You, F., 2017. Shale gas process and supply chain optimization. In: Advances in energy systems engineering. (Eds) Kopanos, G.M., Liu, P., Geeorgiadis, M.C. Switzerland: Springer International Publishing. 21-46,

Gao, J., You, F., 2015a. Shale gas supply chain design and operations toward better economic and life cycle environmental performance: MINLP model and global optimization algorithm. Journal of ACS Sustainable Chemistry and Engineering 3, 1282-1291.

Guerra, O.J., Calderon, A.J., Papageorgiou, L.G., Siirola, J.J., Reklaitis, G.V., 2016. An optimization framework for the integration of water management and shale gas supply chain design. Journal of Computer and Chemical Engineering 92, 230-255.

Yang, L., Grossmann, I.E., Mauter, M.S., Dilmore, R.M., 2015. Investment optimization model for freshwater acquisition and wastewater handling in shale gas production, Journal of American Institute of Chemical Engineers 61, 1770-1782.

Yun, Y., Ma, R., Zhang, W., Fane, A.G., Li, J., 2006. Direct contact membrane distillation mechanism for high concentration NaCl solutions. Desalination 188, 251–262.

CHAPTER FIVE

USING ULTRAFILTRATION FOR FLOWBACK WATER MANAGEMENT IN SHALE GAS EXPLORATION: MULTICONTAMINANT CONSIDERATION

Introduction

Selection of appropriate water management option in hydraulic fracturing involves consideration of many factors, which includes operational, environmental and economic factors. The previous chapters have focused on membrane distillation as a desalination technology capable of treating hydraulic fracturing wastewater effectively with focus on total dissolved solid (TDS) as the main contaminant of concern in wastewater reuse for fracturing. However, it is important to consider the multi-contaminant property of flowback water as flowback water is not a uniform raw material from a process development perspective. An example of this multi-contaminant property is given in Table 5.1.

Table 5.1. Random flowback water composition from Barnett and Appalachian plays (Carrero –Parreño et al., 2017)

Parameter	Well 1	Well 2	Well 3	Well 4
TDS (mg/L)	200,006	54,230	110,847	9,751
TSS (mg/L)	3,220	881	1,530	168
TOC (mg/L)	200	89	138	38
Fe (mg/L)	92	60	105	40
Ca (mg/L)	14,680	4,800	3600	241
Mg (mg/L)	4,730	1,707	899	49
Ba (mg/L)	98	112	127	1
Oil and grease (mg/L)	0	0	18	0

Through implementation of an on-site pre-treatment technology to remove contaminants like TSS, oil, grease and scaling materials, specification for water reuse as depicted in Table 5.2 can be achieved thereby blending the pre-treated water with freshwater in order to reduce other critical contaminants like TDS. Therefore, this chapter looks at the role that low pressure membrane can play in maximizing wastewater reuse in hydraulic fracturing with focus on ultrafiltration (UF) membrane technology. The study considered detailed ultrafiltration model in order to evaluate the sustainability of the system in terms of energy consumption and associated costs. The study also looked into the feasibility of using the gas that would otherwise be flared to generate electrical energy for the membrane system via an onsite gas generator. Thereby developing a systematic approach for scheduling and design of a mobile, cost-effective membrane-based pre-treatment technology for wastewater management in hydraulic fracturing.

Table 5.2. Specification for flowback water reuse in Marcellus Shale play (Carrero –Parreño et al., 2017)

Parameter	Maximum value recommended	
	1	2
TSS (mg/L)	50	
TDS (mg/L)	50,000-65,000	50,000
TOC (mg/L)	<25	
Total hardness (mg/L)	2,500	26,000
Total alkalinity (mg/L)		300
pH	6-8	
Bacteria (/mL)	<100	
Chloride (mg/L)	20,000-30,000	45,000
Sulfates (mg/L)		50
Ca (mg/L)		8000
Fe (mg/L)	20	10
Na (mg/L)		36,000
K (mg/L)		1,000
Ca (mg/L)		8,000
Mg (mg/L)		1,200
Ba (mg/L)		10
Sr (mg/L)		10
Mn (mg/L)		10

5.1. Problem statement

The problem addressed in this chapter is stated as follows:

Given:

- Number of freshwater sources (interruptible and uninterruptible)

- Set of wellpads *S* to be fractured with known volume of water required for fracturing and maximum allowable contaminant concentration in the fracturing fluid.
- Set of contaminants to be removed from flowback water
- Total number of frac stages for each wellpad
- Earliest fracturing date for each wellpad
- Set of wastewater injection wells *D*
- Volume of water required per stage
- Minimum and maximum number of stages that can be fractured per day
- Time horizon of interest
- Network of regenerator for pre-treatment only
- Performance of regenerator
- Gas storage facility
- Historical stream data for the interruptible source
- Gas generator to generate the electrical energy needed for the regenerator

Determine the optimal configuration of the total network that gives:

- Optimal fracturing schedule of the wellpads
- Minimum freshwater intake and wastewater generation
- Optimal operation and design conditions of the regenerator such as number of membrane modules and the energy consumption
- Feasibility of using flared gas as energy source for the regenerator.

The assumptions made in the model formulation are as follows:

- The wells in each wellpad are aggregated (Yang et al., 2015).
- Each wellpad is connected to exactly one of the impoundment through piping (Yang et al., 2014a).

- The number of fracturing stages that could be fractured per day is kept constant at 4
- The flowback water from the fractured wellpad is assumed to be 25% (Bartholomew and Mauter, 2016) of the initial water used.
- The capacity of the fracturing tank on each wellpad varies depending on its water requirement.
- The shale gas production profile of each wellpad is known
- The water pre-treatment unit is located onsite and can be moved from one wellpad to the other.
- The historical flowrate data for the interruptible water source from each calendar year is treated as a scenario each with equal probability (Yang et al 2014a).
- The regeneration task starts immediately the fracturing task ends.
- The regenerator is only used for basic pre-treatment (to remove oil and grease, total organic compound (TOC), Total suspended solid (TSS), bacteria and viruses)).
- The membrane geometry is tubular
- The membrane cleaning time is negligible

5.2. Superstructure representation

Based on the problem statement, the superstructure in Figure 5.1 is developed. In the superstructure, two types of freshwater sources are considered (interruptible and uninterruptible sources) (Yang et al., 2014a). Uninterruptible source is a big water body with guaranteed water availability throughout the year but the mode of transportation is through trucking. The interruptible source is a nearby source that requires piping but with uncertain water availability all year round. The water from any of these sources can be stored in any of the impoundment *t* prior to its usage. *S* represents a set of wellpad to be fractured in which the fracking fluid is blended using freshwater from the impoundment and the recycled water from the fracturing tank. The maximum concentration of TDS into the wellpads is kept at an upper limit of 50,000 ppm (Yang et al., 2015, Bartholomew and Mauter, 2016) while the concentration of other important contaminants are based on the data provided in Table 2. The flowback water generated from the fractured wellpad in the first two weeks after fracturing is assumed to be 25% of the initial water used (Bartholomew and Mauter, 2016) with known inlet state and concentrations of TDS, TSS, TOC, Fe, Ca, Mg, Ba, and oil. This flowback water can be sent to regenerator *R* for pre-treatment or any of the injection well *D* for disposal. The flowback water sent to regenerator *R* is pre-treated before it is sent to the fracturing tank for reuse in the next wellpad. The product of a particular wellpad after stimulation can be either oil and gas or gas only depending on the geological formation of the shale play. For a wellpad that produces oil and gas, the co-produced gas can be captured and stored in the gas storage facility from where it is supplied to the regenerator *R* as fuel, which in turn produces the energy needed, by the regenerator while the oil is sent to the market. In the case of gas producing well, part of the gas can be diverted into the gas storage facility for wastewater treatment while the rest can be sent to the market.

The mode of operation of the regenerator is as stated below:

- Transfer of water from the wellpad to the regenerator *R* is done provided there is a wellpad fractured at that time point. Whenever the regenerator starts operation, it operates continuously until the volume of water designated for treatment becomes zero.
- The regenerator only operates provided there is volume of water designated for treatment when a wellpad is fractured at a particular time point.
- The performance of the regenerator is specified based on a fixed removal ratio

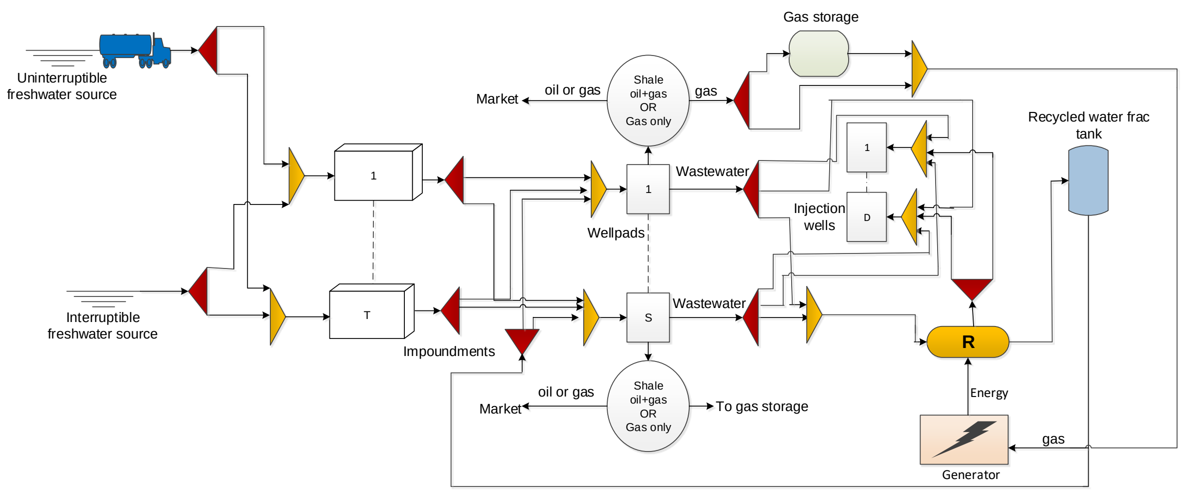

Figure 5.1. Superstructure representation of the water network.

5. 3. Model formulation

The mathematical framework presented in this chapter incorporate regeneration such that the fracturing schedule and water network that correspond to optimum water and energy requirement are determined simultaneously. The framework is based on the superstructure depicted by Figure 4.1, which is an extension of the superstructure presented in chapter one. The problem is formulated as a mixed integer nonlinear programming (MINLP) model which encompasses both scheduling framework and detailed ultrafiltration design model.

5.3.1. Scheduling framework

The scheduling framework captures the time dimension associated with the process. It captures the time a specific task is performed for example wellpad fracturing, regeneration, water transfer in and out of the frac tank etc. The framework adopted here is a slot-based formulation, which is based on the state task network (STN), and unequal discretization of time horizon, that involves time point *n* occurring at unknown time.

5.3.1.1. Allocation constraint

Equation (5.1) is the allocation constraint which specifies that each wellpad *s* has to be fractured exactly once at a given time point *n* in the time horizon. A time point is a precise moment within a given horizon (H) when an event occurs.

$$\sum_n w_{s,n} = 1 \quad \forall s \in S \tag{5.1}$$

Equation (5.2) states that the time at which time point *n* occurs tt_n must correspond with the availability time AT_s of wellpad *s*. Where $w_{s,n}$ is the binary variable that indicate if wellpad *s* is fractured at time point *n*.

$$tt_n \geq \sum_s \left(AT_s w_{s,n} - H\left(1 - w_{s,n}\right)\right) \quad \forall n \in N \tag{5.2}$$

5.3.1.2. Wellpad scheduling

The duration of each wellpad $du_{s,n}$, is calculated by Equation (5.3) where TR_s is the time required to fracture wellpad *s*. Equation (5.4) and (5.5) gives the finish time of each wellpad $tf_{s,n}$ expressed with big-M constraints, which are only active if wellpad *s* is stimulated at time point *n* where $ts_{s,n}$ is the start time of fracturing wellpad s at time point n .

$$du_{s,n} = TR_s w_{s,n} \quad \forall s \in S, n \in N \tag{5.3}$$

$$tf_{s,n} \leq ts_{s,n} + du_{s,n} + H\left(1 - w_{s,n}\right) \quad \forall s \in S, n \in N \tag{5.4}$$

$$tf_{s,n} \geq ts_{s,n} + du_{s,n} - H\left(1 - w_{s,n}\right) \quad \forall s \in S, n \in N \tag{5.5}$$

Equation (5.6) is the sequence dependent change over time between wellpad *s* and $s^{'}$. It states that the start time of wellpad $s^{'}$ at time point *n* must be equal or greater than the finish time of wellpad *s* at previous time point plus the crew transition time $CT_{s}^{s^{'}}$ between wellpad s and s'.

$$ts_{s^{'},n} \geq tf_{s,n-1} + CT_{s}^{s^{'}} w_{s^{'},n} \quad \forall s \in S, s^{'} \in S, s^{'} \neq s, n \in N, n \geq 2 \tag{5.6}$$

5.3.1.3. Regenerator scheduling

Equation (5.7) relates the regeneration and fracturing task that takes place at time point *n*. It states that transfer of water into regenerator *R* depends on the occurrence of fracturing task *s* as fracturing task must be scheduled to take place prior to water been sent for regeneration. However, because fracturing task took place does not guarantee water been sent to the regenerator, it can as well be sent to the injection well for disposal. Equation (5.8) and (5.9) ensure that the time at which regeneration starts tr_{n}^{in} coincide with the finish time $tf_{s,n}$ of wellpad *s* at time point *n*. Equation (5.10) gives the duration of regeneration where tr_{n}^{out} is the finish time of regeneration at time point *n*, f_{n}^{UF} is the total volume of water into the regenerator at time point n and ff^{UF} is the feed flowrate into the regenerator.

$$wr_{n} \leq \sum_{s} w_{s,n} \quad \forall n \in N \tag{5.7}$$

$$tr_{n}^{in} \geq \sum_{s} tf_{s,n} - H\left(2 - wr_{n} - \sum_{s} w_{s,n}\right) \quad \forall n \in N \tag{5.8}$$

$$tr_{n}^{in} \leq \sum_{s} tf_{s,n} + H\left(2 - wr_{n} - \sum_{s} w_{s,n}\right) \quad \forall n \in N \tag{5.9}$$

$$tr_{n}^{out} = tr_{n-1}^{in} + \left(\frac{f_{n-1}^{UF}}{ff^{UF}}\right) wr_{n-1} \quad \forall n \in N, n \geq 2 \tag{5.10}$$

5.3.1.4. Frac tank scheduling

Water usage in hydraulic fracturing and water transfer from the frac tank are linked by equation (5.11). It states that water can only be transferred from the frac tank to wellpad *s* if fracturing task takes place at that time point. Equation (5.12) and (5.13) ensure that the transfer time of water from the frac tank coincide with the start time of the fracturing task taking place at the time point.

$$wv_{s,n}^{out} \geq w_{s,n} \quad \forall s \in S, n \in N \tag{5.11}$$

$$tv_{s,n} \geq tf_{s,n} - H\left(2 - wv_{s,n}^{out} - w_{s,n}\right) \quad \forall s \in S, n \in N \tag{5.12}$$

$$tv_{s,n} \leq tf_{s,n} + H\left(2 - wv_{s,n}^{out} - w_{s,n}\right) \quad \forall s \in S, n \in N \tag{5.13}$$

5.3.2. Mass Balance Constraints

5.3.2.1. Around the wellpad

The volume of water require to fracture each wellpad is supplied with freshwater from the impoundment $f_{s,n}^{fw}$ and/or recycled water from the frac tank $f_{s,n}^{ww}$, which is obtained by Equation (4.14).

$$f_{s,n} = f_{s,n}^{fw} + f_{s,n}^{ww} \quad \forall s \in S, n \in N, n \geq 2 \tag{5.14}$$

The flowback water generated $f_{s,n}^{fbw}$ after fracturing a particular wellpad is assumed to be 25 % of the initial water used as represented in Equation (4.15). Equation (4.16) gives the contaminants concentration $c_{s,c,n}^{fbw}$ in the flowback water while Equation (4.17) states that the flowback water generated can be sent to the injection wells for disposal or sent to the treatment unit where $f_{s,n}^{dis}$ is the volume of wasewater sent to disposal and $f_{s,n}^{trt}$ is the volume of wastewater sent to the treatment unit.

$$f_{s,n}^{fbw} = 0.25 f_{s,n} \quad \forall s \in S, n \in N \tag{5.15}$$

$$c_{s,c,n}^{fbw} = CS_{s,c} w_{s,n} \quad \forall s \in S, c \in C, n \in N \tag{5.16}$$

$$f_{s,n}^{fbw} = f_{s,n}^{trt} + f_{s,n}^{dis} \quad \forall s \in S, n \in N \tag{5.17}$$

5.3.2.2. Around the regenerator

The total volume of water designated for treatment at a particular time point *n* is sent to the regenerator as indicated by Equation (4518). The volume of flowback water designated for treatment at time point *n* should be within the capacity range of the regenerator as given in

Equation (5.19) where $v^{\min}$ and $v^{\max}$ are the minimum and maximum capacity of the treatment unit respectively. Equation (5.20) states that the total volume of water into the regenerator f_n^{UF} at time point *n* is the sum of the volume collected as permeate f_n^{perm} and the volume collected as concentrate f_n^{con}. The contaminant balance around the regenerator is given in Equation (5.21) where $c_{c,n}^{perm}$ is the outlet concentration from the regenerator and $c_{c,n}^{con}$ is the amount of contaminant removed by the regenerator at time point *n*

$$\sum_s f_{s,n}^{trt} = f_n^{UF} \quad \forall n \in N \tag{5.18}$$

$$v^{\min} wr_n \le f_n^{UF} \le v^{\max} wr_n \quad \forall n \in N \tag{5.19}$$

$$f_n^{UF} = f_n^{perm} + f_n^{con} \quad \forall n \in N \tag{5.20}$$

$$f_n^{UF} \sum_s c_{s,c,n}^{fb} = f_n^{perm} c_{c,n}^{perm} + f_n^{con} c_{c,n}^{conc} \quad \forall c \in C, n \in N \tag{5.21}$$

The performance of the regenerator is a function of the removal ratio (*RR*) of contaminants as stated in Equation (5.22). The quantity of water to be collected as permeate and concentrate depends on the recovery ratio (*LR*) as stated in Equation (5.23) and (5.24) respectively.

$$c_{c,n}^{perm} = \sum_s c_{s,c,n}^{fbw} \left(1 - RR_c\right) \quad \forall c \in C, n \in N \tag{5.22}$$

$$LRf_n^{reg} = f_n^{perm} \quad \forall n \in N \tag{5.23}$$

$$f_n^{con} = \left(1 - LR\right) f_n^{reg} \quad \forall n \in N \tag{5.24}$$

Equation (5.25) states that the inlet contaminant concentration into the regenerator should not exceed the maximum it can take where $c_c^{\max}$ is the maximum inlet concentration into the regenerator. The amount of wastewater reused at any time point is supplied through the permeate stream from the regenerator as given in Equation (5.26) while Equation (5.27) states that the capacity of frac tank on a particular wellpad *s* is bounded by the maximum amount of wastewater used at the wellpad. Equation (5.28) ensures that the maximum allowable concentration into the wellpad is not exceeded where $CS_c^{\max}$ is the maximum inlet contaminant concentration into wellpad *s*.

$$\sum_{s} c_{s,c,n}^{fb} \leq C_c^{\max} \qquad \forall c \in C, n \in N \tag{5.25}$$

$$f_n^{perm} = \sum_{s} f_{s,n}^{ww} \qquad n \in N \tag{5.26}$$

$$v_{s,n}^{ft} \geq f_{s,n}^{ww} \qquad \forall s \in S, n \in N \tag{5.27}$$

$$f_n^{perm} c_{c,n}^{perm} \leq CS_c^{\max} \sum_{s} f_{s,n} \qquad \forall c \in C, n \in N \tag{5.28}$$

5.3.3. Ultrafiltration (UF) design model

The detailed design model for ultrafitration presented in this section is based on the work of Guadix et al.(2004). An ultrafiltration plant can be designed to operate with cross flow or dead end flow. The dead-end flow is more suitable to batch processes with low suspended solids as solid accumulation on the membrane surface requires frequent backflushing and cleaning to maintain high flux while cross flow is more preferred in continous operation as solids are flushed from the membrane surface continually to lower the resistance to permeation (Farahbakhsh et al., 2003, Igunnu and Chen,2012, Thoola, 2014). The focus of this study is on cross flow mode of operation, although dead end flow has been found to require low amount of energy but as a result of rapid backwash and chemical cleaning require to control the effect of fouling, crossflow is still preffered regardless of high energy demand (Thoola, 2014). Figure 5.2 illustrates a schematic representation of a typical cross flow filtration. The feed stream entering the system is pressurised to the work pressure by means of a feed pump. The membrane unit consists of number of modules from where the stream yields a permeate stream and a retentate stream.

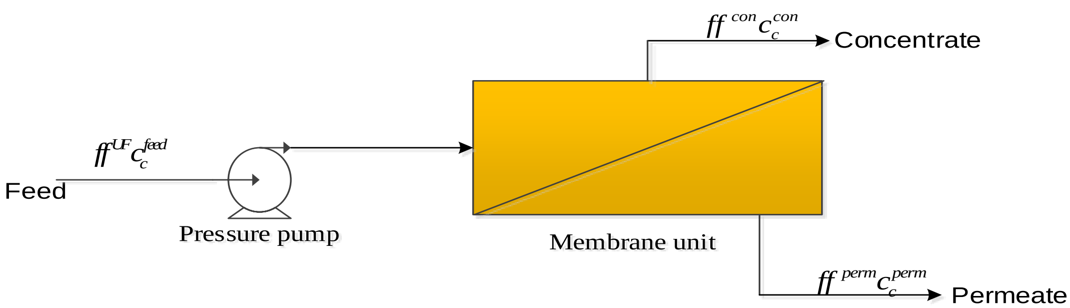

Figure 5.2. Schematic of a crossflow ultrafiltration plant

The description of the process is based on material balances and equipment performance equations that incoporate the following assumptions:

- The membrane geometry is tubular
- The membrane cleaning time is negligible
- The contaminants considered are TSS, TOC, Fe, TDS, Ba, Mg and Ca
- The concentration of Ba, Mg and Ca in the flowback water is taken care of by softening before the water is sent into UF

For practical applications of membrane processes, appropriate model equation to estimate permeate flux is very important. Generally, in membrane processes solute rejected by the membrane accumulate along the membrane surface thereby resulting in a higher concentration at the membrane surface than in the bulk creating a phenomenon called polarization. In the boundary layer between the bulk solution and the membrane surface, the concentration gradient is developed, and accumulated solutes diffuse back into the bulk solution along this gradient (Nakao et al., 1979; Kovasin, 2002; Wenten, 1996). The available models in literature for predicting permeate flux are the gel model, the resistance in series model and the osmotic pressure model. The gel layer model predicts the flux to be independent of operating pressure. It assumes the formation of gel layer at the membrane surface where concentration is constant and only depends on the solute. An increased pressure merely results in a thicker gel layer, which retards the flux to its original value (Wenten, 1996; Guadix et al., 2004; Nakao et al., 1979). The resistance in series model relates permeate flux to the transmembrane pressure and several resistances to flow due to concentration polarization and fouling (Guadix et al., 2004). The osmotic pressure model justifies the limiting flux by the increased osmotic pressure produced by high concentration of the rejected solute near the membrane surface. This effect generally will be most pronounced for small solutes, which tend to have large osmotic pressures (Jonsson, 1984). In the case of ultrafiltration, the solutes are macromolecules and colloids and are tend to form gel layer on the membrane layer (Nakao et al., 1979, Wenten, 1996). If the gel layer is formed, it gives resistance to the flow of the solvent in series to that of membrane and the flux is given by Equation (5.29).

$$J_w = \frac{\Delta p}{R_m + R_g} \tag{5.29}$$

Where Δp is the transmembrane pressure, J_w is the flux, R_m and R_g are the membrane resistance and gel layer resistance respectively.

With the assumption that the formation of gel layer is negligible, the above equation becomes:

$$J_w = \frac{\Delta p}{R_m} \tag{5.30}$$

The transmembrane pressure Δp is the pressure difference between permeate and the feed side of the membrane as given in Equation (5.31) (Micro and utrafiltration, 2018; Falsanisi et al., 2010; Amoosa et al., 2016; Muro et al., 2012) where p_f is the feed pressure, p_p is the permeate pressure and p_r is the pressure of the retentate.

$$\Delta p = \frac{p_f + p_r}{2} - p_p \tag{5.31}$$

The volumetric and salt balance around the UF unit is conducted in accordance with Figure 5.2 as given in Equation (5.32) and (5.33) where ff^{Uf} is the total volumetric flowrate into the UF unit, ff^{perm} and ff^{con} are the permeate and concentrate flowrate respectively.

$$ff^{Uf} = ff^{perm} + ff^{con} \tag{5.32}$$

$$ff^{Uf} cf_c^{feed} = ff^{perm} cp_c^{perm} + ff^{con} cr_c^{con} \quad \forall c \in C \tag{5.33}$$

The permeate flow from the UF unit is calculated through Equation(5.34) where A is the membrane area.

$$ff^{perm} = AJ_w \tag{5.34}$$

For a tubular system, the membrane area is calculated according to Equation (5.35) (Guadix et al., 2004) where N is the number of membrane modules, T is the number of tubes per module, D is the tube diameter and l is the tube length.

$$A = NT\pi Dl \tag{5.35}$$

The energy requirement in ultrafiltration is mainly the energy require by the feed pump in pumping the feed water into the UF unit as given in Equation (5.36). The continous variable W^{fp} represents the energy required by the feed pump and η is the pump efficiency.

$$W^{fp} = \frac{ff^{Uf}\left(p_f - p_p\right)}{\eta} \tag{5.36}$$

The liquid recovery “LR”is the fraction of the feed into the regenerator that is recovered as permeate. The fraction of water recovery by the UF unit is given by Equation (5.37).

$$LR = \frac{ff^{perm}}{ff^{Uf}} \tag{5.37}$$

The removal ratio “RR” is the mass load of contaminant in the concentrate stream of the regenerator as a fraction of the feed. It is assumed to be fixed in this work and is defined as given in Equation (5.38).

$$RR_c = \frac{ff^{con} cr_c^{con}}{ff^{Uf} cf_c^{Uf}} \quad \forall c \in C \tag{5.38}$$

The capital costs of the pump and the membrane are given in Equation (5.39) and (5.40) (Guadix et al., 2004) where CC^{fp} is the capital cost of the feed pump, CC^{m} is the capital cost of membrane, a and b are the pump cost coefficient and pump cost exponent while c and d are the membrane cost coefficient and membrane cost exponent respectively.

$$CC^{fp} = a\left(W^{fp}\right)^{b} \tag{5.39}$$

$$CC^{m} = cA^{d} \tag{5.40}$$

The operating cost of the feed pump is given by Equation (5.41) where C^{ele} is the cost of electricity and AOT is the annual operating time.

$$OC^{fp} = W^{fp} C^{ele} AOT \tag{5.41}$$

The cost of chemical pretreatment is given by Equation (5.42) where C^{che} is the cost incurred per meter cube of water.

$$OC^{che.ptrt} = ff^{Uf} C^{che} AOT \tag{5.42}$$

Figure 5.3 represent the design connection between the flare gas, generator and the membrane unit.

The volume of gas needed by the generator v^{gas} to generate a kWh of energy is given by Equation (5.43) where Gen^{eff} is the generator thermal efficiency/heat rate and HC^{fuel} is the heat content of the gas.

$$v^{gas} = \frac{Gen^{eff}}{HC^{fuel}} \tag{5.43}$$

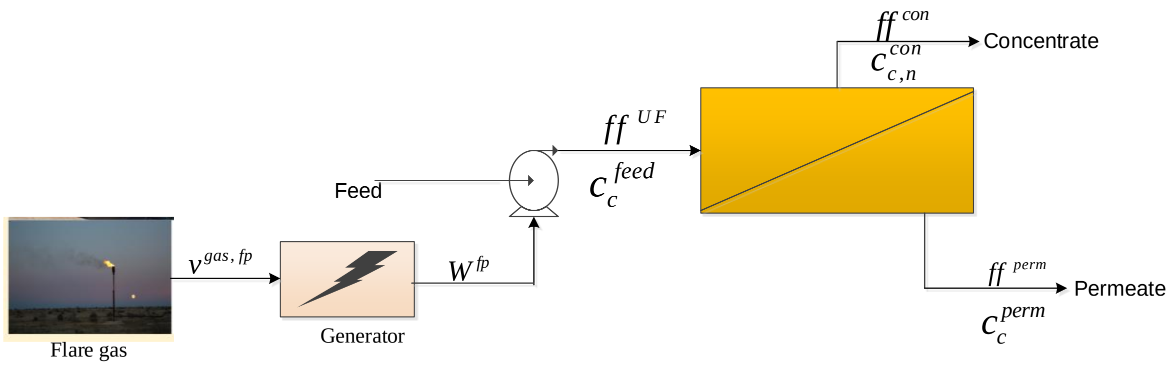

Figure 5.3. Schematic representation of generator and membrane unit

The volume of gas needed to generate the energy required by the feed pump $v^{gas,fp}$ is indicated in Equation (5.44) as:

$$v^{gas,fp} = v^{gas} W^{fp} \tag{5.44}$$

The operating cost of the generator is given in Equation (5.45) where C^{gas} is the cost of gas.

$$oc^{gen} = v^{gas,fp} C^{gas} AOT \tag{5.45}$$

The regeneration network takes into account all the costs associated with regeneration and these are incorporated in the objective function so as to optimize the associated costs as well as the energy consumed in regeneration together with water usage.

5.3.4. Objective function

The objective which aims at maximizing profit is given in Equation (5.46) and it comprises of the following terms: (1) revenue from gas production, (2) freshwater transportation cost, (3) cost associated with regeneration network, (4) disposal cost, (5) wastewater storage cost, and (6) pumping cost to treatment facility.

$$\max profit = SP^{gas}\sum_{s}\sum_{n} p_{s,n} - \left[\begin{array}{l} \left(OC^{truck,fw}\sum_{t}\sum_{n}\sum_{y}\frac{f_{t,n,y}^{truck}}{NY} + OC^{pump,fw}\sum_{t}\sum_{n}\sum_{y}\frac{f_{t,n,y}^{pump}}{NY}\right) \\ +\left(\frac{\left(a\left(W^{fp}\right)^{b} + cA^{d} + CC^{pipe} + CC^{gen}\right)}{L^{\max}} + W^{fp}C^{ele}AOT + ff^{Uf}C^{chem}AOT + v^{gas,fp}W^{fp}AOT\right) \\ +\left(OC^{dis}\sum_{s}\sum_{n} f_{s,n}^{dis}\right) + OC^{dis}\sum_{n} ff_{n}^{con} \\ +\left(OC^{st,ww}\left(\sum_{s}\sum_{n} v_{s,n}^{ft}\right)\right) \\ +OC^{pump,ww}DS_{s}\left(\sum_{s}\sum_{n} f_{s,n}^{trt} + \sum_{n} f_{n}^{perm}\right) \end{array}\right] \quad (5.46)$$

5.4. Case study

In order to demonstrate the applicability of the proposed model, an example taken from Yang et al. (2014a) is considered. This case study represents the typical Marcellus Shale play. The example considered 14 wellpads, 540 days time horizon, one uninterruptible freshwater source and two interruptible sources connected to impoundments as illustrated in Table 5.3 years historical data were provided for the two interruptible sources. The parameters and cost coefficient for the case study is provided in Table 5.4. The selected ultrafiltration membrane geometry is tubular and operate in a cross flow mode and the details of this membrane module are given in Guadix et al. (2004).

Table 5.3 Wellpad Data (Yang et al., 2014a)

Wellpads	S1	S2	S3	S4	S5	S6	S7	S8	S9	S10	S11	S12	S13	S14
Match with takepoints, $TP_{s,t}$	*t2*	*t1*	*t1*	*t1*	*t1*	*t2*	*t2*	*t2*	*t2*	*t2*	*t2*	*t1*	*t1*	*t2*
Earliest frac day	1	1	1	1	1	39	1	273	273	273	396	379	379	1
# of stages	57	61	54	55	64	26	97	88	86	76	63	100	100	87

Table 5.4. Parameters and cost coefficients.

Parameter	Value
Crew transition time (day)	5
Volume of frac fluid used per stage (m^3)	950
Freshwater used (%)	85
Wastewater storage cost ($/$m^3$)	0.59
Freshwater trucking cost ($/$m^3$)	29.35
Freshwater pumping cost ($/$m^3$)	15.93
Disposal cost ($/m3)	134.18
Wastewater pumping cost($/km/m3)	0.28
Pump coefficient ($)	2,590
Pump cost exponent	0.79
Piping and instrumentation cost ($)	20,000
Membrane cost coefficient ($)	1,000
Membrane cost exponent	0.9
Tube diameter (m)	0.004
Electricity cost ($/kWh)	0.07
Tube length	1.02
Plant life (h)	87,600
Number of tubes per module	361
Natural gas price ($/$m^3$)	0.12
Pump efficiency	0.8

5.4.1. Results and discussion

The resulting model, which is a mixed integer nonlinear programm (MINLP) consists of 9,345 constraints, 6,691 continuous variables, 436 binary variables and 1,759 non-linear terms. The model was implemented in GAMS and solved using the general-purpose global optimization (BARON) in CPU time of 1235.6 s. The optimal schedule for the case study is given in Figure 5.4, the figure shows that the fracturing schedule of the wellpads are carried out based on the availability date of each wellpad except for wellpad S6. Although wellpad S6 is available right from day 1 of the time horizon and is the wellpad with the least number of stages, thereby requiring the least volume of water for fracturing, it is fractured last in order to minimize the volume of flowback water that will be disposed at the end of the time horizon.

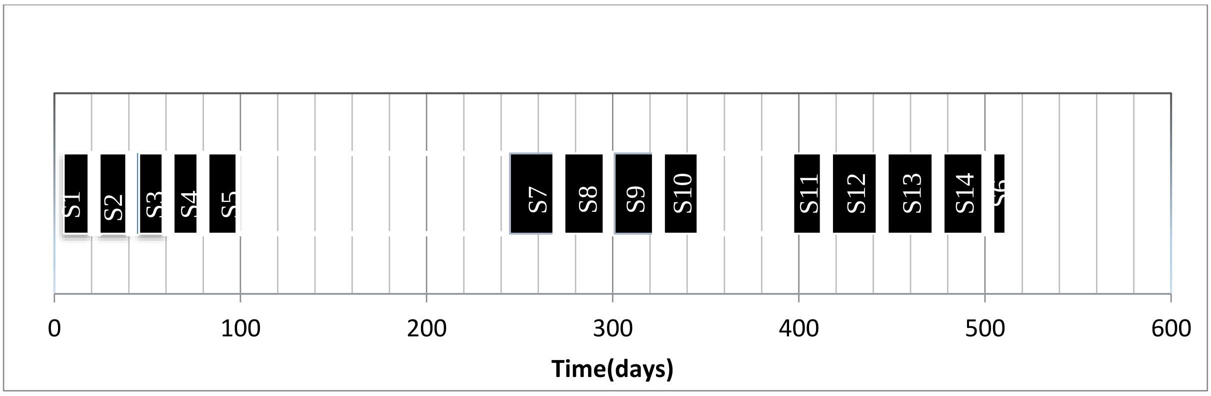

Figure 5.4. Fracturing schedule for the optimal solution

The detail analysis for the case study is given in Table 5.5. The total revenue generated is \$261.24 million with water and wastewater management costs of \$13.03 million. The water and wastewater management cost is capped at 3.9 % of the revenue which is found to be below the industry average according to Bartholomew and Mauter (2016). The optimal result is characterized by the following attributes: (a) freshwater transportation through piping is considered the best option from the source to the impoundments, (b) 90.3 % of the flowback water generated is sent to the regenerator for basic treatment and reused, (c) the remaining 9.6 % is sent to the injection well for disposal.

Table 5.5. Optimal analysis of the case study

Parameter	Optimum value
Freshwater pumped (1,000 m^3)	643.1
Freshwater trucked (1,000 m^3)	0
Freshwater save (%)	21.4
Freshwater trucking cost (\$ 1,000)	0
Freshwater pumping cost (\$ 1,000)	10,164
Disposal cost (\$ 1,000)	1,933
Wastewater pumping cost (\$ 1,000)	11.1
Wastewater storage cost (\$ 1,000)	106.6
Treatment cost (\$ 1,000)	21.9
Revenue (\$ 1,000)	261,240
Profit (\$ 1000)	249,003

The total water requirement for the 14 wellpad is 818,805 m^3 of which 21.4 % is supplied through flowback water reused. The percentage of wastewater to freshwater used in fracturing is given in Figure 5.5. From the figure, for wastewater with TDS concentration of up to 300,000 ppm, the percentage of wastewater in the blended frac fluid never exceeds 16.7 %. For example, in fracturing wellpad S2, 11,506.88 m^3 of flowback water is available from wellpad S1 but only 8,209.58 m^3 could be reused in order to be able to meet the maximum TDS level required. Another significant impact of this is observed in wellpad S6, about 95 % of water required for fracturing this wellpad could have been supplied through wastewater generated by wellpad S14 but only 40 % is supplied in order to meet the required TDS level. In general, despite reuse of flowback water with total dissolved solid (TDS) concentration as high as 300,000 ppm (as the membrane under consideration is not capable of removing salts from the flowback water), the concentration of the blended frac fluid never exceeded the maximum required (50,000 ppm). This result is in agreement with the work of Bartholomew and Mauter (2016) which showed that with basic treatment, wastewater with high salinity could be reused.

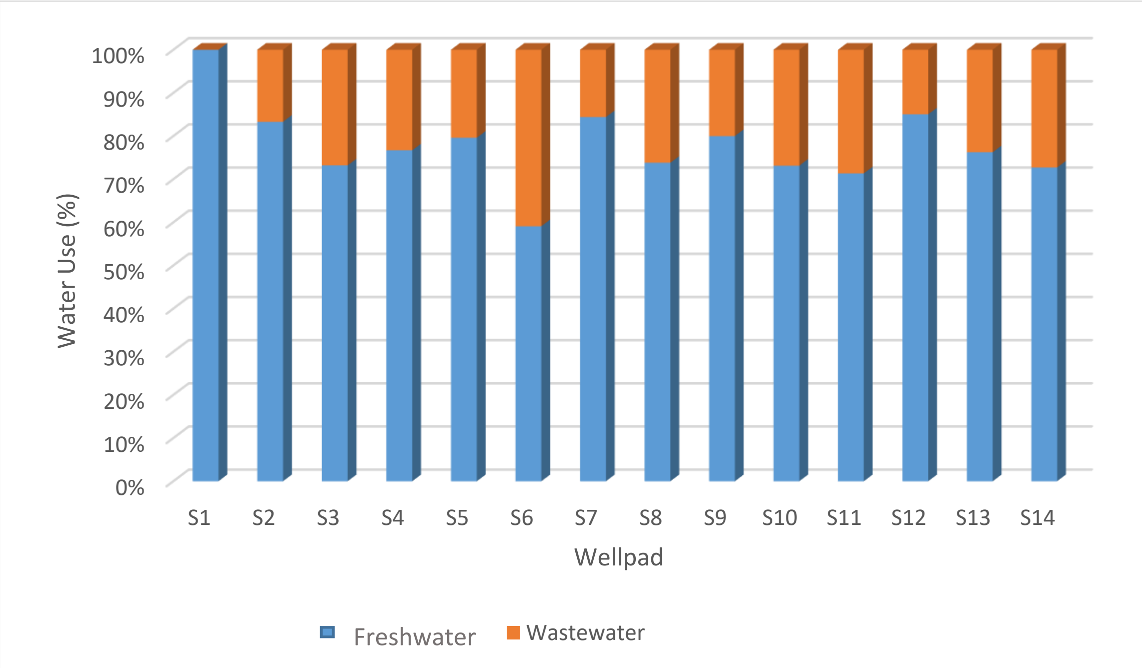

Figure 5.5. Percentage of water used in fracturing operation

In order to account for the energy requirement of the membrane regenerator considered, analysis based on the detailed model and UF standalone model was performed. The optimum throughput from the detailed model was used in the UF standalone model in order to determine the actual energy needed for regeneration. When UF standalone model is considered, the membrane operated at the feed pressure of 401.64 kPa (4.01 bar) which resulted in 7.58 kW power consumption by the feed pump. The simultaneous optimization of both energy and water within the network results in 10.3 % reduction in the amount of energy required by the regenerator. The amount of power consumption by the feed pressure pump is reduced from 7.58 kW (181.92 kWh) to 6.8 kW (163.2 kWh) as the feed pressure is reduced to 369.51 kPa (3.69 bar). The power consumption is in the order of 0.109 kWh/m^3 of water, which is found to be lower than the energy requirement reported in literature (WaterWorld, 2014; Howe et al., 2012; Micro and Ultrafiltration, 2018; Pearce, 2008). The WaterWorld (2014) estimated the typical energy requirements for reclamation and reuse of different sources of water, especially when membrane filtration is involved, to be within the range of 0.8–1.0 kWh/m^3 for wastewater and brackish water systems. The energy requirement in this study is in agreement with other studies in literature (Gander et al. 2000; Amoosa et al. 2016; Löwenberg et al., 2014; Massé et al., 2011) which have reported similar values of energy consumption for UF.

The volume of gas needed to generate the energy required (163.2 kWh) is 15.88 m^3. This indicates a higher feasibility of supplying the gas through flared gas. Glaizer et al. (2014) reported an average estimate of 9600 m^3 of gas being flared per well per day in shale plays that produce oil and associated gas in Texas, although this might be lower in shale play where gas production is dominant.

The optimal design and design specifications for the UF membrane are given in Figure 5.6 and Table 5.6 respectively. For the optimal design given in Figure 5.6, the feed pump power is 6.8 kW with 25 membrane modules that require work pressure of 369.51 kPa.

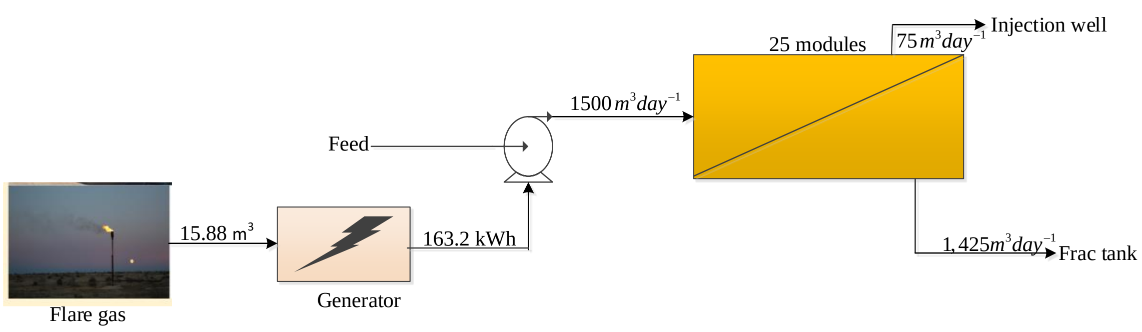

Figure 5.6. Optimal design and design specifications for the UF membrane

The membrane area required, the permeate flux and the transmembrane pressure are given in Table 5.6. The cost incurred in the regeneration network is made up of 72.91 % capital costs and 27.09 % operating costs. The detailed analysis of the costs incurred in the regeneration network is given in Table 5.7 of which the membrane capital cost takes the highest value of

50.52 %, the contribution from feed pressure pump capital cost and piping account for 8.35 % and 14.04 % of the total cost respectively. The operating cost of the feed pump accounts for 27.09 %.

Table 5.6**.** Design specification for UF.

Design variables	Optimum values
Power (kW)	6.8
Membrane area (m^2)	115.70
Transmembrane pressure (kPa)	184.75
Number of membrane modules	25
Permeate flux (m/h)	0.49*

*Conventional unit for membrane permeates flux is L/m^2h. The conversion to the unit shown in this table is 10^3 L/m^2h = 1 m/h (Howe et al., 2012).

Table 5.**7.** Annual regeneration cost breakdown ($/yr.).

	Cost	Percentage
Capital cost	10,383.40	72.91
Pressure pump	1,189.17	8.35
Membrane	7,194.20	50.52
Piping and instrumentation	2,000	14.04
Operating cost	3,857.66	27.09
Pressure pump	3,857.66	27.09

Using the gas that would otherwise be flared in the process however rendered the operating cost of the pressure pump zero since the power required by the feed pump can be generated onsite via a gas generator. Although, there is an additional cost related to the purchase of the generator (capital cost of the generator), the operating cost of the generator will be zero as gas required is supplied through the gas that would otherwise be flared. This study assumed the capital cost of generator to be $ 15,000 with 10 yr. plant life, which make the annualized capital cost of the generator to be $ 1,500/yr. Comparing this with the annual operating cost of the feed pump that is mainly the cost of electrical energy supplied to the feed pump, there is 61 % saving in the cost required if the electrical energy is generated onsite.

5.5. Conclusion

This chapter has explored the role of membrane filtration treatment technology in maximizing wastewater reuse in hydraulic fracturing. The multi-contaminant property of flowback water is captured using detailed ultrafiltration membrane system. The results of this study are employed as requisite data for further investigation on hybrid regeneration process/plant designs in the next chapter. Further studies using the combination of electrical driven membrane and thermal energy driven membrane is explored to better capture the reuse potential of flowback water at different operation conditions as volume of flowback water expected after fracturing fluctuates and the TDS concentration in the flowback water depends on the type of frac fluid employed.

Nomenclature

Sets

D	$\{d \mid d$ = injection well$\}$
N	$\{n \mid n$ = time point$\}$
S	$\{s \mid s$ = wellpad$\}$
T	$\{t \mid t$ = an interruptible source and its corresponding impoundment$\}$
$TP_{s,t}$	Match between wellpad s and source t
Y	$\{y \mid y$ = historical river flowrate data year$\}$

Parameters

AT_s	Availability time of wellpad s, day
AOT	Annual operating time, hr
a	Pump cost coefficient, $
b	Pump cost exponent
c	Membrane cost coefficient, $
$C_c^{\max}$	Maximum inlet concentration into treatment unit, mg/L
Cf_c^{UF}	Concentration of the feed water into UF, mg/L
$CS_c^{\max}$	Maximum inlet concentration into wellpad s, mg/L
$CS_{s,c}$	Flowback water contaminant concentration in wellpad s, mg/L

$CT_{s}^{s'}$	Crew transition time between wellpads, day
c^{che}	Unit cost of chemical pre-treatment, \$/m^3
d	Membrane cost exponent
D	Tube diameter, m
DS_s	Distance from wellpad *s* to treatment facility, km
e	Electricity cost, \$/kWh
Gen^{eff}	Thermal efficiency/heat rate of the generator
H	Time horizon of interest, day
Hc^{fuel}	Heat content of natural gas, Btu/m^3
l	Tube length, m
$L^{\max}$	Plant life, yr
LR	Liquid recovery for the regenerator
NY	Number of historical year, yr
$OC_{s}^{pump,fw}$	Freshwater pumping cost, \$/m^3
$OC_{s}^{truck,fw}$	Freshwater trucking cost, \$/m^3
$OC_{s}^{pump,ww}$	Wastewater pumping cost, \$/m^3/km
OC^{dis}	Cost of wastewater disposal, \$/m^3
$OC_{s}^{st,ww}$	Cost of wastewater storage, \$/m^3
P_s	Gas production of wellpad *s*, m^3
R_m	Membrane resistance, kPahm^2/L
R_g	Gel layer resistance
RR_c	Removal ratio of the contaminants

SP^{gas} Unit price of natural gas, \$/m^3

ST_s Availability date of wellpad *s*, day

T Number of tubes per module

TR_s Time required fracturing wellpad *s,* day

$V^{\max}$ Maximum capacity of treatment unit, m^3

$V^{\min}$ Minimum capacity of treatment unit, m^3

WR_s Amount of water required to fracture wellpad *s*, m^3

η Pump efficiency

Binary variables

$w_{s,n}$ Defines the beginning of stimulating each wellpad *s* at time point *n*

$wv_{s,n}^{out}$ Transfer of water from frac tank to wellpad *s* at time point *n*

wr_n Transfer of water to regenerator at time point *n*

Continuous variables

A Required membrane area, m^2

$c_{s,c,n}^{fbw}$ Flowback water concentration of wellpad *s* at time point *n*, mg/L

$c_{c,n}^{perm}$ Outlet concentration of contaminant from the regenerator at time point *n*, mg/L

$c_{c,n}^{con}$ Contaminant concentration removed by the regenerator at time point *n*, mg/L

cp_c^{perm} Permeate concentration from UF, mg/L

cr_c^{con} Retentate concentration from MD, mg/L

cc^{fp} Capital cost of feed pump, \$

cc^{m} Capital cost of membrane, \$

$du_{s,n}$	Duration of wellpad *s* at time point *n*, day
$f_{s,n}$	Total water required to fracture wellpad *s* at time point *n*, m^3
$f_{t,n,y}^{pump}$	Water pumped from interruptible source at time point *n* in scenario year *y*, m^3
$f_{t,n,y}^{truck}$	Water trucked from uninterruptible source at time point *n* in scenario year *y*
$f_{s,n}^{fw}$	Freshwater required to fracture wellpad *s* at time point *n*, m^3
$f_{s,n}^{ww}$	Wastewater required to fracture wellpad *s* at time point *n*, m^3
$f_{s,n}^{fbw}$	Flowback water from wellpad *s* at time point *n*, m^3
$f_{s,n}^{trt}$	Flowback water sent to the treatment unit from wellpad *s* at time point *n*, m^3
$f_{s,n}^{dis}$	Flowback water sent to disposal from wellpad *s* at time point *n*, m^3
f_n^{UF}	Total flowback water to be treated at time point *n*, m^3
f_n^{perm}	Amount of water collected as permeate from the regenerator at time point *n*, m^3
f_n^{con}	Amount of retentate from the regenerator at time point *n*, m^3
ff^{UF}	Total flowrate into UF, m^3/day
ff^{perm}	Permeate flowrate from UF, kg/day
ff^{con}	Retentate flowrate from UF, kg/day,
Jw	Water flux across the membrane, L/ (m^{2}h)
N	Number of membrane modules
oc^{fp}	Operating cost of the feed pump, $
$oc^{che,ptrt}$	Cost of chemical pre-treatment, $/m^3

oc^{gen} Operating cost of generator, $

$p_{s,n}$ Expected gas production of wellpad *s* at time point *n*, m^3

p_r Pressure of the retentate, kPa

p_p Permeate pressure, kPa

p_f Feed pressure, kPa

$ts_{s,n}$ Start time of wellpad *s* at time point *n*, day

$tf_{s,n}$ Finish time of wellpad *s* at time point *n*, day

tt_n Time that correspond to time point *n*, day

tr_n^{in} Start time of regeneration at time point *n*, day

tr_n^{out} Duration of regeneration at time point *n*, day

$tv_{s,n}$ Time at which water is transferred from the frac tank to wellpad *s* at time point *n*, day

$v^{gas,fp}$ Volume of gas required to generate the energy required by the feed pump, m^3

v^{gas} Volume of gas required to generate a kWh of energy, m^3

W^{fp} Power of the feed pump, kW

$v_{s,n}^{ft}$ Capacity of fracturing tank on wellpad *s* at time point *n*, m^3

Δp Transmembrane pressure, kPa

Superscript

con Concentrate

cons Consumption

che Chemical

dis	Disposal
ele	Electricity
eff	Efficiency
feed	Feed
ft	Fracturing tank
fp	Feed pump
fw	Freshwater
fbw	Flowback water
fuel	Fuel
gas	Gas
m	Membrane
max	Maximum
min	Minimum
pump	Pumping
perm	Permeate
reg	Regenerator
ptrt	Pretreatment
total	Total
truck	Trucking
UF	Ultrafiltration
vap	Vapour
ww	Wastewater

Subscript

m	Membrane

References

Bartholomew, T.V., Mauter, M.S., 2016. Multiobjective optimization model for minimizing cost and environmental impact in shale gas water and wastewater management. Journal of ACS Sustainable Chemistry and Engineering 4, 3728-3735.

Amosa, M.K., Jami, M.S., Alkhhatib, M.F.R., Majozi, T., 2016. Technical feasibility study of a low-cost PAC-UF system for wastewater reclamation and reuse: a focus on feedwater production for low-pressure boilers. Journal of Environmental Science Pollution Research 23, 22554-22567.

Carrero-Parreño, A., Onishi, V.C., Salcedo-Díaz, R., Ruiz-Femenia, R., Fraga, E. S., Caballero, J.A., Reyes-Labarta, J. A., 2017. Optimal pretreatment system of flowback water from shale gas production. Journal of Industrial and Engineering Chemistry Research 56, 4386−4398.

Farahbakhsh, K., Adham, S.S., Smith, D.W., 2003. Monitoring the integrity of low pressure membrane. Journal of American Water Works Association 95(6), 95-107.

Falsanisi, D., Liberti, L., Notarnicola, M., 2009. Ultrafiltration (UF) pilot plant for municipal wastewater reuse in agriculture: Impact of the operation mode on process performance, Water 1, 872-885.

Gander, M., Jefferson, B., Judd, S., 2000. Aerobic MBRs for domestic wastewater treatment: a review with cost considerations. Journal of Separation and Purification Technology 18, 119-130.

Glazer, Y.R., Kjellsson, J.B., Sanders, K.T., Webber, M.E., 2014. Potential for using energy from flared gas for on-site hydraulic fracturing wastewater treatment in Texas. Environmental Science and Technology Letters 1,300-304.

Guadix, A., Sorensen, E., Papageorgiou, L.G., Guadix, E.M., 2004. Optimal design and operation of continuous ultrafiltration plants. Journal of Membrane Science 235, 131-138.

Howe, K.J., Hand, D.W., Crittenden, J.C., Trussell, R.R., Tchobanoglous, G., 2012. Principles of water treatment, John Wiley & Sons, Inc., Hoboken.

Igunnu, E.T., Chen, G.Z., 2012. Produced water treatment technologies. International Journal of Low-Carbon Technology 9, 157–177.

Jonsson, G., 1984. Boundary layer phenomena during ultrafiltration of dextran and whey protein solutions. Desalination 51.

Kovasin, K., 2002. Modeling ultrafiltration and filtration phenomena applied in chemical pulping processes. Chemical Engineering Report Series, Helsinki University of Technology Report No. 44, Espoo 2002.

Löwenberg, J., Zenker, A., Baggenstos, Koch, M.G., Kazner, C., Wintgens, T., 2014. Comparison of two PAC/UF processes for the removal of micropollutants from wastewater treatment plant effluent: process performance and removal efficiency. Water Research 56, 26–36.

Micro and Ultrafiltration, 2018. https://ocw.tudelft.nl/wp-content/uploads/Micro-and-ultrafiltration-1.pdf. Accessed August 2018.

Muro, C., Riera, F., Díaz, M.C., 2012. Membrane separation process in wastewater treatment of food industry, https://www.intechopen.com/books/food-industrial-processes-methods-and-equipment/membrane-separation-process-in-wastewater-treatment-of-food-industry. Acessed 17th August, 2018.

Nakao, S., Nomura, T., Kimura, S., 1979. Characteristics of macromolecular gel layer formed on Ultrafiltration tubular membrane. Journal of American Institute of Chemical Engineer 25(4), 615-622.

Pearce, G.K., 2008. UF/MF pre-treatment to RO in seawater and wastewaterreuse applications: a comparison of energy costs. Desalination 222, 66–73.

Thoola, M.I., 2014. Performance characteristics of bio-ultrafiltration on local surface water. Master dissertation. Durban University of Technology.

WaterWorld, 2014. Membrane filtration for wastewater reuse current. PennWell Corporation. http://www.waterworld.com/articles/wwi/print/volume-25/issue-5/regional-spotlight/north-american-caribbean/membrane-filtrationfor-wastewater-reuse-current.html. Accessed 10 September 2018.

Wenten, I.G., Ganesha, J., 1996. Ultrafiltration in water treatment and its evaluation as pre-treatment for reverse osmosis system. Research Report. Institut Teknologi Bandung, Indonesia.

Yang, L., Grossmann, I.E., Mauter, M.S., Dilmore, R.M., 2015. Investment optimization model for freshwater acquisition and wastewater handling in shale gas production, Journal of American Institute of Chemical Engineers 61, 1770-1782.

Yang, L., Grossmann, I.E., Manno, J., 2014a. Optimization models for shale gas water management. Journal of American Institute of Chemical Engineers 60(10), 3490-3501.

CHAPTER SIX

HYBRID REGENERATION NETWORK FOR FLOWBACK WATER MANAGEMENT

Introduction

This chapter presents the importance/ effect of using multiple/ hybrid treatment technologies in maximizing hydraulic fracturing wastewater reuse. The proposed model is aimed at developing a systematic approach for design and optimization of multi-regenerator networks that accounts for both pre-treatment and desalination alternatives for flowback water management within hydraulic fracturing scheduling framework. The detaitailed design of ultrafiltration and membrane distillation network will help in determining the optimal operating conditions and design specifications and the sustainability of the process in terms of energy and costs to allow for beneficial use of wasted energy from flaring. The proposed options for flowback water management within the process is given in Figure 6.1.

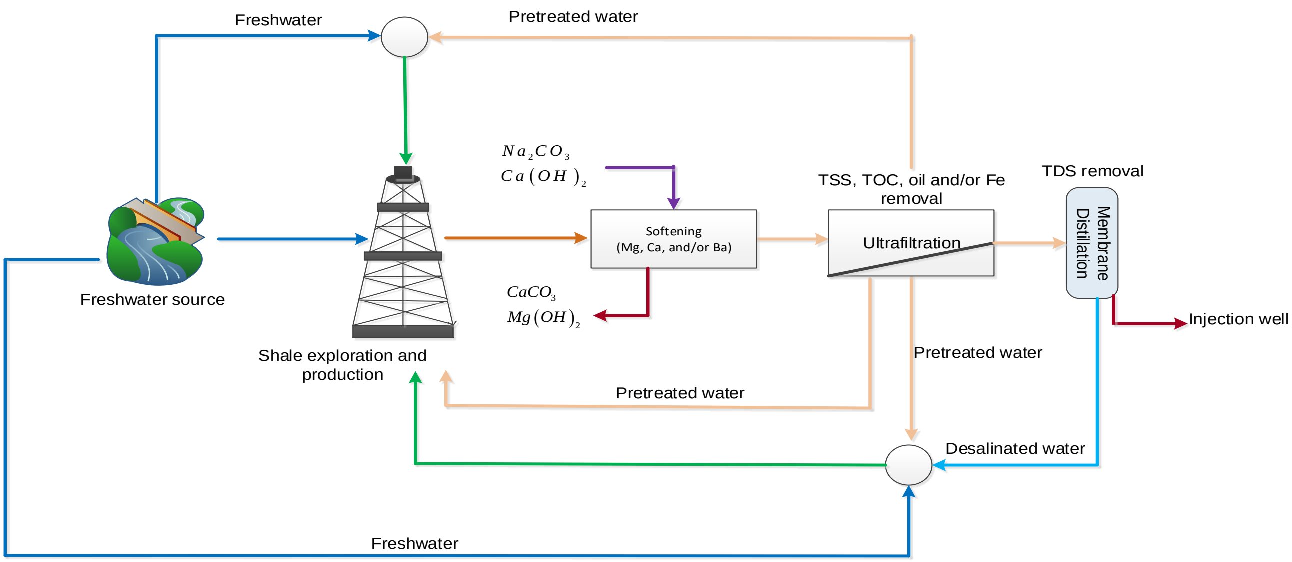

Figure 6.1: Proposed flowback water management options

6.1. Problem statement

The problem addressed in this chapter can be stated as follows: It is assumed that we are given a number of freshwater sources with location and water availability data, set of wellpads *S* to be fractured with known volume of water required for fracturing, maximum allowable contaminant concentration in the fracturing fluid and the availability date of each wellpad. Also given are set of wastewater injection wells *D*, time horizon of interest, network of regenerators and the performance and gas storage facility. The goal is to determine the optimal fracturing schedule of the wellpads that minimise freshwater and maximize wastewater use, preferred sources to obtain freshwater, optimal operation and design conditions of the regenerators such as number of membrane modules and energy consumption, the effect of using multiple regenerators in maximizing wastewater reuse and the feasibility of using flared gas as energy source for the regenerators.

The assumptions made in the model formulation are as follows:

- The wells in each wellpad are aggregated.
- Each wellpad is connected to exactly one of the impoundments through piping.
- The number of frac stages that could be fractured per day is kept constant at 4 instead of allowing it to be variable between 2-4 stages (Yang et al., 2014a).
- The capacity of the wastewater tank and frac tank on each wellpad varies depending on its water requirement.
- The water treatment units are located onsite and can be moved from one wellpad to the other.
- The wastewater undergoes softening process to remove scale-forming contaminants such as Ca, Mg and Ba. These contaminants can produce fouling in pipes by the increase in the temperature, promoting the diminution of the performance of the thermal technologies (Carrero-Parreño et al., 2017).
- While regenerator *Ra* can provide adequate removal of contaminants such as TSS, TOC, heavy metals, oil and grease and/or bacteria and viruses, regenerator *Rb* is capable of desalination (TDS removal).
- There are existing pipelines between the interruptible water source and the impoundment.
- The historical flowrate data for the interruptible water source from each calendar year is treated as a scenario each with equal probability (Yang et al., 2014a).

6.2. Superstructure representation

Based on the problem statement, the superstructure in Figure 6.2 is developed. In the superstructure, two types of freshwater sources are considered (interruptible and uninterruptible sources) based on the mode of transportation and water availability. The water from any of these sources can be stored in any of the impoundment *t* prior to its usage. *S* represents a set of wellpad to be fractured in which the fracking fluid is blended using freshwater from the impoundment and the recycled water from the frac tank. The flowback water generated from the fractured wellpad in the first two weeks after fracturing can be sent to regenerator *Ra* to remove basic contaminants like total organic compound (TOC), total suspended solid (TSS), Heavy metals (e.g. Fe), oil and grease and/or viruses and bacteria or any of the injection well *D* for disposal. The flowback water from regenerator *Ra* either goes to the frac tank from where it is blended with freshwater based on the total dissolved solid (TDS) level to be reused in the next wellpad or passes through regenerator *Rb* which is capable of removing the total dissolved solid as this is the major contaminant of interest in wastewater reuse for hydraulic fracturing before it is sent to the frac tank for reuse in the next wellpad. The product of a particular wellpad after stimulation can be either oil and gas or gas only depending on the geological formation of the shale play. For a wellpad that produces oil and gas, the co-produced gas can be captured and stored in the gas storage facility from where it is supplied to both regenerator *Ra* and *Rb* as fuel, which in turn produces the electrical and heat energy needed by the regenerators respectively while the oil is sent to the market. In the case of gas producing well, part of the gas can be diverted into the gas storage facility for wastewater treatment while the rest can be sent to the market.

The two regenerators operate as follow:

- Water is sent to regenerator *Ra* from the wastewater tank *a* provided there is a wellpad fractured and water is only sent to regenerator *Rb* from wastewater tank *b* only if there is a wellpad to be fractured. Whenever any of the regenerators is active, it operates in a continuous mode with steady inlet and outlet streams until the wastewater tanks become empty.
- Both regenerators operate intermittently with *Ra* only active after a wellpad has been fractured and *Rb* is only active if there is a wellpad to be fractured, otherwise they both remain in the passive mode.
- The regenerators performance is given in terms of fixed removal ratios, however while the liquid recovery for *Ra* is fixed, it is allowed to be a variable in *Rb.*

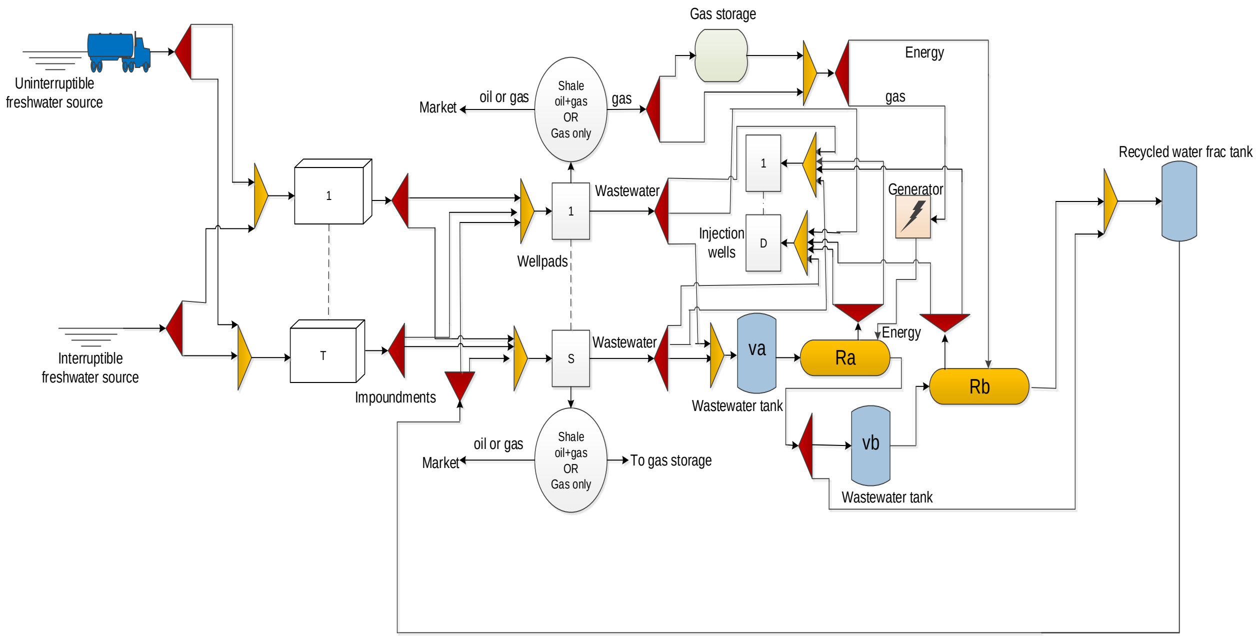

Figure 6.2. Superstructure representation of the water network.

6.3. Model formulation

The superstructure depicted in Figure 6.2 serves as the basis on which the mathematical model presented in this section is built. The problem is formulated as a mixed- integer nonlinear programming (MINLP) model, which is divided into three sections developed inside the same structure to simultaneously optimize water and energy. The first section focuses on mass balance and scheduling, the second is based on the detailed membrane distillation model while the third is based on detailed ultrafiltration model. The resulting model was implemented in GAMS and solved using the general-purpose global optimization solver (BARON). The scheduling framework adopted here is based on the state task network (STN) representation for batch scheduling and unequal discretization of time horizon, which involves time point *n* occurring at unknown time.

6.3.1. Mass balance constraints

6.3.1.1. Around the wellpad

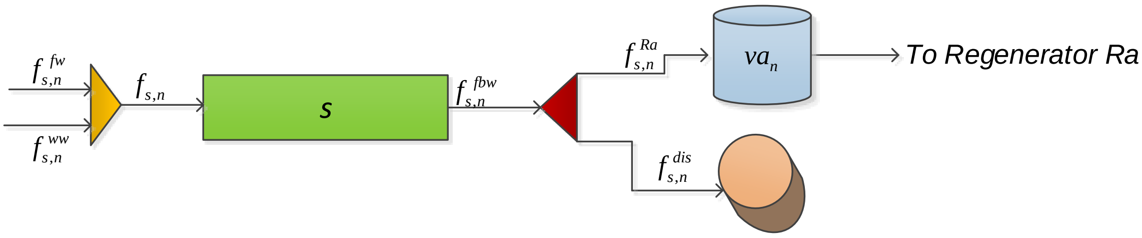

Figure 6.3. Mass balance around wellpad *s*.

Mass balance around wellpad *s* is carried out according to Figure 6.3. Equation (6.1) gives the total volume of water $f_{s,n}$ required to fracture wellpad *s* at time point *n* where WR_s is the volume of water required by wellpad *s* and $w_{s,n}$ is the binary variable that shows if wellpad *s* is stimulated at time point *n*. The water balance into a particular wellpad *s* fractured at time point *n* is the combination of freshwater from the impoundment $f_{s,n}^{fw}$ and/or reuse water from the frac tank $f_{s,n}^{ww}$ as given in Equation (6.2).

$$f_{s,n} = WR_s w_{s,n} \quad \forall s \in S, n \in N \tag{6.1}$$

$$f_{s,n} = f_{s,n}^{fw} + f_{s,n}^{ww} \quad \forall s \in S, n \in N, n \geq 2 \tag{6.2}$$

Equation (6.3) states that the volume of flowback water generated in the first two weeks after comlpeting wellpad *s* $f_{s,n}^{fbw}$ is a fraction of the initial water used. This is assumed to be 25 % of the initial water used for fracturing. This flowback water can be sent to storage tank *a* prior to pretreatment or injection well *d* for disposal as given in Equation (6.4) where $f_{s,n}^{Ra}$ is the volume of flowback water sent to the storage and $f_{s,n}^{dis}$ is the volume to be discarded as effluent. The contaminants concentration in the flowback water $c_{s,c,n}^{fbw}$ is given in Equation (6.5) where $CS_{s,c}$ is the flowback water contaminants concentration of wellpad *s*.

$$f_{s,n}^{fbw} = 0.25 f_{s,n} \quad \forall s \in S, n \in N \tag{6.3}$$

$$f_{s,n}^{fbw} = f_{s,n}^{Ra} + f_{s,n}^{dis} \quad \forall s \in S, n \in N \tag{6.4}$$

$$c_{s,c,n}^{fbw} = CS_{s,c} w_{s,n} \quad \forall s \in S, c \in C, n \in N \tag{6.5}$$

Equations (6.6) and (6.77) describes the water balance around the impoundment. The total volume of water used from impoundment *t* at time point *n* $i_{t,n}^{fw}$ is given in Equation (6.6) where $TP_{s,t}$ is the piping connection between wellpad *s* and impoundment *t.* Equation (6.7) describes the volume of impoundment *t* at any time point *n* for a given scenario year *y* where $f_{t,n,y}^{pump}$ represents the volume of water supplied through piping to the corresponding impondment *t* at time point *n* and $f_{t,n,y}^{truck}$ is the volume supplied by trucking.

$$i_{t,n}^{fw} = \sum_{s \in TP_{s,t}} f_{s,n}^{fw} \quad \forall t \in T, n \in N \tag{6.6}$$

$$vi_{t,n,y} = vi_{t,n-1,y} + f_{t,n,y}^{pump} - i_{t,n}^{fw} + f_{t,n,y}^{truck} \quad \forall t \in T, n \in N, y \in Y \tag{6.7}$$

The amount of water to be disposed at time point *n* fd_n consists of effluent from wellpad *s* and concentrate stream from the regenerator $f_n^{con,Rb}$ as given in Equation (6.8). This volume of water can be injected into any of the injection well *d* as given in Equation (6.9) where Equation (6.10) indicates that the capacity of each injection well should not be exceeded. ff_n^{dis} indicates the throughput of an injection well *d* at time point *n* and $DI^{\max}$ is the maximum capacity of an injection well.

$$fd_n = \sum_s f_{s,n}^{dis} + f_n^{con,Rb} \quad \forall n \in N \tag{6.8}$$

$$fd_n = \sum_d ff_{d,n}^{dis} \quad \forall n \in N \tag{6.9}$$

$$fd_n \le DI^{\max} \quad \forall n \in N \tag{6.10}$$

The expected gas production from wellpad *s* at time point *n* is given in Equation (6.11) where p_s is a prameter indicating gas production of wellpad *s*.

$$p_{s,n} = P_s w_{s,n} \quad \forall s \in S, n \in N \tag{6.11}$$

The mass balances around the storage tanks and the regnerators as presented in the next sub-sections are done according to Figure 6.4.

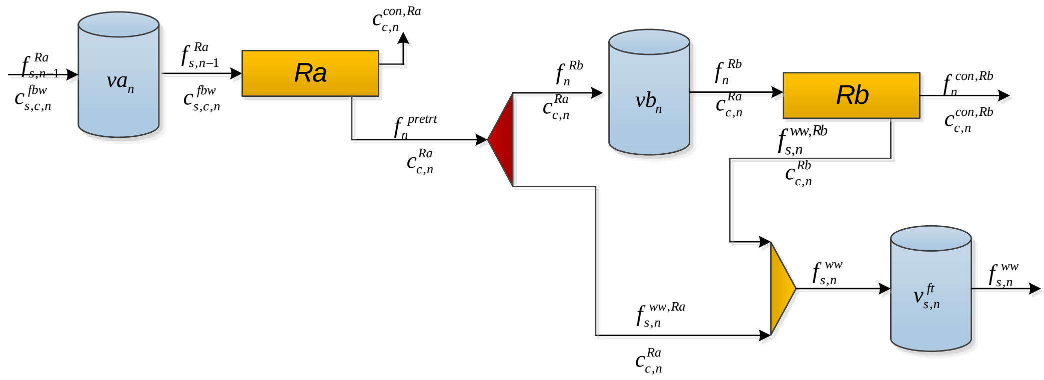

Figure 6.4. Mass balances around the storage tanks and the regenerators

6.3.1.2. Around the storage tank *va* and regenerator *Ra*

It is assumed that storage tank *va* serves as a holding tank for regenerator *Ra* and the total volume of water sent to this storage tank is treated which indicates that the volume of this storage tank at a particular time point *n* depends on the volume of water designated for treatment at a time point. Equation (6.12) is the water balance around regenerator *Ra*; it states that the total volume of water out of the regenerator f_n^{pretrt} at time point *n* is the total volume of water sent to the regenerator at the previous time point $f_{s,n-1}^{Ra}$. This captures the fact that no water is lost or produced during the regeneration operation as ultrafiltration has been reported to have a very high water recovery mostly greater than 95 % (ERM 2014, Dahmn and Chapman, 2014).

$$\sum_s f_{s,n-1}^{Ra} = f_n^{pretrt} \quad \forall n \in N, n \geq 2 \tag{6.12}$$

The contaminant balance around regenerator *Ra* is described in Equation (6.13) where $c_{c,n}^{Ra}$ represents the outlet concentration of contaminant from the regenerator and $c_{c,n}^{con,Ra}$ is the contaminant concentration removed from the water by the regenerator at time point *n.* The regenerator performance as a function of removal ratio RRa_c of contaminants is given in Equation (6.14).

$$\sum_s f_{s,n-1}^{Ra} c_{s,c,n-1}^{fbw} = f_n^{pretrt} c_{c,n}^{Ra} + c_{c,n}^{con,Ra} \quad \forall c \in C, n \in N, n \geq 2 \tag{6.13}$$

$$c_{c,n}^{Ra} = \sum_s c_{s,c,n}^{fbw} \left(1 - RRa_c\right) \quad \forall c \in C, n \in N \tag{6.14}$$

The total volume of water out of regenerator *Ra* f_n^{pretrt} at time point *n* is the sum of the amount sent to the frac tank to be reused in the next wellpad $f_{s,n}^{ww,Ra}$ as generally according to literature (Yang et al., 2014a, Yang et al., 2015, Batrholomew and Mauter, 2016, Carrero-Parreño et al., 2017), wastewater after pre-treatment to remove basic contaminants can be blended with freshwater to reduce TDS level in order to meet fracturing fluid demand and the volume sent to regenerator *Rb* for desalination as expressed in Equation (6.15).

$$f_n^{pretrt} = \sum_s f_{s,n}^{ww,Ra} + f_n^{Rb} \quad \forall n \in N \tag{6.15}$$

The capacity of *Ra* wastewater tank va_n , at time point *n* is bounded by the volume of flowback water f_n^{pretrt} treated at time point *n* as given in Equation (6.16). Equations (6.17) and (6.18) ensure that the maximum capacity of the tank is not exceeded where $V^{\max}$ and $V^{\min}$ are parameters that indicate the maximum and minimum capacity of the wastewater storage tank respectively. Equation (6.19) ensures that no water is stored in the storage tank at the end of the time horizon.

$$va_n = f_n^{pretrt} \quad \forall n \in N \tag{6.16}$$

$$va_n \le v^{\max} \quad \forall n \in N \tag{6.17}$$

$$v^{\min} wv_{s,n-1}^{va} \le f_{s,n-1}^{Ra} \le v^{\max} wv_{s,n-1}^{va} \quad \forall s \in S, n \in N, n \ge 2 \tag{6.18}$$

$$va_n = 0 \quad \forall n = /N/ \tag{6.19}$$

6.3.1.3. Around the storage tank *vb* and regenerator *Rb*

The capacity of the treatment wastewater tank vb_n , at time point *n* is bounded by the volume of pre-treated water f_n^{Rb} designated for desalination from *Ra* at time point *n* as given in Equation (6.20). Equation (6.21) describes the total volume of water into regenerator *Rb* at time point *n* as the sum of the amount collected as permeate $f_{s,n}^{ww,Rb}$ and concentrate f_n^{con} .The comtaminant mass balance around *Rb* is given in Equation (6.22) where $c_{c,n}^{Rb}$ represents the outlet concentration of contaminant from the regenerator and $c_n^{con,Rb}$ is the contaminant concentration removed from the water by the regenerator at time point *n*

$$vb_n = f_n^{Rb} \quad \forall n \in N \tag{6.20}$$

$$f_n^{Rb} = \sum_s f_{s,n}^{ww,Rb} + f_n^{con} \quad \forall n \in N \tag{6.21}$$

$$f_n^{Rb} c_{c,n}^{Ra} = \sum_s f_{s,n}^{ww,Rb} c_{c,n}^{Rb} + f_n^{con} c_{c,n}^{con,Rb} \quad \forall c \in C, n \in N \tag{6.22}$$

The concentration of the inlet contaminants into *Rb* should not exceed the maximum it can take as given in Equation (6.23) where $C_c^{\max,Rb}$ is the maximum inlet concentration into regenerator *Rb*. The performance of the regenerator is a function of the removal ratio RRb_c of contaminants as stated in Equation (6.24). Equations (6.25) and (6.26) specifies the amount of water to be collected as permeate and concentrate as a function of the recovery ratio ((*LR*) respectively.

$$c_{c,n}^{Ra} \le C_c^{\max,Rb} \quad \forall c \in C, n \in N \tag{6.23}$$

$$c_{c,n}^{Rb} = c_{c,n}^{Ra}\left(1 - RRb_c\right) \quad \forall c \in C, n \in N \tag{6.24}$$

$$LRf_n^{Rb} = \sum_s f_{s,n}^{ww,Rb} \quad \forall n \in N \tag{6.25}$$

$$f_n^{con} = \left(1 - LR\right) f_n^{Rb} \quad \forall n \in N \tag{6.26}$$

6.3.1.4. Around the recycled water frac tank

The amount of wastewater designated for reuse $f_{s,n}^{ww}$ at a particular time point *n* determines the capacity of the fracturing tank $v_{s,n}^{ft}$, on wellpad *s* as defined in Equation (6.27). This volume of wastewater is supplied through part of the permeate stream from regenerator *Ra* and the permeate stream from regenerator *Rb* as represented in Equation (6.28). Equation (6.29) ensures that the contaminants concentration in the fracturing fluid do not exceed the maximum where $CS^{\max}$ is the maximum contaminant concentration in the frac fliud.

$$v_{s,n}^{ft} \ge f_{s,n}^{ww} \quad \forall s \in S, n \in N \tag{6.27}$$

$$f_{s,n}^{ww} = f_{s,n}^{ww,Ra} + f_{s,n}^{ww,Rb} \quad \forall s \in S, n \in N \tag{6.28}$$

$$f_{s,n}^{ww,Ra} c_{c,n}^{Ra} + f_{s,n}^{ww,Rb} c_{c,n}^{Rb} \le CS_c^{\max} f_{s,n} \quad \forall s \in S, c \in C, n \in N \tag{6.29}$$

6.3.2 Scheduling constraints

The framework presented in this section consists of sequencing constraints, which account for the time dimension related to the process. These are divided into different sections as follow:

- Wellpad scheduling
- Wastewater storage tank *va* scheduling
- Regenerator *Ra* scheduling
- Regenerator *Rb* scheduling

6.3.2.1. Wellpad scheduling

The allocation constraint, which specifies that each wallpad *s* has to be fractured exactly once at a given time point *n* in the time horizon is given in Equation (6.30). Equation (6.31) specifies that no task can start at the end of the time horizon while the duration $du_{s,n}$ of each wellpad is represented through Equation (6.32). The finish time $tf_{s,n}$ of wellpad *s* fractured at time point *n* is represented by big-M constraints which are active if wellpad *s* is fractured at time point *n* as given in Equations (6.33) –(6.34) where $ts_{s,n}$ is the start time of fracturing wellpad *s*.

$$\sum_n w_{s,n} = 1 \quad \forall s \in S \tag{6.30}$$

$$w_{s,n} = 0 \quad \forall s \in S, n \in N, n = /N/ \tag{6.31}$$

$$du_{s,n} = TR_s w_{s,n} \quad \forall s \in S, n \in N \tag{6.32}$$

$$tf_{s,n} \le ts_{s,n} + du_{s,n} + H\left(1 - w_{s,n}\right) \quad \forall s \in S, n \in N \tag{6.33}$$

$$tf_{s,n} \ge ts_{s,n} + du_{s,n} - H\left(1 - w_{s,n}\right) \quad \forall s \in S, n \in N \tag{6.34}$$

The sequence dependent change over time between wellpad *s* and s' is given in Equation (6.35). It states that the start time of wellpad s' at time point *n* must be equal or greater than the finish time of wellpad *s* at previous time point plus the crew transition time $CT_s^{s'}$ between wellpad s and s'. Equation (6.36) states that the time at which time point *n* occurs must correspond with the availability time AT_s of wellpad *s*.

$$ts_{s',n} \ge tf_{s,n-1} + CT_s^{s'} w_{s',n} \quad \forall s \in S, s' \in S, s' \ne s, n \in N, n \ge 2 \tag{6.35}$$

$$tt_n \ge \sum_s \left(AT_s w_{s,n} - H\left(1 - w_{s,n}\right)\right) \quad n \in N \tag{6.36}$$

6.3.2.2. Storage tank *va* scheduling

The required criteria for water to be transferred to storage tank *va* is described in Equations (6.37) – (6.39). Equation (6.37) specifies that for water to be transferred from wellpad *s* to storage tank *va* at time point *n*, fracturing of wellpad *s* has to be scheduled to take place at that time point. However, fracturing of wellpad *s* can still take place without sending the generated wastewater to the storage tank as the wastewater can as well be sent to the injection well for disposal. Equations (6.38) and (6.39) together ensure that the time at which water is transferred $tv_{s,n}^{va}$ to the storage tank *va* from wellpad *s* fractured at time point *n* coincide with the finishing time $tf_{s,n}$ of wellpad *s*.

$$wv_{s,n}^{va} \le w_{s,n} \quad \forall s \in S, n \in N \tag{6.37}$$

$$tv_{s,n}^{va} \ge tf_{s,n} - H\left(2 - wv_{s,n}^{va} - w_{s,n}\right) \quad \forall s \in S, n \in N \tag{6.38}$$

$$tv_{s,n}^{va} \le tf_{s,n} + H\left(2 - wv_{s,n}^{va} - w_{s,n}\right) \quad \forall s \in S, n \in N \tag{6.39}$$

6.3.2.3. Regenerator *Ra* scheduling

The relationship between transfer of water to storage tank *va* and regeneration of water by regenerator *Ra* is given in Equation (6.40). It states that water regeneration by *Ra* can only take place if water is transferred to storage tank *va* from wellpad *s* fractured at time point *n* i.e. the occurrence of regeneration task *Ra* depends solely on if water is transfer to *va* or not. Equations (6.41) and (6.42) ensure that the time at which regeneration task starts tr_n^{Ra} in *Ra* corresponds to the time $tv_{s,n}^{va}$ at which water is transferred to *va*. The duration of regeneration for *Ra* is given in Equation (6.43) where ttr_n^{Ra} is the finish time of regeneration at time point *n*, $f_{s,n}^{Ra}$ is the total volume of water into the regenerator at time point n and ff^{Ra} is the feed flowrate into the regenerator.

$$wr_n^{Ra} \ge wv_{s,n}^{va} \quad \forall s \in S, n \in N \tag{6.40}$$

$$tr_n^{Ra} \ge tv_{s,n}^{va} - H\left(2 - wr_n^{Ra} - wv_{s,n}^{va}\right) \quad \forall s \in S, n \in N \tag{6.41}$$

$$tr_n^{Ra} \le tv_{s,n}^{va} + H\left(2 - wr_n^{Ra} - wv_{s,n}^{va}\right) \quad \forall s \in S, n \in N \tag{6.42}$$

$$ttr_n^{Ra} = tr_{n-1}^{Ra} + \left(\frac{\sum_s f_{s,n-1}^{Ra}}{ff^{Ra}} \right) wr_{n-1}^{Ra} \quad \forall n \in N \tag{6.43}$$

6.3.2.4. Regenerator *Rb* scheduling

Equation (6.44) describes the relationship between the regeneration of water by regenerator *Rb* and fracturing task occurring at time point *n*. It states that water regeneration by regenerator *Rb* can only takes place if there is a wellpad scheduled to be fractured at that time point i.e. water is only transferred to *Rb* from *vb* if there is a fracturing task requiring that water. However, it is not a pre-requisite for regeneration task by *Rb* to occur as the pre-treated water or combination of freshwater and pre-treated water can supply the water needed for fracturing. Equations (6.45) and (6.46) ensure that the time tr_n^{Rb} at which regeneration task starts in *Rb* coincide with the start time $ts_{s,n}$ of wellpad s scheduled to be fractured at that time point. The duration of regeneration for *Rb* is given in Equation (6.47) where ttr_n^{Rb} is the finish time of regeneration at time point *n*, f_n^{Rb} is the total volume of water into the regenerator at time point n and ff^{Rb} is the feed flowrate into the regenerator.

$$wr_n^{Rb} \geq wv_{s,n} \quad \forall s \in S, n \in N \tag{6.44}$$

$$tr_n^{Rb} \geq ts_{s,n} - H\left(2 - wr_n^{Rb} - w_{s,n}\right) \quad \forall s \in S, n \in N \tag{6.45}$$

$$tr_n^{Rb} \leq ts_{s,n} + H\left(2 - wr_n^{Rb} - w_{s,n}\right) \quad \forall s \in S, n \in N \tag{6.46}$$

$$ttr_n^{Rb} = tr_n^{Rb} + \left(\frac{f_n^{Rb}}{ff^{Rb}} \right) wr_n^{Rb} \quad \forall n \in N \tag{6.47}$$

6.3.3 Tightening constraint

Equation (6.48) impose the requirement that the sum of the fracturing durations of all the wellpads $du_{s,n}$ should be lesser or equal to the time horizon H while Equation (6.49) restricts the sum of the fracturing time of all wellpads starting after tt_n to be smaller than the remaining time where tt_n is the time at which time point *n* occurs.

$$\sum_s \sum_n du_{s,n} \leq H \tag{6.48}$$

$$\sum_s \sum_{n' \geq n} du_{s,n'} \leq H - tt_n \quad \forall n \in N \tag{6.49}$$

6.3.4. Regenerators design models

The detailed design models for the two regenerators are presented in this section. It is worth mentioning that the membrane distillation design model has been presented in detail in chapter three while the detailed design model for Ultrafiltration has also been presented in chapter five, hence, will not be presented in detail in this chapter. However, critical constraints in the models are provided to facilitate better understanding.

6.3.4.1. Ultrafiltration model

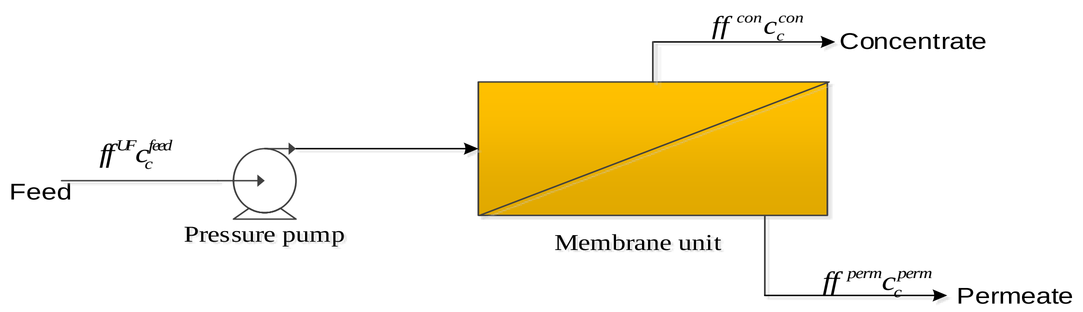

Figure 6.5. Schematic of a crossflow ultrafiltration plant

The detailed design model for ultrafiltration presented in this section is based on the work of Guadix et al. (2004). The water flux across the ultrafiltration membrane J^{UF} is dependent on the transmembrane pressure Δp and the membrane resistance R_m as given in Equation (6.50). Equation (6.51) (Micro and utrafiltration, 2018, Falsanisi et al., 2010, Amoosa et al, 2016 , Muro et al., 2012) describes the transmembrane pressure as the pressure difference between permeate and the feed side of the membrane where p_f is the feed pressure, p_p is the permeate pressure and p_r is the pressure of the retentate.

$$J^{UF} = \frac{\Delta p}{R_m} \tag{6.50}$$

$$\Delta p = \frac{p_f + p_r}{2} - p_p \tag{6.51}$$

The mass balance around the ultrafiltration membrane unit is conducted based on Figure 6.5 as given in Equations (6.52) and (6.53) where ff^{Ra} is the total flowrate into the UF unit and $ff^{Ra,perm}$ is the permeate flowrate from the UF unit.This balance captures the assumption that during the operation of the UF unit, water is neither lost nor produced.

$$ff^{Ra} = ff^{Ra,perm} \tag{6.52}$$

$$ff^{Ra}Cf_c^{Ra} = ff^{Ra,perm}cp_c^{Ra,perm} + cr_c^{Ra,con} \quad \forall c \in C \tag{6.53}$$

For a tubular system, the membrane area is calculated according to Equation (6.54) (Guadix et al., 2004) where N is the number of membrane modules, T is the number of tubes per module, D is the tube diameter and l is the tube length.

$$A = NT\pi Dl \tag{6.54}$$

The energy requirement in ultrafiltration is mainly the energy require by the feed pump in pumping the feed water into the UF unit as given in Equation (6.55).The continous variable W^{fp} represents the energy required by the feed pump and η is the pump efficiency.

$$W^{fp} = \frac{ff^{Ra}\left(p_f - p_p\right)}{\eta} \tag{6.55}$$

The performance of ultrafiltration is specified in terms of removal ratio“RR_c^{Ra}”. It is assumed to be fixed in this work and is defined as given in Equation (6.56).

$$cp_c^{Ra,perm} = cf_c^{Ra,perm}\left(1 - RR_c^{Ra}\right) \tag{6.56}$$

The capital costs of the pump and the membrane are given in Equations (6.57) and (6.58) (Guadix et al., 2004) where CC^{fp} is the capital cost of the feed pump, CC^{m} is the capital cost of membrane, a and b are the pump cost coefficient and pump cost exponent while c and d are the membrane cost coefficient and membrane cost exponent respectively.

$$CC^{fp} = a\left(W^{fp}\right)^{b} \tag{6.57}$$

$$CC^{m} = cA^{d} \tag{6.58}$$

The operating cost of the feed pump is given by Equation (6.59) where C^{ele} is the cost of electricity and AOT is the annual operating time.

$$OC^{fp} = W^{fp}C^{ele}AOT^{UF} \tag{6.59}$$

6.3.4.2. Membrane distillation model

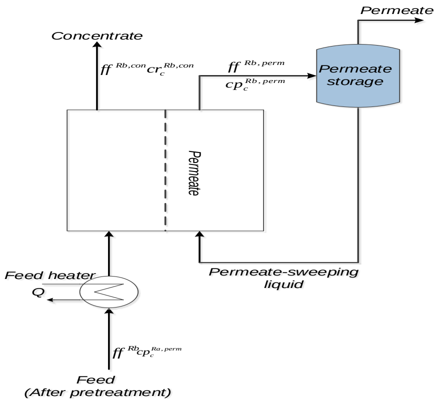

Figure 6.6. Schematic representation of a typical direct contact membrane distillation.

The work of Elsayed et al. (2013) form the basis on which the membrane distillation model presented in this section is built. The driving force for the water flux across the membrane, J^{MD}, is the difference in pressure of the water vapour and is defined in Equation (6.60) as:

$$J^{MD} = Bw\left(p_{wf}^{vap} \gamma_{wf} x_{wf} - p_{wp}^{vap} \right) \tag{6.60}$$

where Bw is the membrane permeability, p_{wf}^{vap} ,is the water vapour pressure of the feed, p_{wp}^{vap} is the water vapour pressure of the permeate, γ_{wf} is the activity coefficient of water in the feed and x_{wf} is the mole fraction of water in the feed.

The activity coefficient is dependent on concentration and on the assumption of NaCl as the primary solute, Equation (6.61) (Yun et al., 2006) can be used to estimate the activity coefficient where x_{NaCl} is the molar concentration of NaCl in the feed.

$$\gamma_{wf} = 1 - 0.5 x_{NaCl} - 10 x_{NaCl}^2 \tag{6.61}$$

The permeability of the membrane Bw depends on the membrane temperature, T_m which differs based on the kind of diffusion. The permeability of membranes in which molecular diffusion occurs is calculated through Equation (6.62) as proposed by Elsayed et al. (2013) where B_{wb} is the temperature-independent base value of membrane permeability.

$$Bw = B_{wb} T_m^{1.334} \tag{6.62}$$

Mass and contaminant balance around the MD unit is conducted in accordance with Figure 6.6 as given in Equations (6.63) and (6.64). Removal ratio refers to the mass load of contaminant exiting in the concentrate stream of the regenerator as a fraction of the feed. It is assumed to be fixed in this work and is defined as given in Equation (6.65).

$$ff^{Rb} = ff^{Rb,perm} + ff^{Rb,con} \tag{6.63}$$

$$ff^{Rb} cp_c^{Ra} = ff^{Rb,perm} cp_c^{Rb,perm} + ff^{Rb,con} cr_c^{Rb,con} \quad \forall c \in C \tag{6.64}$$

$$RR_c^{Rb} = \frac{ff^{Rb,con} cr_c^{Rb,con}}{ff^{Rb} cp_c^{Ra,perm}} \tag{6.65}$$

The amount of permeated water is highly dependent on the energy Q provided to the unit. Therefore, the heat required by the feed is given by Equation (6.66).

$$Q = ff^{Rb} C_p \left(T_{bf} - T_{sf}\right) \tag{6.66}$$

The membrane area A_m is calculated by dividing the permeate flow rate by the water flux as given in Equation (6.67).

$$A_m = \frac{ff^{Rb,perm}}{J^{MD}} \tag{6.67}$$

The annualized fixed cost of the MD network, AFC, as proposed by Elsayed et al. (2013) is given by Equation (6.68).

$$AFC = 58.5 A_m + 1115 ff^{Rb} \tag{6.68}$$

The annual operating cost excluding heating, AOC, as proposed by Elsayed et al. (2013) is given by Equation (6.69), where u, is the ratio of recycled reject to raw feed.

$$AOC = \left(1411 + 43\left(1 - LR\right) + 1613\left(1 + u\right)\right) ff^{Rb} \tag{6.69}$$

The annual heating cost AHC, is given by Equation (6.70): where AOT is the annual operating time, Q is the heat requred by the feed into MD and OC^{ht} is a parameter indicating the cost of heating.

$$AHC = AOT^{MD}\left(Q OC^{ht}\right) \tag{6.70}$$

6.3.4.3. Energy consideration

As membrane processes for wastewater treatment have been considered as energy intensive, integrating these processes with industrial processes can offer several advantages in terms of cost and energy consideration. Excess low-heat or waste heat from industrial processes can be channelled to drive these membrane processes. In hydraulic fracturing, the co-produced gas from wells that produce oil and gas can be channelled towards this course instead of wasting it through flaring. Generally, flaring is initiated for all wells after the completion of hydraulic fracturing whether for oil and gas producing or only gas producing well, for the purpose of well testing. This has been considered as source of wasted energy, which can be channelled towards providing the energy requirement in wastewater treatment (Elsayed et al., 2015). The proposed methodology to incorporate this possibility is shown in Figure 6.7.

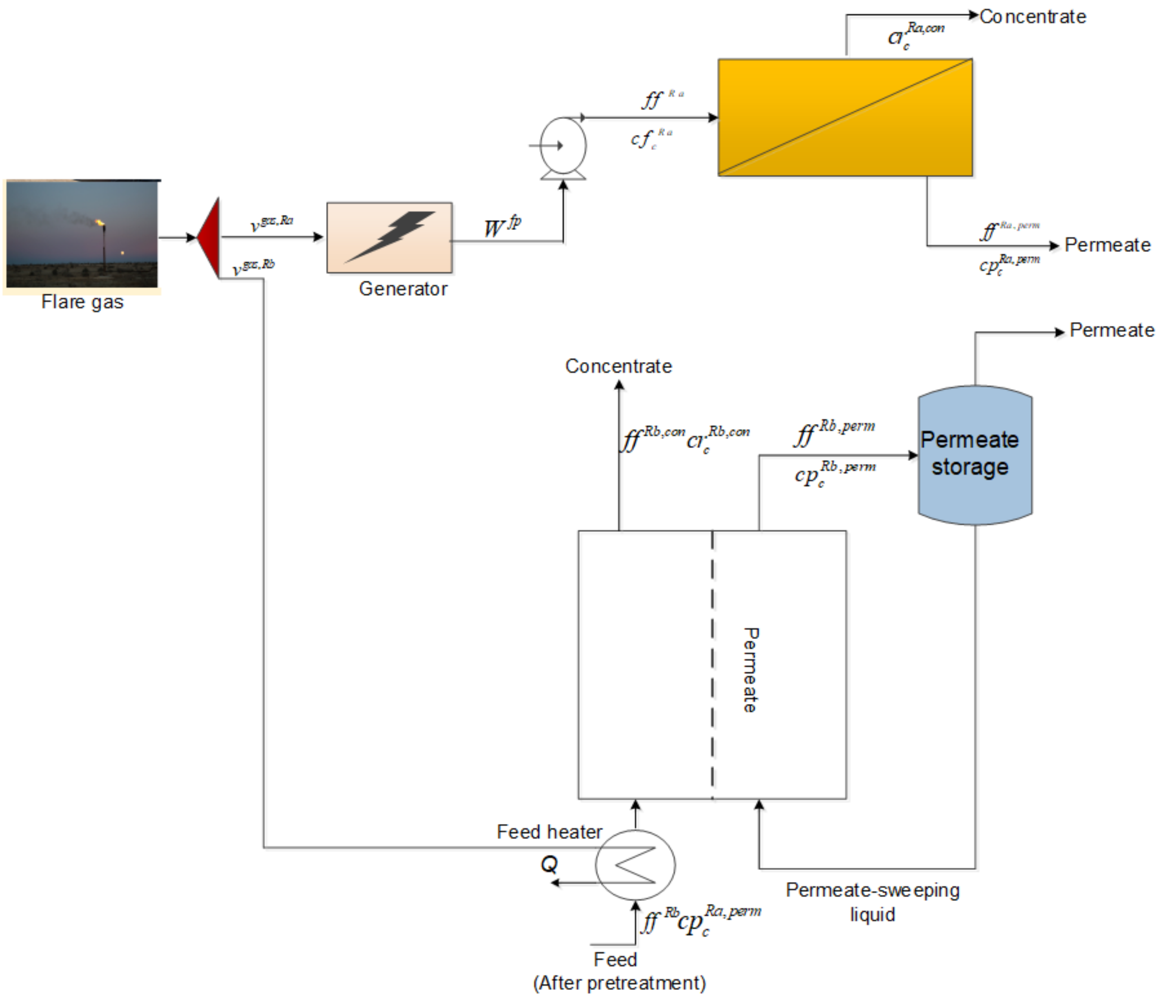

Figure 6.7. Flaring as possible energy source for the regenerators

The volume of gas needed by the generator v^{gas} to generate a kWh of energy required by regenerator Ra (ultrafiltration) is given by Equation (6.71) where Gen^{eff} is the generator thermal efficiency/heat rate and HC^{fuel} is the heat content of the gas.

$$v^{gas} = \frac{Gen^{eff}}{HC^{fuel}} \tag{6.71}$$

The volume of gas needed to generate the energy required by the feed pump $v^{gas,Ra}$ is given in Equation (6.72)

$$v^{gas,Ra} = v^{gas}W^{fp} \tag{6.72}$$

The operating cost of the generator is given in Equation (6.73) Where C^{gas} is the cost of gas.

$$oc^{gen} = v^{gas,Ra}C^{gas}AOT^{UF} \tag{6.73}$$

The volume of gas needed $v^{gas,Rb}$ to supply the required thermal energy for Regenerator *Rb* (membrane distillation) is given in Equation (6.74) where ∂_{ED} is the energy density

$$V^{gas,Rb} = \frac{Q}{38300\partial_{ED}} \tag{6.74}$$

6.3.5. Objective function

The objective which aims at maximizing profit is given in Equation (6.75) and it comprises of the following terms: (1) revenue from gas production, (2) freshwater transportation cost, (3) cost associated with ultrafiltration regeneration network, (4) cost associated with membrane distillation regeneration network, (4) disposal cost, (5) wastewater storage cost, and (6) pumping cost to treatment facility.

$$\max profit = SP^{gas}\sum_{s}\sum_{n} p_{s,n}$$

$$-\left[\begin{array}{l}\left(OC^{truck,fw}\sum_{t}\sum_{n}\sum_{y}\frac{f_{t,n,y}^{truck}}{NY}+OC^{pump,fw}\sum_{t}\sum_{n}\sum_{y}\frac{f_{t,n,y}^{pump}}{NY}\right)\\ +\left(\frac{\left(a\left(W^{fp}\right)^{b}+cA^{d}+CC^{pipe}+CC^{gen}\right)}{L^{\max}}+W^{fp}C^{ele}AOT+ff^{Ra}C^{chem}AOT+v^{gas,Ra}C^{gas}AOT\right)\\ +\left(\left(58.5A_{m}+1115ff^{Rb}\right)+\left(1411+43\left(1-LR\right)+1613\left(1+u\right)\right)ff^{Rb}+AOT\left(QOC^{ht}\right)\right)\\ +\left(OC^{dis}\sum_{s}\sum_{n} f_{s,n}^{dis}\right)+OC^{dis}\sum_{n} f_{n}^{con}\\ +\left(OC^{st,ww}\left(\sum_{s}\sum_{n} v_{s,n}^{ft}\right)\right)\\ +OC^{pump,ww}DS_{s}\left(\sum_{s}\sum_{n} f_{s,n}^{trt}+\sum_{n} f_{n}^{perm}\right)\end{array}\right] \tag{6.75}$$

6.4. Case study

The proposed model is applied to a case study from Yang et al. (2014a) which considered 14 wellpads; 540 days time horizon, one uninterruptible freshwater source and two interruptible sources connected to impoundments as illustrated in Table 6.1. Thirty years historical data were provided for the two interruptible sources. The selected ultrafiltration membrane geometry is tubular and operate in a cross flow mode and the details of this membrane module are given in Guadix et al. (2004). The selected membrane distillation is a polyvinylidene fluoride used in direct-contact membrane distillation and detail of this membrane has been reported in chapter three. In order to allow for detailed analysis of the case study, two different scenarios are considered to cover possible flowback water composition in hydraulic fracturing. The difference in the two scenarios lie in the degree of salinity in terms of TDS concentration of the flowback water generated after hydraulic fracturing. In scenario 1, the concentration of contaminants such as TOC, TSS, and Fe are based on the data provided in Table 6.2 while the TDS concentration is considered to be moderate with values lie between 60,000 mg/l and 100,000 mg/l in most wellpads while in some wellpads the value is allowed to go up to 300, 000 mg/l. In scenario2, the concentration of TDS considered for the wellpads are in the range of 122,000 – 300, 0000 mg/l. This is considered because the case study is reported to be a representative of Marcellus shale play (Yang et al., 2014a) and according to the report in literature, Marcellus play has the tendency of producing high salinity flowback water (Onishi et al., 2017b, Hayes, 2009, Acharya et al., 2011, Jiang et al., 2013, Yang et al., 2015). The removal ratio for each of the contaminant in the treatment unit as well as the parameters and cost coefficient for the case study are provided in Table 6.3 and 6.4 respectively.

Table 6.1. Wellpad Data (Yang et al., 2014a)

Wellpads	S1	S2	S3	S4	S5	S6	S7	S8	S9	S10	S11	S12	S13	S14
Match with takepoints, $TP_{s,t}$	*t2*	*t1*	*t1*	*t1*	*t1*	*t2*	*t2*	*t2*	*t2*	*t2*	*t2*	*t1*	*t1*	*t2*
Earliest frac day	1	1	1	1	1	39	1	273	273	273	396	379	379	1
# of stages	57	61	54	55	64	26	97	88	86	76	63	100	100	87

Table 6.2. Random flowback water composition from Barnett and Appalachian plays (Carrero –Parreño et al., 2017)

Parameter	Well 1	Well 2	Well 3	Well 4
TDS (mg/L)	200,006	54,230	110,847	9,751
TSS (mg/L)	3,220	881	1,530	168
TOC (mg/L)	200	89	138	38
Fe (mg/L)	92	60	105	40
Ca (mg/L)	14,680	4,800	3600	241
Mg (mg/L)	4,730	1,707	899	49
Ba (mg/L)	98	112	127	1
Oil and grease (mg/L)	0	0	18	0

Table 6.3. Contaminants removal ratio

Contaminant	Removal ratio UF	MD
TSS	0.95	0.99
TOC	0.5	0.5
Fe	0.8	0.99
TDS	0	0.99

Table 6.4. Parameters and cost coefficients.

Parameter	Value
Crew transition time (day)	5
Volume of frac fluid used per stage (m^3)	950
Freshwater used (%)	85
Wastewater storage cost ($/$m^3$)	0.59
Freshwater trucking cost ($/$m^3$)	29.35
Freshwater pumping cost ($/$m^3$)	15.93
Disposal cost ($/m3)	134.18
Wastewater pumping cost($/km/$m^3$)	0.28
Pump coefficient ($)	2,590
Pump cost exponent	0.79
Piping and instrumentation cost ($)	20,000
Membrane cost coefficient ($)	1,000
Membrane cost exponent	0.9
Tube diameter (m)	0.004
Electricity cost ($/kWh)	0.07
Tube length	1.02
Plant life (h)	87,600
Number of tubes per module	361
Natural gas price ($/$m^3$)	0.12
Pump efficiency	0.8
Temperature-independent base value ($kg/m^2.s.pa.K^{1.334}$)	$7.5*10^{-11}$
Membrane thickness (mm)	0.65
Annual operation time (h)	8000
Heating cost ($/109J)	5
Supply temperature (K)	293

6.4.1. Results and discussion

The resulting model is a mixed integer nonlinear programming (MINLP) which was formulated in GAMS and solved using BARON. The model has 11,517 constraints, 7,344 continuous Variables, 451 binary variables and 5,451 non-linear terms. The optimum number of time points is 15 with 14 number of slots and CPU time of 14,871.4 s. The schedule obtained for the two scenarios are presented in Figure 6.8 and 6.9 respectively. From Figure 6.8, wellpad S1 which is among the wellpads with the lower number of stages is fractured first. This allow for minimum freshwater withdrawal at the beginning of the time horizon. Although, this is followed by wellpad that require significant volume of water (S14). Fracturing wellpad S1 first allowed for 16.38% of water required by wellpad S14 to be supplied by S1. In most cases in this figure, the schedule indicates fracturing wellpad with higher number of stages followed by one with lower number of stages or fracturing wellpads with close number of stages after one another to allow full wastewater reuse in wellpads with lower number of stages. A significant example of this is the fracturing schedule of wellpad S14 and S3 as 40.28 % of water required by S3 is supplied by S14. This is also significant in the schedule of S11 and S6 as 55.26 % of water required by S6 is supplied by wastewater from wellpad S11.

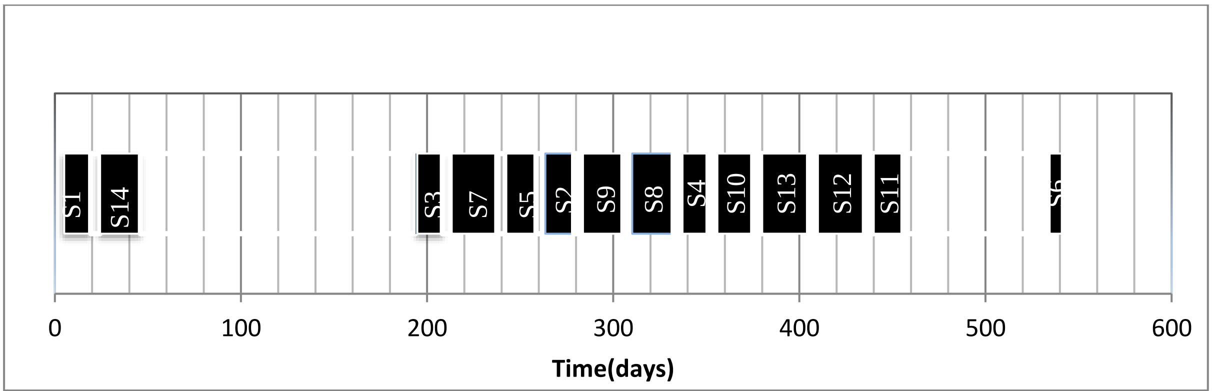

Figure 6.8. Fracturing Schedule: scenario 1

The optimal schedule obtained in scenario 2 indicate that the first 9 wellpads fractured in this scenario followed the same trend as scenario 1 whereby wellpad with high number of stages is fractured followed by wellpad with lower number of stages or wellpads with close number of stages are fractured after one another. However, the group of five wellpads (S12, S9, S13 S8 and S6) fractured towards the end of the time horizon are mostly wellpads with the largest number of stages (except wellpad S6) thereby requiring significant volume of water. Fracturing these wellpads in this sequence will allow full maximisation of flowback water within these wellpads. The effect of this sequence is also significant in wellpad S6; fracturing wellpad S8 before wellpad S6 results in 80 % of water required by S6 to be supplied by wastewater from S8. The major difference in this scenario compared to scenario 1 lies in the sequence of fracturing as both scenarios chose to fracture one of the wellpad with least number of stages first, resulting in minimum freshwater withdrawal at the beginning of time horizon and minimum wastewater discharge from wellpad S6 at the end of time horizon.

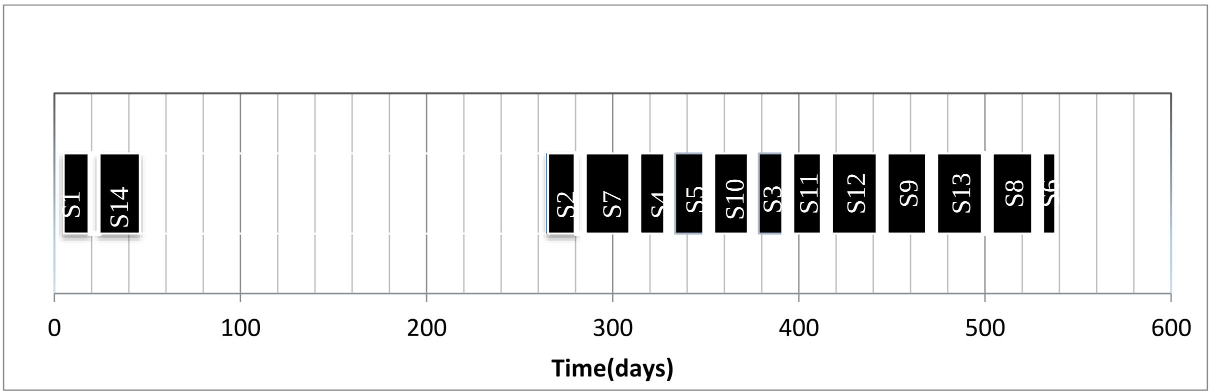

Figure 6.9. Fracturing Schedule: scenario 2

The detail analysis of both scenarios is presented in Table 6.5. The total revenue in the two scenarios are the same with the value of \$261.24 million while the profit is \$247 million for scenario 1 and \$246 million for scenario 2. The total water required is 818,805 m^3 of which 624,494 m^3 fresh water is supplied through piping and 23.73 % through regenerated water in scenario 1, while in scenario 2, 24.13 % of water required is supplied by regenerated water and the remaining 621,219 m^3 is supplied by freshwater through piping. In addition, of the total wastewater used in scenario 1, 6.4 % is supplied by desalinated water from membrane distillation and 93.6 % by pre-treated water from ultrafiltration while in scenario 2, 18.9 % is supply by desalinated water and 81.1 % by pre-treated water. It is worth mentioning that direct flowback water reuse is not considered in this study as it has been reported in literature that this option can cause operational problems mainly because of high level of contaminants that can compromise the well exploration (Carrero-Parreño et al., 2017, Hayes and Severin, 2012). The percentage of wastewater to freshwater used in the schedule for both scenarios is presented in Figures 6.10 and 6.11 respectively. For scenario 1, Figure 6.10 shows that the water needed for most of the wellpads is supplied through the combination of freshwater and pre-treated water as higher percentage of total wastewater used in this scenario comes from pre-treated water. This is possible because of moderate TDS concentration of most of the wellpdads in this scenario.

As the flowback water salinity becomes higher in scenario 2, there is reduction in the volume of pre-treated water used, therefore in most cases the percentage of wastewater requirement comes from desalinated water or combination of pre-treated water and desalinated water. The exceptional case in this scenario is wellpad S6 that uses a significant volume of desalinated water which is capped at 80 % of total water required in fracturing this wellpad.

Table 6.5. Optimal analysis of the case study

Parameters	Scenario 1	Scenario 2
Total water used (1,000 m^3)	818.8	818.8
Freshwater pumped (1,000 m^3)	624.5	621.2
Freshwater trucked (1,000 m^3)	0	0
Regenerated water (1,000 m^3)	194.3	197.6
Freshwater save (%)	23.73	24.13
Wastewater supplied by UF (%)	93.6	81.1
Water supplied by MD (%)	6.4	18.9
Freshwater cost ($ 1,000)	9,948	9,896
Revenue ($ 1,000)	261,240	261,240
Profit ($ 1,000)	247,060	246,107

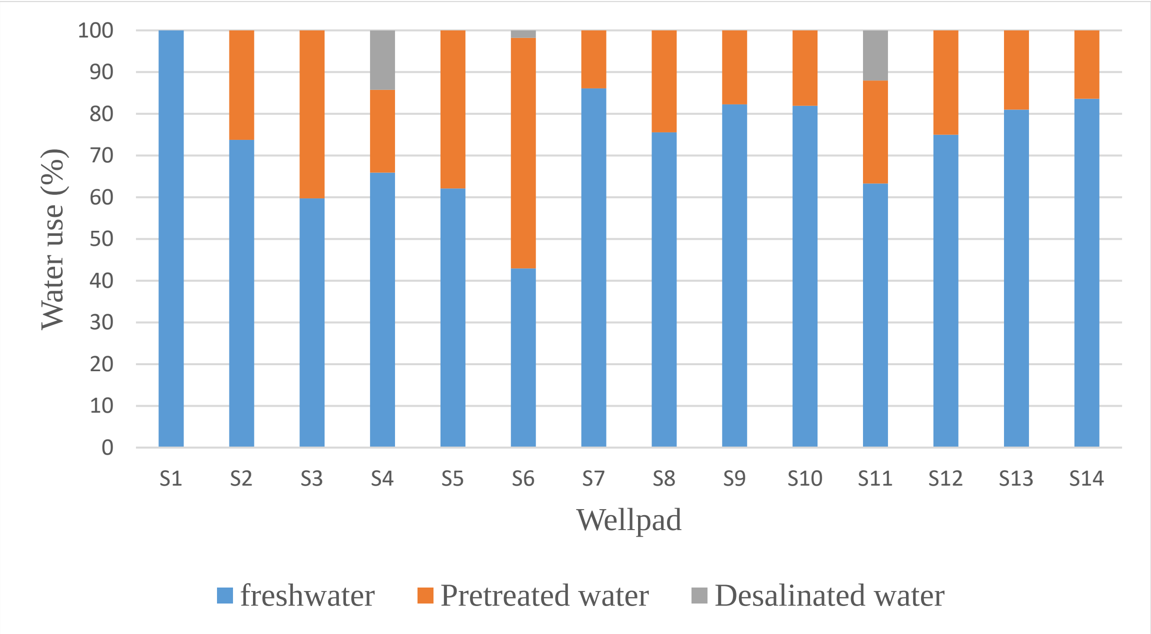

Figure 6.10. Percentage of water used in fracturing operation (Scenario 1)

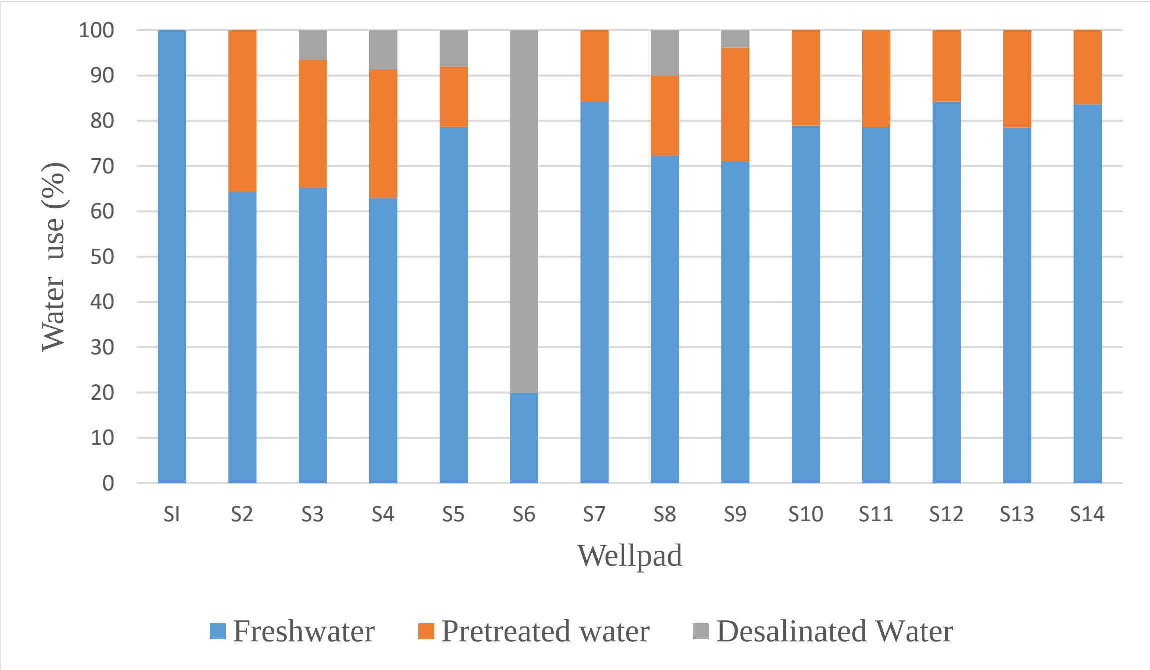

Figure 6.11. Percentage of water used in fracturing operation (Scenario 2)

In order to determine the energy requirement for the multi regenerator water network so as to account for the feasibility of using the onsite flare gas as source of this energy, analysis based on the detailed multiregenerator model and standalone model (for each regenerator) was done. The optimum flowrate from the detailed network was used in the standalone models to in order to determine the actual needed energy for regeneration.

For ultrafiltration membrane, the membrane feed pressure is reduced from 405.16 kPa (4.05 bar) equivalent to 7.65 kW (183.6 kWh) power consumption in standalone to 373.99 kPa (3.73 bar) equivalent to 6.99 kW (167.76 kWh) power consumption by the feed pump in the detailed model. The percentage reduction in the power consumption is capped at 8.62 %. The low percentage of energy saving in ultrafiltration means operating at high pressure which leads to maximization of flux across the membrane, lower membrane area and fixed cost. The primal cost in the UF network is the cost of membrane and operating at lower pressure will have a huge effect on the membrane cost if the flux is minimized and the membrane area is increased. The power consumption is in the order of 0.112 kWh/m^3 of water, which is found to be lower than the estimated energy requirement reported for reclamation and reuse of different sources of water in membrane filtration (WaterWorld, 2014; Howe et al., 2012; Micro and Ultrafiltration, 2018; Pearce, 2008). The reported value is within the range of 0.8–1.0 kWh/m^3 for wastewater and brackish water systems (WaterWorld, 2014). However, as membrane distillation is more energy intensive than ultrafiltration, the simultaneous energy and water

optimization within the multiregenerator water network leads to 31.6 % reduction in the energy require for the membrane distillation regenerator. The feed temperature required in the standalone membrane distillation model is found to be 363 K, which is reduced to 340.9 K in the detailed model. Although operating at the maximum feed temperature results in water flux maximization across the membrane, which leads to the minimization of both the membrane area and the fixed cost but this, does not necessarily correspond to the optimal performance of the membrane. The amount of energy required is reduced from 700×10^6 kJ to 479×10^6 kJ. The thermal energy require is in the order of 191×10^3 kJ/m^3 of water.
The volume of gas needed to generate the required energy (167.76 kWh) for ultrafiltration is 16.33 m^3 while 12,507 m^3 of gas is needed to generate 479×10^6 kJ of energy needed for the membrane distillation based on throughput per day. Glaizer et al. (2014) reported an average estimate of 9,600 m^3 of gas been flared per well per day in shale plays that produce oil and associated gas in Texas, although this might be lower in shale play where gas production is dominant. Assuming an average of 4 wells per wellpad, there is a high feasibility of converting the wasted energy through flaring into useful source of energy for these regenerators. Using this gas as a source of energy for the regenerators will render the operating cost of the feed pump in ultrafiltration and the heating cost in membrane distillation zero. Although, for ultrafiltration network, additional capital cost for the gas generator will be incurred, however as the gas needed is supplied onsite, the operating cost of the generator will be zero. The capital cost of generator is assumed to be $ 15,000 with 10 yr. plant life, resulting in annualized capital cost of $ 1,500/yr. This leads to 61.65 % saving in the cost incurred if the electrical energy is generated onsite.

The design specifications for the two regenerators are given in Tables 6.6 and 6.7 respectively. The membrane area required, the permeate flux and other design specifications are given in Table 6.6 and 6.7 respectively. The detailed analysis of the cost indicates that for ultrafiltration network, the primal cost is the capital cost especially the cost of membrane while in membrane distillation, the primal cost is found to be the operating cost. This may justify the reason while in ultrafiltration detailed model, the percentage of power saving is lower so as to maximize the flux while keeping the membrane area low, hence minimal membrane cost while in membrane distillation, there is significant reduction in the feed temperature hereby lowering the energy requirement thereby minimizing the operating cost.

Table 6.6. Design specification for UF.

Design variables	Optimum values
Power (kW)	6.99
Feed pressure (kPa)	373.99
Transmembrane pressure (kPa)	186.99
Number of membrane modules	26
Permeate flux (m/h)	0.52

Table 6.7 Design specification for MD.

Design variables	Optimum values
MD feed temperature (K)	340.9
Thermal efficiency	0.97
Thermal energy (kJ/day)	4.79×10^8
Membrane area (m^2)	2.535×10^3
Permeate flux (kg/m^2s)	0.008

6.5. Conclusion

This study has considered a systematic approach for scheduling and design of multi-regenerator water network for effective flowback water management in hydraulic fracturing. It focused on detailed ultrafiltration and membrane distillation processes to account for some of contaminants that are considered to be of paramount importance in hyraulic fracturing wastewater reuse. The results showed that in the case where moderate salinity is considered, high percentage of flowback water is pre-treated and reused by combining with freshwater to meet the fracturing requirement in terms of contaminants concentration. However, as the degree of salinity increased ,the water requirement is supplied through the combination of freshwater, pre-treated water and/or desalinated water with different percentage for each wellpad depending on the volume of water required for fracturing and the degree of salinity of the wastewater. The effect of fouling and cake compressibility especially in ultrafiltration can also be incorporated as these are considered to be important for design and scale-ups in membrane processes.

Nomenclature

Sets

D	$\{d \mid d$ = injection well$\}$
N	$\{n \mid n$ = time point$\}$
S	$\{s \mid s$ = wellpad$\}$
T	$\{t \mid t$ = an interruptible source and its corresponding impoundment$\}$
$TP_{s,t}$	Match between wellpad *s* and source *t*
Y	$\{y \mid y$ = historical river flowrate data year$\}$

Parameters

AT_s	Availability time of wellpad *s*, day
AOT^{UF}	Annual operating time, hr
AOT^{MD}	Annual operating time, day
a	Pump cost coefficient, \$
B_{wb}	Temperature independent base value for the permeability, kg/m^2.s.pa.K$^{1.334}$
b	Pump cost exponent
c	Membrane cost coefficient, \$
$C_c^{\max,Ra}$	Maximum inlet concentration into treatment unit *Ra*, mg/L
$C_c^{\max,Rb}$	Maximum inlet concentration into treatment unit *Ra*, mg/L
Cf_c^{Ra}	Concentration of the feed water into UF, mg/L
$CS_c^{\max}$	Maximum inlet concentration into wellpad *s*, mg/L
$CS_{s,c}$	Flowback water contaminant concentration in wellpad *s*, mg/L
$CT_S^{S'}$	Crew transition time between wellpads, day
c^{che}	Unit cost of chemical pre-treatment, \$/m^3
C^{gas}	Cost of gas, \$/m^3
d	Membrane cost exponent
D	UF tube diameter, m
$DI^{\max}$	Maximum capacity of the injection well, m^3
DS_s	Distance from wellpad *s* to treatment facility, km
e	Electricity cost, \$/kWh
Gen^{eff}	Thermal efficiency/heat rate of the generator

H	Time horizon of interest, day
Hc^{fuel}	Heat content of natural gas, Btu/m^3
l	UF tube length, m
$L^{\max}$	Plant life, yr
NY	Number of historical year, yr
$OC_s^{pump,fw}$	Freshwater pumping cost, \$/m^3
$OC_s^{truck,fw}$	Freshwater trucking cost, \$/m^3
$OC_s^{pump,ww}$	Wastewater pumping cost, \$/m^3/km
OC^{dis}	Cost of wastewater disposal, \$/m^3
$OC_s^{st,ww}$	Cost of wastewater storage, \$/m^3
OC^{ht}	Cost of heating, \$/10^{9}J
P_s	Gas production of wellpad *s*, m^3
R_m	Membrane resistance, kPahm^2/L
RRa_c	Removal ratio of contaminants by regenerator *Ra*
RRb_c	Removal ratio of contaminants by regenerator *Rb*
SP^{gas}	Unit price of natural gas, \$/m^3
ST_s	Availability date of wellpad *s*, day
T	Number of tubes per module
TR_s	Time required fracturing wellpad *s*, day
T_{sf}	Temperature of feed water into the treatment unit, K
u	Ratio of recycled reject to raw feed
$V^{\max}$	Maximum capacity of treatment unit, m^3
$V^{\min}$	Minimum capacity of treatment unit, m^3
WR_s	Amount of water required to fracture wellpad *s*, m^3
X_{NaCl}	Molar concentration of NaCl in the feed
η	Pump efficiency
∂_{ED}	Energy density, kJ/ m^3

Binary variables

$w_{s,n}$	Defines the beginning of stimulating each wellpad *s* at time point *n*
$wv_{s,n}^{va}$	Transfer of water from wellpad *s* to storage tank *va* at time point *n*
wr_{n}^{Ra}	Transfer of water to regenerator *Ra* at time point *n*
wr_{n}^{Rb}	Transfer of water to regenerator *Rb* at time point *n*

Continuous variables

A	Required UF membrane area, m^2
A_m	Required MD membrane area, m^2
AFC	Annualized fixed capital cost for MD, \$/yr
AHC	Annualized heating cost for MD, \$/yr
AOC	Annualized operating cost for MD, \$/yr
Bw	Membrane permeability, kg/ (m^2.pa)
$c_{s,c,n}^{fbw}$	Flowback water concentration of wellpad *s* at time point *n*, mg/L
$c_{c,n}^{Ra}$	Outlet contaminant concentration from regenerator *Ra* at time point *n*, mg/L
$c_{c,n}^{Rb}$	Outlet contaminant concentration from regenerator *Rb* at time point *n*, mg/L
$c_{c,n}^{con,Ra}$	Contaminant concentration removed by regenerator *Ra* at time point *n*, mg/L
$c_{c,n}^{con,Rb}$	Contaminant concentration removed by regenerator *Rb* at time point *n*, mg/L
$cp_{c}^{Ra,perm}$	Permeate concentration from UF, mg/L
$cr_{c}^{Ra,con}$	Retentate concentration from UF, mg/L
$cp_{c}^{Rb,perm}$	Permeate concentration from MD, mg/L
$cr_{c}^{Rb,con}$	Retentate concentration from MD, mg/L
cc^{fp}	Capital cost of feed pump, \$
cc^{m}	Capital cost of membrane, \$
$du_{s,n}$	Duration of wellpad *s* at time point *n*, day
$f_{s,n}$	Total water required to fracture wellpad *s* at time point *n*, m^3
$f_{t,n,y}^{pump}$	Water pumped from interruptible source at time point *n* in scenario year *y*, m^3
$f_{t,n,y}^{truck}$	Water trucked from uninterruptible source at time point *n* in scenario year *y*, m^3
$f_{s,n}^{fw}$	Freshwater required to fracture wellpad *s* at time point *n*, m^3

$f_{s,n}^{ww}$	Wastewater required to fracture wellpad *s* at time point *n*, m^3
$f_{s,n}^{ww,Ra}$	Volume of pre-treated water sent to the frac tank at time point *n*, m^3
$f_{s,n}^{ww,Rb}$	Volume of desalinated water sent to the frac tank at time point *n*, m^3
f_{n}^{Rb}	Volume of pre-treated water sent to *Rb* for desalination at time point *n*, m^3
$f_{s,n}^{fbw}$	Flowback water from wellpad *s* at time point *n*, m^3
$f_{s,n}^{Ra}$	Flowback water sent to the treatment unit *Ra* from wellpad *s* at time point *n*, m^3
$f_{s,n}^{dis}$	Flowback water sent to disposal from wellpad *s* at time point *n*, m^3
f_{n}^{UF}	Total flowback water to be treated at time point *n*, m^3
f_{n}^{pretrt}	Total volume of water out of regenerator *Ra* at time point *n*, m^3
f_{n}^{con}	Amount of retentate from regenerator *Rb* at time point *n*, m^3
fd_{n}	Total volume of water disposed at time point n, m^3
ff^{Ra}	Total flowrate into UF, m^3/day
$ff^{Ra,perm}$	Permeate flowrate from UF, m^3/day
ff^{Rb}	Total flowrate into MD, m^3/day
$ff^{Rb,perm}$	Permeate from MD at time point *n*, m^3
$ff^{Rb,con}$	Retentate from MD at time point *n*, m^3
$ff_{d,n}^{dis}$	Amount of water sent to an injection well *d* at time point *n*,
$i_{t,n}^{fw}$	Total amount of water used from impoundment *t* at time point *n*
J^{UF}	Water flux across the UF membrane, L/ (m^{2}h)
J^{MD}	Water flux across the MD membrane, kg/(m^2.s)
LR	Liquid recovery for regenerator *Rb*
N	Number of UF membrane modules
oc^{fp}	Operating cost of the feed pump, $
$oc^{che,ptrt}$	Cost of chemical pre-treatment, $/m^3
oc^{gen}	Operating cost of generator, $
$p_{s,n}$	Expected gas production of wellpad *s* at time point *n*, m^3

p_r	Pressure of the retentate, kPa
p_p	Permeate pressure, kPa
p_f	Feed pressure, kPa
p_{wf}^{vap}	Water vapour pressure of the feed in MD, pa
p_{wp}^{vap}	Water vapour pressure of the permeate in MD, pa
Q	Heat required by the feed into MD, kJ/day
$ts_{s,n}$	Start time of wellpad *s* at time point *n*, day
$tf_{s,n}$	Finish time of wellpad *s* at time point *n*, day
tt_n	Time that correspond to time point *n*, day
tr_n^{Ra}	Start time of regeneration by regenerator *Ra* at time point *n*, day
ttr_n^{Ra}	Duration of regeneration *Ra* at time point *n*, day
tr_n^{Rb}	Start time of regeneration by regenerator *Ra* at time point *n*, day
ttr_n^{Rb}	Duration of regeneration *Rb* at time point *n*, day
$tv_{s,n}^{va}$	Time at which water is transferred from wellpad *s* to *va* at time point *n*, day
T_m	Membrane average temperature, K
T_{bf}	Temperature of the feed in the bulk, K
va_n	Capacity of regenerator *Ra* wastewater tank, m^3
vb_n	Capacity of wastewater tank *vb* at time point n, m^3
$v^{gas,Ra}$	Volume of gas required to generate the energy required by the feed pump, m^3
v^{gas}	Volume of gas required to generate a kWh of energy, m^3
$v^{gas,Rb}$	Volume of gas required by regenerator *Rb*
$v_{s,n}^{ft}$	Capacity of fracturing tank on wellpad *s* at time point *n*, m^3
$vi_{t,n,y}$	Volume of impoundment *t* at time point *n*
W^{fp}	Power of the feed pump, kW
Δp	Transmembrane pressure, kPa
x_{wf}	Mole fraction of water in the feed

γ_{wf}	Activity coefficient of water in the feed to the membrane distillation

Superscript

con	Concentrate
che	Chemical
dis	Disposal
ele	Electricity
eff	Efficiency
feed	Feed
fuel	Fuel
ft	Fracturing tank
fp	Feed pump
fw	Freshwater
fbw	Flowback water
fuel	Fuel
gas	Gas
ht	Heating
m	Membrane
MD	Membrane distillation
max	Maximum
min	Minimum
pump	Pumping
perm	Permeate
Ra	Regenerator a
Rb	Regenerator b
Pretrt	Pre-treatment
total	Total
truck	Trucking
UF	Ultrafiltration
vap	Vapour
va	Wastewater tank a
vb	Wastewater tank b
ww	Wastewater

Subscript

bf	*Feed bulk*
ED	Energy density
sf	*Supply feed*
m	Membrane
p	Pressure
f	Feed
r	Retentate
wp	Permeate water
wf	Feed water

References

Acharya, H.R., Henderson, C., Wang, H., 2011. Cost effective recovery of low-TDS frac flowback water for re-use. Global Research, 1–100.

Amosa, M.K., Jami, M.S., Alkhhatib, M.F.R., Majozi, T., 2016. Technical feasibility study of a low-cost PAC-UF system for wastewater reclamation and reuse: a focus on feedwater production for low-pressure boilers. Journal of Environmental Science Pollution Research 23, 22554-22567.

Bartholomew, T.V., Mauter, M.S., 2016. Multiobjective optimization model for minimizing cost and environmental impact in shale gas water and wastewater management. Journal of ACS Sustainable Chemistry and Engineering 4, 3728-3735.

Carrero-Parreño, A., Onishi, V.C., Salcedo-Díaz, R., Ruiz-Femenia, R., Fraga, E. S., Caballero, J.A., Reyes-Labarta, J. A., 2017. Optimal pretreatment system of flowback water from shale gas production. Journal of Industrial and Engineering Chemistry Research 56, 4386−4398.

Dahm, K., Chapman, M., 2014. Produced water treatment primer: Case studies of treatment applications. Science and Technology Research Report, 1-70.

Elsayed, N.A., Barrufet, M.A., Eljack, F.T., El-Halwagi, M.M., 2015. Optimal design of thermal membrane distillation systems for the treatment of shale gas flowback water. International Journal of Membrane Science and Technology 2, 1-9.

Elsayed, N.A., Barrufet, M.A., El-Halwagi, M.M., 2013. Integration of thermal membrane distillation networks with processing facilities. Journal of Industrial and Engineering Chemistry Research 53, 5284-5298.

Environmental report management (ERM), 2014. Recovered water management study in shale wells. ERM project 0243719 final report, 1-61.

Falsanisi, D., Liberti, L., Notarnicola, M., 2009. Ultrafiltration (UF) pilot plant for municipal wastewater reuse in agriculture: Impact of the operation mode on process performance, Water 1, 872-885.

Glazer, Y.R., Kjellsson, J.B., Sanders, K.T., Webber, M.E., 2014. Potential for using energy from flared gas for on-site hydraulic fracturing wastewater treatment in Texas. Environmental Science and Technology Letters 1,300-304.

Guadix, A., Sorensen, E., Papageorgiou, L.G., Guadix, E.M., 2004. Optimal design and operation of continuous ultrafiltration plants. Journal of Membrane Science 235, 131-138.

Hayes, T., Severin, B. F., 2012. Barnett and Appalachian shale water management and reuse technologies. Project report by Gas Technology Institute for Research Partnership to Secure Energy for America (RPSEA); RPSEA: Houston, TX, 1−125.

Hayes, T., 2009. Sampling and analysis of water streams associated with the development of Marcellus shale gas. Report by Gas Technology Institute, Des Plaines, IL, Marcellus Shale Coalit.

Howe, K.J., Hand, D.W., Crittenden, J.C., Trussell, R.R., Tchobanoglous, G., 2012. Principles of water treatment, John Wiley & Sons, Inc., Hoboken.

Micro and Ultrafiltration, 2018. https://ocw.tudelft.nl/wp-content/uploads/Micro-and-ultrafiltration-1.pdf. Accessed August 2018.

Muro, C., Riera, F., Díaz, M.C., 2012. Membrane separation process in wastewater treatment of food industry, https://www.intechopen.com/books/food-industrial-processes-methods-and-equipment/membrane-separation-process-in-wastewater-treatment-of-food-industry. Acessed 17th August, 2018.

Pearce, G.K., 2008. UF/MF pre-treatment to RO in seawater and wastewaterreuse applications: a comparison of energy costs. Desalination 222, 66–73.

WaterWorld, 2014. Membrane filtration for wastewater reuse current. PennWell Corporation. http://www.waterworld.com/articles/wwi/print/volume-25/issue-5/regional-spotlight/north-american-caribbean/membrane-filtrationfor-wastewater-reuse-current.html. Accessed 10 September 2018.

Yang, L., Grossmann, I.E., Mauter, M.S., Dilmore, R.M., 2015. Investment optimization model for freshwater acquisition and wastewater handling in shale gas production, Journal of American Institute of Chemical Engineers 61, 1770-1782.

Yang, L., Grossmann, I.E., Manno, J., 2014a. Optimization models for shale gas water management. Journal of American Institute of Chemical Engineers 60(10), 3490-3501.

Yun, Y., Ma, R., Zhang, W., Fane, A.G., Li, J., 2006. Direct contact membrane distillation mechanism for high concentration NaCl solutions. Desalination 188, 251–262.

CHAPTER SEVEN

CONCLUSIONS AND RECOMMENDATIONS

7.1. Conclusions

Introduction

Associated with shale gas development are environmental issues such as water usage and wastewater discharge as well as flaring of co-produced gas. As global shale gas reserves and exploration is increasing, there is a need for accurate and efficient method for proper water management as this is one of the important issues that has impeded the process of shale exploration around the world. Due to the importance of water in the process of hydraulic fracturing, industries are faced with challenges of defining wastewater management strategies that are sustainable environmentally and economically. For effective management strategies, water and energy usage in shale gas development are interdependent. Thus, it is imperative to develop a more integrated approach to address the challenges of the water-energy nexus in shale gas production. Therefore, the main objective of this work was to investigate the possibility of finding a better strategy that can alleviate the environmental issues in terms of water usage, wastewater generation and gas flaring associated with hydraulic fracturing simultaneously.

In order to investigate this possibility, the objectives of the study were defined as:

- To synthesize an optimal integrated water, shale gas and membrane network and to determine the design of the ultrafiltration and membrane distillation subnetworks that correspond with the optimal network. The optimal configuration is one that minimizes freshwater use and regeneration energy.
- To develop a mathematical model for hydraulic fracturing scheduling based on continuous time formulation.
- To investigate the feasibility of using co-produced gas that would otherwise be flared as energy source for ultrafiltration and membrane distillation.
- To investigate the effect of optimizing water, energy and shale gas production simultaneously on the overall process.
- To explore the practical application of using ultrafiltration membrane technology as a pre-treatment for membrane distillation.

- To investigate the application of the proposed model in a typical shale gas site using literature case studies.

7.1.1. Simultaneous energy and water optimization in shale exploration

This chapter explored simultaneous water and energy optimization in shale play using continuous time formulation with the incorporation of detailed MD model within the water network. The goal was to balance the trade-off between water acquisition from interruptible and uninterruptible water sources. It has been shown that water acquisition from interruptible source through piping can lead to reduction in both freshwater cost and high environmental impact associated with trucking water from uninterruptible source. The results have also demonstrated that for the considered case study, membrane distillation is capable of handling wastewater from hydraulic fracturing effectively, 99.4% of flowback water generated is treated and reused. The importance of simultaneously optimizing fracturing schedule with water and energy management was demonstrated. The approach indicated that optimizing energy and water simultaneously results in significant reduction in the amount of thermal energy required for regeneration. Although it is difficult to find the specific amount/volume of gas flared per each wellpad in literature. However, based on the average data gathered from literature, the amount of gas that is flared in most of the shale play is sufficient to provide the energy needed for regeneration.

7.1.2. On the optimization of water-energy nexus in shale gas exploration: consideration of production, processing, distribution, power generation and transmission

The continuous time scheduling formulation for water-energy nexus optimization developed in the previous chapter was extended to capture the aspect of shale gas production and infrastructure development with emphasis on shale gas production, processing, distribution, power generation and transmission. This entailed incorporating detailed MD model within the network to capture the energy requirement associated with water management in shale gas production. Consideration is also given to both wet and dry gas in order to capture the impact the type of gas produced in a particular shale play will have on the infrastructure development and economic performance. The resultant model was applied to a case study comprised of 14 wellpads that are geographically distributed in two clusters in a given region. The result showed that freshwater transportation using pipeline appeared as the preferred option in both geographical areas which results in lower freshwater cost compare to trucking. The study has also shown that with proper water management technology and efficient scheduling framework, flowback water can be managed and reused effectively. The efficient reuse of wastewater leads to 23.2 % reduction in the amount of freshwater required and 18.6 % in the total cost of freshwater. The approach indicates that optimizing energy, water and gas simultaneously results in significant reduction in the amount of thermal energy required for regeneration. 42.7 % reduction is achieved in the thermal energy required. The tightness in the fracturing activities also ensure the steady supply of gas to meet the necessary market demand. The main cost in both scenarios considered was the cost of shale gas production, which is more than half of the total cost incurred. The type of shale gas to be produced from wellpads in a particular region can have significant effect on the infrastructure development required and the overall economic performance, which has indicated 41.76 % increase in the cost incurred in wet gas network compared to dry gas network.

7.1.3. Using ultrafiltration for flowback water management in shale gas exploration: multicontaminant consideration

The previous chapters focused on membrane distillation as a desalination technology capable of treating hydraulic fracturing wastewater effectively with focus on total dissolved solid (TDS) as the main contaminant of concern in wastewater reuse for fracturing. This was extended to capture the multi-contaminant property of flowback water by investigating the role that low-pressure membrane can play in maximizing wastewater reuse in hydraulic fracturing with focus on ultrafiltration (UF) membrane technology. The study showed that with treatment of flowback water to remove basic contaminants, wastewater with TDS concentration as high as 300,000 ppm can still be reused which led to the saving of 21.4 % in the amount of water required for fracturing. The energy consumption of the system and the cost implication was evaluated by incorporating detailed UF model into the water network in order to optimize water and energy simultaneously. The simultaneous optimization led to 10.3 % reduction in the amount of energy required and 61 % in the operating cost of the feed pump if the electrical energy is generated onsite via the gas that would otherwise be flared. The main cost in the regeneration network was found to be the cost of membrane, which was capped at 50.52 % of the total regeneration cost. The results of this study could be employed as requisite data for further investigation on hybrid regeneration process/plant designs.

7.1.4. Hybrid regeneration network for flowback water management

Finally, the effect of hybrid regeneration network was investigated by designing a systematic approach for scheduling and design of multi-regenerator water network for effective flowback water management in hydraulic fracturing. It focused on detailed ultrafiltration and membrane distillation processes to account for some of contaminants that are considered to be of paramount importance in hydraulic fracturing wastewater reuse. The results showed that in the case where moderate salinity was considered, high percentage of flowback water was pre-treated and reused by combining with freshwater to meet the fracturing requirement in terms of contaminants concentration. However, as the degree of salinity increased, the water requirement was supplied through the combination of freshwater, pre-treated water and/or desalinated water with different percentage for each wellpad depending on the volume of water required for fracturing and the degree of salinity of the wastewater. The effective maximization of wastewater reuse within the network resulted in 24.13 % reduction in the volume of freshewater required for fracturing. In terms of energy consideration, the study led to 31.6 % reduction in the amount of thermal energy required in membrane distillation and 8.62 % in the energy requirement for UF when compared with standalone model. This was considered to be as a result of the fact that the primal cost in the membrane distillation network was the operating cost which was capped at more than 75 % of the total cost while in ultrafiltration network, the primal cost was the capital cost capped at 73.2 % of the total cost with cost of membrane found to be 69.9 % of the total capital cost.

In all cases, the performance of the regenerators when applied as a standalone technology and when incorporated within the hydraulic fracturing process network was determined. Optimising energy and water simultaneously within a background process has led to a significant reduction in the required energy by the regeneration network. This reflects the significance of incorporating the regeneration network within the background process network and not as a standalone.

7.2. Recommendations for future work

There are various uncertainties associated with shale gas/oil development. Considering the uncertainties associated with shale gas exploration in terms of water usage for hydraulic fracturing, flowback water generation, cost associated with water management, demand and price of natural gas, NGLs and electricity, future work should address the uncertainties associated with the process and the possible impact on the overall project.

Future work can also consider multiple desalination technologies and the integration of fossil energy with renewable sources to reduce the carbon footprint of the resulting network. Hence, sustainability-based objective functions can be used to optimize the system design.

Given the multiple years time horizon been considered and some conditions that may affect the membrane efficiency, it may be necessary to consider explicitly the life span of the membranes used in the models. Although membranes can normally operate for couple of years under good conditions, their life span depends on many factors such as the contaminant level in the wastewater.

Finally, it is recommended that the effect of fouling and cake compressibility especially in ultrafiltration be investigated, as these are considered important for design and scale-ups in membrane processes.